

Escuela Técnica Superior de Ingeniería Agronómica y Biociencias

DEPARTAMENTO DE INGENIERÍA

Doctorado en Ciencias y Tecnologías Industriales

ASSESSMENT AND MODELING OF THE
GENERATION AND TRANSPORT OF WATER AND
SOLUTES IN REPRESENTATIVE WATERSHEDS
OF NAVARRE (SPAIN): TOWARDS AN OPTIMAL
AND SUSTAINABLE AGRARIAN ACTIVITY

Doctoral Thesis



Iker Hernández García

Pamplona-Iruñea, 2021

Thesis advisors:

Javier Casalí Sarasibar

Miguel Ángel Campo Bescós

Daniel Merchán Elena

<https://doi.org/10.48035/Tesis/2454/41130>

ACKNOWLEDGMENTS/ AGRADECIMIENTOS/ESKER-EMATEAK

La realización de esta tesis es el resultado de un gran esfuerzo continuo y constante que no hubiera sido posible sin la colaboración y apoyo de las personas e instituciones que cito a continuación.

A mis directores, el Dr. Javier Casalí y el Dr. Miguel Ángel Campo, que me han acompañado en mi formación y desarrollo como investigador aportando paciencia y apoyo, sabiendo transmitir todo su conocimiento en este proceso de crecimiento personal. A mi director, el Dr. Daniel Merchán, que además de ser mi guía en esta carrera de fondo, principalmente en los primeros pasos en los que uno está más perdido, ha sido compañero de viaje en mis primeras conferencias internacionales, aconsejándome en todo momento y serenándome cuando era necesario.

A mi compañero de despacho en los últimos meses de tesis, Eduardo, por compartir conmigo inquietudes, conocimientos y buen humor. Asimismo, quiero agradecer a todos los compañeros del grupo THERRAE, tanto los que han estado a lo largo de todo el periodo de la tesis, como a los que han estado de paso, por ayudarme con sus aportaciones en los seminarios y por disipar los malos momentos durante la hora del café.

Quiero también agradecer al antiguo Ministerio de Economía y Competitividad Gobierno de España la destinación de recursos a las ayudas a jóvenes investigadores de la que he sido beneficiario, permitiéndome así cumplir un importante hito en mi vida académica. También quiero agradecer a la Universidad Pública de Navarra por facilitarme recursos para poder desarrollar mi tesis, incluidos las tramitaciones de temas burocráticos como mi estancia, o la ayuda concedida para la participación en el Concurso Internacional de Evaluación de Suelos en Río de Janeiro. Y al Gobierno de Navarra, en especial a Javier Eslava, por su predisposición ante mis peticiones.

No me quiero olvidar de todos aquellos que, aun no perteneciendo en la Universidad Pública de Navarra, han sido vitales en el desarrollo de mi tesis. Mi más sincero agradecimiento al Dr. Ron Bingner por permitirme disfrutar de mi estancia en Sedimentation Lab del USDA-ARS en Oxford, Mississippi, y por su plena disponibilidad para explicarme todos los entresijos del modelo AnnAGNPS, thank you very much, and I hope we can share experiences soon, y a Vance Justice, por ayudarme en los primeros pasos de mi estancia, y hacer de mi estancia en Oxford una experiencia más cómoda. Thank you for sharing those afternoons of sports in the soccer stadium.

Al Dr. Manuel López Vicente, por su paciencia y disponibilidad, y por compartir conmigo reflexiones y momentos de la vida científica. Al Dr. Ray Huffaker, por su capacidad de transmitir con serenidad conceptos que nunca imaginé que pudiera llegar a entender, It is a pity that the current pandemic situation has not allowed us to enjoy more of your stay in Pamplona. Y al Dr. Rafael Muñoz Carpena, por aportar ese importante empujón que necesitaba la tesis y permitirme aumentar mi capacidad crítica en ciencia mediante sus seminarios sobre la redacción y evaluación de artículos.

Además de aquellas personas que han formado parte en la producción científica, quiero agradecer de forma especial a todos los que me han acompañado, aguantado y que han confiado en mí a lo largo de esta carrera de fondo.

A Irati, por su paciencia, cariño y comprensión a lo largo de estos cuatro años. Por esa capacidad de motivarme y alegrarme en los momentos que más lo necesitaba, haciéndome ver las cosas que realmente importan en la vida. Zurekin batera ezinezkoa iruditzen zuen bidaia askoz errazagoa izan da, eskerrik asko beti nire ondoan egoteagatik eta nire bertsio hoberena ateratzen laguntzegtatik.

A mi familia, en especial a mis padres y a mis hermanas, por ese apoyo incondicional en todo lo que hago y esa confianza ciega ante todos mis proyectos de vida. Por poder seguir compartiendo todos juntos momentos inolvidables.

A mis amistades más cercanas que, aunque en muchas ocasiones no tuvieran mucha idea de lo que estaba haciendo, siempre han estado ahí dispuestos a compartir buenos momentos y experiencias.

A todos ellos, muchas gracias, thank you very much, mila esker.

ABSTRACT

The overarching aim of this thesis is to expand the knowledge base on the dynamics of total dissolved solids, with special focus on the most widespread nutrients in agricultural systems (N, and to a lesser extent P). To this end, (1) the exports of dissolved solids and their dynamics in a watershed network have been quantified, considering different agrosystems of the region of Navarre (Spain). Recognizing the influence of these compounds on different water bodies, and with the aim of shedding more light on the black box watershed approach in water quality, (2) the relatively recent concept of overland flow connectivity has been assessed through an Overland Flow Connectivity index. This index is based on broadly adopted overland flow connectivity indices, and implemented at two rainfed winter cereal watersheds (*Latxaga* and *La Tejería*). Regarding nutrients, and focusing on nitrate and phosphate dynamics, (3) these two watersheds have been characterized in terms of concentration and exports of nitrate and phosphate, for a range of temporal scales, with insights on the controlling factors of these processes. Finally, (4) the nutrient controlling factors previously identified have been quantified considering different possible scenarios. The AnnAGNPS model capacity has been evaluated for dissolved nitrogen exports at the two rainfed winter cereal watersheds.

Total dissolved solids (TDS) are considered relevant environmental problems related to a wide range of on-site and off-site impacts, such as salinization of water bodies. In Chapter 3, the dynamics of TDS concentration and loads were assessed in all the watersheds that constitute the Navarrese network, which covered representative agricultural land uses in Navarre (*Latxaga*, *La Tejería*, *Landazuría*, *Oskotz*, and the forested sub-watershed of *Oskotz*). Discharge and TDS concentration data were collected during ten hydrological years at the outlet of each watershed, and loads were computed from discharge and concentration values. TDS concentration followed a seasonal pattern imposed by the availability of water, with higher concentrations recorded in low-flow periods and lower concentrations during high-flow periods. Temporal variations (intra- and inter-annual) in TDS loads were explained by differences in runoff. These temporal patterns were observed for both agricultural (this study) and non-agricultural (scientific literature) watersheds. Navarrese watershed data and literature data corroborated that agricultural land use, in general, leads to an increase in the concentration of TDS. The effects of agricultural land use on TDS yields are controlled by changes in runoff rather than by (small) changes in TDS concentration. In this

sense, the changes in land use that were expected to increase runoff (i.e., a shift from forested to arable or from rainfed to irrigated agriculture) also increase TDS yields. In the Navarrese watersheds, TDS yields ranged from 1.1 to 2.2 Mg ha⁻¹ year⁻¹. TDS yields seem to dominate under non-agricultural conditions and in most agricultural land uses at the small watershed scale. On the other hand, suspended sediments were dominant in watersheds with increased soil erosion as a consequence of arable land use over erosion-prone watersheds.

Chapter 4 developed and evaluated an overland flow connectivity index (OFC). The OFC index was based on the established flow connectivity index of Borselli et al. (2008) and on the modifications proposed by Cavalli et al. (2013) and Lopez Vicente Ben Salem (2019). These indices are obtained by calculating the upstream and downstream components of a given reference particle (cell, represented by a pixel) within the watershed. For the computation of the index, parameters related to area, slope, and resistance to flow (weighting factors) are required. Regarding the selection of weighting factors, The RUSLE C factor was selected as the most suitable, as other factors generated unrealistic results or did not provide relevant information. For the calculation of the contributing area, the D-infinite algorithm was used. Application of the OFC index at Latxaga and La Tejería watersheds yielded realistic OFC results, despite some limitations. The semi-quantitative aspect of OFC does not enable the comparison of connectivity between different watersheds. In addition, in agricultural areas with tile drainage, higher relevance to this management practice must be incorporated to reflect the resulting change in OFC.

Chapter 5 assesses nutrient dynamics and factors that control nutrient exports at two watersheds of the Navarrese network, Latxaga and La Tejería. These watersheds present similar climatic and management characteristics, and were monitored throughout 10 years (2007–2016). Similar patterns were observed at both watersheds regarding intra-annual and inter-annual dynamics, with higher NO₃⁻ concentration and NO₃⁻-N yields during the humid seasons (i.e., winter and hydrological year 2013). Regarding concentration, La Tejería presented ca. 73 ± 25 mg NO₃⁻ L⁻¹ and Latxaga presented an almost three times lower concentration, with ca. 21 ± 15 mg NO₃⁻ L⁻¹ throughout the study period. Latxaga presented a more pronounced decrease in nitrate due to the higher development of vegetated areas. High discharge events produced nitrate dilution due to the presence of tile drainage at La Tejeria. At Latxaga, there is no tile drainage and an increase in concentration occurred as a response to high discharge events. Similar patterns were observed for the NO₃⁻-N yield, with 32 kg NO₃⁻-N ha⁻¹ year⁻¹ and 17 kg NO₃⁻-N ha⁻¹ year⁻¹ at La Tejería and

Latxaga, respectively. Regarding phosphorous, the observed concentrations were $0.20 \pm 0.72 \text{ mg PO}_4^{3-} \text{ L}^{-1}$ and $0.06 \pm 0.38 \text{ mg PO}_4^{3-} \text{ L}^{-1}$ at La Tejería and Latxaga, respectively, with $\text{PO}_4^{3-}\text{-P}$ yields being $71 \text{ g PO}_4^{3-}\text{-P ha}^{-1} \text{ year}^{-1}$ and $33 \text{ g PO}_4^{3-}\text{-P ha}^{-1} \text{ year}^{-1}$. In summer, a highly erosive rainfall event mobilized sediments and probably generated desorption of phosphorous in the stream channel, increasing phosphate concentration. The annual $\text{PO}_4^{3-}\text{-P}$ yield distribution in both watersheds followed similar patterns of the $\text{NO}_3^-\text{-N}$ yield, with higher yields in the humid season. This research fills a knowledge gap regarding the dynamics of nutrients and the controlling factors in complex agricultural systems with Mediterranean characteristics. In particular, it highlights the importance of specific controlling factors, such as the presence of vegetation or tile drainage, on the N dynamics in the rainfed cereal watersheds of the network.

Finally, chapter 6 evaluates the capability of the AnnAGNPS model to simulate dissolved N at the Latxaga and La Tejería watersheds, to quantify the effect of the major controlling factors such as the presence of vegetation (spontaneous and riparian) and tile drainage. Simulations encompassed other possible scenarios controlled by these factors. The model has been evaluated by calibration of runoff, and calibration and testing of dissolved N yield at the watershed outlet, using the inverse calibration method. This method consists of three steps: (a) *global search*, in which the analysis of the possible range of the most sensitive variables is performed; (b) *local refinement*, a process in which the number of the most sensitive parameters and/or the range of values of these parameters is decreased; and (c) *model performance*, a process in which the optimal simulation is obtained. The most sensitive variables detected during runoff calibration were the curve number values in the wet periods and in the periods of soil crack appearance. The most sensitive variables detected in the dissolved N yield calibration were the crop yield and the decomposition coefficient. The runoff calibration results at Latxaga and La Tejería were $\text{NSE}=0.72$ and $\text{NSE}=0.76$ respectively, and the dissolved N yield calibration and testing results were $\text{NSE}=0.52$ and $\text{NSE}=0.45$ at Latxaga and $\text{NSE}=0.72$ and $\text{NSE}=0.51$ at La Tejería. Even though some limitations have been observed, model fit showed satisfactory results, in accordance with the thresholds reported in scientific literature. In the simulations for the quantification of the factors controlling the dynamics of dissolved N, it was observed that replacing the vegetated areas at Latxaga with cultivated land would imply an increase of 11.9% in N dissolved yield. Eliminating tile drainage at La Tejería would imply a decrease of 12.4% in dissolved N yield. In the simulated scenarios with different management options, increasing the vegetation area from 12% to 25% at Latxaga

leads to a decrease of 15.8% in the dissolved N yield at the watershed outlet. Replacing the vegetated areas of the watershed by cultivated areas with tile drainage (to improve production capacity) would increase dissolved N yield by 19.2%. At La Tejería, an increase from 16% to 37% in the cultivated area with tile drainage would not lead to significant differences in the export of dissolved N. However, replacing the areas with tile drainage by vegetated areas would decrease the N dissolved yield at the watershed outlet by 26%.

RESUMEN

El objetivo general de esta tesis es ampliar la base de conocimiento sobre la dinámica de los sólidos disueltos totales, con especial atención a los nutrientes más extendidos en los sistemas agrícolas (N, y en menor medida P). Para ello, (1) se han cuantificado las exportaciones de los sólidos disueltos totales y su dinámica en la red de cuencas experimentales de Navarra, considerando diferentes agrosistemas de la región de Navarra (España). Reconociendo la influencia de estos compuestos en diferentes masas de agua, y con el objetivo de arrojar más luz sobre el enfoque de la caja negra de las cuencas en la calidad del agua, (2) se ha evaluado el concepto relativamente novedoso de conectividad de flujo superficial a través de un índice de conectividad del flujo superficial. Este índice se basa en índices de conectividad de flujos superficiales ampliamente contrastados, aplicándose en dos cuencas de secano con cultivo de cereal de invierno (*Latxaga* y *La Tejería*). En cuanto a los nutrientes, y centrándonos en la dinámica de los nitratos y fosfatos, (3) se ha caracterizado la concentración y la exportación de nitratos y fosfatos en diferentes escalas temporales en estas dos cuencas. En ellas se han identificado los factores controladores de estas dinámicas para estas dos cuencas. Por último, (4) se han cuantificado los factores controladores de nutrientes previamente identificados considerando diferentes escenarios posibles, y se ha evaluado la capacidad del modelo AnnAGNPS para las exportaciones de nitrógeno disuelto en las dos cuencas de secano con cultivo de cereal de invierno.

Los sólidos totales disueltos (SDT) generan importantes problemas ambientales relacionados con una amplia gama de impactos in situ y ex situ, como la salinización de las masas de agua. En el capítulo 3 se evaluó la dinámica de la concentración y las cargas de SDT exportadas a la salida de cada una de las cuencas que componen la red de cuencas de Navarra, que abarcan usos agrícolas representativos de Navarra (*Latxaga*, *La Tejería*, *Landazuría*, *Oskotz* y la subcuenca forestal de *Oskotz*). Se recogieron datos de caudal y concentración de SDT durante diez años hidrológicos en la salida de cada cuenca, y las cargas exportadas de SDT se calcularon a partir de los valores de caudal y concentración. La concentración de SDT siguió un patrón estacional establecido por la disponibilidad de agua, con concentraciones más altas registradas en los períodos de bajo caudal y concentraciones más bajas durante los períodos de alto caudal. Las variaciones temporales (intra e interanuales) en las cargas exportadas de SDT se dieron por las diferencias en la esorrentía. Estos patrones temporales se observaron tanto para las cuencas agrícolas (este estudio) como para

las no agrícolas (literatura científica). Los datos de las cuencas de Navarra y los datos de la literatura científica corroboraron que el uso de suelo agrario, en general, produce un aumento de la concentración de SDT. Los efectos del uso de suelo agrario en la exportación de SDT están controlados por los cambios en la escorrentía más que por los (pequeños) cambios en la concentración de SDT. En este sentido, los cambios en el uso de suelo que se esperaba que aumentaran la escorrentía (es decir, un cambio de bosques a cultivos o de agricultura de secano a regadío) también aumentan las exportaciones de SDT. En las cuencas navarras, las exportaciones de SDT oscilaron entre 1,1 y 2,2 Mg ha⁻¹ año⁻¹. Estas exportaciones de SDT parecen dominar en las condiciones no agrícolas y en la mayoría de los usos agrícolas del suelo a escala de cuenca pequeña. Por otro lado, los sedimentos en suspensión fueron dominantes en las cuencas con una alta proporción de tierras de cultivo y condiciones ambientales propicias para una alta erosión.

En el capítulo 4 se desarrolló y evaluó un índice de conectividad de flujo superficial (CFS). El índice CFS se basó en el índice de conectividad de flujo superficial establecido por Borselli et al. (2008) y en las modificaciones propuestas por Cavalli et al. (2013) y López Vicente y Ben Salem (2019). Estos índices se obtienen calculando las componentes aguas arriba y aguas abajo de una determinada partícula de referencia (celda, representada por un píxel) dentro de la cuenca. Para el cálculo del índice se requieren parámetros relacionados con el área, la pendiente y la resistencia al flujo (factores de ponderación). Dentro de estos factores de ponderación, se seleccionó el factor C de RUSLE como el más adecuado, descartando otros por su generación de resultados poco realistas o por no proporcionar información relevante. Para el cálculo del área contributiva se utilizó el algoritmo D-infinite. La aplicación del índice CFS en las cuencas de Latxaga y La Tejería mostró resultados realistas, a pesar de presentar algunas limitaciones, ya que el aspecto semicuantitativo del CFS no permite comparar la conectividad entre diferentes cuencas. Además, en las zonas con drenaje artificial subsuperficial, la incorporación de parámetros que reflejen una mayor relevancia en este tipo de manejo agrícola es necesaria, ya que de esta manera se podrá observar la influencia de este factor en el resultado de CFS.

El capítulo 5 evalúa la dinámica de nutrientes y los factores controladores de las exportaciones de nutrientes en dos cuencas de la red de Navarra, más concretamente en Latxaga y La Tejería. Estas cuencas presentan características climáticas y de manejo agrícola similares, y fueron monitorizadas a lo largo de 10 años (2007-2016). En ambas cuencas se observaron patrones similares en cuanto a la dinámica intra-anual e inter-anual, con una mayor concentración de NO₃⁻

y carga específica exportada de NO_3^- -N durante las estaciones húmedas (es decir, invierno y año hidrológico 2013). En cuanto a la concentración, La Tejería presentó ca. $73 \pm 25 \text{ mg NO}_3^- \text{ L}^{-1}$ y Latxaga ca. $21 \pm 15 \text{ mg NO}_3^- \text{ L}^{-1}$ (casi tres veces menor) a lo largo del periodo de estudio. Latxaga presentó una disminución más pronunciada de los nitratos debido al mayor desarrollo de las zonas con vegetación. Los eventos de alta descarga produjeron una dilución de los nitratos debido a la presencia de drenaje artificial subsuperficial en La Tejería. En Latxaga, no hay este tipo de drenaje, por lo que se produjo un aumento de la concentración como respuesta a los eventos de alto caudal. Se observaron patrones similares para la carga exportada de NO_3^- -N, con $32 \text{ kg NO}_3^- \text{ N ha}^{-1} \text{ año}^{-1}$ y $17 \text{ kg NO}_3^- \text{ N ha}^{-1} \text{ año}^{-1}$ en La Tejería y Latxaga, respectivamente. En cuanto al fósforo, las concentraciones observadas fueron de $0,20 \pm 0,72 \text{ mg PO}_4^{3-} \text{ L}^{-1}$ y $0,06 \pm 0,38 \text{ mg PO}_4^{3-} \text{ L}^{-1}$ en La Tejería y Latxaga, respectivamente, siendo la carga exportada de PO_4^{3-} -P de $71 \text{ g PO}_4^{3-} \text{ P ha}^{-1} \text{ año}^{-1}$ y $33 \text{ g PO}_4^{3-} \text{ P ha}^{-1} \text{ año}^{-1}$. En verano, los eventos tormentosos altamente erosivos produjeron una alta movilización de sedimentos y probablemente generaron una desorción de fósforo en el cauce, aumentando la concentración de fosfato. La distribución de la carga anual exportada de PO_4^{3-} -P en ambas cuencas siguió patrones similares a la carga exportada de NO_3^- -N, con mayores exportaciones en la estación húmeda. Este estudio aporta un aumento de conocimiento en la dinámica de los nutrientes y los factores de control en sistemas agrícolas complejos con características mediterráneas. En particular, destaca la importancia de factores controladores específicos, como la presencia de vegetación o el drenaje artificial subsuperficial, en la dinámica del N en las cuencas cerealistas de secano de la red.

Por último, en el capítulo 6 se evalúa la capacidad del modelo AnnAGNPS para simular el N disuelto en las cuencas de Latxaga y La Tejería, con el fin de cuantificar el efecto de los principales factores de control como la presencia de vegetación (espontánea y riparia) y drenaje artificial subsuperficial. También se realizaron simulaciones que abarcaron otros posibles escenarios controlados por estos factores. El modelo ha sido evaluado mediante la calibración de la escorrentía, y la calibración y testado de carga exportada de N disuelto a la salida de la cuenca, utilizando el método de calibración inversa. Este método consta de tres pasos: (a) la *búsqueda global*, en la que se realiza el análisis del posible rango de las variables más sensibles; (b) *el refinamiento local*, proceso en el que se disminuye el número de los parámetros más sensibles y/o el rango de valores de estos parámetros; y (c) *el ajuste del modelo*, proceso en el que se obtiene la simulación óptima. Los parámetros más sensibles detectados durante la calibración de la

escorrentía fueron los valores del número de curva en los periodos húmedos y en los periodos de aparición de grietas en el suelo. Las variables más sensibles detectadas en la calibración de la carga específica exportada de N disuelto fueron la productividad del cultivo y el coeficiente de descomposición. Los resultados de la calibración de la escorrentía en Latxaga y La Tejería fueron $NSE=0,72$ y $NSE=0,76$ respectivamente, y los resultados de la calibración y testado del ajuste de N disuelto fueron $NSE=0,52$ y $NSE=0,45$ en Latxaga y $NSE=0,72$ y $NSE=0,51$ en La Tejería. Aunque se han observado algunas limitaciones, el ajuste del modelo mostró resultados satisfactorios, de acuerdo con los umbrales reportados en la literatura científica. En las simulaciones para la cuantificación de los factores que controlan la dinámica del N disuelto, se observó que la sustitución de las zonas con vegetación en Latxaga por tierras de cultivo implicaría un incremento del 11,9% en la carga exportada de N disuelto. Por otro lado, la eliminación del drenaje artificial subsuperficial en La Tejería implicaría una disminución del 12,4% en la carga exportada de N disuelto. En cuanto a los escenarios simulados con diferentes opciones de manejo agrícola, el aumento de la superficie de vegetación del 12% al 25% en Latxaga supone una disminución del 15,8% en la carga exportada de N disuelto en la salida de la cuenca. Por otro lado, la sustitución de las zonas con vegetación de la cuenca por zonas de cultivo con drenajes artificiales subsuperficiales (para mejorar la capacidad de producción) aumentaría la carga exportada de N disuelto en un 19,2%. En La Tejería, un aumento del 16% al 37% de la superficie cultivada con drenajes artificiales subsuperficiales no supondría diferencias significativas en la exportación de N disuelto. Sin embargo, la sustitución de las zonas con drenajes artificiales subsuperficiales por zonas con vegetación disminuiría la carga exportada de N disuelto en la salida de la cuenca en un 26%.

LABURPENA

Tesi honen helburu orokorra disolbatutako solido totalen dinamikari buruzko ezagutza-oinarria zabaltzea da, nekazaritza-sistemetan gehien hedatuta dauden nutrienteetan arreta berezia jarritz (nitratoak, eta neurri txikiagoan fosfatoak). Horretarako, (1) disolbatutako solido totalen esportazioak eta horien dinamika kuantifikatu dira Nafarroako arro esperimentalen sarean, Nafarroako (Espainia) hainbat agrosistema ezberdin kontuan hartuta. Konposatu horiek ur-gorputz ezberdinetan duten eragina ezagututa, eta arroen kutxa beltzak uraren kalitatean duen ikuspegian argi gehiago emateko helburuarekin, (2) gainazaleko fluxuaren konektibitatearen kontzeptu nahiko berritzailea ebaluatu da, gainazaleko fluxuen konektibitate-indize baten bidez. Indize hori zabalki egiaztatuta dauden gainazaleko fluxuen konektibitate-indizeetan oinarritzen da, eta lehorreko neguko zereala duten bi arrotan aplikatu da (*Latxaga* eta *La Tejería*). Nutrienteei dagokienez, eta nitratoen eta fosfatoen dinamikan arreta jarrita, (3) bi arro horietan denbora-eskala desberdinetan nitratoen eta fosfatoen kontzentrazioa eta esportazioa karakterizatu dira. Bi arro hauetan nutriente hauen dinamika kontrolatzen dituzten faktoreak identifikatu dira. Azkenik, (4) aurretik identifikatutako nutrienteen faktore kontroladoreak kuantifikatu dira, hainbat egoera posible kontuan hartuta, eta AnnAGNPS modeloak disolbatutako nitrogenoaren esportazioetarako duen gaitasuna ebaluatu bi arrotan.

Disolbatutako solido totalak (DST) ingurumenean arazo larriak sortzen dituzte in situ eta ex situ inpaktuekin lotuta, hala nola, ur gorputzen gazitzea. 3. kapituluan, Nafarroako arroen sarea osatzen dituzten arroen irteera puntuetan kontzentrazioaren dinamika eta esportatutako DST kargak ebaluatu ziren. Arro hauek, Nafarroako nekazaritza-erabilera adierazgarriak hartzen dituzten arroak dira (*Latxaga*, *La Tejería*, *Landazuría*, *Oskotz* eta *Oskotz* baso azpi-arroa). Arro bakoitzaren irteera puntuan emari eta DST kontzentrazioari buruzko datuak bildu ziren hamar urte hidrokologikotan zehar, eta DST esportatutako kargak emari eta kontzentrazio balioetatik abiatuta kalkulatu ziren. DST kontzentrazioak urak ezarritako urtaroko antzeko patroia jarraitu zuen, emari baxuko aldietan kontzentrazio altuagoekin eta emari altuko aldietan kontzentrazio baxuagoekin. DST-aren kontzentrazioa uraren kantitatean oinarritutako urtaroko patroia bat jarraitu zuen, kontzentrazio altuenak emari baxuko denboraldietan erregistratuz eta kontzentrazio baxuenak emari altuko denboraldietan. DST esportatutako kargen garai-aldaketak (urte barrukoak eta urte artekoak) ur isurketaren diferentziengatik gertatu ziren. Denbora-patroi horiek nekazaritza-

arroetan (azterlan honetan) zein nekazal erabilera ez dituzten arroetan (literatura zientifikoa) behatu ziren. Nafarroako arroen datuek eta literatura zientifikoaren datuek berretsi zuten nekazaritza-lurren erabilerak, orokorki, DST kontzentrazioaren areagotzea erakartzen duela. Nekazaritzako lurak erabiltzearen ondorioak DST-en esportazioan uraren isurketaren aldaketek kontrolatzen dituzte, DST-en kontzentrazioaren aldaketa (txikiek) baino gehiago. Ildo horretan, lurzoruen erabilera aldaketekin, uraren isurketa handitzea espero zen (hau da, baso erabileratik laborantzara edo lehorreko laborantzatik ureztatura aldatzea), eta ondorioz, DST-en esportazioak ere areagotu ziren. Nafarroako arroetan, DST esportazioak 1,1 eta 2,2 Mg ha⁻¹ urte⁻¹ artekoak izan ziren. Badirudenez, DST esportazio hauek nagusitzen dira nekazaritza-egoeretatik kanpo zein nekazaritza erabilera duten lurzoru gehienetan arro txikiko eskalan. Esekitako solidoak nagusi izan ziren laborantza-lurren proportzio handia eta higadura handiko prozesuak bultzatzeko ingurumen baldintza aproposak zituzten arroetan.

4. kapituluak gainazaleko fluxuaren konektibitate indizea (GFK) garatu eta ebaluatu zen. GFK indizea Borselli et al.-ek (2008) ezarritako fluxu-konektibitatearen indizean oinarritu zen (2008), eta Cavalli et al. (2013) eta López Vicente eta Ben Salem-ek (2019) proposatutako aldaketetan. Indize hauek, arroaren barruan erreferentziazko partikula jakin baten (pixel batez irudikatutako zelda) uretan gora eta behera dauden osagaiak kalkulatuaz lortzen dira. Indizea kalkulatzeko, azalarekin, maldarekin eta fluxuarekiko erresistentziarekin lotutako parametroak behar dira (haztapen-faktoreak). Haztapen-faktore horien artean, RUSLE-ren C faktorea aukeratu zen egokiena. Beste faktore batzuk errealistak ez ziren emaitzak sortzen zituztelako edo informazio garrantzitsurik ematen ez zutelako baztertu egin ziren. Azalera kontributiboa kalkulatzeko D-infinitive algoritmoa erabili zen. Latxaga eta La Tejería arroetan GFK indizeak emaitza errealistak erakutsi zituen, naiz eta muga batzuk izan arren. GFK-ren alderdi erdi-kuantitatiboak ez ditu arroen arteko konektibitate konparaketak baimentzen. Gainera, lur azpiko drainatze artifiziala duten eremuetan, beharrezkoa da nekazaritza-erabilera mota horretan garrantzi handiagoa erakusten dituzten parametroak txertatzea, faktore horiek GFK-n dituzten eraginak behatzeko.

5. kapituluak Nafarroako sareko bi arrotan, Latxagan eta La Tejerían, nutrienteen dinamika eta nutrienteen esportazioen faktore kontrolatzaileak ebaluatzen ditu. Arro hauek antzeko ezaugarri klimatikoak eta nekazaritza-erabilerak dituzte, eta 10 urtez monitorizatu ziren (2007-2016). Bi arroetan antzeko patroiak ikusi ziren urte barruko eta urte arteko dinamikari dagokionez, NO₃⁻

kontzentrazio handiagoarekin eta esportatutako NO_3^- -N karga espezifiko handiagoarekin urtaro hezeetan (hau da, negua eta 2013-ko urte hidrologikoa). Kontzentrazioari dagokionez, La Tejería ca. $73 \pm 25 \text{ mg NO}_3^- \text{ L}^{-1}$ eta Latxaga ca. $21 \pm 15 \text{ mg NO}_3^- \text{ L}^{-1}$ (ia hiru aldiz txikiagoa) aurkeztu zituzten azterketa-aldian zehar. Latxagak nitratoen beherakada nabarmenagoa izan zuen, landaredia zuten eremuak gehiago garatu zirelako. La Tejería dagoen lurrazpiko drainatze artifizialaren ondorioz, deskarga altuko gertaerak nitratoen diluzio bat eragin zuten. Latxagan aldiz, drainatze mota hori ez dagoenez, emari handiko gertakarien ondorioz kontzentrazioak gora egin zuen. Antzeko patroiak ikusi ziren NO_3^- -N esportatutako kargarako, $32 \text{ kg NO}_3^- \text{ N ha}^{-1} \text{ urte}^{-1}$ eta $17 \text{ kg NO}_3^- \text{ N ha}^{-1} \text{ urte}^{-1}$ esportazioarekin La Tejería eta Latxagan, hurrenez hurren. Fosforoari dagokionez, behatutako kontzentrazioak $0,20 \pm 0,72 \text{ mg PO}_4^{3-} \text{ L}^{-1}$ eta $0,06 \pm 0,38 \text{ mg PO}_4^{3-} \text{ L}^{-1}$ -koak izan ziren La Tejería eta Latxagan, hurrenez hurren, PO_4^{3-} -P esportazio karga $71 \text{ g ha}^{-1} \text{ urte}^{-1}$ eta $33 \text{ g PO}_4^{3-} \text{ P ha}^{-1} \text{ urte}^{-1}$ izanik. Udan, higadura handiko ekaitz-gertaerak sedimentuen mobilizazio handia eragin zuten fosforo-desorzio bat eraginez erreka ubidean, fosfato-kontzentrazioa areagotuz. Bi arroetan PO_4^{3-} -P-ren urteko esportatutako kargaren banaketak, NO_3^- -N esportatutako kargaren antzeko patroiak jarraitu zituen, urtaro hezean esportazio handiagoak izanik. Ikerketa honek ezaugarri mediterraneoak dituzten nekazaritza-sistema konplexuetan nutrienteen dinamikan eta kontrol-faktoreetan ezagutza areagotu dela nabarmentzen du. Bereziki, nabarmentzekoa da N dinamikan faktore kontrolatzaile espezifikoek duten garrantzia, hala nola landarediaren presentzia edo lurrazpiko drainatze artifiziala, sareko lehorreko arro zerealistetan.

Azkenik, 6. kapituluan, AnnAGNPS modeloak Latxaga eta La Tejería arroetan disolbatutako N-a simulatzeko duen gaitasuna ebaluatzen da, faktore kontrolatzaile nagusien eragina kuantifikatzeko helburuarekin, hala nola landarediaren presentzia (espontaneo eta urbazterrekoa) eta lurrazpiko drainatze artifiziala. Gainera, simulazio batzuk bideratu ziren faktore hauek kontrolatutako egoera desberdinak behatzeko. Modeloa ebaluatzeko, ur isurketa kalibratu da, eta arroaren irteera puntuan disolbatutako N karga esportatua kalibratu eta testatu da, alderantzizko kalibratio-metodoa erabiliz. Metodo horrek hiru urrats ditu: (a) *bilaketa globala*, aldagai sentikorrenen balizko tartearen analisisa egiten duena; (b) *tokiko finketa*, parametro sentikorrenen kopurua eta/edo parametro horien balio-tartea murrizten den prozesua; eta (c) *modeloaren doikuntza*, simulazio optimoa lortzen den prozesua. Ur isurketaren kalibratioan hautemandako aldagai sentikorrenak kurba zenbakiaren balioak izan ziren, aldi hezeetan eta lurzoruan arrailak agertzen diren aldietan.

Disolbatutako N karga espezifikorearen kalibrazioan hautemandako aldagai sentikorrenak laborearen produktibitatea eta deskonposizio-koefizientea izan ziren. Ur isurketaren kalibrazioaren emaitzak Latxagan eta La Tejerían $NSE = 0,72$ eta $NSE = 0,76$ izan ziren, hurrenez hurren, eta disolbatutako N-aren kalibrazioaren eta doikuntza-testatuaren emaitzak $NSE = 0,52$ eta $NSE = 0,45$ izan ziren Latxagan eta $NSE = 0,72$ eta $NSE = 0,51$ La Tejerían. Muga batzuk ikusi diren arren, modeloaren doikuntzak emaitza onak erakutsi zituen, literatura zientifikoa emandako limiteen arabera. Disolbatutako N dinamikak kontrolatzen dituzten faktoreak kuantifikatzeko burutu ziren simulazioetan ikusi zenez, Latxagan landaredia duten eremuak laborantza-lurrekin ordezkaturik gero, esportatutako N disolbatuaren karga % 11,9-an handituko litzateke. Bestalde, La Tejerían lurrazpiko drainatze artifiziala kenduz gero, esportatutako N disolbatuaren karga % 12,4-an murriztuko litzateke. Nekazaritza-erabilera aukera desberdinak dituzten simulatutako egoerei dagokienez, Latxagan landarediaren azalera %12tik %25era igotzeak, disolbatutako N-aren esportatutako kargaren %15,8-ko murrizketa suposatuko zuen. Bestalde, arroetan dauden landaredi eremuak lurrazpiko drainatze artifizialak dituzten laborantza-zonengatik ordezkaturik gero (ekoizpen-gaitasuna hobetzeko), disolbatutako N karga esportatua % 19,2-an handituko zen. La Tejerían, lurrazpiko drainatze artifizialak dituzten landatutako eremuen %16tik %37rako handipena ez litzuke desberdintasun adierazgarriarik ekarriko N disolbatuaren esportazioan. Hala ere, lurrazpiko drainatze artifizialak dituzten eremuak landaretza duten zonekin ordezkaturik gero, arroaren irteera puntuan disolbatutako N karga esportatua %26-an murriztuko litzateke.

Contents

Chapter 1: Introduction and Objectives

1.1 INTRODUCTION AND OBJECTIVES	12
---------------------------------------	----

Chapter 2: Materials and Methods

2.1. DESCRIPTION OF AGRICULTURAL WATERSHED NETWORK OF THE GOVERNMENT OF NAVARRE.	27
2.1.1. Latxaga experimental watershed	28
2.1.2. La Tejería experimental watershed.....	31
2.1.3. Oskotz experimental watershed.....	33
2.1.4. Landazuría experimental watershed	35
2.2. SAMPLING, DATA COLLECTION, AND DATA ANALYSIS AT EACH WATERSHED	38
2.2.1. Load computation	40
2.3. AnnAGNPS MODEL	42
2.3.1. AnnAGNPS input data	44
2.3.2. Simulated processes with AnnAGNPS.....	47
2.3.2.1. Surface runoff.....	47
2.3.2.2. N cycle in AnnAGNPS	50
2.4. HIGH COMPUTING PERFORMANCE (HPC).....	58

Chapter 3: Total Dissolved Solids dynamics from the Navarrese agricultural watershed network: A 10-year study

3.1. INTRODUCTION	62
3.2. METHODS	65
3.2.1. Experimental watersheds and data collection and analysis	65
3.3. RESULTS	67
3.3.1. Precipitation and discharge.....	67
3.3.2. Dynamics in dissolved solids and suspended sediment concentration.....	68
3.3.3. Dynamics in the exported loads of TDS and SS	72
3.3.4. Estimation of annual TDS and SS yield during the hydrological years 2007-2016... 75	
3.4. DISCUSSION	77
3.4.1. Total dissolved solids concentration and loads	77

3.4.2.	Total Dissolved solids in small watersheds	78
3.4.3.	Total dissolved solids yield in small watersheds	79
3.4.4.	Contribution of total dissolved solids to total loads.....	80
3.5.	CONCLUSIONS.....	82

Chapter 4: Evaluation of an Overland Flow Connectivity index at two Mediterranean agricultural watersheds

4.1.	INTRODUCTION	84
4.2.	METHODS	87
4.2.1.	Experimental watersheds of the study	87
4.2.2.	Overland Flow Connectivity index.....	87
4.2.2.1.	OFC index modifications	89
4.2.3.	Data acquisition and processing	90
4.2.4.	Proposal of an OFC index for the conditions of the Navarrese watersheds	91
4.3.	RESULTS AND DISCUSSION	96
4.3.1.	OFC index computation.....	96
4.4.	CONCLUSIONS.....	100

Chapter 5: Assessment of the main factors affecting the dynamic of nutrients in two rainfed cereal watersheds

5.1.	INTRODUCTION	102
5.2.	METHODS	106
5.2.1.	Experimental watersheds and data collection and analysis	106
5.3.	RESULTS	107
5.3.1.	Rainfall and runoff distribution	107
5.3.2.	Nutrient concentration trends at both watersheds.....	108
5.3.3.	Nutrient yields at both watersheds.....	111
5.4.	DISCUSSION	114
5.4.1.	Hydrology patterns at both watersheds	114
5.4.2.	NO ₃ ⁻ dynamics in response to storm events.....	114
5.4.3.	Seasonal NO ₃ ⁻ dynamics	115
5.4.4.	Interannual NO ₃ ⁻ dynamics.....	116
5.4.5.	PO ₄ ³⁻ concentration dynamics	117

5.4.6.	PO ₄ ³⁻ -P yield.....	117
5.4.7.	Nutrient export controlling factors	118
5.4.8.	Comparison with other studies	122
5.5.	CONCLUSIONS.....	123

Chapter 6: On the modeling of two agricultural Mediterranean watersheds to quantify the critical factors affecting dissolved nitrogen exports

6.1.	INTRODUCTION	125
6.2.	METHODS	127
6.2.1.	Experimental watersheds and data collection and analysis	127
6.2.2.	AnnAGNPS model	128
6.2.3.	AnnAGNPS model inputs	128
6.2.4.	Processing of observed data	129
6.2.5.	Runoff calibration.....	130
6.2.5.1.	Global search.....	132
6.2.5.2.	Local Refinement	133
6.2.5.3.	Final runoff calibration.....	134
6.2.6.	Dissolved nitrogen calibration and testing	134
6.2.6.1.	Global search.....	135
6.2.6.2.	Local Refinement	137
6.2.6.3.	Final dissolved N calibration and testing.....	138
6.2.7.	Scenario simulations for controlling factors of dissolved N exports.....	138
6.2.7.1.	Quantification scenarios of dissolved N export by tile drainage and vegetation at La Tejería and Latxaga, respectively.....	138
6.2.7.2.	Scenarios for determining the effect of different tile drainage and spontaneous vegetation management in both watersheds.....	138
6.2.8.	Model Performance Metrics	140
6.3.	RESULTS AND DISCUSSION	141
6.3.1.	Runoff calibration.....	141
6.3.1.1.	Global search.....	141
6.3.1.2.	Local Refinement	143
6.3.1.3.	Model performance	144

6.3.2.	Calibration and testing of dissolved N exports.....	146
6.3.2.1.	Global search.....	146
6.3.2.2.	Local Refinement	147
6.3.2.3.	Model performance and testing.....	148
6.3.3.	Scenario simulations of the controlling factors of dissolved N exports	151
6.3.3.1.	Quantification scenarios of dissolved N export by tile drainage and vegetation at La Tejería and Latxaga, respectively.....	151
6.3.3.2.	Scenarios for determining the effect of different tile drainage and spontaneous vegetation management in both watersheds.	155
6.4.	CONCLUSIONS.....	157
	Conclusions.....	165
	References.....	174
	Annexes	
	ANNEX I: Principal nutrient cycles	188
	ANNEX II: HPC scripts for dissolved nitrogen calibration in the AnnAGNPS model	195
	ANNEX III: Publications in journals and conference proceedings during the doctoral program	202

List of figures

Figure 1.1: Nitrogen balance in the European Union for the period 2012-2015. Source: EEA, 2018.....	16
Figure 1.2: Connectivity index (IC) concept. Source: Borselli et al., 2008.....	18
Figure 1.3: Classification of watershed models. Source: (Novotny, 2009).....	22
Figure 2.1: Digital Elevation Model (DEM) of the watersheds and their location in Navarre. ..	28
Figure 2.2: Maps of the main characteristics of the Latxaga watershed: (a) soil, (b) land use, (c) slope, and (c) elevation.	30
Figure 2.3: Maps of the main characteristics of the La Tejería watershed: (a) soil, (b) land use, (c) slope, and (c) elevation.....	32
Figure 2.4: Maps of the main characteristics of the Oskotz watershed: (a) soil, (b) land use, (c) slope, and (c) elevation.	35
Figure 2.5: Maps of the main characteristics of the Landazuria watershed: (a) soil, (b) land use, (c) slope, and (c) elevation.....	37
Figure 2.6: (A) V-notch weir, (B) H-type flume, and (C.1; C.2) ISCO sampler at the watershed network.	39
Figure 2.7: Determination of the cells and network of channel reaches at La Tejería watershed through TOPAGNPS. (a) Land use map and (b) soil map (Casalí et al., 2008) incorporated in TOPAGNPS creating cells through GIS tools. Example of cells and reaches setup, depicting (c) first-order reaches and (d) higher-order reaches. The legend shows the rotation of land use for each cell, in chronological order during 10 years: "c" cereal, "b" bare soil, "g" sunflower, and "h" broad beans.	43
Figure 2.8: AnnAGNPS topographical processing and input data.	45
Figure 2.9: AnnAGNPS types of inputs: required, required if referenced, and optional. Source: Bingner et al., 2018.....	47
Figure 2.10: Hydrological processes simulated by AnnAGNPS.....	48
Figure 2.11: N-cycle processes, parameters, and pools involved in AnnAGNPS simulations. ..	50
Figure 2.12: Computational procedure of the calibration process with HPC. Please refer to Annex II for detailed scripts.	60
Figure 3.1: Land uses in Navarre (Spain) [Source: CORINE Land Cover 2012, standard legend] and experimental watersheds (black crosses in Navarre map) monitored by the Government of Navarre. In each watershed (orthophotos taken in summer 2017), the hydrological station (blue triangle) and meteorological station (white square) are depicted. In Landazuria, the meteorological station is 5 km south from the watershed. Note that both Oskotz Principal and Forested watersheds share the same meteorological station.....	65
Figure 3.2: Daily total dissolved solids concentration (TDS) and discharge (Q) in the Navarrese watersheds during the hydrological years 2007-2016.	69

Figure 3.3: Relationship (double-logarithmic scale) between discharge (Q) and the concentration of total dissolved solids (TDS) in the Navarrese watersheds. The degree of correlation ($p < 0.05$) between variables is indicated by the Spearman's ρ (Helsel and Hirsch, 2002).	71
Figure 3.4: Median and 95 th percentile of the daily discharge (Q) and total dissolved solids load (TDSL) in the Navarrese watersheds.	73
Figure 3.5: Accumulated discharge (Q), total dissolved solids loads (TDSL) and suspended sediment loads (SSL) <i>versus</i> accumulated time in the Navarrese watersheds.	74
Figure 4.1: Location of the Latxaga and La Tejería watersheds, two experimental agricultural watersheds of the Government of Navarre.	87
Figure 4.2: Flow connectivity index approach proposed in Borselli et al. (2008).	88
Figure 4.3: Soils distribution at La Tejería and Latxaga, and the AIC index proposed by López Vicente and Ben Salem (2019) with non-realistic OFC areas similar to soil cartographic units. 93	93
Figure 4.4: OFC variability in different land uses with the Aggregated Connectivity Index (AIC) proposed by López-Vicente and Ben Salem (2019).	93
Figure 4.5: Semiquantitative results of the OFC index at (A) La Tejería and (B) Latxaga.	96
Figure 4.6: The highest and lowest 10% OFC values (percentile 10, percentile 90) at (A) La Tejería and (B) Latxaga.	97
Figure 4.7: Distribution of OFC values in different land uses with the proposed OFC index in Navarrese watersheds.	98
Figure 5.1: Location of the Latxaga and La Tejería watersheds, two experimental agricultural watersheds of the Government of Navarre.	106
Figure 5.2: Annual (A) and monthly (B) distribution of rainfall, runoff, and median nitrate concentration with 25 th and 75 th percentiles at Latxaga and La Tejería.	107
Fig. 5.3: Rainfall, discharge, and nitrate concentration distribution in a typical hydrological year (2015) at Latxaga (A) and La Tejería (B)	109
Figure 5.4: LOESS smoothing method nitrate results for the Latxaga and La Tejería watersheds	109
Figure 5.5: Nitrate concentration, chloride concentration, and nitrate/chloride ratio at the Latxaga (A) and La Tejería (B) watersheds.	110
Figure 5.6: Annual (A) and monthly (B) distribution of rainfall, discharge, and median phosphate concentration with 25 th and 75 th percentiles at Latxaga and La Tejería.	111
Figure 5.7: Rainfall, discharge, and phosphate concentration distribution in a typical hydrological year (2015) at Latxaga (A) and La Tejería (B)	111
Figure 5.8: Monthly and monthly accumulated nitrate- N yield (A) and annual nitrate-N yield and runoff (B) at the Latxaga and La Tejería watersheds.	112
Figure 5.9: Monthly and monthly accumulated phosphate-P yield (A), and annual phosphate-P yield and runoff (B) at the Latxaga and La Tejería watersheds.	113

Figure 5.10: Schematics of the main controlling factors of nitrate dynamics	118
Figure 6.1: Location of the Latxaga and La Tejería watersheds, two experimental agricultural watersheds of the Government of Navarre.	127
Figure 6.2: Discharge of total flow and baseflow at La Tejería throughout in six days.....	130
Figure 6.3: Schematics of runoff calibration.	131
Figure 6.4: Monte Carlo Filtering of a critical parameter and new range definition.	134
Figure 6.5: Procedure for dissolved N export calibration and testing.	135
Figure 6.6: Increment of (A) tile drainage cells in simulated scenario at La Tejería, and (B) vegetated cells in simulated scenario at Latxaga.	139
Figure 6.7: Sobol first order index distributions for runoff at Latxaga and La Tejería watersheds.	141
Figure 6.8: Observed and simulated values, and NSE probability for runoff at (a) La Tejería and (b) Latxaga watersheds.	146
Figure 6.9: μ vs σ plot for selected parameters: (a) those parameters located above the black dotted line refer to interactions; (b) the $\mu = -/+2$ SEM lines identify the factors with dominant non-additive/non-linear effects.	147
Figure 6.10: Observed and simulated values of dissolved N Yield calibration at La Tejería and Latxaga watersheds.	150
Figure 6.11: Observed and simulated values of dissolved N Yield testing at La Tejería and Latxaga watersheds.	151
Figure 6.12: Average monthly and annual dissolved N yield for calibrated values and proposed scenarios at La Tejería and Latxaga.....	153
Figure 6.13: Dissolved N yield variations at the watershed outlet (a) La Tejería and (b) Latxaga, for calibrated simulation and proposed scenarios.	154
Figure A.I.1: Principal processes of the N cycle.	189
Figure A.I.2: Principal processes of the P cycle.....	192

List of tables

Table 3.1: Number of samples in which suspended sediment (SS), anions and cations were determined; multi-linear regression coefficient of determination (R^2) and Dissolved Solids (TDS) equation for each watershed (all constituents in mg L^{-1}).....	66
Table 3.2: Precipitation values (mm) in each watershed, range of standardized values for the hydrological years (Oct-Sep) 2007-2016.....	67
Table 3.3: Selected statistics of daily average discharge (Q , L s^{-1}) and dissolved solids (TDS, mg L^{-1}) concentration in the studied watersheds for the hydrological years (Oct-Sep) 2007-2016.	68
Table 3.4: Results from different methods for load estimations for total dissolved solids yields. All values in $\text{Mg ha}^{-1} \text{ year}^{-1}$	75
Table 3.5: Runoff (mm), suspended sediment yield (SSY, Mg ha^{-1}) and dissolved solids yield (TDSY, Mg ha^{-1}) for the studied watersheds during the hydrological years 2007-2016. Presented yields were computed by numerical integration method.	76
Table 4.1: Selected weighing factors for different lands.	95
Table 5.1: Parametric and non-parametric statistics of nitrate and phosphate concentration at the Latxaga and La Tejería watersheds in the 2007-2016 period.	108
Table 5.2: Yield estimations of nitrate-N and phosphate-P at Latxaga and La Tejería, with the methods described in Meals et al. (2013)	113
Table 6.1: Curve number and soil hydrological parameters (each soil hydrologic group corresponds to a different parameter).	133
Table 6.2: Parameters that influence the N cycle in AnnAGNPS, processes in which they are involved, and the distribution used in the defined ranges, based on scientific literature. In the case of clay, the variation range comprised the textural class of the horizon to be analyzed in each case, and reported in the soil map developed by the Government of Navarra (e.g. for a silty-clay horizon, the range analyzed was 40-60% clay content).	136
Table 6.3: Sobol first and total order indices, and interactions of runoff parameters for runoff at La Tejería and Latxaga watersheds.....	143
Table 6.4: p-value between non-satisfactory and satisfactory results for each parameter, and first and refined ranges for runoff.	144
Table 6.5: Optimal model fit variables and model performance metrics for runoff at Latxaga and La Tejería.	145
Table 6.6: Range of selected critical parameters.	148
Table 6.7: Optimal combination factors for model performance, and model performance metrics at La Tejería and Latxaga watersheds.....	148
Table 6.8: Annual averages of dissolved N for calibrated values and proposed quantification scenarios.....	152

Table 6.9: Annual averages of dissolved N for calibrated values and proposed scenarios for determining the effect of different tile drainage and spontaneous vegetation management at both watersheds..... 156

CHAPTER 1

Introduction and Objectives

Agriculture has been constantly evolving to supply the food demand required by the growing world population. The limited surface area for its development, in the face of global population increase, forces agriculture to seek constant innovation to overcome this challenge. The development of agriculture, to enhance productivity to ensure food security, has resulted in a significant intensification of agrarian activities, implying an increase in the use of heavy machinery and the application of chemicals (fertilizers, pesticides, etc.). The utilization of different chemicals and machinery can lead to a significant deterioration of the environment.

Among the several effects of agriculture, the increase in total dissolved solids (TDS) can be highlighted due to its negative consequences. Elevated contents of dissolved solids in water bodies can cause the salinization of downstream waters, loss of water for human consumption due to its poor quality, and deterioration of aquatic ecosystems, among other issues.

Regarding the ecological effects caused by TDS, many are associated with a significant impairment of the ecosystem (Hart et al., 1991, 2003; Nielsen and Hillman, 2000; Clunie et al., 2002). For instance, an increase in salinity leads to a decrease in microalgae diversity such as diatoms (Hart et al., 2003) and implies significant adverse effects on microbial biomass (Egamberdieva et al., 2010). In environments with rising salinity, a significant loss of vigor has been observed in aquatic plants such as macrophytes, with lethal levels above the threshold of 1000-2000 mg l⁻¹ (Haller et al., 1974). Riparian vegetation can also be sensitive to increased salinity, with effects such as reduced presence and vigor, and a decline in its sink effect for pollutants (e.g. nutrient, sediments). Besides plants and microorganisms, animal species such as invertebrates or fish are also affected by high salinity levels. Invertebrates are much more sensitive to changes in salinity, with adverse effects verified on some species with mild increases in TDS concentration (Hart et al., 1991, 2003). However, TDS has an important effect on fish growth, producing alterations in their osmoregulation (Bœuf and Payan, 2001). Even though some fish can live in highly saline waters, the survival of their eggs and larvae is negatively affected (Nielsen et al., 2003).

In addition to the direct effects that TDS can produce on the ecosystem, salts can also cause indirect impacts on the environment, with detrimental effects. An increase in soil sodicity due to high levels of TDS can cause a significant dispersion of soil clays (Fitzpatrick et al., 1994; Oster and

Shainberg, 2001), leading to erosion processes and increasing the sediment load in water bodies, which is also a pollutant vector with physical and chemical impacts (Merrington et al., 2002).

Concerning the anthropogenic activities that increase TDS in soils and water bodies, numerous negative environmental impacts have been reported. For instance, the salt used to de-ice roads can lead to an increase of TDS, with a significant contribution to the salinization of water bodies in different world regions (Godwin et al., 2003; Daley et al., 2009). In addition, wastewater effluents generate an important share of TDS. But one of the most widespread activities that is closely related to TDS dynamics is agriculture (Mastrocicco et al., 2009; Anning and Flynn, 2014). Among the problems that TDS can cause in agricultural systems, several studies have shown problems associated with crop growth, such as in winter cereal (Childs and Hanks, 1975; Wiegand et al., 1996). Moreover, an excessive use of fertilizers can cause a significant increase in TDS, which has a significant impact on the ecosystem, primarily in irrigated agriculture (Mastrocicco et al., 2009; Wang et al., 2015).

The use of synthetic fertilizers has increased to satisfy crop necessities and obtain the required productivity. Although the fertilizers used in agriculture can be very different in nature, the most used compounds are based on nitrogen and phosphorus nutrients. Nitrogen (N) is the leading nutrient employed in fertilizers, being the most important to increase crop vigor (Guan et al., 2019; Aranguren et al., 2020). An excess of N applications on agricultural lands can cause nitrogen losses by leaching, primarily in the highly mobile nitrate-N form. Nitrogen is one of the most critical nutrient regarding the impairment of water quality, due to its widespread use and application, along with its consequences on the environment and human health. Mobile nitrate-N form is considered the main reason of eutrophication, and a well-known trigger for its emergence (Durand et al., 2011; Zhou et al., 2017). Eutrophication is a serious problem in aquatic systems, which could lead to the generation of algal blooms. In addition, other consequences of eutrophication include deoxygenation of water, fish mortality, production of hazardous toxins, and changes in the aquatic food chain, which raise concerns and produce a significant impairment to freshwater ecosystems (Merrington et al., 2002), implying in a serious threat to ecosystem sustainability. Human health is also threatened by the presence of nitrate-N in water. The ingestion of high levels of nitrates has been reported as a cause of diverse diseases such as methemoglobinemia - generated by the increase of methemoglobin in the blood, which is known in infants as the blue baby syndrome - and gastric cancer, among other illnesses (World Health Organization, 2011). The global concern

generated by high nitrate contents in freshwater has forced governments and institutions to implement different regulations worldwide, focusing on the control of nitrate concentration in water. In Europe, the EU Nitrates Directive (91/676/CEE) established the nitrate concentration threshold in groundwater at $50 \text{ mg NO}_3^- \text{ L}^{-1}$. In the USA, the Safe Drinking Water Act (1974, with subsequent amendments in 1986 and 1996) regulates the amounts and concentrations of different pollutants in water, and establishes a threshold of $10 \text{ mg N-NO}_3^- \text{ L}^{-1}$ (ca. $44 \text{ mg NO}_3^- \text{ L}^{-1}$) for nitrate concentration in drinking water.

Regarding phosphorous (P), its application in agricultural systems has also increased with productivity necessities. P is one of the most used nutrients in fertilizers and is considered a trigger factor for the emergence of eutrophication in freshwater ecosystems (Daniel et al., 1998). A P increase of 0.01 mg L^{-1} can be significant and enough to transform oligotrophic inland waters into eutrophic (Merrington et al., 2002). Nevertheless, P is not as available as other nutrients. The availability of the most common soluble form of P, phosphate-P, depends on the pH, which becomes crucial in the presence of reactive P in freshwater ecosystems. Unlike N, the soluble form of P is not its most frequent form and is highly dependent on soil conditions. Therefore, a detailed study of soil characteristics is necessary for a correct evaluation of phosphorus leaching (Djodjic et al., 2004).

As previously mentioned, the increased application of nutrients has had significant consequences on the water quality of different streams and rivers. Regarding the situation of large rivers across the world, the upward trend in nutrient content is evident. In North America, an increasing concentration of N in the Mississippi river has led to an average nitrate yield export rate 2-3 times higher in the 1980s-1990s than reported in the 1950s-1960s, reaching a maximum of $1,800 \text{ T N yr}^{-1}$ in 1993, almost an order of magnitude greater than recorded in 1963, at ca. 192 T N yr^{-1} (USEPA, 2015). Even though the 2000s and 2010s have not seen such high N export peaks, the export trend in recent decades remains similar to that observed in the 1980s-1990s, much higher than in the 1950s (USEPA, 2015). In Asia, the Yangtze river doubled its N concentration from the 1960s to the late 1980s (Jingsheng et al., 2000). The N concentration of some samples taken in the summer was approximately 3 times higher than the threshold marked by the Nitrates Directive in Europe. The nutrient concentration in the Nile river in Africa has increased since the 1990s, with high concentrations reported for ammonia, nitrite, nitrate, and phosphate, among other components (e.g., Badr et al., 2013). The Amazon basin, the largest basin in the world, has experienced

significant changes in recent years. By 2012, 20% of the Brazilian Amazon forest has been cleared for the implementation of agricultural activities – and this percentage has increased over the years (Bustamante et al., 2015). This deforestation produces important biogeochemical and hydrological changes (Neill et al., 2006), increasing the input of fertilizers in the basin. This is a major concern for the quality of water in the area, where the major output of N is riverine (Bustamante et al., 2015).

The effect of nutrients on water quality has raised important concerns around the world. Regarding Europe, as displayed in Fig. 1.1, the N balance (an estimate of the potential surplus or deficit of nitrogen in agricultural lands) is positive for all countries, with an average N loss of $50.1 \text{ kg N ha}^{-1}$. The situation is alarming, particularly in Western Europe and in some Mediterranean countries (EEA, 2018). Several countries have already taken measures to know, quantify and understand the effects of agricultural nutrients on water bodies. A large part of countries belonging to the European Union has implemented an experimental watershed network (Deelstra et al., 2014; Fučík et al., 2017), focusing efforts on the detection and assessment of the effects of agriculture on water quality. This type of watershed study enables the evaluation of different processes under real conditions, from a systemic perspective, establishing relationships and their influence on the different factors involved (García-Ruiz and López-Bermúdez, 2009). There are several examples of these watershed study networks around the continent: in Baltic countries, monitored watersheds provide water quality information, as reported in Latvia (Lagzdins et al., 2012), Sweden (Kyllmar et al., 2014), Estonia (Iital et al., 2014) and Lithuania (Povilaitis et al., 2014). Other European areas, such as the Mediterranean region and British islands, have also installed different networks to monitor, assess, and study water quality. In the Mediterranean, studies have reported water quality data for rainfed (e.g. Pieri et al., 2011) and irrigated watersheds (Merchán et al., 2015), as irrigation is important to guarantee productivity in arid areas. British examples of watershed monitoring have mainly focused on major nutrients such as N and P (e.g. Hooda et al., 1997; Lloyd et al., 2016; Ockenden et al., 2017).

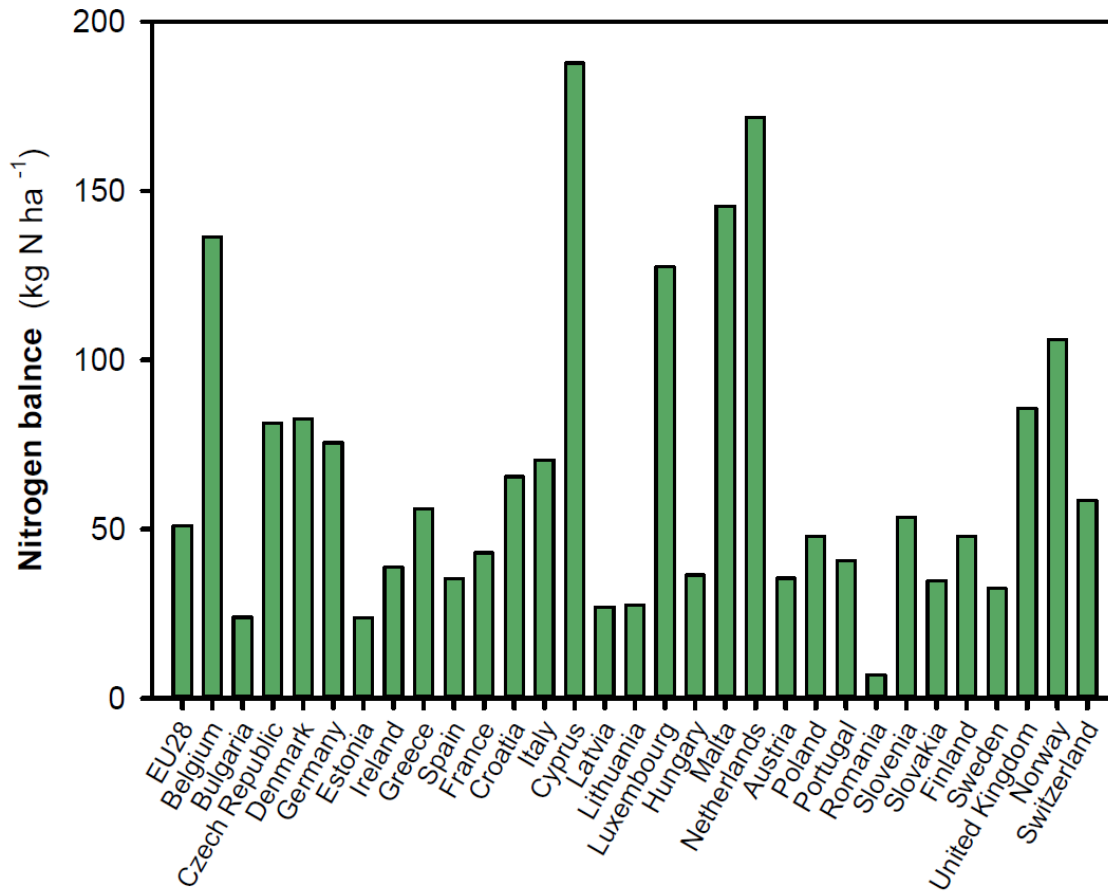


Figure 1.1: Nitrogen balance in the European Union for the period 2012-2015. Source: EEA, 2018

In Navarre, Northern Spain, the consequences of agricultural activity on the environment have raised great concern. The former Department of Agriculture, Livestock, and Food of the Government of Navarre implemented a network of experimental watersheds to provide data for the assessment of the effects of agricultural activities on soil erosion and water quality. These watersheds are located in areas with the most representative agricultural land uses (rainfed winter cereal, forests, grazed pastures, and irrigated land), and under typical management practices of the region.

Several studies have been carried out using the data collected from this network of watersheds. These studies have mainly focused on hydrological and soil erosion characterization (Casalí et al., 2008, 2010), controlling factors of sediment exports (Giménez et al., 2012), and the assessment of the AnnAGNPS model for runoff and sediment yield simulation (Chahor et al., 2014). However, only one study focused on an irrigated watershed (Merchán et al., 2018), although some

information about nutrient dynamics was succinctly introduced by Casalí et al. (2008, 2010). The efforts of the aforementioned studies have mainly concentrated on soil erosion in this territory. Therefore, a complete evaluation of the effects of agriculture on this region requires the study of TDS, and especially of the effects of nutrients, to further expand the knowledge base.

In recent decades, the strategy most employed to identify agricultural effects on the environment has been mainly based on gauged watershed networks. The analysis at the watershed scale offers the possibility of studying soil erosion, dissolved solids dynamics, and particle transport under real conditions from a systemic perspective. This type of study helps relate and prioritize the influence of the different factors involved in the hydrological cycle, along with transportation of dissolved solids and production of sediments, also incorporating the effects of changes in land use (García-Ruiz and López-Bermúdez, 2009). Nevertheless, the watershed approach has its limitations, particularly in larger ones (i.e., Likens, 2001). Traditionally, watersheds have been described using the “black-box” approach (Black, 1996). This approach is not sufficiently accurate to understand the future impacts of anthropogenic actions and climatic conditions on the streamflow (Frisbee et al., 2012). Another significant limitation of the watershed approach is the need for long data series, throughout several years under the same land use and management. Several approaches and tools have been developed (modeling, sediment indexes, etc.) to help hydrologists and environmental managers understand the internal processes of watersheds. One of these approaches is the concept of hydrological or flow connectivity, which tries to explain the internal processes occurring in a watershed. Flow connectivity aims to describe the linkages of the different landscape components within a watershed, regarding flow and related substances such as sediments and nutrients. However, the definition of flow connectivity is not well-established: Ali and Roy (2009) reported 11 different connectivity definitions. Among these definitions, the most accepted defines flow connectivity as the connection, via overland and subsurface flow, between the riparian and the upland zones (Vidon and Hill, 2004; Ocampo and Oldham, 2006; Bracken et al., 2013). Bracken and Croke (2007) describe flow connectivity as a concept related to hydrology and geomorphology, divided into three types: (1) landscape connectivity, related to the form of terrain in a watershed, which can favor the movement of materials; (2) hydrological connectivity, related to the movement of water from one part to another; and (3) sedimentological connectivity, related to the physical transfer of sediments and soil-attached pollutants. As Bracken and Croke (2007) reported, the flow connectivity concept can be understood and partially explained by the

integration of five major components in watersheds: (1) climatic conditions, (2) hillslope runoff potential, (3) landscape position, (4) lateral buffering, and (5) delivery pathway. Building upon this concept, Borselli et al. (2008) developed the overlandflow connectivity index (IC) to characterize connectivity in a semi-quantitative form (Fig. 1.2). IC is based on downslope and upslope components, which are obtained by parameters derived from a Digital Elevation Model (DEM) of the analyzed watershed and a weighting factor (which in this case was the C factor of RUSLE). After the implementation of IC in different watersheds, Cavalli et al. (2013) optimized this index by using the surface roughness as a weighting factor and implementing the D-infinite algorithm in the flow direction parameter, which was closer to the environmental reality. López-Vicente and Ben-salem (2019) developed the Aggregated Connectivity Index (AIC), which added other weighting factors to Cavalli's index version, such as soil physical properties, vegetation and crop management and rainfall erosivity – some of which are very interesting for an analysis of the spatial-temporal variation. With AIC, Lopez-Vicente and Ben-salem (2019) obtained a representation of flow connectivity that not only shows the structural connectivity (potential connectivity) of a watershed but also reveals functional connectivity that changes in time and space.

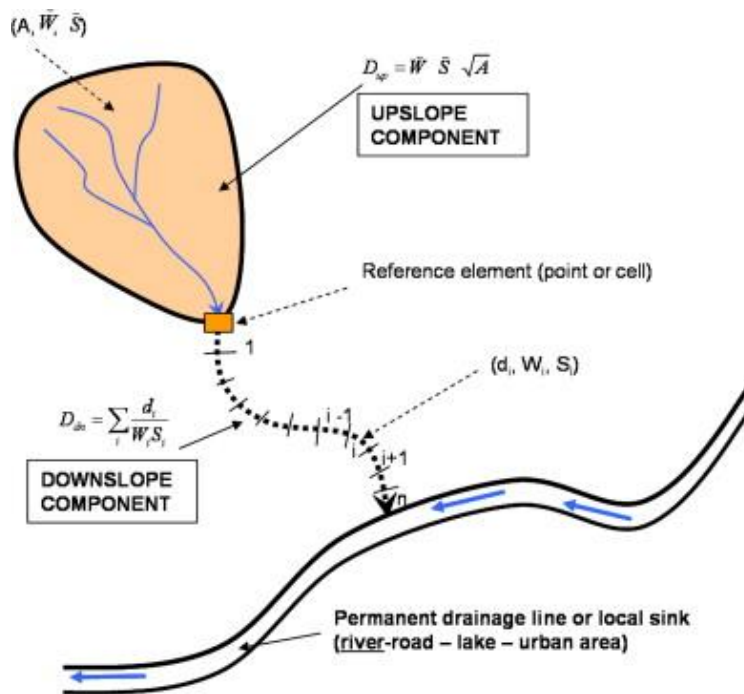


Figure 1.2: Connectivity index (IC) concept. Source: Borselli et al., 2008

Adequate characterization of the processes occurring in a watershed is essential for the correct understanding of these processes. The first step for an adequate assessment of pollutants in an agricultural watershed is the determination of the elements that influence their dynamics and transport. Nutrient controlling factors in a watershed may differ in nature and are divided into intrinsic and anthropogenic elements of the watershed.

Regarding the intrinsic elements that determine pollutant loads, the size and shape of the watershed can be important in the dynamics of nutrient exports. A more circular watershed implies a lower residence time of water in the watershed (Black, 1996). In turn, there is a shorter time available for the degradation of the nutrients in the watershed and thus increases the nutrient loads (Black, 1996; Merrington et al., 2002). Highly sloped areas, particularly near stream channels, also produce a decrease in water residence time and, as a consequence, reduce the nutrient degradation time. These steep-sloped areas can be considered non-productive zones, and are occupied by spontaneous vegetation or riparian vegetation, becoming a nutrient sink (Dosskey et al., 2010; Casal et al., 2019). Soil properties (e.g. texture, bulk density, presence of cracks, etc.) are considered important intrinsic characteristics regarding nutrient dynamics in a watershed (Brady and Weil, 2008; Lehmann and Schroth, 2003). Water infiltration, runoff generation, lateral flow, denitrification processes, and preferential flow, among other factors, are controlled by soil properties and are considered crucial elements in the exports of agricultural pollutants into freshwater ecosystems.

The anthropogenic factors that control nutrient exports are primarily a consequence of the field management adopted by farmers. As previously reported, fertilization is considered a trigger in nutrient exports to streams. An excess of nutrients provided to agricultural fields is frequently the reason for nutrient leaching, which generates several problems in freshwater ecosystems and is the main cause of eutrophication of water bodies (Merrington et al., 2002; Lehmann and Schroth, 2003). Other factors derived from anthropogenic activities have been studied, such as the use of heavy machinery (Miller et al., 2004) and the presence of tile drainage (McIsaac and Hu, 2004; Randall and Goss, 2008), among others, with results indicating significant impacts on the dynamics of nutrient exports.

The detection of controlling factors in exports is not an easy task, and is frequently even more complicated when the interaction between factors is attempted to be quantified. Generally, in

natural ecosystems the interactions between components are not static - this means that the interactions change along with ecosystem factors (Deyle et al., 2016). For instance, a higher fertilization doses can suppose fewer nutrient exports if the presence of spontaneous vegetation increases (Casalí et al., 2008). This variability hinders the assessment of agricultural pollution. The quantification and identification of processes in large extensions of land is not a simple task either. In response to these challenges, the development of watershed models is a considerable advance for a better understanding of environmental processes and the identification of vulnerable areas.

Watershed models are representations of systems or processes involved in a specific area, being essential tools for hydrologists since the 1950s, when the first model was developed: the Stanford Watershed Model (SWM) (Crawford and Burges, 2004). The SWM was a more advanced tool to help understand the trends and dynamics of water resources. In the 1970s, the developers of SWM created the Hydrocamp Simulation Program (HSP), which included the ability to simulate water quality processes, being able to evaluate diffuse pollution loads. Since the 1980s, the increase in computer resources combined with increased knowledge capacity and the development of new technologies have encouraged the emergence of a wide range of models (Novotny, 2008), which represents an opportunity for land management by hydrologists and environmental managers.

Watershed models, as shown in Fig. 1.3, can be classified into different types. Physical models were primarily used in the first steps of modeling, to better understand processes at the watershed scale. These types of models are still used in some laboratories but are more focused on a reduced scale and controlled simulations, with small relevance to natural ecosystems (Novotny, 2008). Physical analog models are rarely used and are primarily focused on groundwater processes. The most frequent watershed models employed nowadays are mathematical, which can include three spheres (atmosphere, lithosphere, hydrosphere).

Within the mathematical models, there are deterministic and indeterministic models. The latter are generally developed from collected data – there can be a high amount of data involved as these models are developed from current and historical information. Indeterministic models have a strong statistical basis, with the outputs generally being probability distributions (not an exact value). If these indeterministic models also consider the randomness of one or more inputs over time, models are considered stochastic. In addition to the strong statistical basis of these models,

in recent decades, the development of artificial intelligence and its application to these models has led to a significant improvement in their optimization.

Deterministic models, also referred to as mechanistic, are developed from a subset of well-known processes (hydrological processes, rainfall-runoff transformation, accumulation of pollutants, vegetation growth, etc.) (Novotny, 2009). These processes are tested through monitoring and then are calibrated and validated with field-collected data. Deterministic models do not consider random variables and produce fixed and reproducible results from a unique input dataset (Novotny, 2009). Generally, deterministic models are composed of five components: inputs or forcing functions, state variables, mathematical equations, parameters, and constants (Jørgensen and Bendricchio, 2001). The output, contrary to what is obtained from indeterministic models, is an exact value. Deterministic models are considered compartmental models and perform mass balance calculations in each interval of time for each compartment, based on well-known process equations. The most usual components in watershed models are hydrological parameters, soil dynamics and its interaction with pollutants, and erosion (Novotny, 2008). Within deterministic models, there are two approaches to model processes: lumped and distributed models. Lumped models consider the watershed, or the subwatersheds inside it, as a homogeneous unit. Owing to the enormous variability of parameters in small areas of the watershed, the characteristics are lumped together for the entire unit. The empirical equations of lumped models simplify the computation between parameters within the homogeneous unit. The simplicity of these models, and the consideration of the watershed unit as a homogeneous and basic unit, implies that the output data of the model is limited only to the data obtained at the outlet, with no information about what happens at intermediate points in the watershed. Regarding distributed models, the computational subunits where the watershed is divided are smaller than those of lumped models. These unit sizes can vary over a wide range and can be smaller than one hectare in some cases. Each unit is homogeneous and receives external and internal inputs from surrounding units. An important advantage of distributed models over lumped models is the possibility to obtain output information in each unit of the watershed. This allows the observation of different output data at different points of the watershed, enabling the spatial discretization of results. These distributed models are very suitable for the simulation of non-point source pollution, as the processes occurring are highly dependent on spatially distributed parameters. Currently, the potential and usefulness of this type of model have been boosted thanks to the development of new technologies,

which include Geographic Information Systems (GIS). GIS facilitates the management of spatial data and remote sensing, providing a higher number of parameters along with their spatial and temporal variation (Gastesi, 2014). In addition to the different types of models based on their spatial distribution, each deterministic model can have a different functional transfer depending on the system's functional response. For instance, if there is a stationary system with low variability, the model becomes stationary - however if the system has important changes in time and functional transfer, the model becomes dynamic (Novotny, 2003).

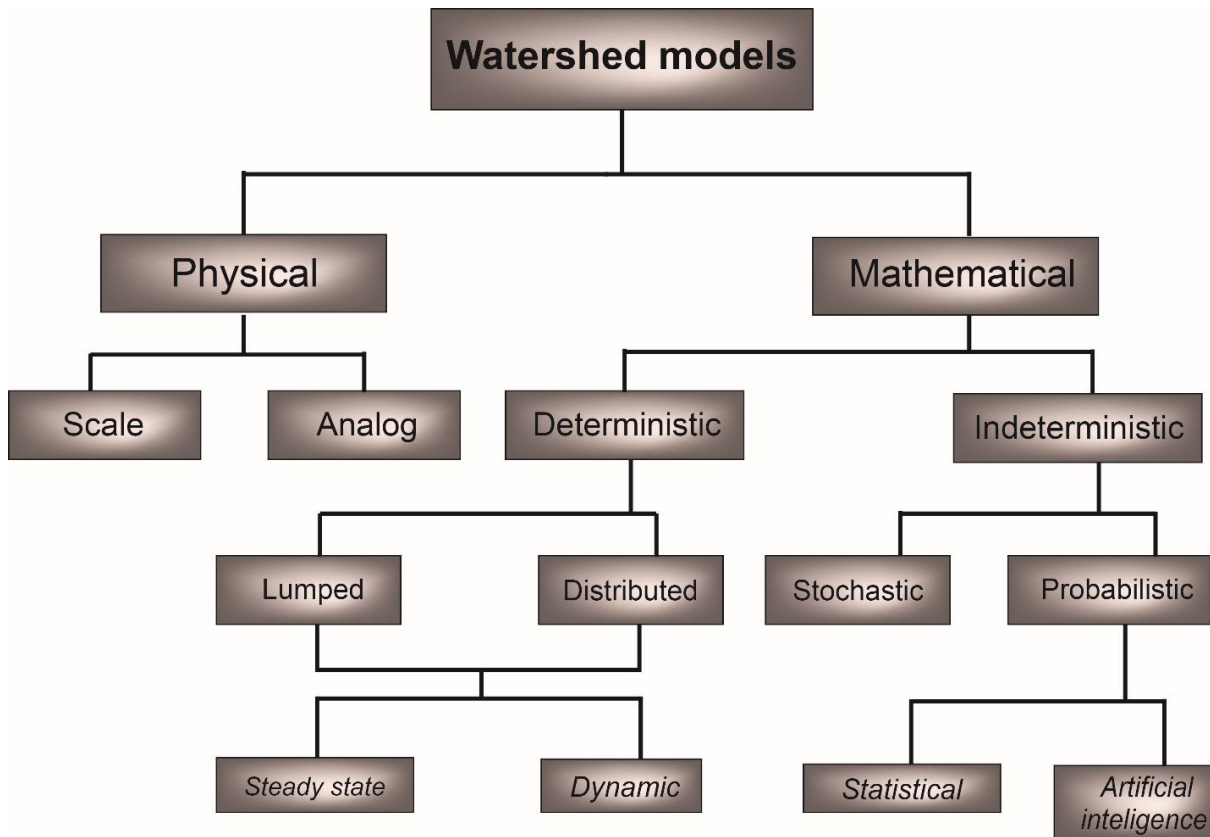


Figure 1.3: Classification of watershed models. Source: (Novotny, 2009)

As reported herein, the emergence of models for hydrological management in watersheds began in the 1950s. Currently, there are several models focused on hydrological resources, many of which simulate hydrological processes and transportation of sediments and chemicals. The Chemicals, Runoff, and Erosion from Agricultural Management System (CREAMS) (Knisel, 1980) is a plot-scale model that simulates runoff, erosion, and chemicals in agricultural soils. The Hydrological Simulation Program for FORTRAN (HSPF) (Johanson et al., 1984) estimates daily runoff and

sediment loads, and long-term amounts of nutrients, pesticides, and other toxics. Still focusing on different model examples, the Agricultural Non-Point Source Pollution model (AGNPS) (Young et al., 1989) is an event-based model that simulates soil erosion and nutrient transports in a watershed. The Soil and Water Assessment Tool (SWAT) (Arnold et al., 1993, 2012) is a watershed-scale model used to simulate surface and groundwater, with the possibility of predicting the environmental impact of land use, land management practices, and climate change. SWAT has been used for the assessment of soil erosion prevention and of non-point source pollution such as nutrients. Over time, many improvements have been made to this model – the most recent version is SWAT+. Regarding models that focus on water quality simulations, the CE-QUAL-W2 (Environmental and Hydraulics Laboratory, 1986) is a water quality and hydrodynamic model for rivers, estuaries, lakes, reservoirs, and watershed systems. This model simulates basic eutrophication processes such as temperature-nutrient-algae-dissolved oxygen-organic matter and sediment relationships. The CE-QUAL-W2 is in continuous development since the late 1970s, with the most recent version being 4.2.2. The Water Quality Analysis Simulation Program (WASP) (Di Toro et al., 1983) also simulates water quality in rivers, lakes, estuaries, coastal wetlands, and reservoirs (Wang et al., 2013). The Environmental Fluid Dynamics Code (EFDC) is a surface water model that simulates hydrodynamic, sediment-contaminant, and eutrophication components in water bodies. This model has been applied to rivers, lakes, reservoirs, wetlands, estuaries, and coastal ocean regions. The MIKE project consists of a compendium of hydrological models that determine different hydrological aspects of different water bodies. Regarding watershed analysis, the physical model MIKE SHE (Danish Hydraulics Institute, 1993) can simulate the processes that occur in surface and groundwater, including also nutrient dynamics. The Better Assessment Science Integrating Point and Nonpoint Sources (BASINS) (USEPA, 2000) is an example of a watershed-centered model based on the HSPF, which focuses primarily on the water quality of watersheds. BASINS is under continuous updating, with the most recent version being BASINS 4.5 (USEPA, 2019). Another model example is the Hydrodynamic, Sediment, and Contaminant Transport Model (HSCTM2D) that simulates 2D surface water flow, sediment, and pollutants in rivers and estuaries (Hayter et al., 1995).

As reported herein, there is a high number of models for the simulation of nutrient content in different systems, and therefore the selection of a suitable model is crucial to achieving the expected results. Bingner et al. (2001) developed a model based on the event model AGNPS, the

Annualized Agricultural Non-Point Source model (AnnAGNPS), which can simulate water, sediment (by particle size class and source of erosion), and chemical dynamics (nitrogen, phosphorus, organic carbon, and pesticides) (Bingner et al., 2018). AnnAGNPS is a mathematical, distributed, and dynamic model, under continuous development, that is based on interactions between components through processes in different unit areas. However, its theoretical simplicity does not lead to poor or bad results, and several studies have presented satisfactory results using AnnAGNPS (Yuan et al., 2011; Chahor et al., 2014; Que et al., 2015). AnnAGNPS can discretize the watershed into smaller size cells that act as small sub-watersheds, enabling a high prediction resolution. This high resolution provides a spatial sectorization of the watershed, identifying the most vulnerable areas in each simulation (Gastesi, 2014). AnnAGNPS is a compartmental model that bases the hydraulic component on the curve number technique, with sediment transport in each cell based on the well-known Revised Universal Soil Loss Equation (RUSLE) (Renard et al., 1997) and the chemical loads based on a mass balance between the three spheres (hydrosphere, atmosphere, and lithosphere). AnnAGNPS is a well-equipped model with validated tools for the simulation of agricultural systems, suitable for different watershed sizes. Furthermore, the cell division of the watershed is an advantage over other simulation models, making AnnAGNPS very adequate for hydrological simulations at small agricultural watersheds. This watershed model has been applied to different locations with satisfactory results in the assessments of nutrient loads. Li et al. (2015) employed AnnAGNPS to simulate water runoff and nutrients in a medium-size watershed in Eastern China, demonstrating an adequate fit of the model for runoff and nitrogen loads. Yuan et al. (2003) assessed nitrogen loads with AnnAGNPS at a small watershed of Mississippi (USA), reporting good results in short-term periods. However, few studies are evaluating the nitrogen component with AnnAGNPS in Mediterranean watersheds – this type of study would be very enriching to evaluate the capability of the model in Mediterranean climates. In Navarre, some previous versions of the AnnAGNPS model have been used to simulate water and sediment components, with good results (Chahor et al., 2014; Gastesi, 2014). Given the characteristics of the AnnAGNPS model and the conditions of the Navarrese region, utilization of this model to evaluate nutrient loads in Navarre is a natural step, and be a useful management tool in the area.

In light of the above, the overarching aim of this work is to characterize, understand, and quantify the dynamics of nutrients and other solutes in the watershed network of the Government of Navarre

and explore the factors that control these dynamics. To this end, the following specific objectives have been proposed:

- To characterize and quantify the exports of total dissolved solids and their dynamics in the watershed network of the Government of Navarre, using the available database;
- To propose an overlandflow connectivity index building upon existing indices, and evaluate this index at two agricultural watersheds with similar characteristics;
- To deepen knowledge on the dynamics of nitrate and phosphate and identify the controlling factors of these nutrients by comparing two watersheds with similar characteristics;
- To evaluate the capacity of the AnnAGNPS model for simulating dissolved nitrogen exports in the watershed network and quantify nutrient controlling factors in different scenarios.

CHAPTER 2:

Materials and Methods

This chapter presents a thorough description of the watersheds that constitute the network of experimental agricultural watersheds implemented by the former Department of Agriculture, Livestock, and Food of the Government of Navarra. The main materials and methods employed throughout this thesis are also reported. In addition, each of the following chapters includes a ‘Methods’ section that describes the specific methods and techniques utilized.

2.1. DESCRIPTION OF AGRICULTURAL WATERSHED NETWORK OF THE GOVERNMENT OF NAVARRE.

As reported previously, the analysis of the pollution caused by agricultural activity is not a trivial task. Environmental concerns have led to the implementation of a watershed network by the former Department of Agriculture, Livestock, and Food of the Government of Navarra. The aim is to gather actual data to assess water quality and soil erosion in this region, located in Northern Spain. These watersheds are located in headwater areas, do not have significant flood plains or groundwater inputs/outputs, and present uniform climate across the watershed area.

The watersheds are located in different areas of Navarra (Fig. 2.1), covering the most representative land uses throughout the Navarrese climatic gradient (Mediterranean in Landazuria, Sub-Mediterranean in Latxaga and La Tejería, and Sub-Atlantic in Oskotz). Regarding land use, Latxaga and La Tejería are rainfed winter cereal watersheds located in the center of the region. Both watersheds have similar climatic conditions and management. Landazuría, situated in the South of Navarra, is an excellent example of irrigated agriculture of the region, with a high proportion of the watershed area under pressurized irrigation. Finally, the Oskotz watershed is the Northernmost watershed of the network, where grazed pasture dominates in the lower regions. In the Northeastern part of Oskotz, forest land use predominates. Due to the importance of the representativeness of this type of land use, a forested sub-watershed was implemented in Northeast Oskotz. The general characteristics of each watershed are described next, and the information on annual productivity, crop management (fertilization, harvest, crop rotation), and climate comprehends the 2007-2016 study period.

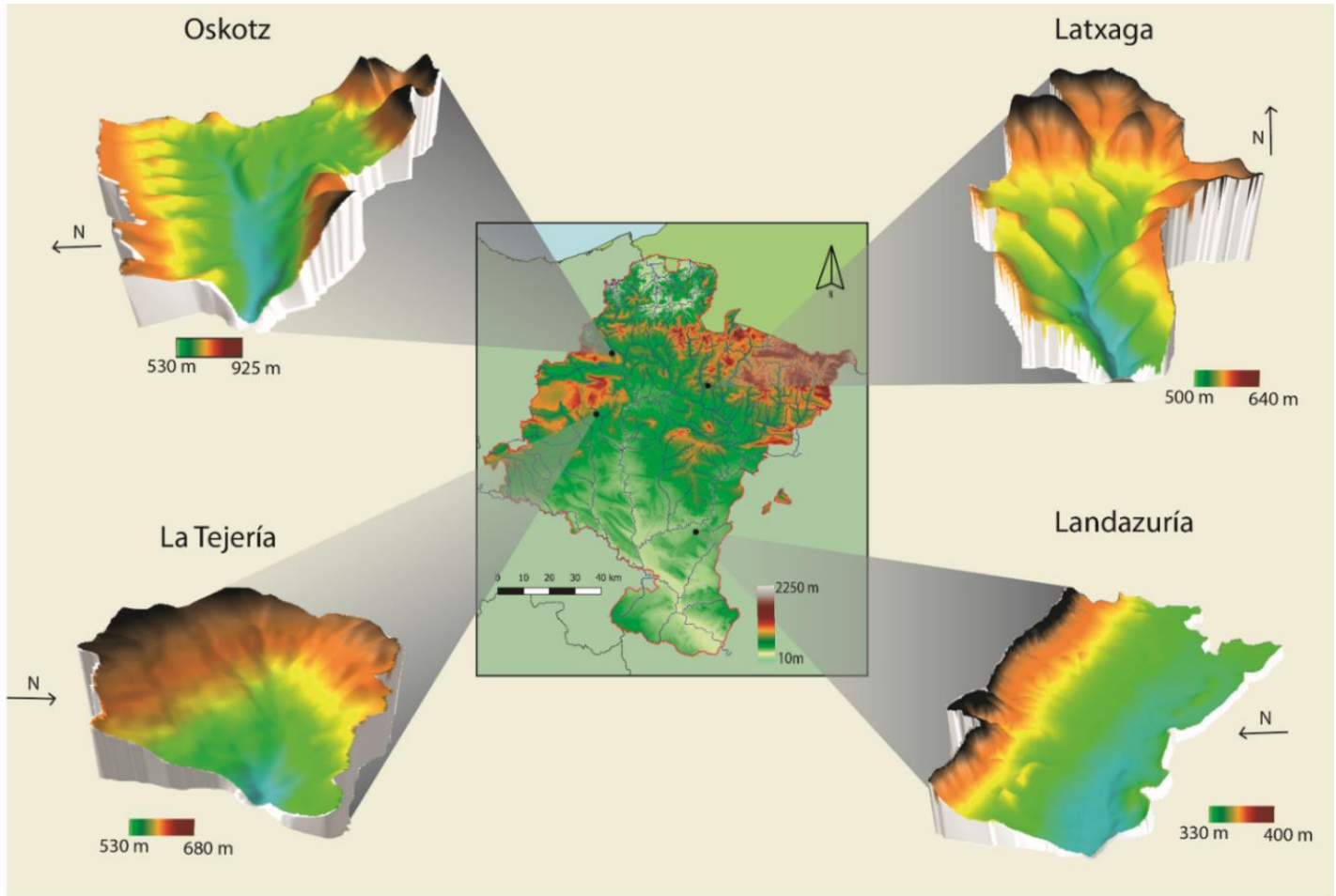


Figure 2.1: Digital Elevation Model (DEM) of the watersheds and their location in Navarre.

2.1.1. Latxaga experimental watershed

The experimental watershed of Latxaga (Fig. 2.1) covers 207 ha. At Latxaga, the average precipitation was ca. 950 ± 285 mm per year with maximum precipitation of $1,665 \text{ mm yr}^{-1}$ in 2013 and a minimum of 600 mm yr^{-1} in 2011. The average annual temperature was $11.8 \text{ }^\circ\text{C}$, with a minimum of $-12.4 \text{ }^\circ\text{C}$ and a maximum of $39.9 \text{ }^\circ\text{C}$ recorded for the study period. Latxaga is located at an altitude range of 502 - 638 m, with an average slope of 17% (Fig. 2.2C, D). The maximum slope reaches 83 %. In the valley, the slopes are generally gentle, under 7%, in opposition to the hillslope, where the slope is around 25 %.

The geology of the watershed includes Tertiary and Quaternary materials. The Tertiary materials of the study area are marls, and to a lesser degree, sandstones and limestones of the Middle Eocene.

Flysch marls predominate, with levels of 50 cm of thickness, alternating with sandstones 1-3 cm thick (Government of Navarre, 1994). Flysch marls are the primary material covering almost the entire watershed, except for the stream bed, where the Quaternary materials predominate. These materials are mainly constituted by valley deposits of silt, gravels, and sands (Government of Navarre, 1994).

Regarding the soil, a detailed map was built with 29 soil observations and pits (Fig. 2.2A) (Government of Navarre, 2005a). There are three predominant soil classes in the watershed. Fluventic Xerorthent is located frequently in valleys and accumulation hillslopes with gentle slopes (Soil Survey Staff, 2014). This soil class was considered the deeper class, with the upper horizon being silty-clay-loam in texture. In the eroded hillslopes, the most frequent soil classes are Typic Xerorthent and Paralithic Xerorthent (Soil Survey Staff, 2014). Typic Xerorthent is considered a deep soil, with the upper horizon being silty-clay-loam in texture. Most Typic Xerorthent at the watershed is located in cultivated areas, with an average slope of ca. 20%. Paralithic Xerorthent is a shallow soil, under 50 cm depth, generally occupied by non-cultivated lands with an average slope of 20.5%. In their upper horizons, the texture of Paralithic Xerorthent is silty-clay-loamy.

Cultivated area covered ca. 85% (175 ha), where the prevailing crop was winter rainfed cereal. Natural non-cultivated regions were also observed, occupying ca. 11% of the area. These areas present shallow soils, pronounced slopes, or riparian vegetation, which limit cultivation. The natural vegetation consisted mainly of herbaceous plants and Mediterranean shrubs. Riparian vegetation includes *Salix alba*, *Populus nigra*, and *Fraxinus angustifolia* tree species (Government of Navarre, 2005a), occupying a continuum in the streambanks. Multiple herbaceous and shrubs species appeared around the channel, where *Buxus sempervirens*, *Rosa Sp.*, *Rubus ulmifolius*, and *Cornus Sanguinea* predominate (Government of Navarre, 2005a). The significant development of riparian vegetation at Latxaga must be emphasized, with a width ranging from 2 m to 5 m, generating a canopy in the channel. This vegetation has considerable density and diversity in comparison with other agrosystems in the region. The remaining 4% of the watershed is covered by rural roads and small constructions (Fig. 2.2B).

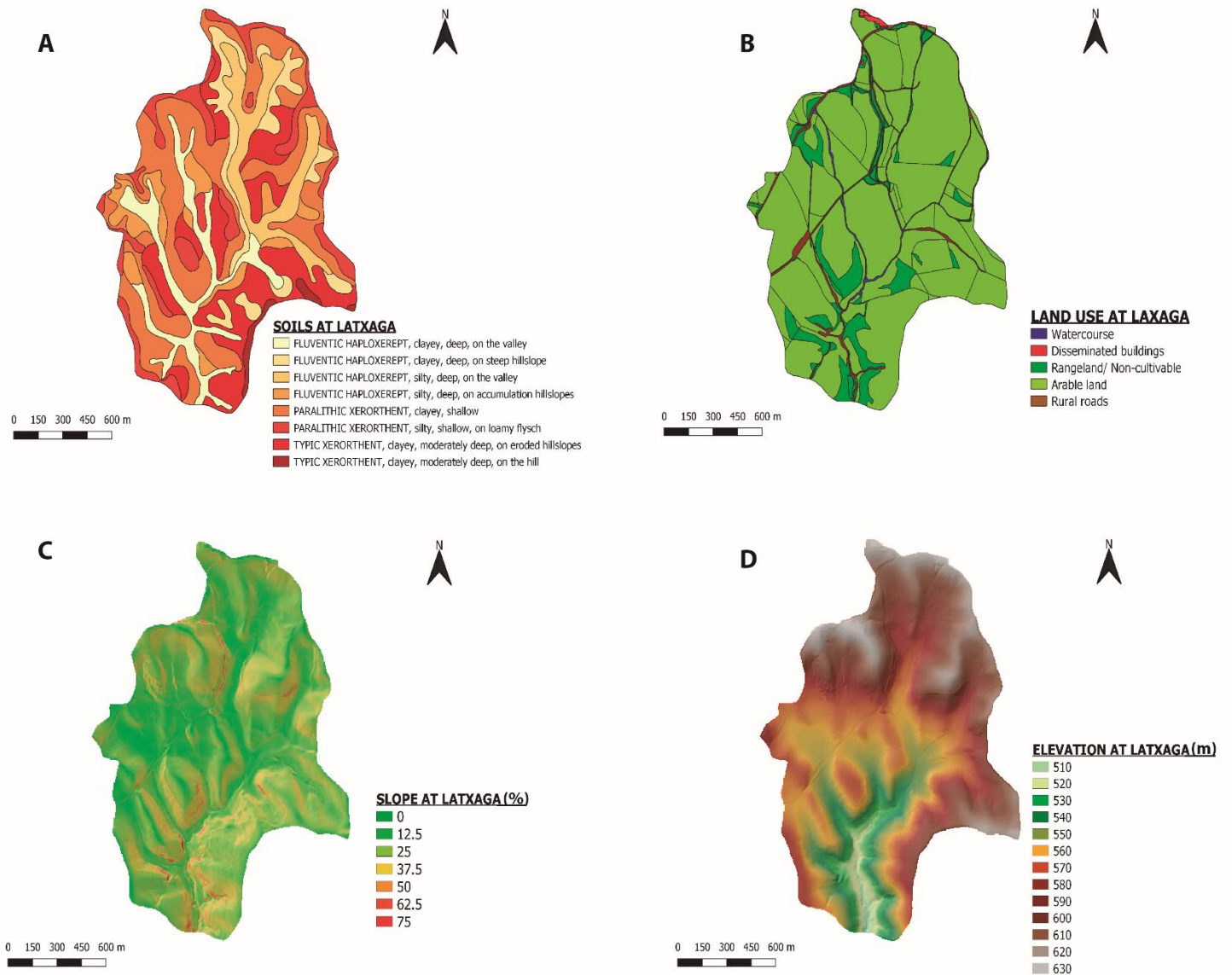


Figure 2.2: Maps of the main characteristics of the Latxaga watershed: (a) soil, (b) land use, (c) slope, and (c) elevation.

According to local institutions, the fertilization rate recommended for the cereal crops at Latxaga was 190 kg N ha^{-1} , considering the typical regional management of the watershed (INTIA, 2018). Fertilization was divided into two stages, with applications approximately in January and March (Casalí et al., 2008). The first application employed slow-release fertilizers at the tillering initiation stage. The second application depended on the crop requirements at the specific year and could utilize quick-release fertilizers, or follow the first application and use slow-release fertilizers such

as urea. Every two or three years, phosphorous (diammonium phosphate) was applied at the sowing stage (Casalí et al., 2008).

During the study period, the productivity of the watershed, considering the production of the study area as representative of the region, was ca. 5,000 kg ha⁻¹ for rainfed wheat and ca. 4,750 kg ha⁻¹ for barley (Government of Navarre, 2020).

2.1.2. La Tejería experimental watershed

The experimental watershed of La Tejería covers 169 ha and is located in the central West of Navarre (Fig. 2.1). Regarding meteorological data, the average precipitation at the watershed was 793±216 mm per year, with maximum and minimum precipitations of 1,324 mm yr⁻¹ in 2013 and 531 mm yr⁻¹ in 2012, respectively. In the study period, the average annual temperature was 12.3 °C, with a minimum of -10.7 °C and a maximum of 42.3 °C. The average altitude ranged between 530 m and 680 m, with an average slope of 15.5% (Fig. 2.3C, D). The steepest slopes can be as high as ca. 50%

The geology of the watershed, as at Latxaga, includes Tertiary and Quaternary materials. The predominant Tertiary materials at the watershed are yellow silts and clays with occasional alternation of sandstones of the Middle Miocene (Government of Navarre, 1996). The Quaternary materials are located in the bed channel and also at the Northwestern side of the watershed. The bed channel is composed of valley deposits of silt, gravel, and sands. The Quaternary materials of the hillslope consist of a mixture of colluvial fragments from upper sites in a silty-clay matrix (Government of Navarre, 1996).

A detailed soil map was also developed for La Tejería watershed (Government of Navarre, 2005b), with three predominant soil classes. Like Latxaga, at la Tejería the most frequent soil in the valley is also Fluventic Xerorthent (Soil Survey Staff, 2014). This soil class is deep, over 1 m, and with the upper horizon being silty-clay-loam/silty-loam in texture. The most usual soil class found in the eroded hillslopes was Vertic Haploxerept, covering almost half of the watershed (Soil Survey Staff, 2014). The depth of these soils ranged between 0.5 - 1 m, and the upper horizon is silty-clay in texture. Soil cracks with a width of 1-2 cm are observed in the upper horizon. In addition to eroded hillslopes, this soil is also found in accumulation areas but generally with higher depths

(>1 m). Typic Calcixerept is also found at eroded hillslopes (Soil Survey Staff, 2014), which presents depths higher than 0.5 m and the upper horizon with silty-clay texture (Fig. 2.3A).

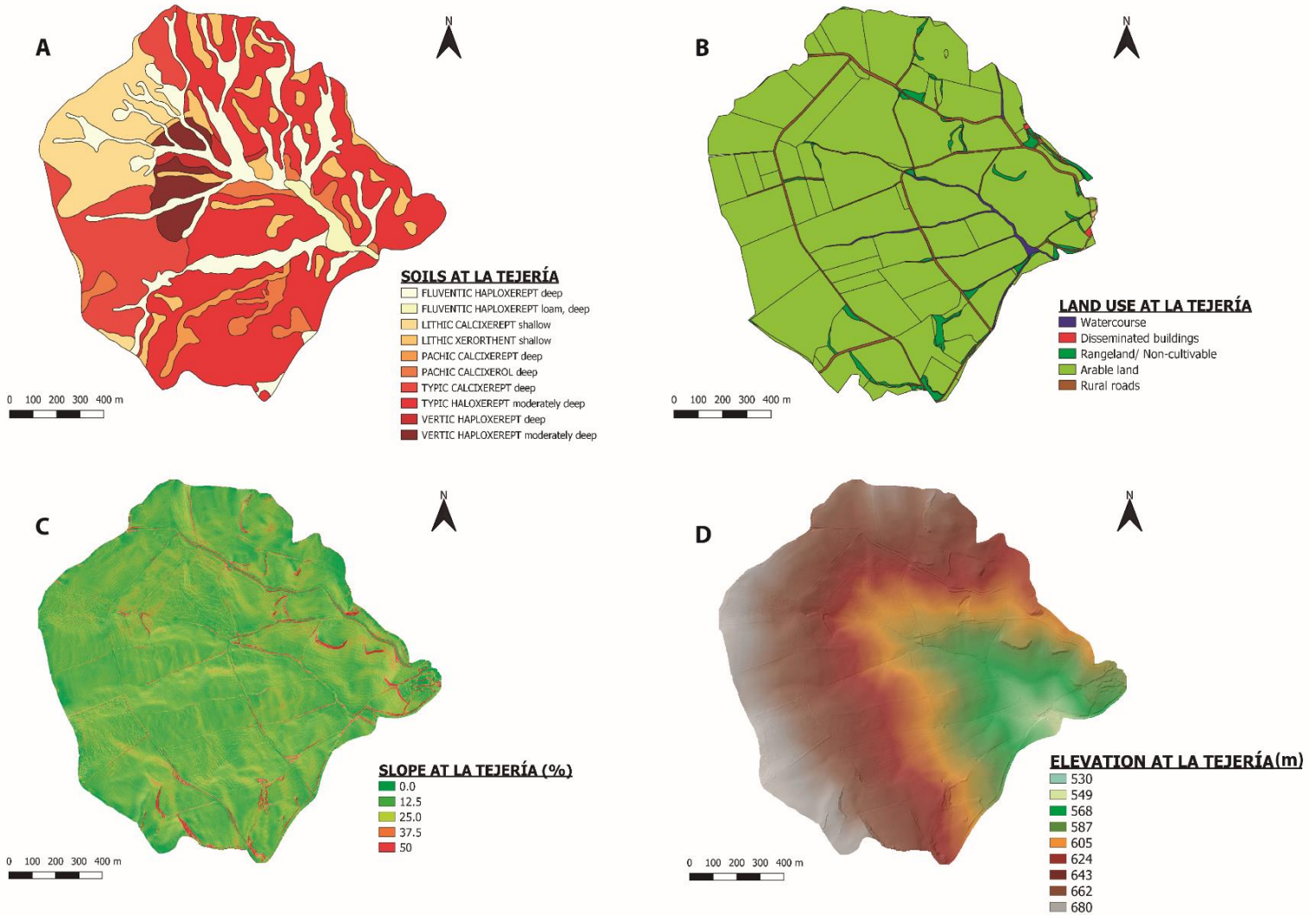


Figure 2.3: Maps of the main characteristics of the La Tejería watershed: (a) soil, (b) land use, (c) slope, and (c) elevation.

The cultivated area of La Tejería is also vast compared to the remainder of land uses (ca. 93%, 157 ha), with winter rainfed cereal prevailing. To a lesser degree, other natural non-cultivated areas are occupied with natural grassland vegetation and an emerging forest, covering approximately 2 % (4 ha) of the watershed, located principally on high slopes. In opposition to Latxaga, riparian vegetation at La tejería is limited. Even though the species observed are similar, the density, size, and width occupied is reduced, with completely bare streambank reaches. The width of riparian

vegetation in the streambank does not exceed 3 m. The remaining 5% of the surface area, as at Latxaga, is occupied by rural roads and small isolated buildings (Fig. 2.3B). According to Navarrese institutions, the recommended fertilization rate of cereals at La Tejería is 170 kg N ha⁻¹ and considers typical management practices at the watershed (INTIA, 2018). The fertilization calendar follows Latxaga (Casalí et al., 2008), with the same application peculiarities. Every two or three years, an application of phosphorous is carried out at the sowing stage with diammonium phosphate (Casalí et al., 2008).

At La Tejería, tile drainage is frequent in plots with drainage issues, located near the main channel. Tile drainage avoids problems such as waterlogging, reducing the moisture content of the soil, thereby increasing soil air in its pores so as to increase conditions for optimal growth of crops. The drainage density in the area close to the channel was estimated at 25 m ha⁻¹.

The productivity of La Tejería, considering the production of the study area as representative of the region, was ca. 4,500 kg ha⁻¹ for rainfed wheat and ca. 4,100 kg ha⁻¹ for barley throughout the study period (Government of Navarre, 2020).

2.1.3. Oskotz experimental watershed

The experimental watershed of Oskotz is located in the Northern part of the region (Fig. 2.1), covering 1,688 ha of grazed pastures and forested land. A forested sub-watershed is situated within the Northeast section of the watershed, comprising 434 ha (Fig. 2.4). Regarding meteorological data, this watershed is wetter than those described before, with an annual average of ca. 1200 mm, being the average annual temperature around 12 °C. The average altitude of Oskotz ranged between 530 m and 924 m (Fig. 2.4D). Slopes are quite steep, ranging from 10% to 45% in the hillslopes and being gentle in the valleys with a 5% (Fig. 2.4C).

Regarding geology, Oskotz is located over clay marls and Pamplona grey marls of the Tertiary. Quaternary materials are also observed at Oskotz, situated in the bed channel and composed primarily of silt and sands (Government of Navarre, 1995).

According to the soil map (Fig. 2.4A) (Government of Navarre, 2011a), the prevailing classes were Lythic and Typic Ustochrepts in eroded hillslopes, Typic Ustochrepts in accumulation hillslopes,

and Fluventic Ustochrepts in the valley (Soil Survey Staff, 2014). The prevailing soil textures in these soils were clay-loam and silt-clay-loam. The soils in the accumulation hillslopes and valley were relatively deep (over 1 m). Soil located in the eroded hillslopes was shallower, with less than 1 m for all cases and near 0.5 m for most.

The predominant land use at this watershed is forest, with an extension of ca. 1020 ha. The main tree species in the forested area are *Quercus pyrenaica*, *Fagus sylvatica*, and various *Pinus* species (*Pinus pinaster*, *Pinus sylvestris*). Pasture also covers a significant share of Oskotz, ca. 650 ha (Fig. 2.4B).

There were natural and cultivated pastures, with the primary purpose of animal feeding (primarily cows and sheeps). Natural pastures were situated in areas inaccessible to agricultural machinery. The species present in these pastures are mainly *Lolium*, *Festuca*, *Brachypodium*, *Bromus*, *Trifolium*, and *Melilotus* (Casalí et al., 2010; Government of Navarre, 2011a). Cultivated pastures were sown every 4-5 years, in Autumn. Several grass species are grown, with the most usual being *Lolium multiflorum*, *Lolium perenne*, *Trifolium pretense*, and *Trifolium repens*, among others (Casalí et al., 2010; Government of Navarre, 2011a). These grass species are usually cut twice a year, in May and June. The yield of grass cut is around 10,000-14,000 kg ha⁻¹, generally higher in June than in May (Casalí et al., 2010).

P-K-Mg-Z fertilizer is applied at approximately 450 kg ha⁻¹ in mid-Autumn. Then, in May, when animals are allowed to graze (rotating the fields), a dose of 150 kg ha⁻¹ is applied. In addition to this application, animal slurry is sprinkled over the soil surface in April, implying an additional amount of 13 P kg ha⁻¹ and 22 N kg ha⁻¹ (Casalí et al., 2010). Abandoned plots are normally fertilized with urea or slurry.

Within Oskotz, there is a forestal subwatershed located in the Northeast. This subwatershed covers 434 ha, of which 83% is forested (Casalí et al., 2010).

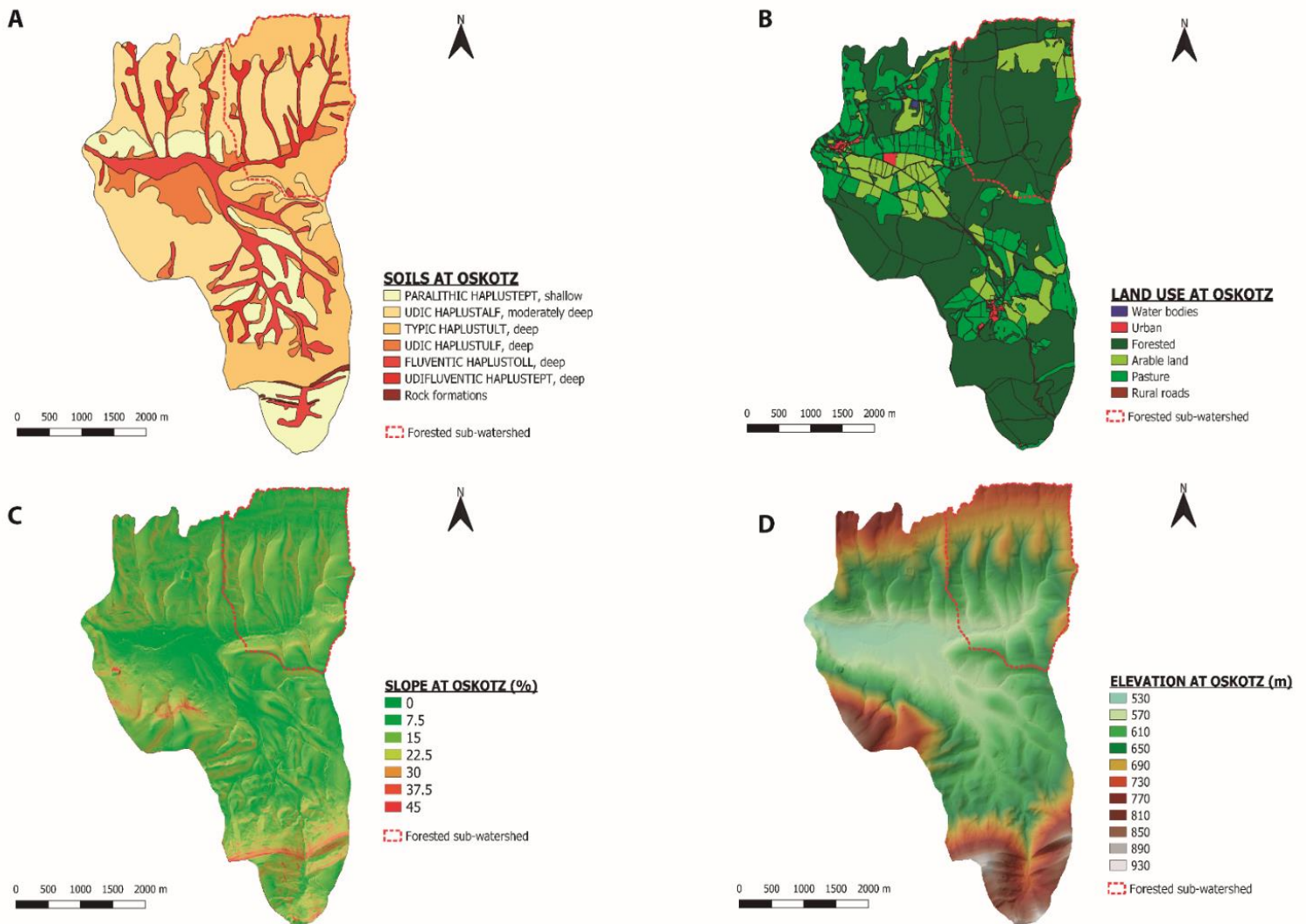


Figure 2.4: Maps of the main characteristics of the Oskotz watershed: (a) soil, (b) land use, (c) slope, and (c) elevation.

2.1.4. Landazuría experimental watershed

The watershed of Landazuría is the Southern watershed of the network, covering 480 ha (Fig. 2.1). The altitude of Landazuría ranged between 339 m and 415 m (Fig. 2.5D). In opposition to the previous watersheds, Landazuría is relatively flat, with slopes between 3.5 -5% (Fig. 2.5C). Landazuría is a dry Mediterranean climate watershed, with an average precipitation of ca. 430 mm, and an average annual temperature of 14 °C. The minimum temperature registered was -8 °C in Winter, with a maximum of 41 °C reached in Summer. According to the Penman-Monteith

equation (Allen et al., 1998), evapotranspiration was 1350 mm, almost three times higher than precipitation.

The geology in Landazuria is represented by Tertiary and Quaternary materials. The Tertiary materials appear as a bottom layer several hundred metres thick, composed of alternating gypsum, and red clays, with occasional intercalations of fine (centimetres to decimetres) limestone layers (Government of Navarre, 2003a, 2003b). The Quaternary materials cover in most of the watershed surface the Tertiary materials, and they are composed mainly by detrital sediments, gravels with some limestone clasts, alternating with sands, silt and clays (glacis) of Pleistocene-Holocene age. The synclinal structure and extremely low hydraulic conductivity of the Tertiary materials avoids deep percolation of water within the watershed (Government of Navarre, 2003a, 2003b).

As for all watersheds in the network, a detailed soil map was built based on 78 soil samples (Government of Navarre, 2011b). The prevalent soil classes at this watershed are Typic Haplustepts and Typic Calcicustolls, located in the high and low hillslopes (Soil Survey Staff, 2014). Generally, these soils are clay-loamy and silty-loamy in texture and are relatively deep (over 1m), except on the eroded hillslopes where the soil is shallower (Fig. 2.5A). Although this watershed is widely irrigated, the soil does not present high salinity levels. Only a slight increase in soil salinity was detected in the valleys due to their development over the tertiary marls (Merchán et al., 2018).

At Landazuría, the cultivated area is ca. 88%, with the remaining 12% occupied by roads and spontaneous vegetation, in some cases near the channel. Within the cultivated land area, ca. 170 ha (40%) is occupied by rainfed agriculture, while the other ca. 250 ha is irrigated. Regarding crops, the rainfed areas were mainly covered by winter cereals (barley and wheat), and in some cases, were fallow. Irrigated areas were occupied by maize, winter cereal, tomatoes, and onions. The most common irrigation is sprinkler irrigation, which corresponds to 89% of the irrigated area. Drip irrigation was implemented in some areas for specific vegetables (Fig. 2.5B) (Merchán et al., 2018).

Fertilization at Landazuría differed depending on if the land was rainfed or irrigated. The fertilization rate in the rainfed areas averaged $32 \text{ kg N ha}^{-1} \text{ year}^{-1}$ and was almost six times higher in irrigated areas, $208 \text{ kg N ha}^{-1} \text{ year}^{-1}$. These rates and the proportion of the fallow land in rainfed areas imply a low N fertilization in rainfed regions (less than 5% of the watershed) (Merchán et

al., 2018). According to the Agriculture Institute of Navarre (INTIA, 2017), during the study period, the fertilization of irrigated crops was ca. 225- 425 kg N ha⁻¹ year⁻¹ for maize, 138 kg N ha⁻¹ year⁻¹ for winter cereals, 218 kg N ha⁻¹ year⁻¹ for tomatoes, and 168 kg N ha⁻¹ year⁻¹ for onions.

Regarding the productivity of these crops in the watershed, the average crop productivity during the study period was 11,850 kg ha⁻¹ for maize, over 90,000 kg ha⁻¹ for tomato, 68,500 kg ha⁻¹ for onion, 6,150 and 1,500 kg ha⁻¹ for irrigated and rainfed wheat, respectively, and 5,600 and 2,100 kg ha⁻¹ for irrigated and rainfed barley, respectively (INTIA, 2017).

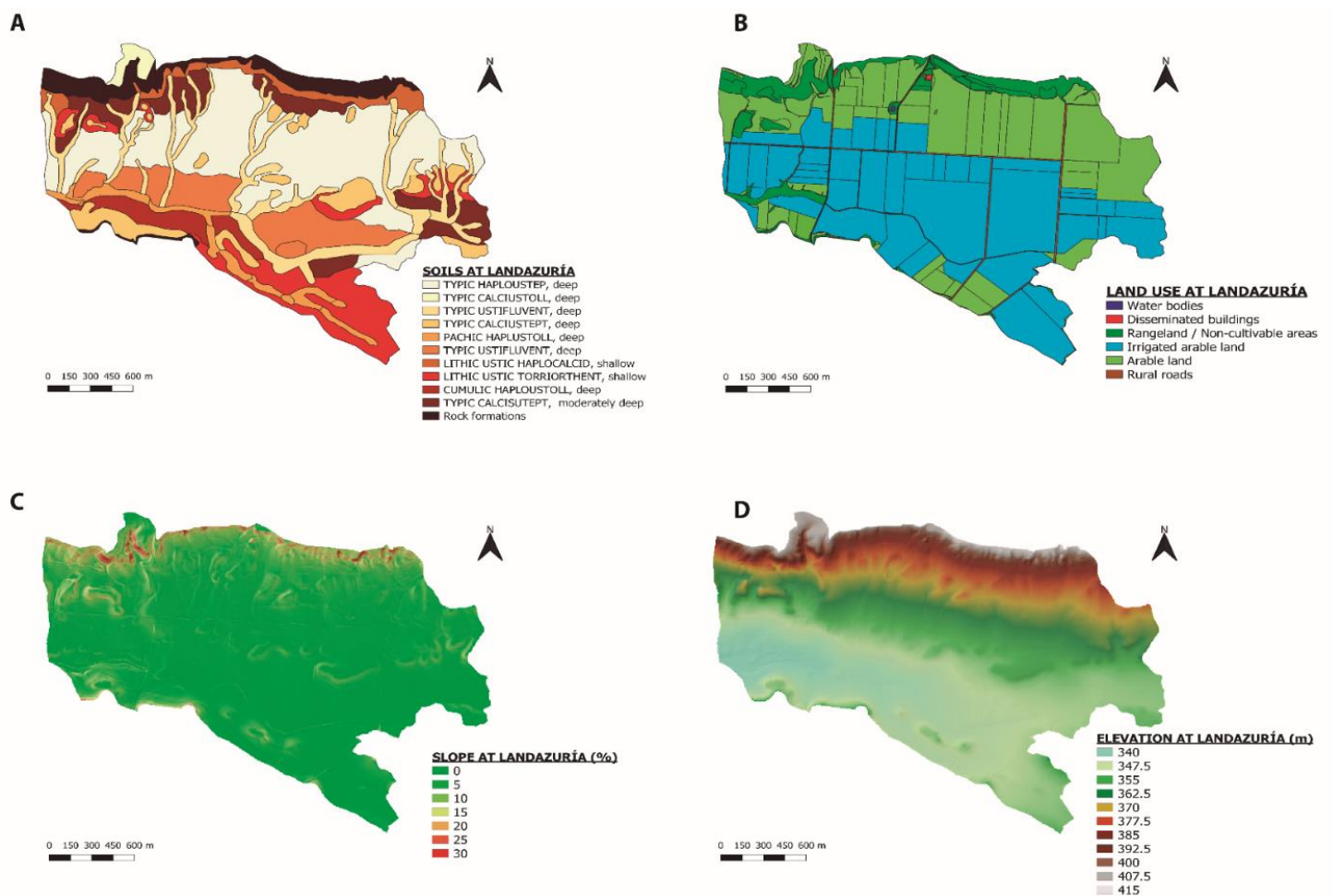


Figure 2.5: Maps of the main characteristics of the Landazuria watershed: (a) soil, (b) land use, (c) slope, and (c) elevation.

2.2. SAMPLING, DATA COLLECTION, AND DATA ANALYSIS AT EACH WATERSHED

Hydrological, meteorological, and water quality data were collected for all watersheds of the network. The Latxaga and La Tejería watersheds have been in operation since 1997, while Oskotz and Landazuría have data registries since 2002 and 2005, respectively. This section describes the main characteristics of data and sample collection for the watershed network.

There is a meteorological station at each watershed. At La Tejería, Latxaga, and Oskotz, the station is located within the watershed, close to the hydrological station. At Landazuria, the meteorological station is located 5 km to the South (meteorological station Bardenas-El Yugo, Government of Navarra). These stations record information on temperature, precipitation, humidity, radiation, and wind speed and direction on a 10-minute basis.

Hydrological stations collected hydrological data at the outlet of each watershed, where the discharge was measured every 10 minutes. The discharge measurement device consisted of a V-notch weir at La Tejería, Latxaga, and Oskotz (main watershed and sub-watershed) (Fig. 2.6A) and an H-type flume at Landazuria (Fig. 2.6B). Discharge computation was based on water level data, which were monitored using electronic limnigraphs and data loggers. In addition, water discharge was also directly measured using a propeller-type current meter and triangular and rectangular sharp-crested weirs.

Water quality was monitored by collecting samples at the outlet of each watershed. Samples were collected every 6 hours, four times a day, and mixed to generate a single composite sample per day, to avoid possible concentration fluctuations that could have occurred during the day. The daily samples were collected from a hemispheric hollow (0.66 m diameter) located just after the V-notch weir and H-Type flume (Fig. 2.6A). The daily samples were stored in an ISCO sampler situated inside the building next to the weir (Fig. 2.6C1; C2) and automated to collect samples throughout 20 days. After this period, the samples were taken to the laboratory. Each composite water sample was analyzed for suspended sediment concentration and major dissolved constituents (Na^+ , K^+ , Ca_2^+ , Mg_2^+ , Cl^- , SO_4^{2-} , HCO_3^- , CO_3^{2-} , NO_3^-), following the analytic methods for water quality parameters established by the Agricultural Laboratory of the Department of Agriculture and Food of the Government of Navarre. Cations were determined by inductively coupled plasma-

optical emission spectrometry (ICP-OES; PerkinElmer DV-2000, Waltham, Massachusetts, U.S). Cl^- , SO_4^{2-} and NO_3^- were quantified by ionic chromatography (HPLC; Thermo Fischer Scientific Dionex DX-120, Bremen, Germany). HCO_3^- and CO_3^{2-} were determined by the acid-base volumetric technique, and suspended sediments were analyzed by the gravimetric method (0.7 μm filter pore size).

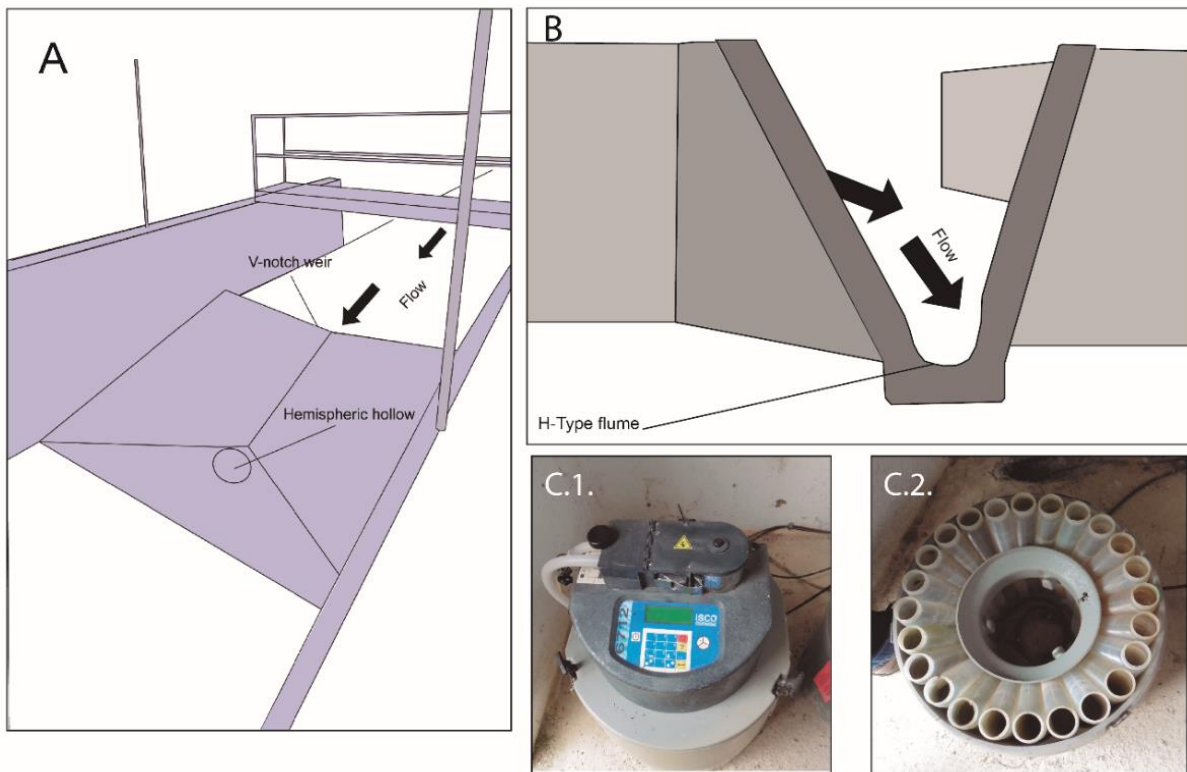


Figure 2.6: (A) V-notch weir, (B) H-type flume, and (C.1; C.2) ISCO sampler at the watershed network.

After preliminary screening of the available database, the period from October 2006 to September 2016 (hydrological years 2007-2016) was selected for this study. This period presented: (1) complete meteorological records, with only a few days of sensor failures; (2) continuous water level records, with only minor (in the order of hours) failures in the recording equipment (<0.05% of the study period), and (3) the most complete water quality data set. 69% of days were sampled at La Tejería, 66% at Latxaga, 87% at Oskotz Principal (main watershed), and 83% at Oskotz Forested (subwatershed) and Landazuria. The lower values of La Tejería and Latxaga are related to the fact that these watersheds are dry (non-measurable discharge) for significant periods in Summer, especially in dry years.

Due to gaps in the database, the load was estimated for the entire study period following the different approaches developed by Meals et al. (2013) (described in section 2.1). In Chapter 6, the gaps in daily nitrate concentration were filled using linear regression and were considered suitable and consistent with the loads estimated.

2.2.1. Load computation

Daily average discharge data were used in combination with daily suspended sediment (SS), total dissolved solids (TDS), and nutrient concentrations for the computation of daily SS loads, daily TDS loads, and daily nutrient loads. Three different approaches were used (Meals et al., 2013) to obtain load estimation for the entire study period:

- a) Numerical integration: based on the integration of daily loads. For those days in which there was no load available, the monthly median concentration of the sampled period (2007-2016) was assigned to the volume of water measured in non-sampled days.

- $Load_{07-16} = \sum_{i=1}^n c_i q_i t_i$

Where c , q , and t are the concentration, discharge, and duration of the i^{th} time interval, respectively, and $Load_{07-16}$ is the load for the entire study period (hydrological years 2007-2016).

- b) Regression: a rating curve was fitted to the observed data and used to estimate the load for the selected study period. Daily loads were estimated based on the relationship between observed loads with discharge, time, and season. This estimation for days with no data was performed using the software developed by the United States Geological Survey (USGS) LOADEST (Runkel et al., 2004).

- $Log(Load) = a_0 + a_1 Log(Q) + a_2 Log(Q^2) + a_3 sin(2\pi dtime) + a_4 cos(2\pi dtime) + a_5 dtime + a_6 dtime^2$

Where $Load$ and Q are, respectively, the daily load and the daily average discharge, $a_0 \dots a_6$ are the seven parameters of the rating curve, and $dtime$ is decimal time (representation of the time of day using decimally related units).

- c) Ratio estimator: this method assumes that the flow weighted concentration in the period with available data represents the entire study period. Therefore, the ratio of complete flow over sampled flow is used to correct the observed load. Some corrections are then applied according to the covariance of loads and flow. In particular, the Beale ratio (Richards, 1998) was used:

- $Load_{07-16} = Load_{obs} \left[\frac{Q_{07-16}}{Q_{obs}} \right] BCT$

Where $Load_{obs}$ and Q_{obs} are, respectively, the total load and discharge of those days that were sampled, while Q_{07-16} is the discharge for the entire study period, and BCT is a bias correction term.

After computation of loads, annual yields were obtained by dividing the annual loads by the watershed surface.

2.3. AnnAGNPS MODEL

This study employs the Annualized Agricultural Non-Point Source Pollution (AnnAGNPS) model (version v5.51), developed from the single event Agricultural Non-Point Source model (AGNPS) watershed model (Young et al., 1989). AnnAGNPS is a batch-process, continuous-simulation, daily time-step, surface-runoff, pollutant loading computer model developed by the United States Department of Agriculture – Agricultural Research Service – Natural Resources Conservation Services (USDA-ARS-NRCS) (Bingner et al., 2018). The basic components of AnnAGNPS are hydrology, sediment, nutrients, and pesticides. The surface of the watershed is represented by land units, defined as cells. Each cell represents landscape components (land use, soil type, agricultural managements, etc.) homogeneously within the watershed. These landscape components are unique to each cell, where those occupying the most significant proportion of the cell can be selected or modified by the user. These cells are generated from a terrain analysis of the digital landscape topography using the TOPographic PARAMeteriZation (TOPAZ) tool (Garbrecht and Martz, 1999) for AGNPS (TOPAGNPS) developed as a tool for use with AnnAGNPS. In addition to the cells generated, the stream network is also generated using TOPAGNPS.

The Critical Source Area (CSA) and Minimum Source Channel Length (MSCL) variables are key input parameters in TOPAGNPS used to generate the cells (which act as small sub-watersheds) and the stream network (composed of different reaches of different magnitude). These variables enable the determination of the size of the cells and the length of the reaches, which are generally determined using expert judgment after a previous characterization of the watershed. Each of the cells, in addition to a homogeneous representation of the characteristics of the territory it comprises, typically defines the predominant land use and the soil unit of the land it occupies (Fig. 2.7a, b), resembling as much as possible the actual conditions of the field. The cells are located in the watershed according to a series of criteria that enable the simulation to resemble actual conditions as closely as possible. Thus, typically three cells are discharged into a Strahler first-order channel reach, with the highest altitude cell draining as the source area to the upstream end of the reach. The other two cells are generated to drain along each side of the reach (Fig. 2.7c). Sections channels greater than first-order reaches receive the contribution of the corresponding lower-order reaches at their upstream. On both sides, as in the previous case, two other cells are placed and flow to each side of the reach (e.g., Strahler second-order reach receives the water and

pollutants from the Strahler first-order reaches at its upstream, and the adjacent cells flow the accumulated runoff water along with the pollutants carried, at its sides) (Fig. 2.7d).

In AnnAGNPS, the use of different techniques enables the model to carry out the processes in each component. The generation of daily direct runoff is obtained by incorporating the SCS curve number technique (USDA, 1972). Daily sediment transport and daily and sheet erosion are simulated by applying RUSLE (Bingner et al., 2018). For nutrients and pesticides, a daily mass balance is computed for each land unit.

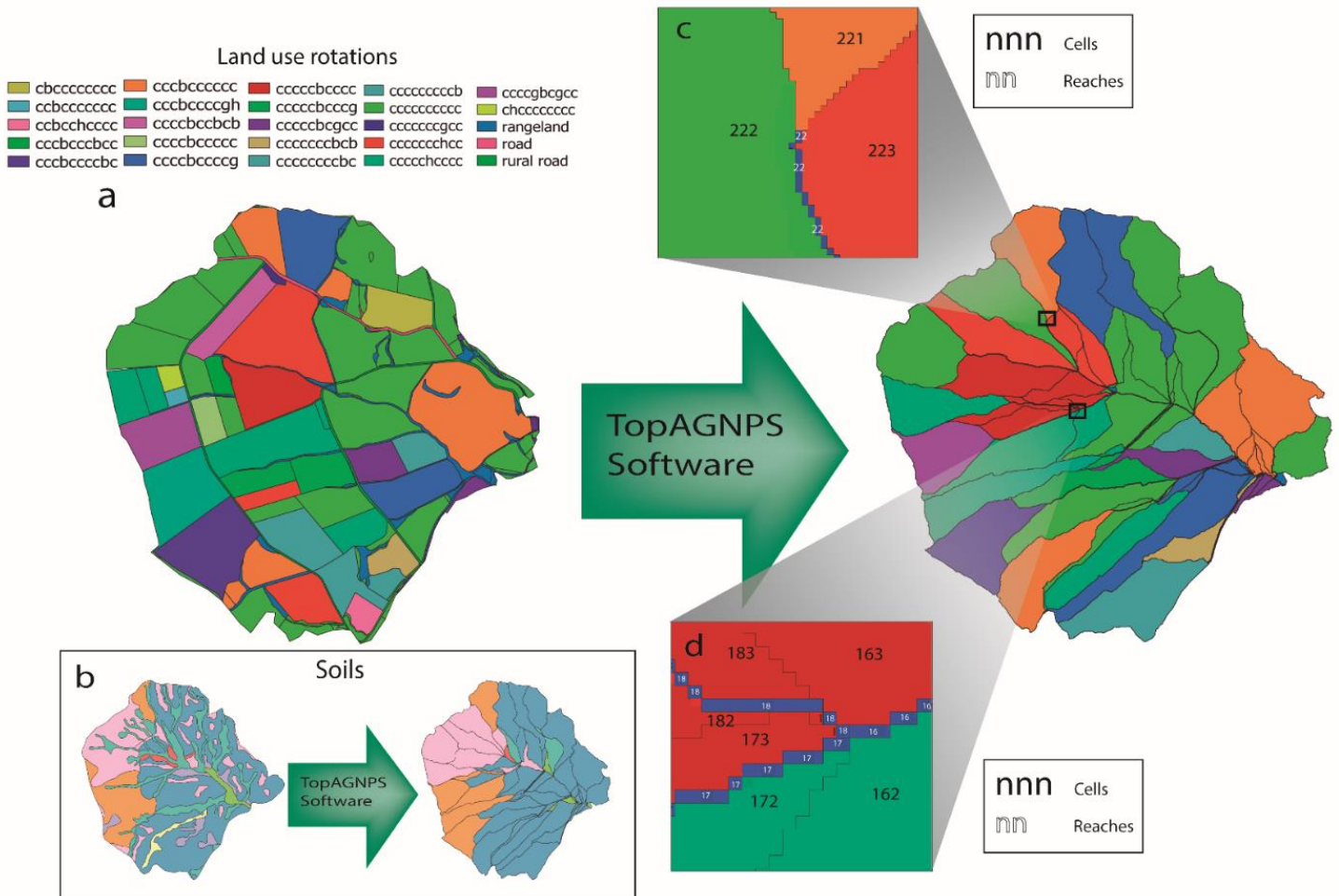


Figure 2.7: Determination of the cells and network of channel reaches at La Tejería watershed through TOPAGNPS. (a) Land use map and (b) soil map (Casalí et al., 2008) incorporated in TOPAGNPS creating cells through GIS tools. Example of cells and reaches setup, depicting (c) first-order reaches and (d) higher-order reaches. The legend shows the rotation of land use for each cell, in chronological order during 10 years: "c" cereal, "b" bare soil, "g" sunflower, and "h" broad beans.

The simulation of N in AnnAGNPS provides a two-stage output: dissolved N, in the soil solution, and N attached to the sediment (Bingner et al., 2018). This study focuses on the dissolved part, using nitrate as dissolved N, which is the most mobile N compound in watersheds (Hernández-García et al., 2020), and the most mobile form of mineral N in the soil (Merrington et al., 2002). The mass balance is developed considering the major components of the N cycle, such as plant uptake, fertilizer application, leaching, denitrification, mineralization, and decomposition. In this work, runoff and N yield have been studied in detail (Chapter 6). Therefore, a more detailed analysis of these components is carried out in section 2.3.2. of this chapter.

2.3.1. AnnAGNPS input data

The effective performance of AnnAGNPS requires a significant number of inputs, including topography, climate, crop growth, crop management, soil, and runoff input factors, as can be observed in Fig. 2.8, with many parameters automatically determined with input data processing tools.

Regarding topography, a digital elevation model (DEM) to generate the land units (cells) and stream reaches with TOPAGNPS software can be utilized to greatly simplify the development of the necessary AnnAGNPS input parameters. The minimum pixel size that this model supports for DEM is 1 m. In addition to DEM, spatial information on soil classes and land use is required for subsequent incorporation into the cells generated. The information related to these soil and land use maps is incorporated in the different sections corresponding to crop, management, and soil data described next.

Concerning crop information, AnnAGNPS requires two types of inputs. The first is crop growth; bi-weekly data are entered on the crop cycle over the entire year, including information on cover, height, and root mass. The second input comprises general characteristics of the crop (e.g., crop yield, residue decomposition coefficient, crop phenological cycle, and N and P uptake).

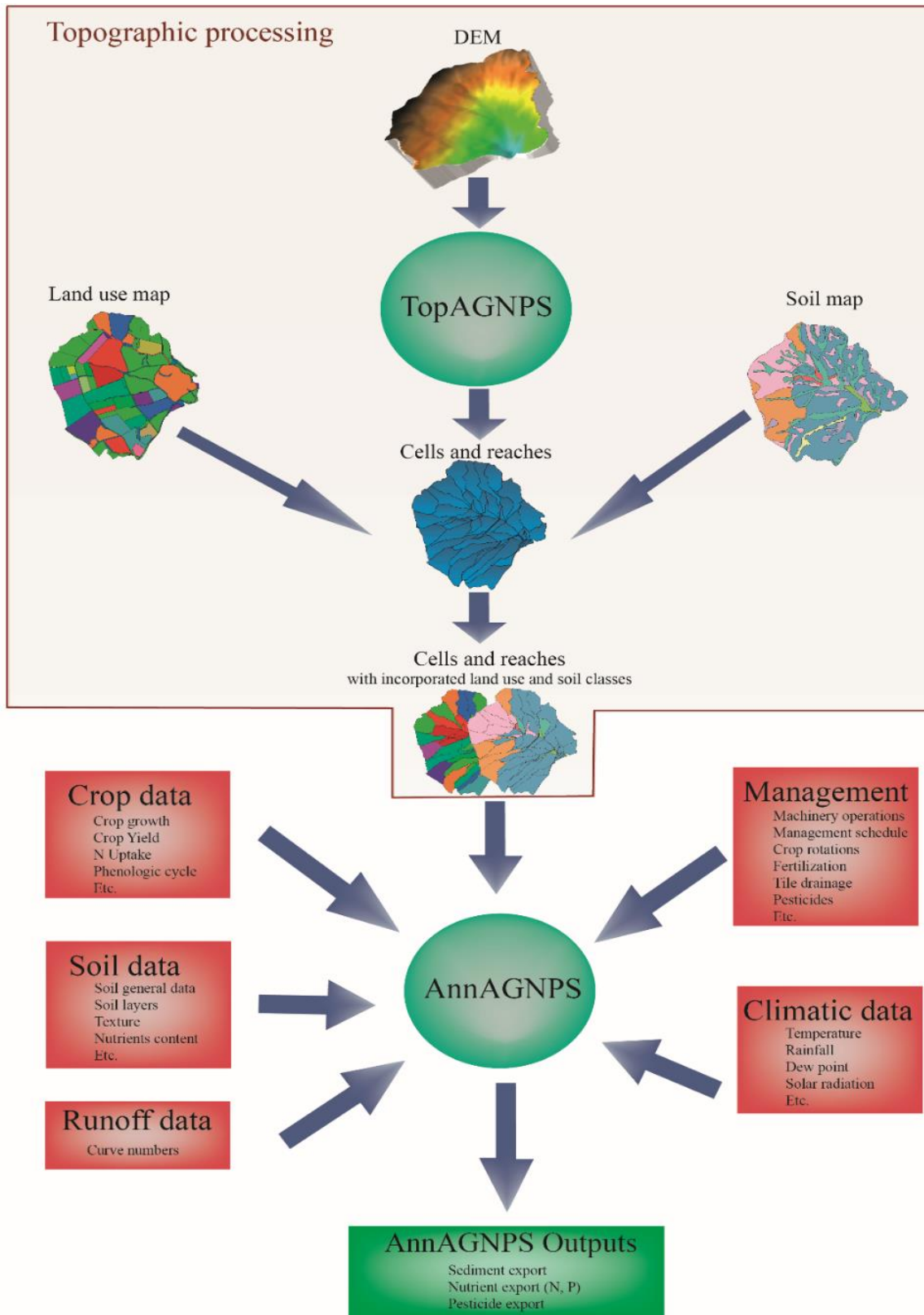


Figure 2.8: AnnAGNPS topographical processing and input data.

Crop management information requires a large amount of data. It is necessary to schedule every operation carried out in each cell. Therefore, crop rotation must be considered, along with operations performed (tillage, fertilization, sowing, harvesting, pesticide application, etc.) and data regarding the year crop rotations began. After completing the crop management schedule, information must be appended to each operation entered in the schedule (e.g., amount of fertilizer applied, soil disturbance when sowing, etc.). For the chemicals (pesticides, nutrients), the model requires the amounts applied. In the case of pesticides, their degradation coefficient is also necessary. AnnAGNPS enables the addition of other types of management such as tile drainage or irrigation.

AnnAGNPS uses the curve number technique to determine runoff, and therefore, the curve number value corresponding to its hydrologic soil group is added for each land use.

For adequate performance, AnnAGNPS requires physical and chemical characteristics of each soil layer. Physical features include texture, field capacity, wilting point, saturated conductivity, among others. The chemical features include pH, nutrient and organic matter contents, and base saturation.

Climate information is crucial to operating the AnnAGNPS model, which requires daily weather data (e.g., maximum and minimum temperatures, precipitation, sky cover, dew point temperature, solar radiation, wind speed, wind direction, and potential evapotranspiration).

Even though the inputs aforementioned are required (mandatory) for the complete simulation, AnnAGNPS accepts additional inputs to characterize the intrinsic characteristics of each watershed (e.g., wetlands, riparian vegetation) or to further explore sediment analysis (e.g., ephemeral gully) (Fig. 2.9, Bingner et al., 2018). These inputs can be *optional*, which provide additional information to the already complete processes in the model, or *required if referenced*, if they are referenced in the inputs required for the model to function (e.g., if irrigation is mentioned in the management calendar, corresponding irrigation input data are needed).

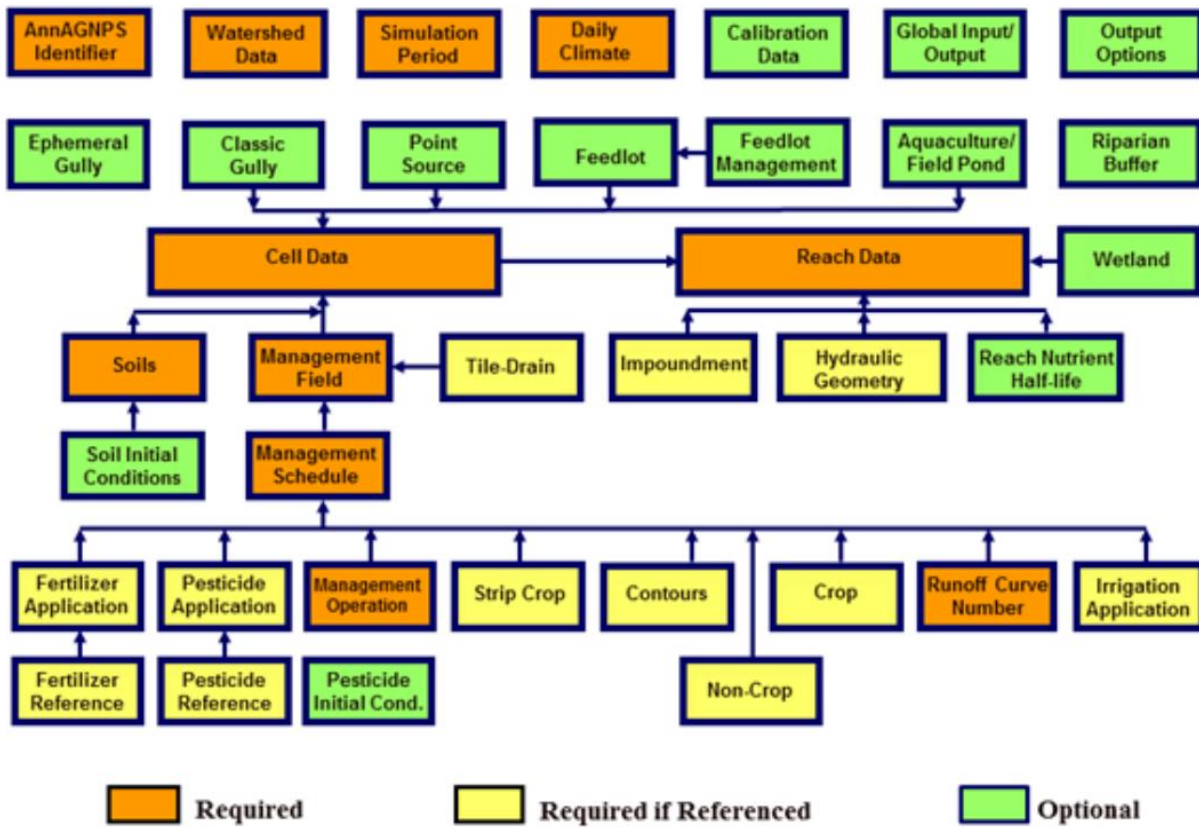


Figure 2.9: AnnAGNPS types of inputs: required, required if referenced, and optional. Source: Bingner et al., 2018

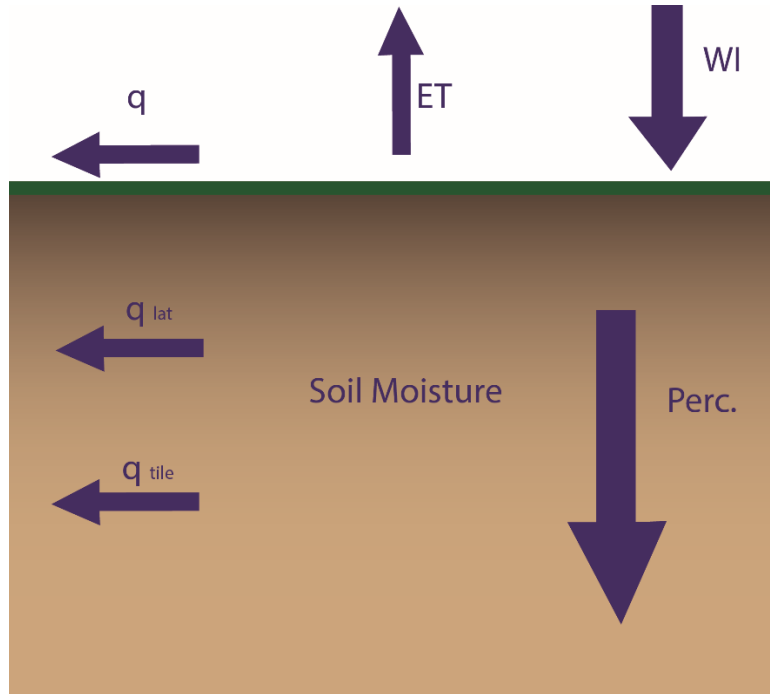
2.3.2. Simulated processes with AnnAGNPS

In this work, the processes simulated with AnnAGNPS were runoff generation and N cycle, to determine the losses of dissolved N in the watershed. The description of these processes in the model is presented next. All processes simulated by AnnAGNPS, in addition to those shown in this section, are thoroughly described in Bingner et al. (2018).

2.3.2.1. Surface runoff

In AnnAGNPS, the SCS curve number technique is used to determine the surface runoff from a field (USDA, 1972), adapted to the soil moisture content at any period of time. AnnAGNPS updates, on a daily scale, the soil moisture content to define the antecedent moisture content. This calculation is based on the moisture content of the previous day and on the water balance

(calculated by adding water inputs and subtracting water losses for the same day). Water inputs to the system are generally rain, snow, or irrigation. Losses include direct runoff, evapotranspiration, percolation, tile drain flow, and subsurface flow (Fig. 2.10).



Where:

- WI: Water inputs (rainfall, snow, irrigation)
- q: Direct runoff
- q_{lat}: Subsurface lateral flow
- q_{tile}: Tile drainage lateral flow
- Perc.: Water percolation
- ET: Evapotranspiration

Figure 2.10: Hydrological processes simulated by AnnAGNPS.

AnnAGNPS simulates soil moisture for two layers. The first layer refers to the surface layer (ca. 20 cm), present in the first centimeters of the soil, generally where tillage occurs (Eq. 2.1). The second layer refers to the remainder of the soil profile (Eq. 2.2).

$$SM_{t,1+1} = SM_{t,1} + \frac{WI_{t,1} - q_{t,1} - Perc_{t,1} - ET_{t,1} - q_{lat,t,1} - q_{tile,t,1}}{D_{SL1}} \quad \text{Eq. 2.1}$$

Where:

- SM_{t,1}**: moisture content for the surface layer at the beginning of the time period (fraction)
- SM_{t+1,1}**: moisture content for the surface layer at the end of the time period (fraction)
- WI_{t,1}**: water input, consisting of precipitation or snowmelt plus irrigation water (mm)

- q_{t,1}**: direct runoff (mm)
PERC_{t,1}: water percolation out of surface soil layer (mm)
ETP_{t,1}: evapotranspiration (mm)
q_{lat t,1}: subsurface lateral flow at surface layer (mm)
q_{tile t,1}: tile drainage flow at surface layer (mm)
D_{SL,1}: thickness of soil layer (mm)

$$SM_{t,2+1} = SM_{t,2} + \frac{\text{Perc}_{t,1} + \text{Inf}_{t,1} - \text{Perc}_{t,2} - \text{ET}_{t,2} - q_{\text{lat } t,2} - q_{\text{tile } t,2}}{D_{\text{SL}2}} \quad \text{Eq. 2.2}$$

Where:

- SM_{t,2}**: moisture content for the remainder of the soil profile at the beginning of the time period (fraction)
SM_{t+1,2}: moisture content for the remainder of the soil profile at the end of the time period (fraction)
PERC_{t,1}: surface layer percolation (mm)
Inf_{t,1}: Surface layer infiltration (mm)
PERC_{t,2}: water percolation out of the remainder of the soil profile (mm)
ETP_{t,2}: evapotranspiration (mm)
q_{lat t,2}: subsurface lateral flow for the remainder of the soil profile (mm)
q_{tile t,2}: tile drainage flow for the remainder of the soil profile (mm)
D_{SL,2}: thickness of soil layer (mm)

After determining the soil moisture content, AnnAGNPS can vary the average CN value (CN₂) by utilizing a CN value for dry conditions (CN₁, Eq. 2.3) or wet conditions (CN₃, Eq. 2.4), depending on the soil moisture content.

$$CN_1 = CN_2 - \frac{20(100-CN_2)}{100-CN_2 + \exp[2.533 - 0.0636(100 - CN_2)]} \quad \text{Eq. 2.3}$$

$$CN_3 = CN_2 \exp[0.0636(100 - CN_2)] \quad \text{Eq. 2.4}$$

2.3.2.2. N cycle in AnnAGNPS

The AnnAGNPS model has been tested to simulate N transport in a watershed. Even though it does not simulate all the nitrogen cycle processes, such as fixation or volatilization (see principal nutrient cycles, Annex I), AnnAGNPS considers the most critical processes such as plant uptake, fertilizer application, leaching, denitrification, and mineralization. The cycle processes that AnnAGNPS simulates are based on user-supplied parameters or processes simulated by the model (Fig. 2.11). The calculation of the main N-cycle processes in the model was described by Bingner et al. (2018) and evaluated by Yuan et al. (2018) and presented next.

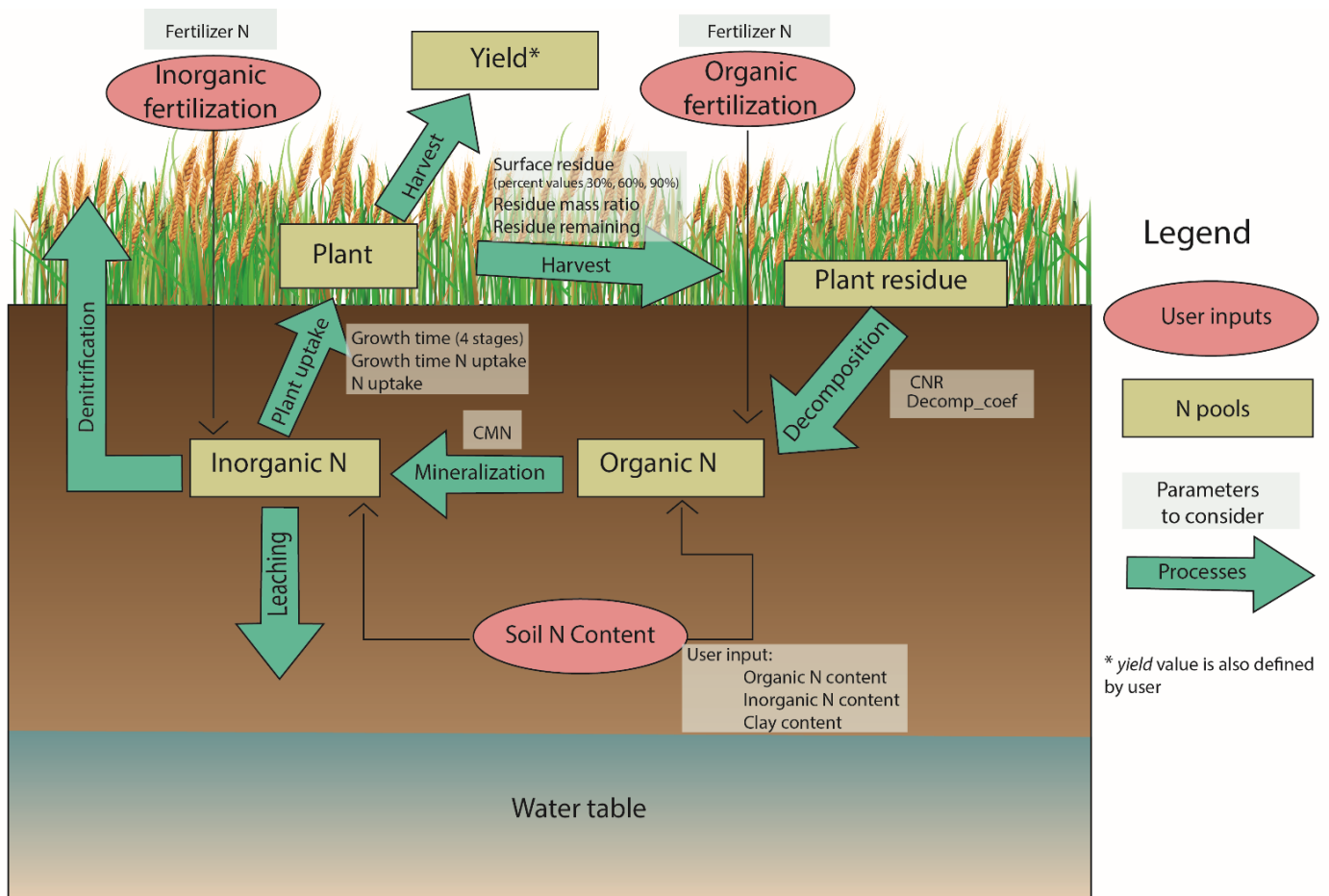


Figure 2.11: N-cycle processes, parameters, and pools involved in AnnAGNPS simulations.

Correct calibration and parameterization of the model input data are essential, which are not easy tasks, as the number of parameters considered in this cycle is very high. In addition to the rates

and ratios required by the model, the initial soil N content (organic and inorganic) is necessary, along with fertilizer applications and amount, percentage of plant residue, and crop productivity.

The decomposition of plant residue in AnnAGNPS depends on the type of residue: crop or non-crop. If the plant residue is a crop, AnnAGNPS requires the carbon-nitrogen ratio (Eq. 2.7), and if the residue is a non-crop, AnnAGNPS obtains the fraction of N corresponding to the biomass (Eq. 2.5). Concerning the daily decomposition, in the case of a crop, it is necessary to add the specific intrinsic factor of each crop (Eq. 2.8). For non-crops, this factor is based on grassland and forest residue decomposition (Eq. 2.6). The temperature correction is important in these processes (Eq. 2.9):

Non-crop decomposition

$$\text{FON} = (\text{Res_decomp}) * \text{NF} \quad \text{Eq. 2.5}$$

Where:

FON: organic N addition from the decomposition of non-crop residue (kg)

Res_decomp: plant residue mass decomposition for the current day (kg)

NF: N fraction of total dry biomass for a non-crop field (kg N/kg biomass)

For non-crops, the calculation of plant residue mass decomposition for the current day is:

$$\text{Res_decomp} = (\text{Res} * [1 - \exp(-\text{TF} * 0.016)]) * \text{A_cell} \quad \text{Eq. 2.6}$$

Where:

Res: surface or subsurface residue, which is computed from RUSLE (kg ha^{-1})

TF: RUSLE temperature correction factor, for non-crop Res_decomp, used to adjust the calculation of residue decomposition based on first-order rate (dimensionless).

A_cell: AnnAGNPS cell area (ha)

Crop decomposition

$$\text{FON} = \frac{(\text{Res_decomp}) * 0.5}{\text{CNR}_{\text{harvest}}} \quad \text{Eq. 2.7}$$

Where:

FON: organic N addition from the decomposition of non-crop residue (kg)

Res_decomp: crop residue mass decomposition for the current day (kg)

CNR_{harvest}: Carbon-N ratio for the crop at harvest

For crops, the calculation of crop residue mass decomposition for the current day is:

$$\text{Res_decomp} = (\text{Res} * [1 - \exp(-\text{TF} * \text{Decomp_coeff})] * \text{A_cell}) \quad \text{Eq. 2.8}$$

Where:

Res: surface or subsurface residue, which is computed from RUSLE (kg ha⁻¹)

TF: RUSLE temperature correction factor (unitless).

A_{cell}: AnnAGNPS cell area (ha)

The RUSLE temperature correction factor for crops is applied to a temperature range of 0-32 °C, and is calculated by Eq. 2.9:

$$\text{TF} = \frac{3200 * [(T_{\text{soil}} + 8)**2] - [(T_{\text{soil}} + 8)**4]}{2560000} \quad \text{Eq. 2.9}$$

Where:

T_{soil}: average cell soil temperature

Regarding mineralization in AnnAGNPS, the organic N is maintained until the end of the day. The amount of active organic N for mineralization is calculated based on the total organic N in soil, and the fraction of active N, which is based on the period of cultivation before the simulation starts (Eq. 2.10).

Temperature (which also plays an important role in decomposition) and soil moisture content are essential factors in mineralization, as shown in Eq. 2.10.

$$\text{HMN} = \text{CMN} * \text{AON} * (\text{SWF} * \text{TF})^{0.5} \quad \text{Eq. 2.10}$$

Where:

HMN: mineralization rate of humus organic N ($\text{kg ha}^{-1} \text{ day}^{-1}$)

CMN: constant rate for N mineralization from humus, 0.0003 day^{-1}

AON: active organic N content of soil layer (kg ha^{-1})

SWF: soil water fraction

TF: RUSLE temperature correction factor (dimensionless).

The calculation of soil water fraction is expressed by Eq. 2.11:

$$\text{SWF} = \frac{\text{SW}}{\text{PO}} \quad \text{Eq. 2.11}$$

Where:

SW: water content of the soil layer on a given day (mm).

PO: Soil porosity (mm)

Denitrification is a fundamental process in dissolved N dynamics and is regulated by temperature and soil moisture content (Eq. 2.12). High levels of carbon and nitrogen are essential for denitrification.

$$\text{DN} = \text{NO}_3 * [1 - \exp(-1.4 * \text{TF} * \text{OrgC})] \quad \text{Eq. 2.12}$$

Where:

DN: denitrification rate (kg ha^{-1})

NO₃: amount of nitrate in soil layer (kg ha^{-1})

OrgC: organic carbon content (%)

TF: nutrient cycling temperature correction factor, as used for mineralization (dimensionless).

AnnAGNPS calculates the N uptake by the plant based on the stages of the crop - depending on the stage, the plant uptake of N can be higher or lower (Eq. 2.13). In addition to the stage and development period of the crop, the nutrient content of the soil is also a limiting factor in this process.

$$\text{upt.N} = \frac{\text{Growth.N.Uptake} * \text{Crop.Yield} * \text{N.uptake.harvest}}{\text{stage.length}} \quad \text{Eq. 2.13}$$

Where:

upt.N: mass of inorganic N taken up by plant on the current day (kg day⁻¹)

Growth.N.Uptake: fraction of N uptake for current growth stage. (4 stages: initial, development, mature, and senescence).

Crop.Yield: crop yield at harvest (kg ha⁻¹).

N.uptake.harvest: N uptake per yield unit at harvest (kg N/ kg harvest unit)

stage.length: number of growing days for current growth stage (days)

In the N cycle, losses are generated on many occasions, principally in agrosystems, by the excess of nutrients. The AnnAGNPS model considers most of the losses in agrosystems and can simulate N losses by leaching, runoff, and sediment transport.

Leaching losses are calculated using the updated inorganic N content level in the soil and the physical particularities of the soil, such as moisture content and wilting point (Eq. 2.14).

$$\text{N_Leaching} = \frac{\text{Perc_loss}}{\text{SW- Wilting}} * \frac{\text{inorg_N} * \text{conv}}{1000000} \quad \text{Eq. 2.14}$$

Where:

N_Leaching: leaching loss from soil layer (kg)

Perc_loss: percolation loss for the current day (mm)

SW: soil water content (mm)

Wilting: Wilting point (mm)

inorg_N: amount of inorganic N in the soil layer (ppm)

conv: conversion factor

The N loss by runoff in AnnAGNPS considers the soil surface plus the first mm of soil (Eq. 2.15).

AnnAGNPS considers the total N loss, the sum of the nitrogen dissolved in the surface (Eq. 2.16), and

the N lost in the first 10 mm of the soil (interaction layer between the rain and the soil), as shown in Eq. 2.17.

$$\text{Sol_N_runoff} = \text{Cell_soil_sol_N} + \text{Surf_sol_N} \quad \text{Eq. 2.15}$$

$$\text{Surf_sol_N} = \frac{Q_{surf}}{Q_{surf} + inf} * \text{Surf_inorgN} \quad \text{Eq. 2.16}$$

$$\text{Cell_soil_sol_N} = \text{edi} * \frac{\text{inorgN} * \text{conv}}{D * 1000000} \quad \text{Eq. 2.17}$$

Where:

Sol_N_runoff: total mass of inorganic N removed by runoff (kg)

Cell_soil_sol_N: mass of inorganic N removed from the topsoil layer by runoff (kg)

Surf_sol_N: mass of inorganic N in runoff from fertilizer applied on the soil surface (kg)

edi: effective depth of interaction factor (AnnAGNPS uses 10 mm).

inorgN: inorganic N concentration in the soil layer (ppm)

D: depth of soil layer (mm)

Conv: conversion factor

Q_{surf}: surface runoff generated on a given day (mm)

inf: amount of infiltration, calculated in the hydrology module (mm)

surf_inorgN: inorganic N added through fertilizer application on the soil surface (kg).

For the calculation of sediment-attached N transport, AnnAGNPS assumes two situations. Firstly, that the organic N is composed of N attached to the sediment, and secondly, that the organic N is associated with the clay fraction (Eq. 2.18).

$$\text{SedN} = \text{frac_orgN_clay} * [\text{Sed_part}(1,1) + \text{Sed_part}(1,2)] * 1000 \quad \text{Eq. 2.18}$$

Where:

SedN: mass of N attached to sediment loss (kg)

frac_orgN_clay: decimal fraction of organic N in clay in the soil layer

Sed_part(1,1): Current day's mass of sediment by clay (1) under irrigation(1)

Sed_part(1,2): Current day's mass of sediment by clay (1) under no irrigation(2)

Regarding N balance, as well as carrying out the soil moisture balance, AnnAGNPS simulates N for two layers. The first layer refers to the surface layer, which refers to the first centimeters of the soil, generally where tillage occurs. The second layer refers to the remainder of the soil profile. The balances of organic and inorganic N are carried out separately. Each balance is developed based on the N losses or inputs in each cell. In AnnAGNPS, the mineralizable N is not available until the next day in the cell. The model computes the addition of fertilizers firstly, then the losses by absorption, denitrification, or leaching. Finally, daily mineralization is added. Eq. 2.19 and Eq. 2.20 show the organic N balances for the first and second layer, respectively, and Eq. 2.21 and Eq. 2.22 represent the inorganic N balances.

Organic N Balance:

$$\text{OrgN}_t = \text{OrgN}_{t-1} + \frac{\text{FON} + \text{fer}_{\text{orgN}} - \text{HMN} - \text{sedN} * 10}{\text{Conv}} \quad \text{Eq. 2.19}$$

$$\text{OrgN}_t = \text{OrgN}_{t-1} - \frac{\text{HMN} * 1000000}{\text{Conv}} \quad \text{Eq. 2.20}$$

Where:

OrgN_t: concentration of organic N in the total soil layer for the current day (ppm)

OrgN_{t-1}: concentration of organic N in the total soil layer for the previous day (ppm)

FON: organic N addition from the decomposition of non-crop/crop residue for the current day

fer_{orgN}: organic N from fertilizer application such as manure (kg) for the current day

HMN: organic N addition from mineralization of non-crop/crop residue for the current day

SedN: mass of N attached to sediment loss for the current day

Conv: conversion factor

Inorganic N Balance:

$$\text{InorgN}_t = \text{InorgN}_{t-1} + \frac{\text{hmnN} - \text{upt.N} - \text{Sol_N_runoff} - \text{DN} - \text{N_Leaching}}{\text{Conv}} \quad \text{Eq. 2.21}$$

$$\text{InorgN}_t = \text{InorgN}_{t-1} + \frac{\text{hmnN} - \text{upt.N} - \text{DN} - \text{N_Leaching}}{\text{Conv}} \quad \text{Eq. 2.22}$$

Where:

InorgN_t: concentration of inorganic N in the total soil layer for the current day (ppm)

InorgN_{t-1}: concentration of inorganic N in the total soil layer for the previous day (ppm)

hmnN: inorganic N mineralized from organic N in the soil layer for the current day (kg)

upt.N: plant uptake N from growth stage subroutine for the current day (kg)

Sol_N_runoff: inorganic N lost to runoff for the current day (kg)

DN: denitrification loss in the current day (kg)

N_Leaching: leaching loss from soil layer (kg)

Conv: conversion factor

2.4. HIGH COMPUTING PERFORMANCE (HPC)

High-Performance Computing (HPC) utilizes computing power to solve complex problems. In addition, HPC enables simultaneous computation jobs, reducing computation time significantly and allowing multiple iteration processes. The opportunities provided by this type of computing have led to its widespread adoption in areas such as science and engineering. HPC requires computational hardware such as clusters or supercomputers.

The Public University of Navarra has a computational cluster available for research institutes, which allows high-performance computations. The cluster has 26 nodes with 128 GB of RAM. Each node contains 2 CPUs and 16 cores with 32 parallel execution threads. Of the 26 nodes included in the computational cluster, 16 are computing nodes, and 8 are Big Data nodes. The cluster also contains a master node and a graphics processing unit (GPU) node. Each user can employ 30 computing cores within the cluster to execute parallel work with 128 GB RAM and 100 GB hard disk. Regarding the jobs queue, the HPC works with Sun Grid Engine (SGE), a queue management system that optimally selects the solution node for effective and equal job execution.

In this work, HPC has allowed performing multiple runs of the AnnAGNPS model, thus optimizing the model calibration and testing processes (Chapter 6). The calibration process with the HPC followed the methodology developed by Muñoz-Carpena (2019) (Fig. 2.12), modifying the general scripts to the specific conditions.

Firstly, a sampling matrix of the parameters to be considered in calibration is generated from a sequence previously obtained through the appropriate screening methods (Chapter 6). Each of these combinations of values (vectors) is a realization to run in the HPC. The large size of the generated matrix requires very long simulation times with the AnnAGNPS model. Each group of vectors is divided into different jobs, and several vectors are simulated simultaneously to reduce these simulation times. The size of each job is based on the executions to be performed and the parallel computations that can be accomplished (Fig. 2.12, Jobs generation). For instance, if it is necessary to complete 900 simulations that take one minute to run, and it is possible to work simultaneously with 30 computing cores (such as the cluster at the Public University of Navarre), each job will have 30 combinations of vectors to run in the model. In this way, a process that would take 900 minutes on a conventional computer is reduced to 30 minutes. Finally, once the jobs are

performed, they are sent to HPC for execution. After execution, the results are divided into the different jobs (Fig. 2.12, Run in HPC and Outputs). These results are merged into a single matrix. This way, results are obtained for each combination of parameters generated in the matrix.

Each simulation performed by HPC incorporates the corresponding vector values, replacing labels previously incorporated in a labeled input file pattern (Fig. 2.12, Substitution and run in each simulation). This pattern (with the labels substituted by the vector values) is incorporated into the input files. The model is executed, obtaining the results corresponding to the combination of vector parameters in each simulation (Fig. 2.12, Substitution and run in each simulation). Once the model outputs are obtained, the results are processed to obtain the desired output. In this thesis, the Nash-Stucliffe coefficient was used to evaluate the fitting performance between observation and simulation.

Fig. 2.12 depicts the different scripts needed to perform the calibration. The matrix is generated by the *Proc_matrix* script. The different jobs are carried out by the bash script *make_jobs.sh*. The jobs are sent to HPC, and executed by the bash script *class_submit.sh*. The outputs of the model are combined using the *class_merge.sh* bash script. And finally, for the substitution of labels by values in each simulation, the bash script used is *sens_class*. All these scripts developed for the specific case of the runoff calibration in the La Tejería watershed are reported in the Annex II of this thesis.

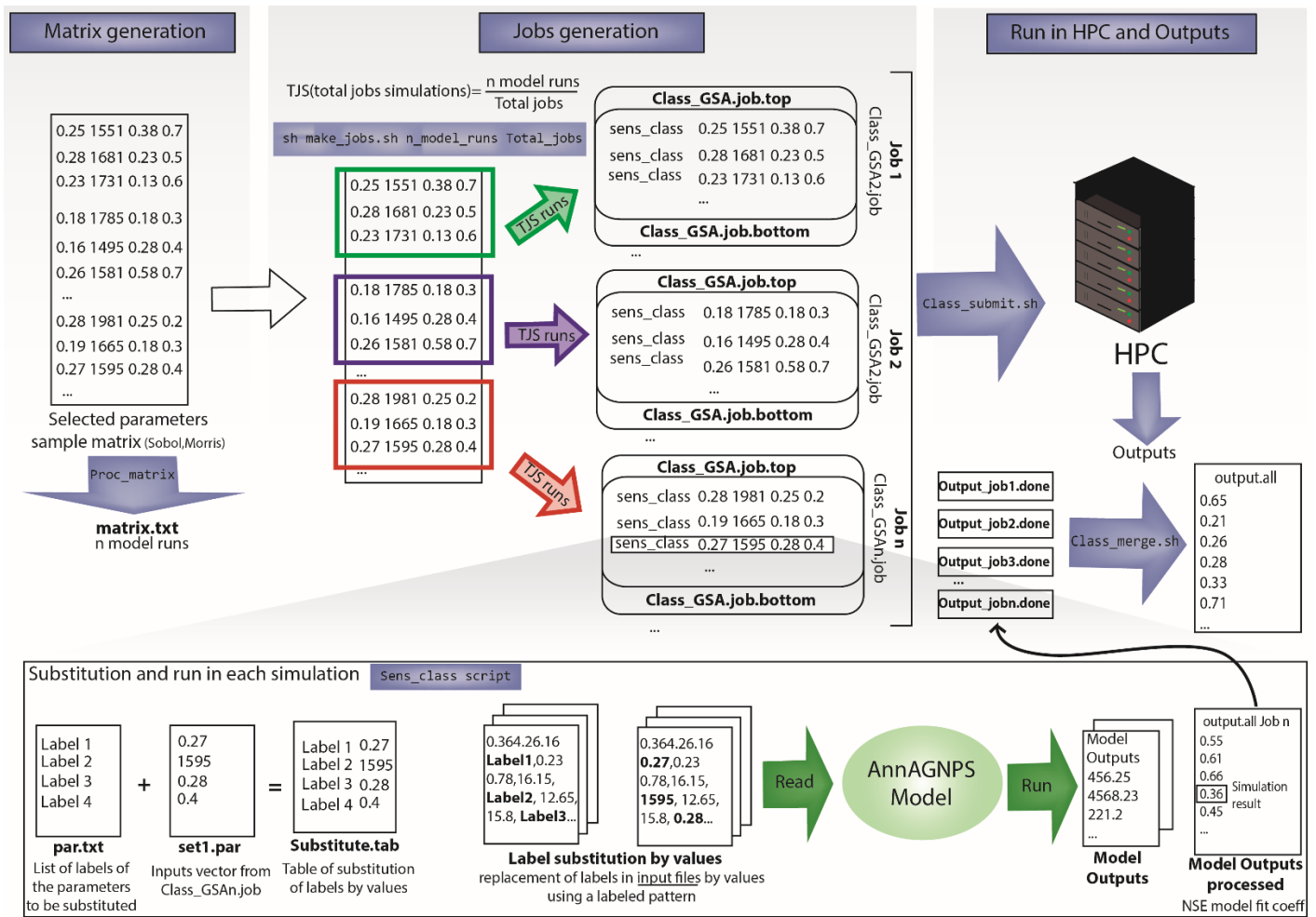


Figure 2.12: Computational procedure of the calibration process with HPC. Please refer to Annex II for detailed scripts.

CHAPTER 3:

Total Dissolved Solids dynamics from the Navarrese agricultural watershed network, Spain: A 10-year study

3.1. INTRODUCTION

Dissolved solids are regarded as an important environmental problem. Dissolved loads contribute to the salinization of downstream water bodies, which can affect its suitability for water consumption or impair its ecosystem value (Nielsen et al., 2003). The solutes delivered to streams depend mainly on lithology and the duration of water circulation, and they are supplied by tributaries as well as surface runoff, interflow and groundwater flow (Swiechowicz, 2002). However, several anthropogenic factors may contribute to the stream soluble load. For instance, de-icing road salts is a significant source of chloride and sodium (e.g., Godwin et al., 2003) and wastewater effluents supply considerable amounts of a wide range of soluble constituents such as chloride, sulphate, sodium, phosphate, etc. In addition, both cultivated land and pastures may contribute to streams salt loads (e.g., Anning and Flynn, 2014).

The role of dissolved loads in streamflow has been extensively studied in watersheds, in many cases related with suspended sediments. For instance, Grove, (1972) studied the dissolved and solid loads by some West African rivers; Subramanian (1979) studied it in Indian rivers; Lewis and Saunders (1989) in the Orinoco River; and Gaillardet et al. (1997) in the Amazon River. These studies (along with others available in the literature) were conducted in regional watersheds (from 103 to 106 km²), they are relatively short termed and present low frequency in data acquisition (e.g., following a biweekly to monthly sampling schemes during one or up to a few years). More recent studies such as those by Negrel et al. (2007) in the Ebro River (Spain) or Ollivier et al. (2010) in the Rhone River (France) partially overcome this weakness with a long-term study (Ebro) or a higher sampling frequency (Rhone). However, in such extensive watersheds, it can be hard to relate observed hydrological behaviour to specific controlling factors such as climate, geology or land use.

In contrast to large regional watersheds, dissolved loads in small watershed (<10 km²) have been studied to a lesser extent. In fact, Llorens et al. (1997) studied particulate and soluble mass transfer in a mountainous 0.4 km² watershed in which terraced-cultivation had been abandoned. Lasanta et al. (2001) studied a 6.5 km² flood irrigated watershed. Outeiro et al. (2010) estimated the contribution of suspended or dissolved loads in relation to specific high-flow events (floods) events in a watershed covered by forest and cultivated fields. Durán Zuazo et al. (2012) studied a 6.5 km²

watershed with mixed land use. Also, Nadal-Romero et al. (2012) reported the proportion of suspended and dissolved loads for four small watersheds in the Pyrenees.

From an operational point of view, small watersheds allow for some degree of homogeneity in climate, geology and land use; have minor or no flood plains; and only local contribution of groundwater flow (Buttle, 1998). Therefore, they may seem to be better suited to understand the specific processes generating the suspended and dissolved loads in streamflow. Despite this advantage, results are not easily extrapolated to larger watersheds due to the scale dependency of many hydrological processes, in particular dissolved solids dynamics (De Vente et al., 2007; Tiwari et al., 2017). As it was the case in large watersheds, most of the available studies are generally short termed, covering from a few flood events (Outeiro et al., 2010) up to three hydrological years (Durán Zuazo et al., 2012; Gao et al., 2014). Therefore, these studies may have low representativeness given the short study period.

In Navarre (northeast Spain), the consequences of agriculture on soil erosion and water quality are investigated in a network of experimental watersheds implemented by the former *Department of Agriculture, Livestock and Food* of the Government of Navarre. Four watersheds covering representative land uses in the region are included in this network. Agricultural management in these watersheds is the typical for the different land uses in the region, since the objective of the network is to adequately characterize the behaviour of these watersheds under standard management conditions. Previous works have described the physical and agronomic characteristics of each watershed, along with the quality of the water generated in terms of suspended sediment, nitrate or phosphate (Casalí et al., 2008, 2010; Merchán et al., 2018). In addition, other studies have been performed in these watershed network. For instance, Giménez et al. (2012) analysed the factors controlling sediment export whereas Chahor et al. (2014) calibrated and validated a model (AnnAGNPS) of sediment yield in one of the watersheds. However, to the date no data have been presented on the different dynamics of the dissolved solids.

In this context, the main objectives of this study were (i) to assess the dynamics of total dissolved solids concentration and loads in small watersheds in Navarre in which the agricultural land use is dominant; (ii) to estimate a long-term (10 years) average total dissolved yield in each of these watersheds, comparing with suspended sediment yield; and (iii) to gain insight in the controlling

factors underpinning these processes through comparisons among watersheds and with information available in the literature.

3.2. METHODS

3.2.1. Experimental watersheds and data collection and analysis

This study was conducted in the experimental watershed network of the Government of Navarra (Fig. 3.1). These watersheds can be considered “small” watersheds (10^{-2} to 10^2 km²) according to the operational definition of Buttle (1998). A detailed description of the experimental watersheds, its agricultural management and its particular characteristics are presented in the Chapter 2, Section 2.1 of this document.

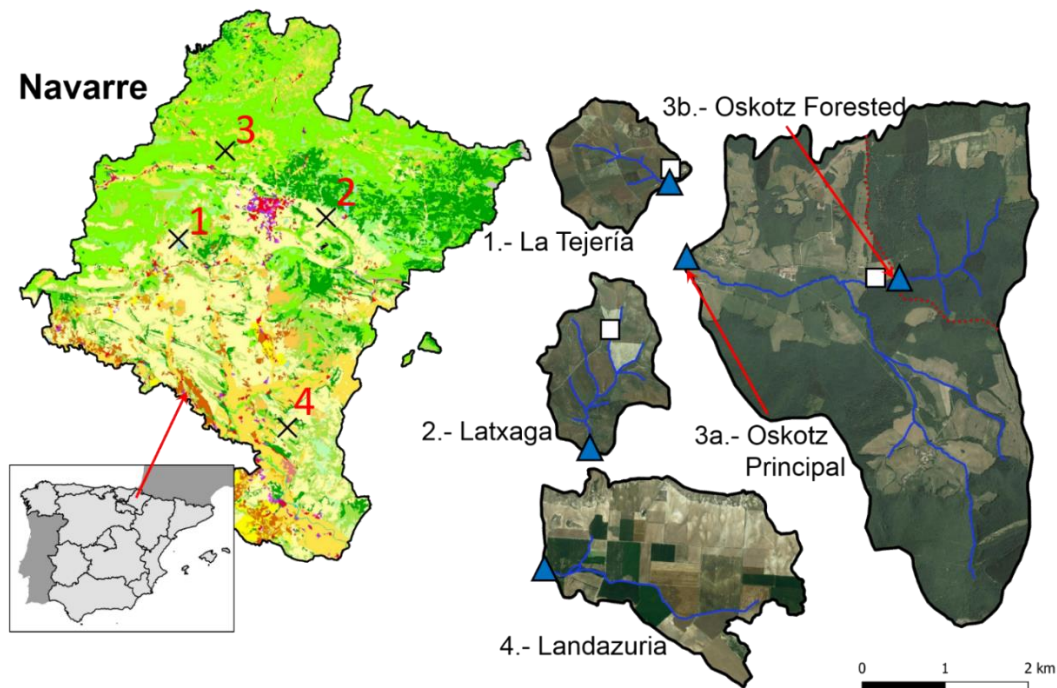


Figure 3.1: Land uses in Navarre (Spain) [Source: CORINE Land Cover 2012, standard legend] and experimental watersheds (black crosses in Navarre map) monitored by the Government of Navarra. In each watershed (orthophotos taken in summer 2017), the hydrological station (blue triangle) and meteorological station (white square) are depicted. In Landazuria, the meteorological station is 5 km south from the watershed. Note that both Oskotz Principal and Forested watersheds share the same meteorological station.

Hydrological and meteorological data, and water quality samples collected in each watershed, with the correspond analysis, are described in the Chapter 2 Section 2.2. Regarding water quality, the charge balance ($100 \cdot [\sum \text{cations} - \sum \text{anions}] / [\sum \text{cations} + \sum \text{anions}]$) of the samples was determined and found to be within $\pm 10\%$ for more than 97% of the samples, suggesting that all relevant constituents were considered in the analysis. Total dissolved solids concentration (TDS) was then

computed by addition of the individual dissolved constituents (Na^+ , K^+ , Ca_2^+ , Mg_2^+ , Cl^- , SO_4^{2-} , HCO_3^- , CO_3^{2-} , NO_3^-).

Since October 2012, the analytical determinations were limited to anions and nutrients. Therefore, a multi-linear regression was obtained from the period in which all major constituents were determined. Samples utilized for each regression, coefficient of determination (R^2) and equations obtained are presented in Table 3.1.

Table 3.1: Number of samples in which suspended sediment (SS), anions and cations were determined; multi-linear regression coefficient of determination (R^2) and Dissolved Solids (TDS) equation for each watershed (all constituents in mg L^{-1}).

Watershed	SS	Anions	Cations	R^2	Equation
La Tejería	4109	4145	3239	0.988	TDS = 15.37 + 1.46·Cl ⁻ + 1.39·SO ₄ ²⁻ + 1.30·HCO ₃ ⁻ + 1.23·CO ₃ ²⁻ + 1.23·NO ₃ ⁻
Latxaga	3977	4103	3159	0.99	TDS = -1.32 + 1.66·Cl ⁻ + 1.38·SO ₄ ²⁻ + 1.31·HCO ₃ ⁻ + 1.08·CO ₃ ²⁻ + 1.30·NO ₃ ⁻
Oskotz Princ.	4009	4071	2800	0.98	TDS = 13.77 + 2.40·Cl ⁻ + 1.65·SO ₄ ²⁻ + 1.25·HCO ₃ ⁻ + 2.05·CO ₃ ²⁻ + 1.11·NO ₃ ⁻
Oskotz For.	4254	4320	3081	0.981	TDS = 7.91 + 1.43·Cl ⁻ + 1.30·SO ₄ ²⁻ + 1.31·HCO ₃ ⁻ + 1.29·CO ₃ ²⁻ + 1.29·NO ₃ ⁻
Landazuria	2961	2982	1722	0.984*	TDS = 88.61 + 1.56·Cl ⁻ + 1.31·SO ₄ ²⁻ + 1.25·HCO ₃ ⁻ + 1.30·NO ₃ ⁻

* For Landazuria the statistical model did not considered estimated CO_3^{2-} concentration in the regression.

The load estimation of TDS and suspended sediments for the whole study period was performed following the Meals et al. (2013) methods for load estimation. These methods description can be observed in the Chapter 2, Section 2.2.1.

3.3. RESULTS

The structure of this section is as follows: the general results regarding precipitation and discharge in the watersheds are briefly described in order to provide the hydrological context of the study period (Section 3.3.1); then, the dynamics in the concentration (Section 3.3.2) and exported loads (Section 3.3.3) of TDS is shown; finally, section 3.3.4 presents the long-term yield estimation for the analysed watersheds.

3.3.1. Precipitation and discharge

During the hydrological years 2007-2016, annual average precipitation ranged between 423 ± 80 mm (average \pm standard deviation) in Landazuria and 1391 ± 326 mm in Oskotz, with intermediate values in La Tejería and Latxaga (793 ± 216 mm and 950 ± 285 mm, respectively) (Table 3.2). The hydrological year 2013 was the wettest for all the watersheds, with precipitation more than two standard deviations higher than the average (Table 3.2). The driest hydrological year differed among watersheds, being 2010 for Oskotz, 2011 for Latxaga and 2012 for La Tejería and Landazuria. In addition, the year 2012 was the second driest year in Oskotz and Latxaga.

Table 3.2: Precipitation values (mm) in each watershed, range of standardized values for the hydrological years (Oct-Sep) 2007-2016

Hydrol. Year	La Tejería	Latxaga	Oskotz	Landazuria	Standardized values range
2007	860	982	1246	445	-0.44 to +0.31
2008	895	841	1179	375	-0.65 to +0.47
2009	682	939	1242	400	-0.52 to -0.04
2010	790	798	1105	400	-0.88 to -0.02
2011	551	600	n.a.	402	-1.23 to -0.27
2012	531	709	1121	302	-1.52 to -0.83
2013	1324	1665	2148	617	+2.32 to +2.50
2014	816	1162	1658	405	-0.22 to +0.82
2015	849	1039	1594	496	+0.26 to +0.92
2016	636	765	1224	386	-0.73 to -0.47
Average \pm S.D.	793 ± 216	950 ± 285	1391 ± 326	423 ± 80	

For the same period, water yield in La Tejería ranged from 4 to 415 mm (222 ± 126 mm), with an average runoff coefficient of 28%; in Latxaga it ranged from 38 to 513 mm (250 ± 129 mm), runoff coefficient of 26%; in Oskotz Principal water yield ranged from 349 to 1161 mm (639 ± 238 mm), runoff coefficient of 46%; in Oskotz Forested it ranged from 353 to 1275 mm (646 ± 265 mm), runoff coefficient of 46%; and finally in Landazuria water yield ranged from 42 to 143 mm

(98 ± 30 mm), with a runoff coefficient of 23%. Note that irrigation is not considered for the computation of runoff coefficient in this last watershed.

3.3.2. Dynamics in dissolved solids and suspended sediment concentration

The degree of variation in TDS concentration in the different watersheds (Fig. 3.2) was relatively low. TDS concentration, average and median values were relatively similar ($\pm 2\%$, Table 3.3), and the coefficient of variation (CV) was low, ranging from 13 to 20% in the different watersheds.

Regarding the specific values obtained (Table 3.3), TDS concentrations were the highest in Landazuria (median: 2275 mg L^{-1} ; inter-quartile range (IQR): 1960 to 2547 mg L^{-1}), followed by La Tejería (median: 547 mg L^{-1} ; IQR: 494 to 612 mg L^{-1}), Latxaga (median: 482 mg L^{-1} ; IQR: 440 to 529 mg L^{-1}), Oskotz Principal (median: 420 mg L^{-1} ; IQR: 376 to 475 mg L^{-1}) and Oskotz Forested (median: 327 mg L^{-1} ; IQR: 300 to 355 mg L^{-1}). Median TDS concentration in each watershed was significantly different (Wilcoxon-Mann-Whitney Rank-Sum Test, $p < 0.001$; Helsel and Hirsch, 2002) than that in any other watershed.

Table 3.3: Selected statistics of daily average discharge (Q , L s^{-1}) and dissolved solids (TDS, mg L^{-1}) concentration in the studied watersheds for the hydrological years (Oct-Sep) 2007-2016.

Watershed	La Tejería		Latxaga		Oskotz Principal		Oskotz Forested		Landazuria	
	Q	TDS	Q	TDS	Q	TDS	Q	TDS	Q	TDS
N	3653	2532	3653	2425	3653	3190	3653	3040	3653	2982
Perc. 05	0	429	0	390	0	279	0	256	5	1620
Quar. 1	0	494	0	440	9	376	3	300	8	1960
Median	1	547	2	482	76	420	19	327	12	2275
Quar. 3	10	612	12	529	280	475	70	355	17	2547
Perc. 95	52	713	80	629	1512	577	415	388	30	2918
Perc. 99	170	768	220	722	4120	637	1047	415	63	3051
Maximum	625	1075	553	1066	10788	958	2840	462	545	3534
IQR	10	119	12	89	271	99	67	55	9	587
Average	12	556	16	492	342	426	89	326	15	2259
S.D.	34	89	41	79	821	87	215	42	17	397
C.V. (%)	284	16	251	16	240	20	242	13	117	18
Avg./Median	8.08	1.02	8.45	1.02	4.51	1.01	4.73	1	1.26	0.99

N: Number of samples; Perc: Percentile; Quar: Quartile; IQR: inter-quartile range; S.D.: Standard deviation; C.V.: Coefficient of variation

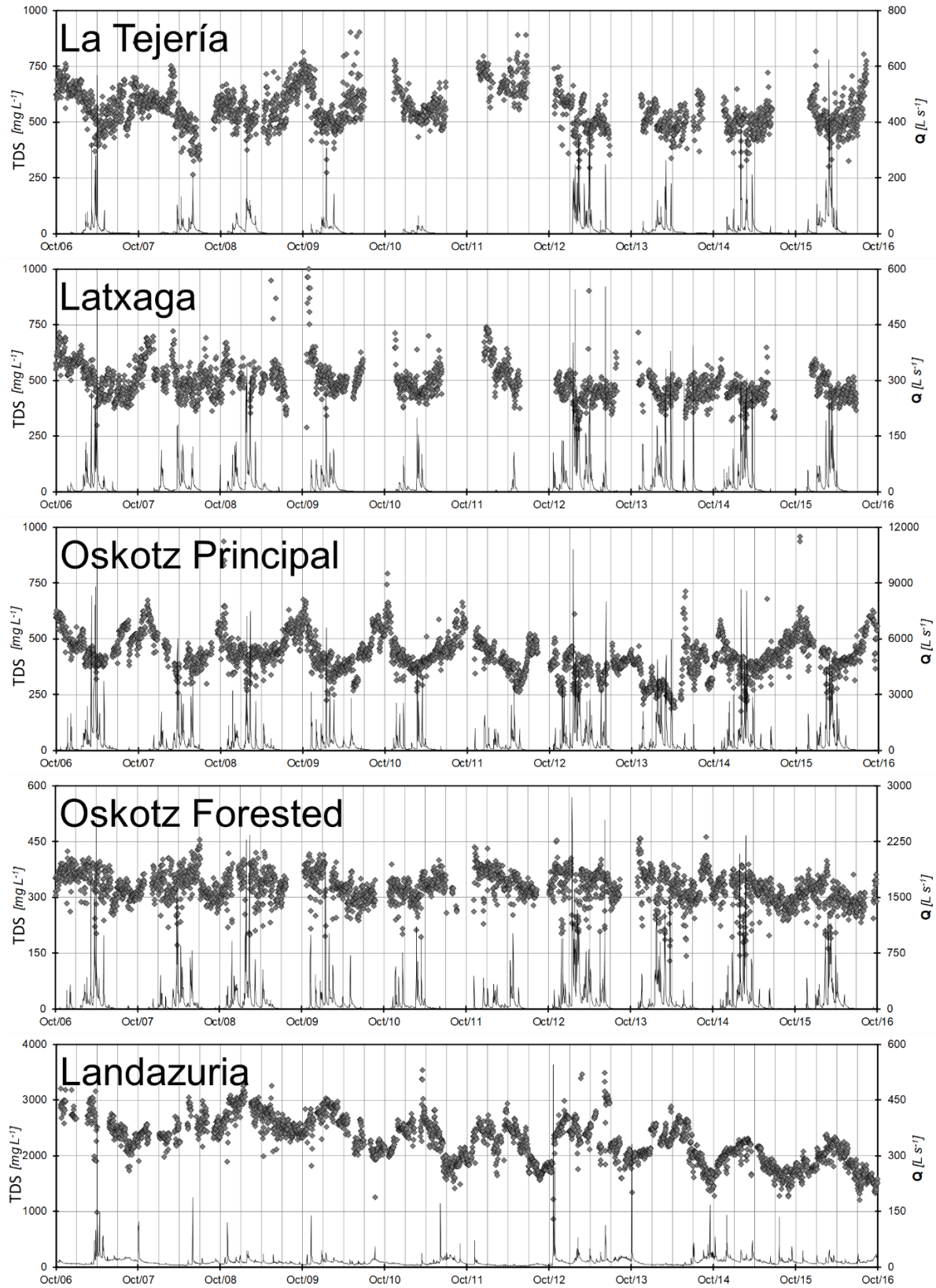


Figure 3.2: Daily total dissolved solids concentration (TDS) and discharge (Q) in the Navarrese watersheds during the hydrological years 2007-2016.

TDS concentration presented a characteristic seasonal pattern in every watershed. In the non-irrigated watersheds (namely La Tejería, Latxaga and both stations in Oskotz), the highest TDS concentrations were observed at the end of the summer, late September to early November (Fig. 3.2). This pattern was detected even in those summers where sampling was cancelled due to low-flow conditions. A clear increasing trend was observed before the summer data gap, while a decreasing trend follows it (example in Fig. 3.2, Latxaga). In contrast, the lowest recorded concentrations tend to occur in winter months, although in some occasions this period is slightly delayed, with lower concentrations in spring months. However, the dynamics of TDS concentration in the irrigated watershed (namely Landazuria) were opposite to that observed in the non-irrigated (Fig. 3.2, Landazuria), with the highest concentrations recorded in late autumn to early winter and the lowest ones in summer, coinciding with the irrigation season.

The seasonal pattern in TDS concentration was clearly related to the available runoff in each watershed. For both the non-irrigated and the irrigated watersheds, the high TDS values correspond with the periods in which discharge is smaller, whereas the low TDS values were recorded during the wet season (in the non-irrigated watersheds) or the irrigated season (in the irrigated watershed). Deviations from this seasonal pattern were observed in all watersheds in response to significantly increased discharge in the outlets (Fig. 3.2). In fact, the lowest TDS concentrations were recorded for individual samples collected in days in which significant hydrograph peaks were also recorded. All in all, a relationship was inferred between discharge (Q) and TDS concentration (Fig. 3), with significant ($p < 0.05$) negative Spearman's ρ (-0.19 to -0.65) (Helsel and Hirsch, 2002). Oskotz Forested was the only exception with a slightly positive correlation (Spearman's $\rho = +0.06$) between Q and TDS, although the lowest TDS in this watershed were recorded for Q values over 1000 L s^{-1} (Fig. 3.3).

Regarding the inter-annual variation, rather similar patterns were observed in TDS concentration throughout the study period, although subtle differences were indeed observed. For instance, both 2011 and 2012 were quite dry in La Tejería (more than one standard deviation below the average, Table 3.2) which may explain the high TDS concentrations recorded in 2012 (Fig. 3.2). In contrast, the years 2013 and 2014 were above average regarding precipitation in Oskotz, which may explain the lowest TDS concentration values in the winter of 2014 (Fig. 3.2).

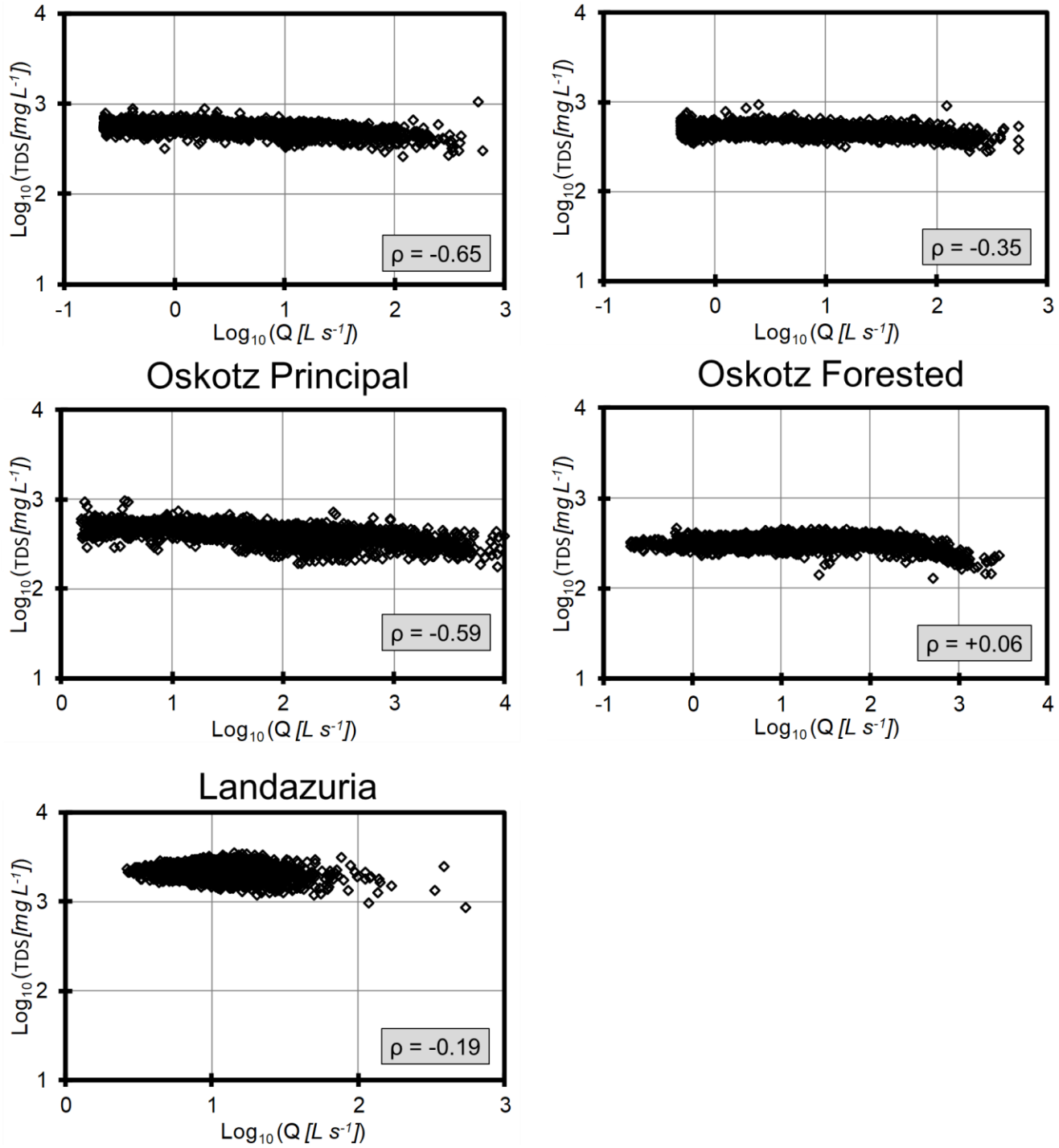


Figure 3.3: Relationship (double-logarithmic scale) between discharge (Q) and the concentration of total dissolved solids (TDS) in the Navarrese watersheds. The degree of correlation ($p < 0.05$) between variables is indicated by the Spearman's ρ (Helsel and Hirsch, 2002).

3.3.3. Dynamics in the exported loads of TDS and SS

The dynamics in the exported loads were greatly conditioned by the availability of runoff water in the case of total dissolved solids loads (TDSL). In fact, the TDSL presented a clear seasonal pattern similar to that of accumulated water yield (Q), both for typical (median) and extreme (95th percentile) hydrological conditions for every single watershed (Fig. 3.4). In contrast, suspended sediment loads (SSL) did not clearly follow the Q pattern (median, Fig. 3.4), being the median SSL negligible for most of the months. However, SSL were severely modified when considering the 95th percentile. Perceptible loads were registered in all watersheds, with a significant contribution to the total load (i.e., both dissolved and suspended loads) in the non-irrigated watersheds (Fig. 3.4). In fact, Latxaga presented SSL in the same order of magnitude than TDSL, whereas La Tejería presented SSL clearly higher than TDSL. It is important to note that those high-flow conditions depicted here by the 95th percentile have a higher weight in determining the total annual loads.

The pattern of Q, TDSL and SSL in relation with the accumulated time is represented in Fig. 3.5. These plots were constructed using only those periods for which there was information available for every variable. In the non-irrigated watersheds, there was a significant proportion of the study period in which the discharge was negligible (the gauging station had no measurable flowing water). For instance, 58% of the time was required to export 5% of the total water yield in La Tejería, 55% in Latxaga, 58% in Oskotz Principal, and 53% in Oskotz Forested, whereas 14% of the time exported 5% of total water in Landazuria (Fig. 3.5). In general, the accumulated TDSL presented a pattern similar to that of the water yield, supporting the conservative behaviour of dissolved solids in water. Regarding SSL, do not follow the water yield pattern. Its episodic character was clearly detectable for all watersheds. Producing in a 5% of the time 85%, 94%, 89%, 93% and 89% of the SSL in La Tejería, Latxaga, Oskotz Principal, Oskotz Forested and Landazuria, respectively (Fig. 3.5).

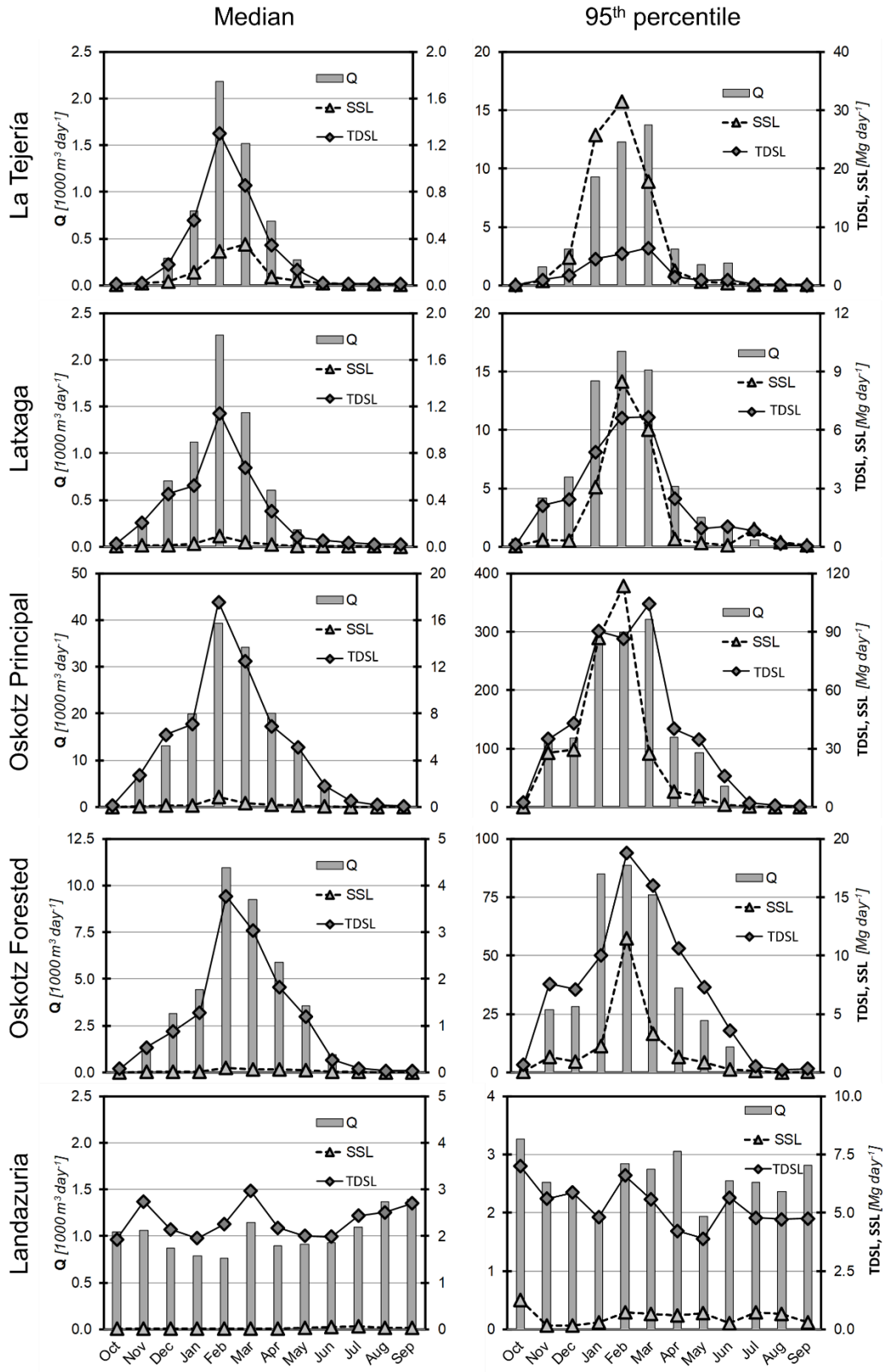


Figure 3.4: Median and 95th percentile of the daily discharge (Q) and total dissolved solids load (TDSL) in the Navarrese watersheds.

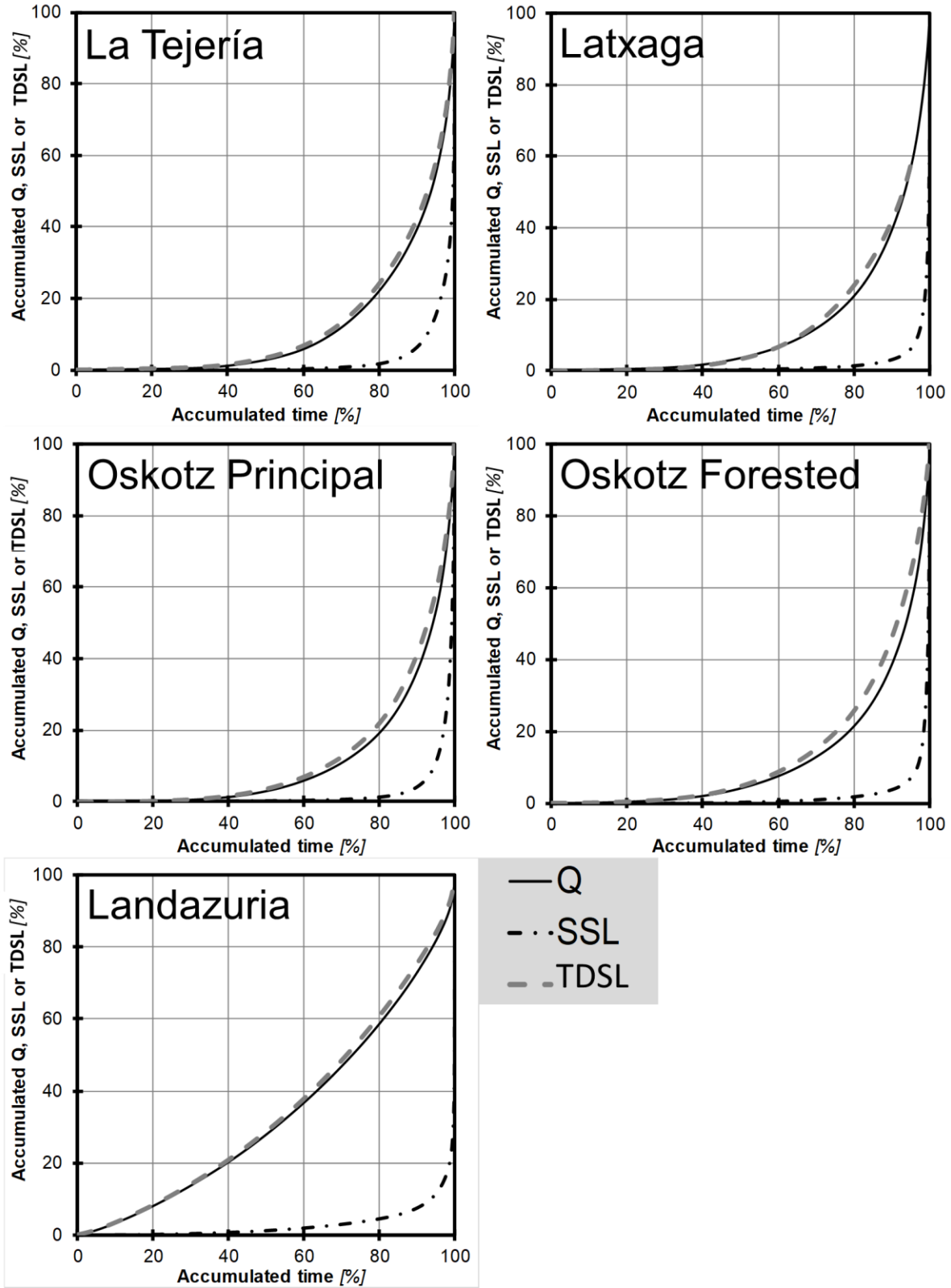


Figure 3.5: Accumulated discharge (Q), total dissolved solids loads (TDSL) and suspended sediment loads (SSL) versus accumulated time in the Navarrese watersheds.

3.3.4. Estimation of annual TDS and SS yield during the hydrological years 2007-2016

The estimated total dissolved solids yield (TDSY) for the different watershed and methods used are presented in Table 3.4. All methods provided consistent results. However, the regression method presented significantly biased estimates (>25%) in four out of five watersheds for suspended sediment. Suspended sediment yield (SSY), were subject to a higher degree of uncertainty than those of TDSY. According to Gulati et al., (2014), regression methods are not appropriate for many agricultural streams, where pollutants concentrations and flows are not correlated.

Table 3.4: Results from different methods for load estimations for total dissolved solids yields. All values in Mg ha⁻¹ year⁻¹.

Estimation method	La Tejería	Latxaga	Oskotz Principal	Oskotz Forested	Landazuria
Numeric Integration	1.07	1.12	2.24	1.88	2.17
Regression	1.06	1.11	2.24	1.91	2.16
Ratio Estimator	1.06	1.10	2.21	1.84	2.13

Representative annual yield estimates (numeric integration method) are presented in Table 3.5. During 2007-2016, the average TDSY in the studied watershed was was 1.1, 1.1, 2.2, 1.9 and 2.2 Mg ha⁻¹ year⁻¹ for La Tejería, Latxaga, Oskotz Principal, Oskotz Forested and Landazuria, respectively.

Table 3.5: Runoff (mm), suspended sediment yield (SSY, Mg ha⁻¹) and dissolved solids yield (TDSY, Mg ha⁻¹) for the studied watersheds during the hydrological years 2007-2016. Presented yields were computed by numerical integration method (see Table 3.4).

	La Tejería			Latxaga			Oskotz Principal			Oskotz Forested			Landazuria		
	Runoff	SSY	TDSY	Runoff	SSY	TDSY	Runoff	SSY	TDSY	Runoff	SSY	TDSY	Runoff	SSY	TDSY
2007	256	1.6	1.4	234	1.4	1.1	802	1	3.3	571	1.1	1.8	130	0.3	3.2
2008	177	2.1	0.8	201	0.5	0.9	575	0.5	2.1	543	0.6	1.7	79	0.1	1.9
2009	267	8.3	1.3	287	5.7	1.4	563	1.2	2.1	727	0.7	2.3	92	0.1	2.5
2010	161	6.1	0.8	185	0.4	0.9	507	1.7	1.8	502	0.4	1.5	89	0	2.2
2011	72	2.3	0.4	127	0.2	0.6	348	1.3	1.3	357	0.3	1	85	0.1	1.8
2012	4	0.1	0	38	0.1	0.2	346	0.2	1.3	353	0.2	1.2	42	0	0.9
2013	415	11.4	1.9	513	2.6	2.2	1151	2.8	3.8	1275	2.5	3.7	143	0.2	3.1
2014	219	1.2	1.1	344	1.5	1.5	712	0.1	2	704	0.8	1.9	94	1.6	1.8
2015	269	2.5	1.2	316	1.2	1.3	768	2.2	2.4	790	1.4	2	133	0.4	2.5
2016	382	7	1.8	249	0.3	1.1	620	0.5	2.2	639	0.6	1.7	96	0	1.8
Average	222	4.3	1.1	250	1.4	1.1	639	1.1	2.2	646	0.9	1.9	98	0.3	2.2
S.D.	126	3.7	0.6	129	1.7	0.5	238	0.9	0.8	265	0.7	0.7	30	0.5	0.7
C.V. (%)	57	87	55	52	123	49	37	76	36	41	83	39	30	172	32
Total Yield (TDSY + SSY)	-	80%	20%	55%	45%		34%	66%		31%	69%		12%	88%	

The highest TDSY were obtained for two rather different watersheds. On the one hand, Oskotz Principal presented one of the highest water yield and one of the lowest TDS concentrations. On the other hand, Landazuria presented the highest TDS concentration and the lowest water yield. However, the TDSY was similar in both watersheds (2.2 Mg ha⁻¹ year⁻¹). The lowest TDSY was estimated for the winter cereal watersheds (La Tejería and Latxaga), which presented similar values despite minor differences in water yields and TDS concentrations. Intermediate values were obtained in Oskotz Forested (1.9 Mg ha⁻¹ year⁻¹). The inter-annual variability in TDSY for all watersheds could be explained mostly by the variability in the water yield, with rather similar CV for water and annual TDSY (Table 5). In fact, the annual TDSY was linearly correlated to water yield (Pearson's *r* between 0.91 and 0.99 for the different watersheds; Helsel and Hirsch, 2002).

Finally, the contribution of TDSY to the total yield (understood in this study as the sum of both SSY and TDSY) differed greatly among watersheds. TDSY represented 20%, 45%, 66%, 69% and 88% of the total yield in La Tejería, Latxaga, Oskotz Principal, Oskotz Forested and Landazuria, respectively, although these percentages were rather variable among different years (Table 3.5). Thus, TDSY dominated in the forests/pastures and irrigated watersheds.

3.4. DISCUSSION

3.4.1. Total dissolved solids concentration and loads

Dissolved solids concentrations in rivers are normally controlled mainly by the geology and the climate of the watershed (Millman and Farnsworth, 2001). However, under similar geological/climatological conditions, the role of other factors can be detected. In fact, several authors have reported higher TDS concentrations in agricultural watersheds than in non-agricultural ones under similar geological/climatological conditions (e.g., Swiechowicz, 2002; Pacheco-Betancur, 2013). The increase in TDS normally is associated with the presence of solutes derived from fertilizers application (such as NO_3^-) (Merrington et al., 2002), but also with some other constituents (such as Ca^{2+} or Mg^{2+}) associated with increased weathering as a consequence of biogeochemical reactions between soil minerals and fertilizers (Menció et al., 2016).

In the Navarrese watersheds, the rainfed winter cereal watersheds (La Tejería and Latxaga) presented relatively similar geological/climatological characteristics. However, La Tejería (median: 547 mg L^{-1}) presented TDS concentrations higher than Latxaga (median: 482 mg L^{-1}), probably as a consequence of the higher NO_3^- concentrations in La Tejería (median: 73.5 mg L^{-1}) than in Latxaga (median: 21.0 mg L^{-1}). In fact, the higher amount of NO_3^- in La Tejería (along with some cations to compensate its negative charge) is enough to explain the differences in TDS concentration between the rainfed winter cereal watersheds.

Oskotz Principal and Forested also presented similar geological and climatological characteristics. In this case, differences in NO_3^- concentrations (medians of 9.6 and 3.6 mg L^{-1} in Principal and Forested, respectively) are not enough to justify the differences in TDS concentration (Principal: 420 mg L^{-1} ; Forested: 376 mg L^{-1}). In Oskotz Principal approximately one third of the watershed surface is covered by pastures and grassland that are intensively managed and grazed, which can explain the increase in TDS concentration in relation with its more forested counterpart (i.e., the contribution of animal urine and faeces to dissolved solids concentration). In addition, there are two small villages (ca. 100 inhabitants in 2014) within the watershed whose wastewater could add some dissolved solids to the stream.

Among the Navarrese watersheds, TDS concentrations were the highest in the irrigated watershed (Landazuria, median of 2275 mg L^{-1}) as a consequence of the high salinity of the soils and

geological materials of the watershed (Merchán et al., 2018). In addition, the seasonal cycle in TDS concentration was different from the one observed in the non-irrigated watersheds as a consequence of the dilution effect of irrigation water applied in summer. Our results are consistent with those reported for other irrigated areas in which lower TDS concentrations were observed during the irrigation season (Tedeschi et al., 2001; Merchán et al., 2013). In fact, a decreasing trend in TDS concentration associated with a wash out of available soluble salts is observed, as reported elsewhere (Merchán et al., 2018).

Finally, all of the Navarrese watersheds reported in this study presented: (i) a clear seasonal cycle in TDS concentration; (ii) a significant negative relationship between discharge and TDS concentration; and (iii) a strong relationship between annual water yield and dissolved solids yield (see Section 3.3.2, 3.3.3, and 3.3.4). Other studies in small watersheds have reported similar seasonal variation in TDS concentration (e.g., Swiechowicz, 2002; Durán Zuazo et al., 2012), significant negative correlation between TDS concentration and discharge (Llorens et al., 1997; Durán Zuazo et al., 2012). In addition, as for the studied watersheds in Navarre, TDSL mirrored the pattern observed in discharge in other studies (e.g., Tedeschi et al., 2001; Durán Zuazo et al., 2012; Merchán et al., 2013). In fact, this pattern is also observed in non-agricultural areas (Hubbard et al., 1990; Butler and Ford, 2018). Besides, similar observations regarding the relationship of TDSY and water yield have been reported in other studies conducted at the small watershed scale (e.g., Pacheco-Betancur, 2013; Swiechowicz, 2002; Tedeschi et al., 2001).

3.4.2. Total dissolved solids in small watersheds

Up to this point in our discussion, comparison with other studies has been made considering general patterns and processes rather than specific values or estimations. It is important to note that the results obtained in the different Navarrese watersheds may be adequately inter-compared, since they follow the same methodology over a long and similar study period. However, any comparison of our quantitative results with any other available in the literature must be considered with caveats. Among the different previous studies, there are differences in the definition of the variables (for instance, constituents considered for TDS computation), in the used sampling strategy (frequency, consideration of flood events sampling, simple or composite samples), in the load estimation methods (from simple interpolation to more complex methods), in the study period (what may influence estimations, especially those of suspended sediment yield), etc. In fact, the

lack of comparability among watersheds due to methodological issues has been manifested by other authors (e.g., Zabaleta et al., 2007; Millman and Farnsworth, 2011; Vanmaercke et al., 2011). For that reasons, in the following sections, any comparison with other studies is intended as an illustrative example rather than an exhaustive analysis of the particular methods used and results obtained in a range of studies, which is out of the scope of this paper.

3.4.3. Total dissolved solids yield in small watersheds

The vast majority of data available in the literature regarding TDSY in small watersheds refers to irrigated areas. In these areas, the accumulation of salts in soils and the leaching of salt are relevant management options and therefore have received considerable attention in research studies. In fact, irrigated areas are usually located in arid and semi-arid areas where salts build up in the soils has occurred historically (e.g., Merchán et al., 2018). For instance, in irrigated areas of the Ebro River Basin (northeast Spain), even after subtracting the inputs from precipitation or irrigation, the net TDSY can reach ca. 20 Mg ha⁻¹ year⁻¹ in flood irrigated saline soils, whereas it can be as low as 0.5 Mg ha⁻¹ year⁻¹ in mature pressurized irrigation systems (data compiled in Merchán et al., 2015). In comparison, scarce data is available in non-irrigated watersheds. For instance, in small watersheds in the Pyrenees (northeast Spain), TDSY ranged from 0.98 to 2.3 Mg ha⁻¹ year⁻¹ (Nadal-Romero et al., 2012). Values of around 1 Mg ha⁻¹ year⁻¹ were reported for watersheds under natural (forest) or semi-natural (recolonization of shrubs and forests) conditions. Higher values were reported for high-mountain watersheds (1.7 Mg ha⁻¹ year⁻¹), probably as a consequence of a higher runoff, and the maximum (2.3 Mg ha⁻¹ year⁻¹) was reported for a watershed with badlands in a significant proportion of its surface (Nadal-Romero et al., 2012). A watershed (6.7 km²) in southern Spain with mixed land use (forest, shrubs, grassland and farms) presented 32.7 Mg ha⁻¹ year⁻¹ (Durán Zuazo et al., 2012). This high value was related to the high salinity of the soils parent material. In England, 1.1 Mg ha⁻¹ year⁻¹ was reported by Carling (1983) in a heavily grassed, relatively undisturbed watershed (2.2 km²).

In the Navarrese watersheds, rainfed winter cereal watersheds presented TDSY values similar to that of natural or seminatural watersheds in the Pyrenees or north England. The forested watershed presented similar values to that reported for other forests in mountainous areas. The irrigated watershed presented the highest TDSY of the Navarrese watersheds, but it is in the lower end of

other irrigated areas, as expected for pressurized irrigation systems with an efficient use of irrigation water (Merchán et al., 2015).

Thus, the differences in TDS exports between agricultural and non-agricultural watersheds are minimal, being these differences justified by other factors, mainly the salinity of soils/geological materials and the climate (Section 4.1). Only in irrigated watersheds, where a huge modification of the water balance is observed (e.g., Tedeschi et al., 2001; Merchán et al., 2013; Merchán et al., 2018), a significant increase in the export of TDS is expected. In this sense, agricultural land uses expected to increase water yield (such as a shift from forested to arable land, or from rainfed to irrigated agriculture) would increase the TDS exports (Scanlon et al., 2007).

3.4.4. Contribution of total dissolved solids to total loads

Among those studies conducted in small watersheds in which TDS and SS have been assessed, TDS contribution tended to dominate the total exported loads. For instance, in a small (36 ha) terraced agricultural watershed that had been abandoned, the estimated TDSY ($0.15 \text{ Mg ha}^{-1} \text{ year}^{-1}$) was almost four times higher than SSY ($0.04 \text{ Mg ha}^{-1} \text{ year}^{-1}$) (monitoring time: 1.5 years; Llorens et al., 1997). TDSY contributed to 80% of total yield in a heavily grassed watershed (2.2 km^2) in north England (Carling, 1983). In a flood-irrigated agricultural watershed (643 ha) 98% of the total load was in soluble form (Lasanta et al., 2001). Both Swiechowicz (2002) and Durán Zuazo et al. (2012) reported TDS loads as 95% of total loads in mixed land use (shrubs, forest and agricultural) watersheds (22.4 and 6.7 km^2 , respectively). Pacheco-Betancur (2013) analysed a watershed with two hydrological stations, one of them draining mainly forest whereas the second one was mainly arable land. This author found that TDS dominate the total load in both the forested and the arable area. In a comprehensive assessment of four watersheds in the Pyrenees considering dissolved, suspended and bed loads, Nadal-Romero et al. (2012) reported the dominance of TDS in the exported loads for the Arnás (natural shrubs and forest colonization, 61% TDS), Izas (high-mountain grasslands, 70% TDS) and San Salvador (natural forest, 74% TDS). Only a watershed severely affected by badlands (26% of its surface) presented dominance of SS (Araguás, 95% SS, Nadal-Romero et al., 2008, 2012).

As can be seen, most of the available studies in the literature were conducted in natural or semi-natural areas. Our results on agricultural watersheds (Section 3.4) in combination with the literature reviewed suggest a shift in the dominance from TDS to SS in the exported loads in small

watersheds. This shift is consistent with the higher SS exports expected in arable lands (e.g., Montgomery, 2007; Cerdan et al., 2010; García-Ruiz et al., 2015) while TDS exports are not severely modified under arable land use (unless the watershed under consideration is irrigated, as elaborated in previous paragraphs). Indeed, as Milliman and Farnsworth (2011) reported for high-order rivers, “it is the difference in physical delivery (or lack thereof) of sediment that seems to be the key factor in determining whether a river is sediment- or dissolved-dominated”.

3.5. CONCLUSIONS

From the presented data in the Navarrese watersheds and that available in the literature, the effects of agricultural land use in the dynamics of concentration and exported loads of TDS at the small watershed scale can be summarized as follows:

- The temporal dynamics of TDS concentration and loads are controlled by the fact that TDS are conservative with water, i.e., its dynamics are associated to that presented by water. As a consequence, TDS concentration and loads are mostly controlled by the geological/climatological characteristics of the watershed and consequently follow a seasonal cycle. There are no important differences in these temporal dynamics among different land uses, as depicted by the similar general behaviour in a range of agricultural and non-agricultural land uses both in the Navarrese watersheds and in the literature.
- Agricultural land use seems to increase the TDS concentration in the drainage water, probably due to the contribution of dissolved constituents via fertilizers or livestock excreta and a more easily chemical weathering of tilled soils. However, the variability among watersheds imposed by natural factors (such as salinity of soils/geological materials or climate) is usually higher than the effect of agricultural land use. Regarding TDS loads, no clear pattern is observed since it is mainly controlled by the water yield dynamics. In this sense, agricultural land uses expected to increase water yield (such as a shift from forested to arable land, or from rainfed to irrigated agriculture) would increase the TDS exports.
- The variability of TDS yield among watersheds with different characteristics (including land use) is mainly explained by differences in water yield, and it is lower than that of SS yield. Out of the total yield (TDS + SS), TDS yield normally dominates under non-agricultural and agricultural land uses. However, SS yield becomes dominant under watersheds with predominantly arable land and environmental conditions that facilitate sediment export.

CHAPTER 4:
**Evaluation of an overland flow connectivity
index at two Mediterranean agricultural
watersheds**

4.1. INTRODUCTION

The environmental impairment caused by agricultural activity is an issue of global concern. As has been reported in previous chapters, agricultural intensification to satisfy world food demands has led to an increase in the use of heavy machinery and fertilizers (Merrington et al., 2002), which can lead to an excess of nutrient inputs to agricultural land, causing nutrient losses. This leaching enhances the negative effects of pollutants on freshwater ecosystems (Durand et al., 2011).

In response to this concern, different governments and institutions have implemented experimental agricultural watershed networks, which are a very widespread measure to control the effects of anthropogenic activity on the environment. In Europe, watershed networks have been implemented in different areas to evaluate and quantify agricultural pollutants, such as in the Baltic region (Lagzdins et al., 2012; Kyllmar et al., 2014; Povilaitis et al., 2014), the British region (Hooda et al., 1997; Lloyd et al., 2014; Ockenden et al., 2017) and the Mediterranean region (Pieri et al., 2011; De Girolamo et al., 2017).

Even though agricultural watershed networks have been an important advance in the understanding of pollutant dynamics in environments affected by anthropogenic activity, these networks have traditionally been described through black-box approaches (Black, 1996). This approach is not sufficiently accurate to understand the effects of anthropogenic activity in the future, nor to determine precisely the causes of the processes occurring in the environment (Frisbee et al., 2012). To better understand the processes occurring in watersheds, in addition to lower-scale component analysis inside the watershed (sub-watershed, plot, or soil profile analysis), different concepts and tools are developed such as watershed modeling or flow connectivity.

Regarding flow connectivity, it is a term that has been described in many ways (Ali and Roy, 2009), even though the most widely accepted definition is the one that understands it as the connection, via overland and subsurface flow system, between the riparian and the upland zones (Bracken et al., 2013). Bracken and Croke (2007) describe connectivity as a concept related to hydrology and geomorphology, which is divided into landscape connectivity, hydrological connectivity, and sedimentological connectivity. The integration of these three types of connectivity (especially hydrological and sedimentological connectivity) results in a combined connectivity concept that Borselli et al. (2008) define as flow connectivity. Borselli et al. (2008)

developed an overland flow connectivity (OFC) index to characterize the flow connectivity in a watershed. OFC attempts to identify flow connectivity of each part of a watershed, in a semi-quantitatively manner, based primarily on a digital elevation model (DEM). This structural connectivity refers to the potential flow connectivity of each reference element in the watershed. The OFC index has undergone modifications in its application in different watersheds. For instance, Cavalli et al. (2013) adapted the index to better identify sediment connectivity in alpine watersheds, while López-Vicente and Ben-Salem (2019) added specific variables that allowed the identification of functional connectivity over time through an aggregated connectivity index (AIC). This functional connectivity represents the flow connectivity of each reference area throughout the different seasons and different vegetation, among other factors. The study of OFC with these indices can be useful in the understanding of nutrient dynamics in different watersheds. The analysis of OFC can be helpful in the identification of different forms of nutrients, both dissolved and sediment-attached. Regarding dissolved compounds, runoff connectivity is an important factor in the analysis of TDS and nutrient dynamics (Merrington et al., 2002). In aquatic ecosystems, one of the most harmful forms of nutrients is nitrate (Durand et al., 2011). This compound is highly soluble and highly mobile and is crucial in eutrophication processes (Merrington et al., 2002). Therefore, correct detection of the OFC of runoff is very important to the analysis of dissolved nutrient dynamics.

In Navarre (northern Spain), the former Department of Agriculture, Livestock, and Food of the Government of Navarre implemented a network of experimental agricultural watersheds to evaluate and monitor soil erosion and water quality in different areas with a representative land use of the region. Several studies have been carried out in these watersheds, focusing on nutrient and salt dynamics (Merchán et al., 2018; Hernández-García et al., 2020) and soil erosion and sediment transportation (Casalí et al., 2008, 2010; Giménez et al., 2012; Merchán et al., 2019). Assessment of connectivity in these watersheds can help to improve the understanding of the dynamics observed in previous works.

Intending to deepen knowledge on the dynamics of dissolved solids (such as nutrients) in agricultural watersheds, the specific objectives of this study are: (a) to implement an OFC index based on Borselli et al. (2008) and the modifications proposed by Cavalli et al. (2013) and López-Vicente and Ben-Salem (2019); and (b) to evaluate the OFC index at two rainfed winter cereal

watersheds with similar management and climatic characteristics, and observe its suitability to explain TDS and nutrients dynamics in typical agricultural environments of Navarre.

To this end, a critical review of the parameters and algorithms of each of the indices was carried out, selecting the most appropriate for subsequent application to the Navarrese watersheds.

4.2. METHODS

4.2.1. Experimental watersheds of the study

This study was carried out in the rainfed cereal watersheds of Latxaga and La Tejería (Fig. 4.1) within the network of experimental watersheds of the Government of Navarre. A detailed description of their particularities can be found in Section 2.1 of Chapter 2

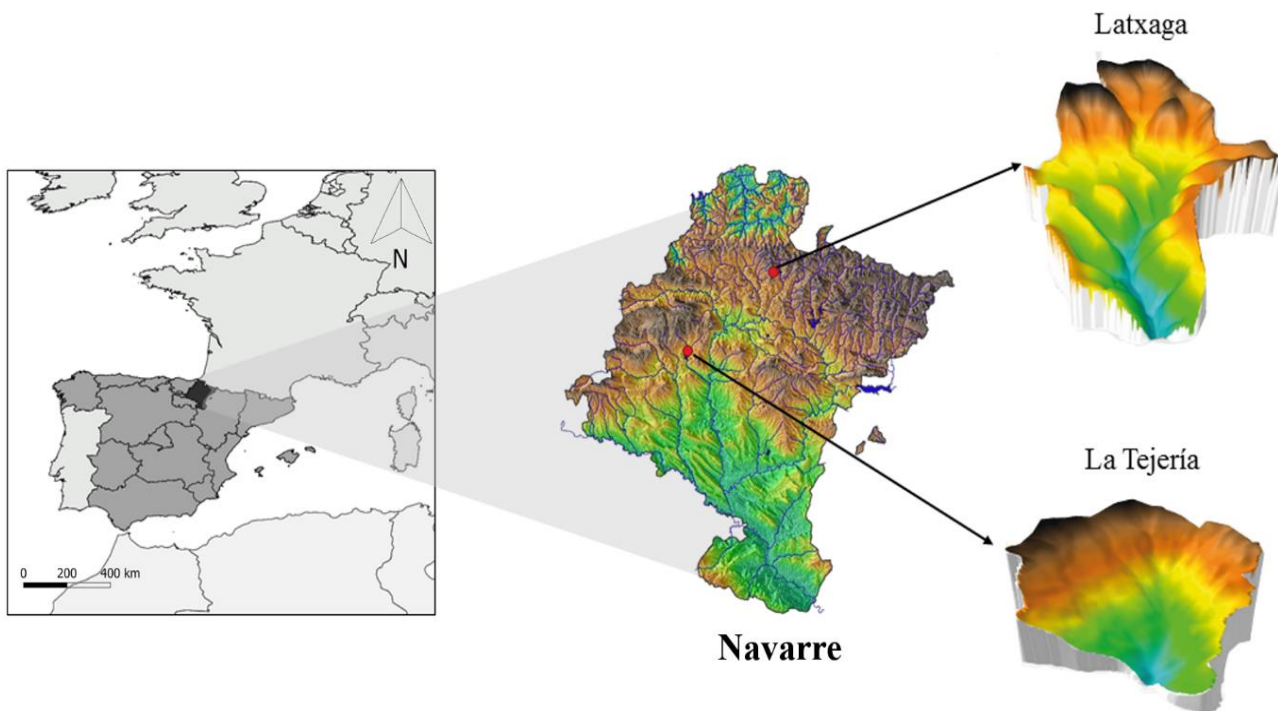


Figure 4.1: Location of the Latxaga and La Tejería watersheds, two experimental agricultural watersheds of the Government of Navarre.

4.2.2. Overland Flow Connectivity index

This study evaluates an OFC index based on Borselli et al. (2008) and the modifications proposed by Cavalli et al. (2013) and López-Vicente and Ben-Salem (2019). This index was developed from the calculations of the three proposed approaches, which are presented next, selecting the more suitable parameters, algorithms, and tools for the Navarrese conditions.

The OFC indices for watersheds presented herein are derived from the original OFC index (Borselli et al., 2008). These semi-quantitative indices are based on the downslope (Ddn) and

upslope (Dup) components, obtained by parameters derived from a DEM (Fig. 4.2) and considering the drainage area and characteristics of the flow path. The Ddn component is based on the runoff or sediment particle capacity of a reference element to arrive at a sink along the flow path. The distance between the source area and the sink is affected by a weighting factor that reflects the impediment for runoff generation or sediment transport, and slope (Eq. 4.1). Dup component is the potential for downward routing of the runoff and sediment produced upslope. In this component, in addition to the weighting factor and slope, the contributing area of the analyzed point is also considered (Eq. 4.1).

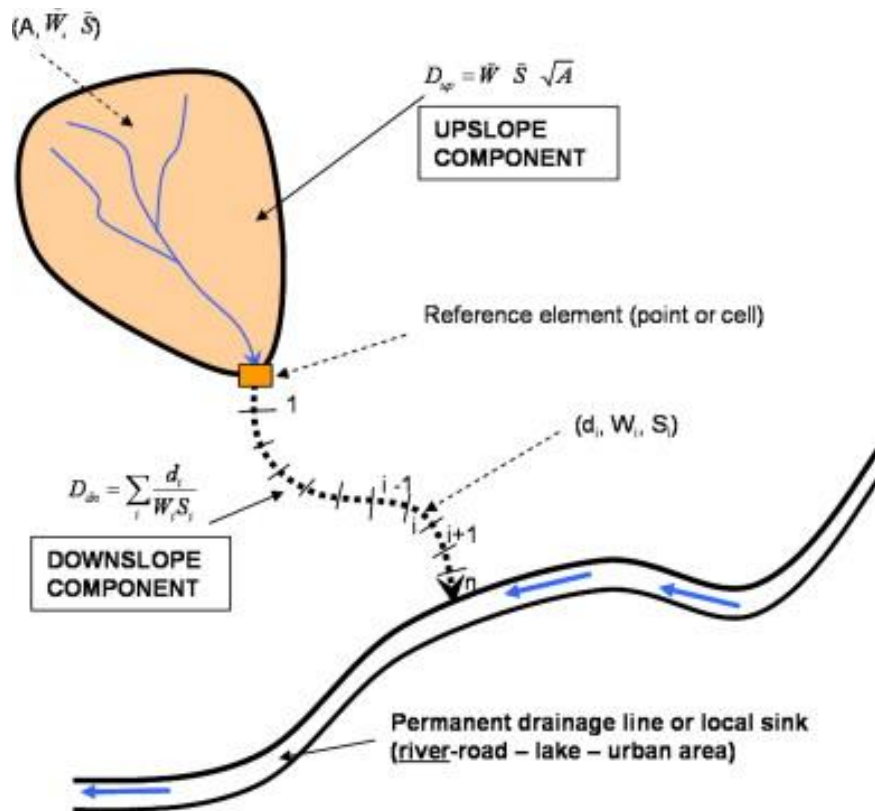


Figure 4.2: Flow connectivity index approach proposed in Borselli et al. (2008)

The computation of the index is performed for each pixel (reference element) of the watershed, whose size is defined by the chosen DEM, and determined by Equation 4.1:

$$IC_k = \log_{10} \left(\frac{D_{up,k}}{D_{dn,k}} \right) = \log_{10} \left(\frac{\bar{W}_k \bar{S}_k \sqrt{A_k}}{\sum_{i=k, n_k} \frac{d_i}{W_i S_i}} \right) \quad \text{Eq. 4.1}$$

For a reference element k , \bar{W} is the weighting factor of the upslope contributing area (dimensionless), \bar{S} is the slope gradient of the upslope contributing area (m/m), A is the upslope contributing area (m²), d_i is the length of the i th cell along the downslope path (m), W_i is the weight of the i th cell (dimensionless), and S_i is the slope gradient of the i th cell (m/m).

Regarding the weighting factor (related to the impediment of runoff generation and sediment transport) used in the original OFC index, Borselli et al. (2008) employed the RUSLE C-factor, which was defined as the proportion of soil loss from land with a specific crop/vegetation, and its value depends on the vegetation cover and management practices. This factor ranges between 0 and 1, reaching its maximum value when the soil is at the highest risk of erosion, and minimum value when soil is protected from erosion (Wischmeier and Smith, 1978). The RUSLE C-factor is very suitable to describe the impediment of runoff and sediment flow processes in agricultural and forest environments (Renard et al., 1997). In the original version of the OFC index, the contributing area was calculated by the single-flow direction algorithm (O'Callaghan and Mark, 1984), and a value of 0.005 m/m was added to the minimum computed values of slope (S) to avoid infinite values of the Ddn component of the index.

4.2.2.1. OFC index modifications

Some authors proposed modifications to the original index of Borselli et al. (2008), to improve adaptability to specific study sites, and enhance the connectivity results in a specific area.

In addition to the lower limit of 0.005 m/m proposed by Borselli et al. (2008), Cavalli et al. (2013) set an upper limit of 1 m/m. The reason for setting this upper value was physical. Cavalli et al. (2013) used an alpine environment as a reference to define this modification. In this case, the areas with high slopes were due to cliffs or very steep slopes with hardly any accumulation of sediment. Therefore, in these environments, particle mobility is more probably caused by rockfall than by sediment or runoff movement, which is more linked to the concept of connectivity.

Regarding the contributing area (A), Cavalli et al. (2013) proposed the use of the D-infinite algorithm (Tarboton, 1997). This algorithm does not restrict the flow direction to only eight directions such as the single-flow algorithm and provides a much more realistic result, avoiding the unrealistic flow overdispersion observed in other algorithms (Cavalli et al., 2013).

Concerning the W parameter, Cavalli et al. (2013) used a roughness index (standard deviation of the residual topography) as a weighting factor. A more objective value was achieved, less conditioned by factors pertaining to agricultural environments (RUSLE C-factor). Cavalli et al. (2013) focused their connectivity work on alpine areas where the RUSLE C-factor is not adequate, as it is intended for agricultural or vegetated areas. The roughness index is more suitable for modeling alpine mass movement processes (e.g. debris flows).

Following the modifications suggested by Cavalli et al. (2013), many studies have modified the characteristics of the original index by adding different weighting factors that adapt to the characteristics of the watersheds under study. Gay et al. (2016) added the factor of persistence of the drainage network, and Chartin et al. (2017) added the erosivity of rainfall to detect periods of greater erosivity and thus achieve a more functional OFC. Building on this concept of functional OFC, López-Vicente and Ben-Salem (2019) developed an index that included weighting factors associated with rainfall erosivity, roughness index related with residual topography, crop management, soil permeability, and physical properties important for soil for erosion or runoff generation. In this way, depending on the different seasons of the year, connectivity varied according to rainfall events and soil characteristics. All weighting parameters were normalized to values between 0 and 1 depending on their influence on connectivity following the methodology proposed by López-Vicente and Ben-Salem (2019).

After calculation of the OFC index proposed by Borselli et al. (2008), and the modifications proposed by Cavalli et al. (2013) and López-Vicente and Ben-Salem (2019), the most suitable index was selected for the study watersheds.

4.2.3. Data acquisition and processing

For the calculation of the indices, a 1-m DEM of the two watersheds was obtained from high-density LiDAR points information from the Government of Navarre (IDENA, 2019). DEM processing yielded the slope, roughness index (through the standard deviation of the residual

topography), and contributing area. The meteorological information for the calculation of the erosivity index was collected from the meteorological stations in each watershed, described in Section 2.2 of Chapter 2. Soil information was obtained from the soil maps available for each of the watersheds (see Chapter 2, Section 2.1), where the physical and chemical characteristics of each soil unit are described. Soil information was used to determine soil permeability by firstly estimating the soil water retention capacity. Field capacity and wilting point were estimated from soil texture (Government of Navarre, 2005a, 2005b). The crop management factor developed by López-Vicente and Ben-Salem (2019) was not considered due to the homogeneity of the crop types in the arable land (rainfed winter cereal) at both watersheds (this factor is negligible in the absence of crop diversity).

ArcGIS© 10.3 was used to compute the index proposed by Borselli et al. (2008), following the steps reported in Appendix A of Borselli et al. (2008). The modification of contributing area introduced by Cavalli et al. (2013), also used in López-Vicente and Ben-Salem (2019), was performed using SAGA© 2.1.2 software, with the D-infinity approach. This software was also used for the calculation of residual topography, using the ‘Residual Analysis (Grid)’ algorithm. The Planchon and Darboux (2001) algorithm was used to remove local depressions of the DEM.

4.2.4. Proposal of an OFC index for the conditions of the Navarrese watersheds

After computation of the three indices, the most suitable parameters were selected to determine the OFC at the rainfed winter cereal watersheds studied herein. The parameters analyzed were the algorithm for the calculation of the flow direction of the contributing area and the weighting factors. The suitability of parameters was based on scientific literature recommendations for the Navarrese environment and results obtained from the observed connectivity characteristics. These aspects are discussed and justified in the following paragraphs. Due to the non-quantitative nature of the index, the selection of the parameters have been partly based on qualitative aspects.

The D-infinite (Tarboton, 1997) algorithm was used for the calculation of flow direction in the contributing area. This algorithm takes advantage of the more restricted single flow method, which restricts flow direction to only eight directions, thereby increasing the grid bias (Cavalli et al., 2013). Its computation has been found to be realistic, differing from other algorithms that generate

flow overdispersion (Hengl and Reuter, 2008). In addition, the use of a small cell size (pixel) such as the one used in this study (1m), can be smaller than the width of many channels throughout the watershed. So the use of the single-flow algorithm to derive flow accumulation would limit high-drainage areas to single cells, underestimating channel widths (Cavalli et al., 2013).

Concerning the soil permeability factor proposed by López-Vicente and Ben-Salem (2019), its computation in small watersheds such as the ones studied herein (ca. 200 ha) generated unrealistic connectivity results. This index shows areas of low flow connectivity, where in practice it is high (e.g. close to the stream bank). Even though the scale of the soil map is considered detailed (1:5,000), the large size of the soil map units (polygons) within the watershed generated connectivity areas with high similarity to the soil map cartographic units, not coinciding with the connectivity reality at the watershed (Fig. 4.3). In addition, this soil permeability factor homogenized the OFC results across the different land uses (Fig. 4.4), diminishing the credibility of results as similar connectivity values across different land uses are not feasible. In watersheds with areas two or three orders of magnitude larger than those studied, this factor could be suitable, but in small watersheds, this factor can generate unreliable results.

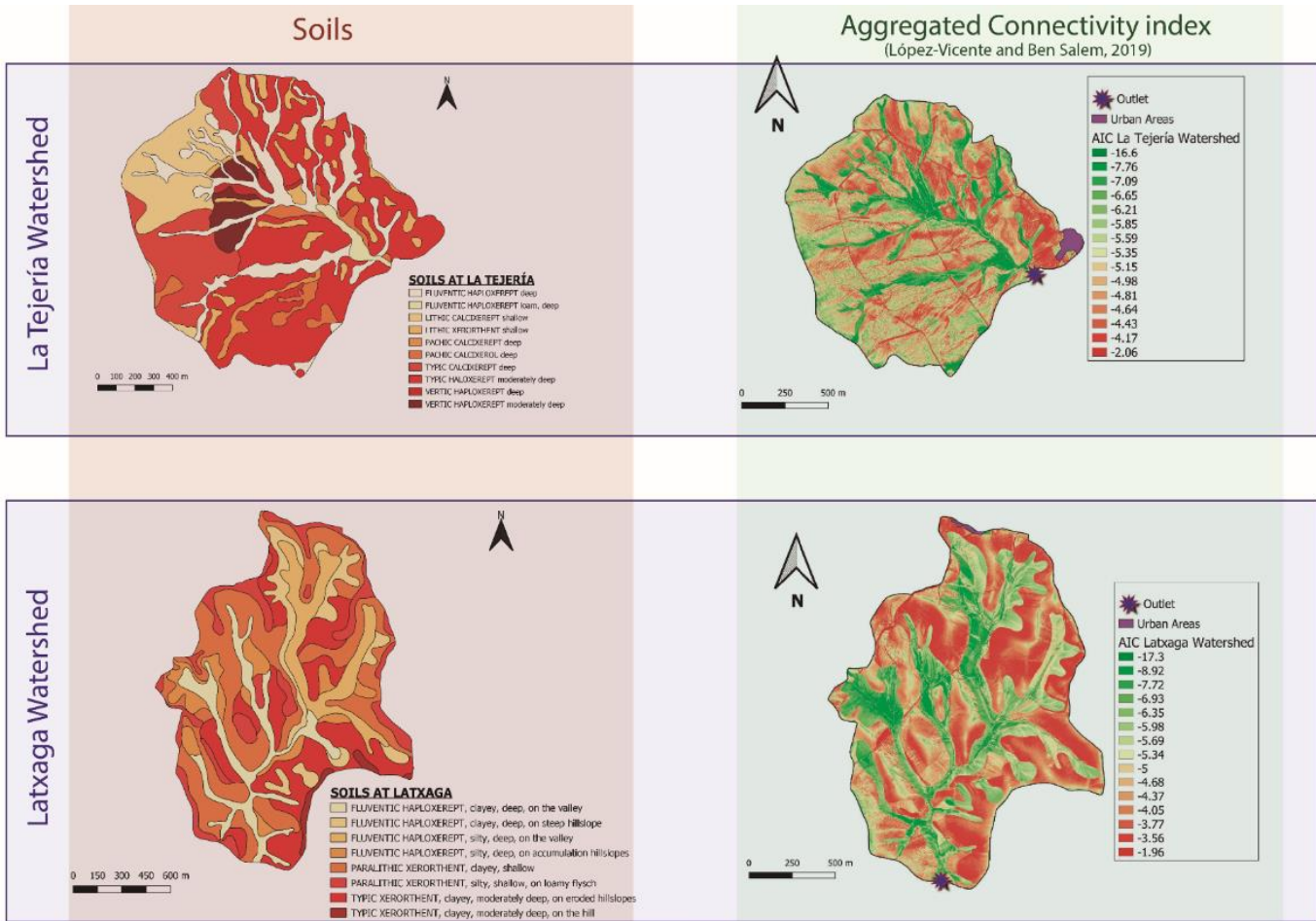


Figure 4.3: Soils distribution at La Tejería and Latxaga, and the AIC index proposed by López Vicente and Ben Salem (2019) with non-realistic OFC areas similar to soil cartographic units.

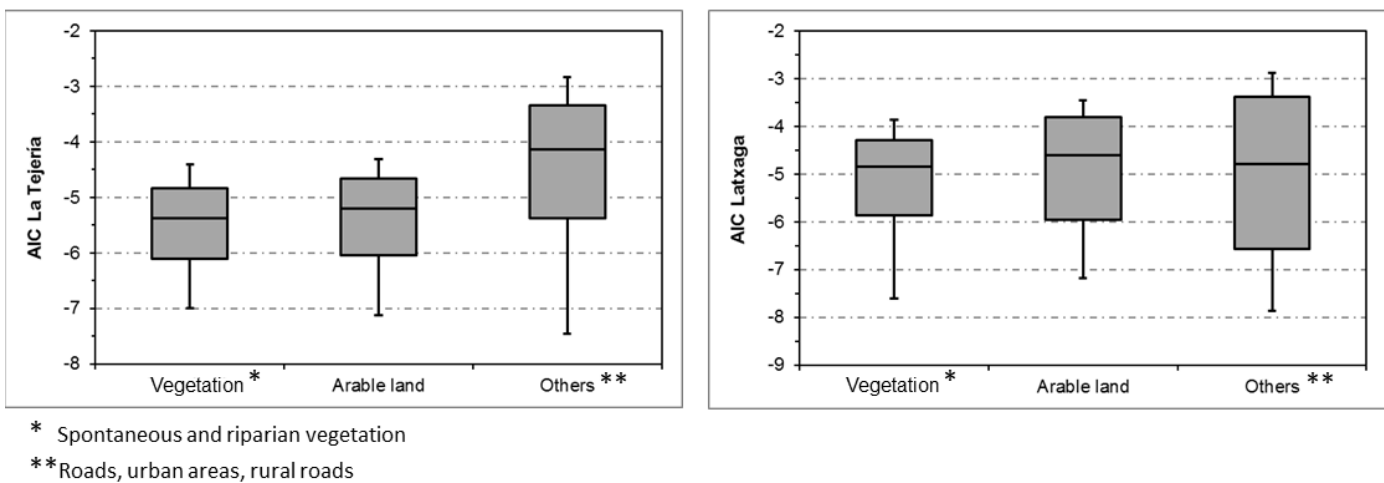


Figure 4.4: OFC variability in different land uses with the Aggregated Connectivity Index (AIC) proposed by López-Vicente and Ben Salem (2019).

Regarding the Aggregated OFC index proposed by López-Vicente and Ben-Salem (2019), the rainfall erosivity factor did not report gradual differences across the watershed. Due to the small size of the watershed, there was no meteorological gradient throughout the watershed and therefore the erosivity index was the same across the watershed areas. Larger watersheds (two or three orders of magnitude larger) could generate different erosivity index values throughout the watershed due to meteorological differences between headwater and outlet areas (López-Vicente and Ben-Salem, 2019). Because a single erosivity value was obtained for the entire watershed, this variable did not provide any information that could modify the OFC in specific parts of the watershed, and was not included in the final computation.

The RUSLE-C factor was selected as the weighting factor related to the impediment of runoff generation and sediment transport. In the modifications of Cavalli et al. (2013) and López-Vicente and Ben-Salem (2019), factors related to roughness (e.g., the roughness index) were used as impediment factors for the generation of runoff and sediment transport. These factors increase the objectivity of the measurement and decrease the influence of agricultural and forested lands. Therefore, in alpine or mountainous areas with a wide variety of bare soils, this factor, represented by roughness, provides more information regarding the OFC. However, this study focuses on two small agricultural watersheds with ca. 90 % of the area covered by arable land. The RUSLE C-factor was considered the most suitable parameter to study the impediment of runoff generation and sediment transport, considering the importance of agricultural land in these watersheds, the absence of mountainous areas studied in other works (such as in Cavalli et al., 2013), and the globally validated RUSLE equation. The RUSLE C-factor values selected in the watersheds were calculated (Renard et al., 1997), and contrasted with other similar Mediterranean agricultural areas (Borselli et al., 2008) (Table 4.1). In addition, Table 4.1 shows that areas with no C-factor value, such as urban areas, have a value of 0.95, which reflects the high runoff connectivity that occurs on these surfaces (high runoff potential). A suitable representation of runoff connectivity in an OFC is very important for the analysis of TDS and nutrient dynamics (Merrington et al., 2002), as it affects the movement of these compounds throughout the watershed.

Table 4.1: Selected weighing factors for different lands.

	C-factor
Natural vegetation (Spontaneous and riparian vegetation)	0.04
Arable areas (Rainfed winter cereal)	0.1
Anthropized areas (Urban, roads and rural roads)	0.95*
Water bodies (stream channel)	1

* Anthropized areas do not have a C-factor value. In this case the value refers to the runoff potential

In summary, after computation of all the indices aforescribed, the most adequate weighting factor was the RUSLE C-factor. The remainder were discarded due to lower suitability, generation of unrealistic artifacts in the index, or irrelevant results that would generate a spatial variation of the OFC. The D-infinite algorithm was used to calculate the flow direction of the contributing area.

4.3. RESULTS AND DISCUSSION

4.3.1. OFC index computation

The results of the OFC index show higher connectivity in urbanized areas and rural roads (in red, Fig. 4.5). For arable area and spontaneous and riparian vegetation, high variability of OFC is observed at both watersheds, where a clear pattern is not easily identified (Fig. 4.5). Observation of the highest and the lowest 10% OFC values at both watersheds (p10, p90) reveals that arable areas with high OFC present higher slopes (Fig. 4.6). Areas with lower OFC (in green) coincide with cultivated areas or areas with spontaneous or riparian vegetation with low slopes (Fig. 4.6).

Higher runoff connectivity in lands with high potential runoff renders this OFC index suitable for the analysis of runoff nutrient dynamics, mainly dissolved nutrients. The observed results agrees with the connectivity definition of Bracken and Croke (2007), as a higher slope allows a greater connection between the riparian and the upland zones. The difference in connectivity in areas close to the channel is remarkable when comparing both watersheds. At La Tejería, these areas do not generally present a low value compared to the remainder of the watershed. Even though some single cells can be observed, there are no significant areas below 10% of the OFC values (p10, Fig. 4.6A). However, at Latxaga, important areas adjacent to the channel present OFC values below 10% (Fig. 4.6B). The increased presence of riparian vegetation increases the OFC impediment in areas close to the channel, reducing the OFC.

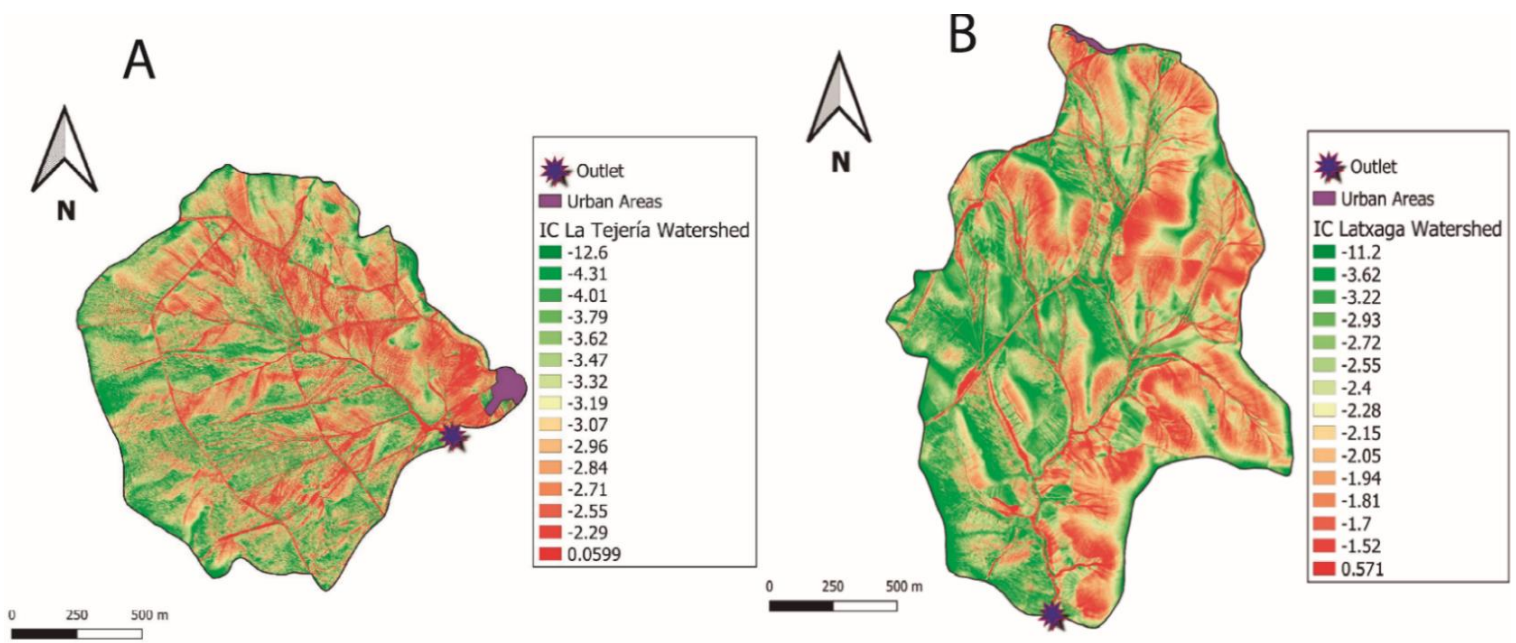


Figure 4.5: Semiquantitative results of the OFC index at (A) La Tejería and (B) Latxaga.

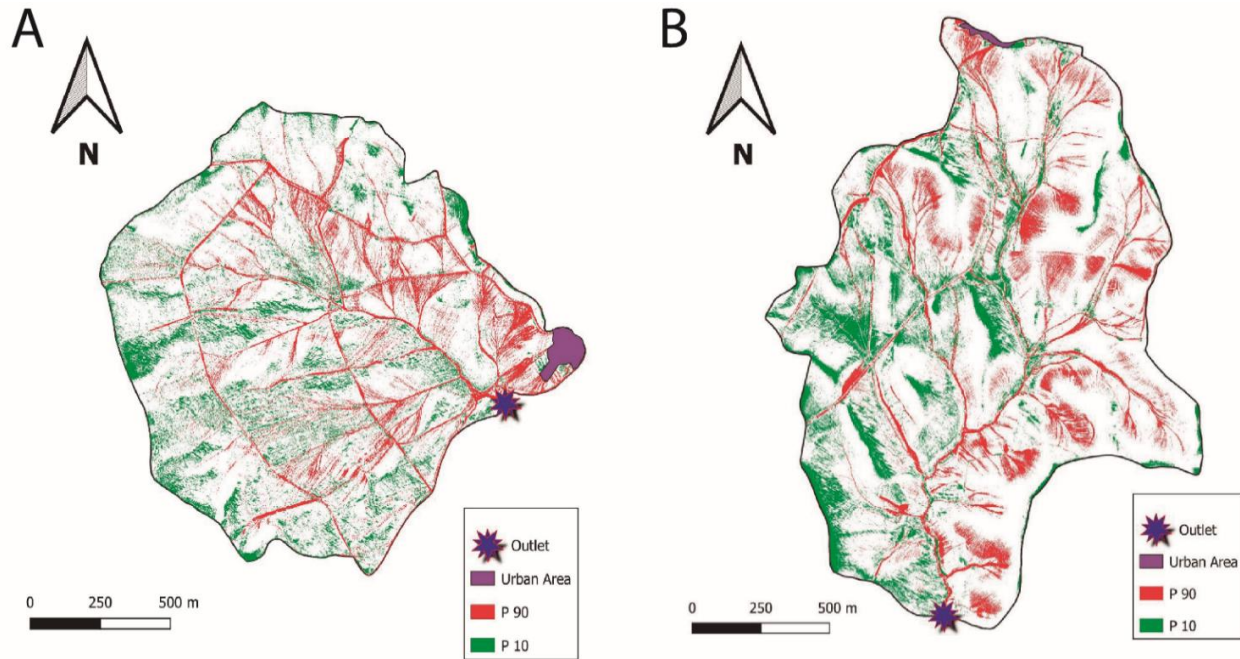


Figure 4.6: The highest and lowest 10% OFC values (percentile 10, percentile 90) at (A) La Tejería and (B) Latxaga.

According to watershed land use and OFC, the highest OFC is observed at anthropized lands (e.g. rural roads, urban infrastructure) followed by arable lands and spontaneous or riparian vegetation respectively (Fig. 4.7). The lack of impediment for the generation of runoff in anthropized lands causes the highest OFC. The weighting factor (W) also generates OFC differences between arable areas and areas with spontaneous or riparian vegetation. The presence of riparian vegetation composed of trees and shrubs improves infiltration, thus reducing runoff and sediment transport potential (Dosskey et al., 2010). In addition, the presence of leafy residues in these areas also hinders the generation of runoff, reducing the potential for sediment transport (Dosskey et al., 2010). These areas are also a nutrient sink in agricultural environments, so the decrease of OFC can help understand the nutrient dynamics in these watersheds (Chase et al., 2016; Neilen et al., 2017). Even though the difference in OFC between arable and riparian and spontaneous vegetation areas is considerable, a greater difference was expected. The main reason for the slight differences observed is the location of the spontaneous vegetation zones. These vegetation fields, generally, have not been cultivated due to shallow soil depth and steep slopes, which lead to slighter OFC differences than expected.

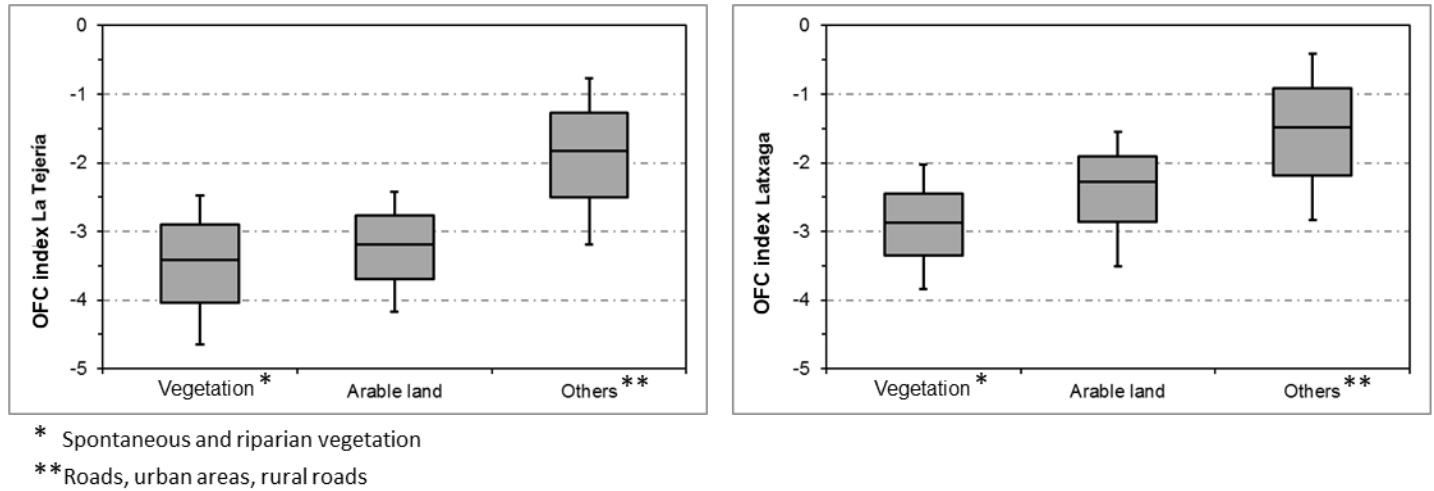


Figure 4.7: Distribution of OFC values in different land uses with the proposed OFC index in Navarrese watersheds.

Even though the reported results are consistent and realistic with the OFC concept and field events, some limitations must be mentioned (Heckmann et al., 2018). The semi-quantitative nature of the index prevented the comparison of watersheds, hindering the identification of crucial factors that explain different behaviors in two similar watersheds. For example, the two watersheds have very similar climatic, crop management, and extension characteristics, but report very different sediment and nutrient yields (La Tejería exports twice more nitrate-N and three times more sediment than Latxaga). The impossibility of comparing their OFC prevents a deeper study of the dynamics.

The selection of the weighting factors in the OFC index relates the result obtained with sediment or particulate and soil-attached nutrients than with dissolved nutrients. However, an accurate characterization of the OFC for runoff enables the consideration of nutrients in runoff within this index.

The OFC index does not adequately consider tile drainage management practices. These practices is considered to be of great importance in the exports of dissolved nutrients (Randall and Goss, 2008; Gramlich et al., 2018). Calsamiglia et al. (2018) attempted to adequately represent the surface drainage where the tile drains discharged in a small agricultural watershed of Mallorca (Spain), in order to consider partially this management in the OFC index. In La Tejería, despite the surface artificial drainage network into which these tile drainages discharge is well represented,

the effect that tile drainage has on the plots in which it is present (increased flow connectivity of the upper watershed with the riparian zone) is not reflected in OFC results. Therefore, its incorporation, for example, as a weighting factor, would improve the OFC results.

4.4. CONCLUSIONS

This work evaluated an OFC index at two agricultural watersheds with Mediterranean characteristics. The RUSLE C-factor was considered more appropriate than the roughness variables for the impediment of runoff generation and sediment transport.

In the selection of the parameters to define the index, it is important to consider their scale and spatial distribution. Large polygons of the different cartographic units occupying a high percentage of the watershed surface can produce inappropriate artifacts in the watershed OFC, generating an important bias if this parameter has an important weight in the final result.

The results reported were consistent with the definitions of flow connectivity, and very realistic with the actual processes occurring in the field. Areas with the steepest slopes and lowest infiltration capacities presented the highest OFC values.

The semi-quantitative nature of these indices does not enable the comparison of OFC values between watersheds, preventing the identification of different dynamics. The quantification of a comparable OFC value would facilitate the understanding of the OFC and allow a deeper comprehension of sediment and nutrient dynamics.

The OFC index is more related to the dynamics of sediment and particulate nutrients than to dissolved nutrients. However, accurate representation of runoff enables the consideration of dissolved nutrients in the runoff.

The absence of management practices such as artificial drainage (a crucial factor in nitrogen nutrient dynamics) decreases the suitability of this index for the assessment of nutrient dynamics in runoff.

Although the OFC indices discretize spatial connectivity around a watershed, a natural next step is to obtain a comparable index to quantify watershed OFC. In addition, the generation of new weighting factors that reflect specific managements, such as tile drainage, is important to expand the knowledge base regarding nutrients dynamics. Moreover, an OFC index that considers parameters related to dissolved nutrients dynamics (e.g., interflow or nutrient uptake) would improve the identification of nutrient dynamics by OFC indices.

CHAPTER 5:
**Assessment of the main factors affecting the
dynamics of nutrients in two rainfed cereal
watersheds**

5.1. INTRODUCTION

The intensification of agricultural activity throughout the world is, at least partially, responsible for the decline of water quality and, as a consequence, of the deterioration of freshwater and coastal ecosystems (Berka et al., 2001; Van Meter et al., 2016). In particular, the application of fertilization doses above crop necessities and/or the intensification of livestock production are usually associated with a surplus of nutrients in soils. This means an excess of available nutrients that are subject to losses via runoff and/or leaching, plus the aforementioned off-site effects (Durand et al., 2011; Merrington et al., 2002).

Nitrogen is considered the nutrient that generates one of the best crop responses, increasing yields. Therefore, nitrogenous fertilization is the most employed in the world, with over 100 million tonnes applied each year (Delgado et al., 2016). N fertilizers are available in a range of forms (straight, such as urea or ammonium, compound forms such as di-ammonium phosphate, or organic fertilization with manure). Soil N is mainly lost in the form of nitrate, via leaching (Oelmann et al., 2007; Billen et al., 2011; Wang et al., 2018), although other types of losses can also be significant (Liu et al., 2003; Huang et al., 2016). Nitrate loss is relevant both from a farmer's perspective, as it entails a loss of economic resources, and due to environmental reasons, worsening water quality for human supply (World Health Organization, 2011) or contributing to eutrophication (Merrington et al., 2002; Le Moal et al., 2019). Other environmental impacts have been reported, such as air pollution or greenhouse gas emissions (Butterbach-Bahl et al., 2011; Moldanová et al., 2011).

In contrast, the effects of phosphorus (P) on the environment are mostly associated with eutrophication, being habitually the limiting nutrient in inland water ecosystems. An increase of 0.01 mg L^{-1} has been reported as sufficient to transform oligotrophic inland waters into eutrophic (Merrington et al., 2002). P exportation is controlled by soil erosion and sediment exports, as a considerable proportion of P is fixed or precipitated due to prevailing soil pH values (Withers and Jarvie, 2008). Although wastewater is commonly the main P-contributor to inland waters, especially in developing countries, agriculture is a proven, but variable, contributor of P to many affected waters (Sharpley, 1995).

There are multiple factors that influence nutrient export processes. Riparian vegetation located near the water bodies act as filters or sinks of sediments and nutrients (Tabacchi et al., 2000; Dosskey et al., 2010; Chase et al., 2016; Neilen et al., 2017). In particular, width, density, and diversity of riparian vegetation have been reported to affect nutrient transport to streams (Broadmeadow and Nisbet, 2004; de Souza et al., 2013). For instance, herbaceous vegetation improves water infiltration and protects from runoff and erosion while woody vegetation protects streambanks from mass failure, and, in the case of senescent species, its leaves increase the soil roughness, reducing runoff (Dosskey et al., 2010). Besides riparian vegetation, the presence of aquatic vegetation can influence the export of nutrients altering the amount in the watershed outlet (Soana et al., 2019). A greater sinuosity of the stream causes a higher interaction of water with the hyporheic zone of the bed (Peterson and Benning, 2013), increasing the potential of denitrification and nitrogen uptake in riparian areas. Soil characteristics such as cracks and tile drainage also influence nitrogen exports, reducing the residence times of dissolved nutrients and decreasing denitrification (Brady and Weil, 2008; Randall and Goss, 2008; Arenas Amado et al., 2017). In addition, other factors have been also reported to significantly influence nutrient export, such as soil pH (Merrington et al., 2002) and climatic conditions (Chen et al., 2002), for example.

These factors, plus other physical factors, can trigger biogeochemical processes such as denitrification (Mastrocicco et al., 2019). Denitrification is the process where microbial activity reduces compounds, namely nitrate, to gaseous forms found in the environment. Denitrification occurs mainly when denitrifying microorganisms do not have sufficient oxygen, and therefore carry out anaerobic respiration, transforming soluble nitrogen compounds into gases such as nitrous oxide and nitrogen (Martens, 2005; Skiba, 2008). Assessment of these factors can underpin the extension of knowledge on the different pathways of nutrients in diverse watersheds.

Rainfed winter cereal is the most extended agricultural land use around the world, representing approximately 20% of the cultivated area (FAO, 2011). For instance, in Europe and Spain, the main rainfed winter crops, wheat, and barley, occupy ca. 36% and 40 % of the total arable area, respectively (EUROSTAT, 2016; MAPAMA, 2018). Although this land use is considered essential to the agriculture sector, the effects on water quality are widely acknowledged (e.g., Durand et al., 2011). The European Union has even promoted the Nitrates Directive to address pollution from agricultural sources (91/676/EEC). Many European countries have implemented networks of agricultural watersheds to investigate diffuse source pollution (e.g., Hooda et al.,

1997; Kyllmar et al., 2006; Lagzdins et al., 2012; Povilaitis et al., 2014; Lloyd et al., 2016; Ockenden et al., 2016; Fučík et al., 2017). However, there is an apparent under-representation of watersheds in Mediterranean climate conditions, which presumably present remarkable differences in nutrient dynamics and exports. In fact, to the best of our knowledge, only a few studies have reported nutrient dynamics for the Mediterranean climate or in locations under its influence (Ferrant et al., 2011; Lassaletta et al., 2012; De Girolamo et al., 2017a). The Mediterranean climate is characterized by mild, wet winters and hot, dry summers. Evapotranspiration is high in summer, with crop management being a challenge, and irrigated agriculture is a frequent practice. Besides, rainfed cereal fertilization in Mediterranean areas occurs at approximately the same period in which most of the runoff is generated. Therefore, its contribution to nutrient exports is significant.

In Navarre (northern Spain), the impact of agriculture on soil erosion and water quality has been analysed in a network of small watersheds implemented by the former Department of Agriculture, Livestock, and Food of the Government of Navarre. These studies have mainly focused on the characterization of hydrological and erosion (Casalí et al., 2008, 2010), factors controlling sediment exports (Giménez et al., 2012), assessment of the AnnAGNPS model for runoff and sediment yield simulation (Chahor et al., 2014), and the dynamics of dissolved solids and suspended sediment (Merchán et al., 2019). Specific work on nutrient dynamics was also conducted at one of these watersheds (Merchán et al., 2018), although some information regarding nutrient dynamics in the remaining watersheds was presented in Casalí et al. (2008, 2010). In a study conducted at two watersheds representing rainfed cereal land use under relatively similar management conditions, surprising different behaviours were reported for nutrient exports (especially nitrate). Although no detailed study was carried out, differences in the watersheds' morphology, riparian and stream channel vegetation were proposed to be the leading causes of the differences observed (Casalí et al., 2008).

This paper builds upon and extends the work of Casalí et al. (2008) by elaborating on nutrient concentration and export dynamics in two relatively similar watersheds, which were expected to behave similarly. However, the watersheds presented distinct behaviours, as previously reported. In this study, we aim to improve the knowledge base on the nutrient dynamics in rainfed agricultural watersheds under the Mediterranean climate and, mainly, on the factors that could explain the differences observed between two similarly managed watersheds. The specific

objectives were: (a) to characterize the behaviour of both watersheds, in terms of concentration and exports of nitrate and phosphate, for a range of temporal scales (in response to rainfall events, seasonally, and inter-annually); (b) to estimate a long-term (10 years) average nitrate-N and phosphate-P concentration and yield in each of the watersheds; and (c) to gain insight on the controlling factors influencing these processes, through comparisons between the watersheds and with information available in scientific literature.

5.2. METHODS

5.2.1. Experimental watersheds and data collection and analysis

This chapter was carried out at the rainfed winter cereal watersheds of the agricultural watershed network of the Government of Navarre (Fig. 5.1). A thorough description of these watersheds highlighting its particular characteristics are in the Section 2.1 of the Chapter 2.

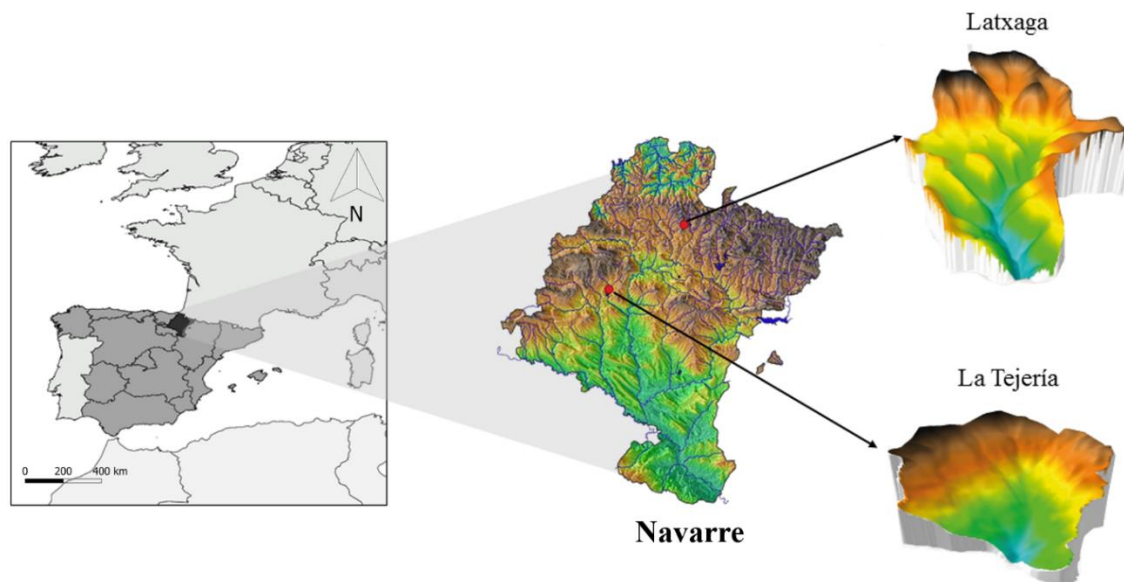


Figure 5.1: Location of the Latxaga and La Tejería watersheds, two experimental agricultural watersheds of the Government of Navarre.

The methodology conducted for hydrological data, meteorological data and water quality samples collected (with the correspond analysis) in each watershed are described in the Section 2.2 of Chapter 2. The load estimation of nitrate-nitrogen (NO_3^- -N) and phosphate-phosphorous (PO_4^{3-} -P) for the whole study period was perform following the Meals et al., (2013) methods for load estimation. These methods description can be observed in the Section 2.2.1 of the Chapter 2. The load result was transformed into a specific load or yield, dividing the load by the watershed surface. Afterward, the yield was aggregated into monthly, annual, and for the entire study period.

A local regression method was used to establish a relationship between time and concentrations and detect seasonal patterns. The regression method selected was the locally estimated scatterplot smoothing (LOESS). The LOESS line was obtained with the R statistical software, and the selected span was 0.33, which was the best fit for the available data.

5.3. RESULTS

5.3.1. Rainfall and runoff distribution

Annual rainfall average and standard deviation were 793 ± 216 mm at La Tejería and 950 ± 285 mm at Latxaga. The driest and wettest years were 2011/2012 and 2013, respectively, with 531 mm and 600 mm for La Tejería in 2012 and for Latxaga in 2011, and 1,324 mm and 1,665 mm at La Tejería and Latxaga in 2013, respectively (Fig. 5.2A). The humid season lasted from November to March in both watersheds, with ca. 100 mm per month at La Tejería and 120 mm per month at Latxaga (Fig. 5.2B).

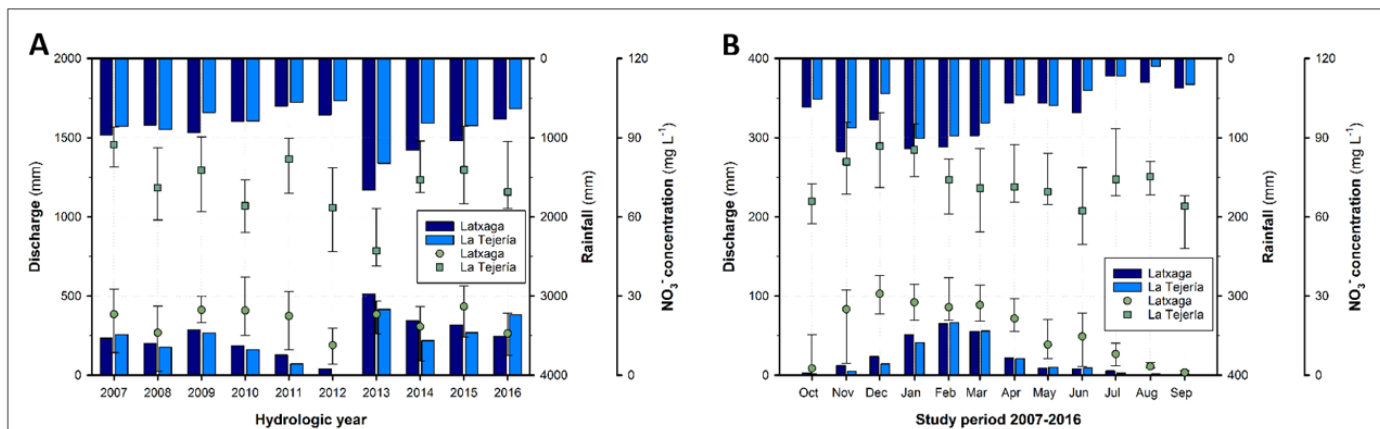


Figure 5.2: Annual (A) and monthly (B) distribution of rainfall, runoff, and median nitrate concentration with 25th and 75th percentiles at Latxaga and La Tejería.

Regarding runoff, the annual average and standard deviation at La Tejería was 222 ± 126 mm, while at Latxaga it was 250 ± 129 mm. The percentage of rainfall converted into runoff was very similar for both watersheds (31% at La Tejería and 33% at Latxaga). The runoff registered in the hydrological year 2012 was the lowest, with 4 mm at La Tejería and 38 mm at Latxaga. In contrast, the following year (2013) was the year with the highest runoffs, with 415 mm at La Tejería and 513 mm at Latxaga (Fig. 5.2A). Seasonally, runoff is dependent on rainfall and similar for both watersheds (Fig. 5.2B). An increase in runoff generally started in November-December, and decreased in May-June-July. Usually, rainfall events in the first part of the hydrological year (October-December) did not generate significant runoff (Fig. 5.2B). In general, hydrograph recessions presented higher slopes (i.e., were faster) at La Tejería than at Latxaga. The events that occurred during or after summer generated less discharge at both watersheds than

those events occurred in spring. The aridity of soil was higher after summer, contrasting with spring, which coincided with the most humid season of the year.

5.3.2. Nutrient concentration trends at both watersheds.

Considering the entire study period, the nitrate concentration (NO_3^-) measured at La Tejería was nearly four times higher than at Latxaga. Median NO_3^- at La Tejería was $73.5 \text{ mg NO}_3^- \text{ L}^{-1}$, which exceeded the $50 \text{ mg NO}_3^- \text{ L}^{-1}$ threshold (e.g., Nitrates Directive). Indeed, 85% of the collected samples were over this value. At Latxaga, median NO_3^- was $21 \text{ mg NO}_3^- \text{ L}^{-1}$. Conversely to La Tejería, only 3% of the collected samples at Latxaga were over $50 \text{ mg NO}_3^- \text{ L}^{-1}$ (Table 5.1).

Table 5.1: Parametric and non-parametric statistics of nitrate and phosphate concentration at the Latxaga and La Tejería watersheds in the 2007-2016 period.

Conc. (mg L^{-1})	NO_3^-		PO_4^{3-}	
	Latxaga	La Tejería	Latxaga	La Tejería
p10	2.09	37.34	0.025	0.025
p25	8.07	62.02	0.025	0.025
p50	20.99	73.49	0.025	0.025
p75	29.76	86.08	0.025	0.089
p90	38.79	98.11	0.083	0.365
Average	20.78	71.81	0.060	0.201
S.D.	14.84	24.62	0.376	0.723

Conc.: Concentration

S.D.: Standard deviation.

Differences in NO_3^- between hydrological years were observed at both watersheds. At La Tejería, the highest median was observed in 2007 ($87.4 \text{ mg NO}_3^- \text{ L}^{-1}$) and the lowest in 2013 ($47.1 \text{ mg NO}_3^- \text{ L}^{-1}$). The minimum concentration coincided with the most humid year (Fig. 5.2A). Oppositely, at Latxaga this pattern was not present, with a maximum median concentration in 2015 ($26.0 \text{ mg NO}_3^- \text{ L}^{-1}$) and a minimum in 2012 ($11.4 \text{ mg NO}_3^- \text{ L}^{-1}$), which was the second driest year of the study period. In contrast with La Tejería, the average and median concentrations in the humid year at Latxaga (2013) increased considerably compared with the previous year, which coincides with the driest year and also with the minimum median of NO_3^- . This demonstrated the different behaviours of the watersheds (Fig. 5.2A).

The seasonal distribution within each year was similar for both watersheds. The high NO_3^- period for both watersheds occurred mainly in late autumn and winter months, whereas lower NO_3^- was

registered after the harvest, during the summer and the early autumn (Fig. 5.2B). September and October presented the lowest NO_3^- values. Regarding the NO_3^- trend throughout the year, for both watersheds, the increase in concentration started with the first rainfall events, reaching its maximum peak in December-January and then decreasing during the spring until the summer. After late March, the concentration at Latxaga decreased, approaching 0 mg L^{-1} in the late summer (Fig. 5.3).

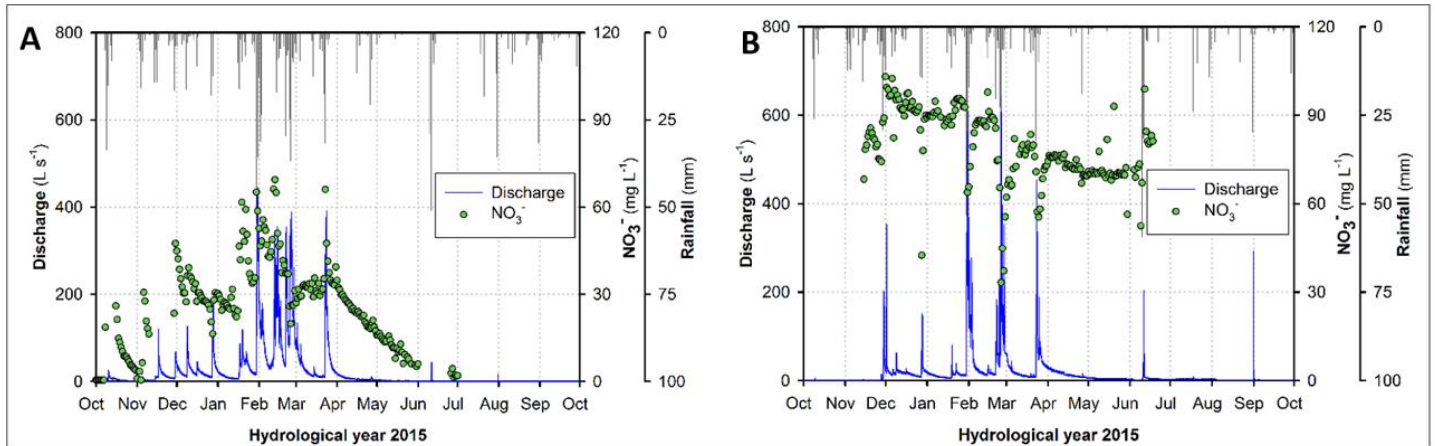


Figure 5.3: Rainfall, discharge, and nitrate concentration distribution in a typical hydrological year (2015) at Latxaga (A) and La Tejería (B)

Although the general patterns observed in the seasonal cycle were similar in terms of NO_3^- , some behaviour differed. Whereas Latxaga presented a relatively stable line (Fig. 5.4), at La Tejería this line presented more ups and downs (see the two local maxima in Fig. 5.4) probably as a consequence of higher inter- and intra-annual variability in concentration.

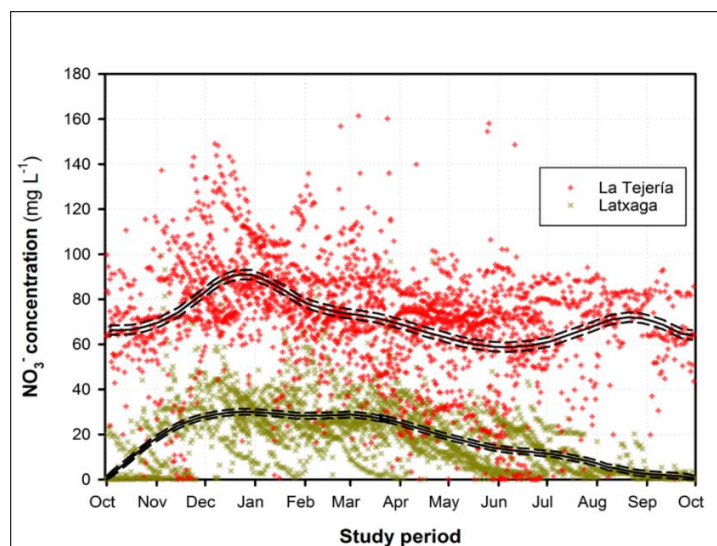


Figure 5.4: LOESS smoothing method nitrate results for the Latxaga and La Tejería watersheds

Remarkably, the response to specific flow events was different for each watershed (Fig. 5.5). At La Tejería, a rainfall event caused an increase in the watershed discharge and a decrease in concentration, generating a dilution effect in the stream. Also, from late march and after the harvest, the concentration of NO_3^- remained stable or decreased slightly over time until the sowing period. Conversely, at Latxaga the NO_3^- concentration increased considerably with a rainfall event, along with runoff. Although the response in terms of NO_3^- concentration was different, the $\text{NO}_3^-/\text{Cl}^-$ ratio demonstrated an important increase in specific flow events at both watersheds (Fig. 5.5).

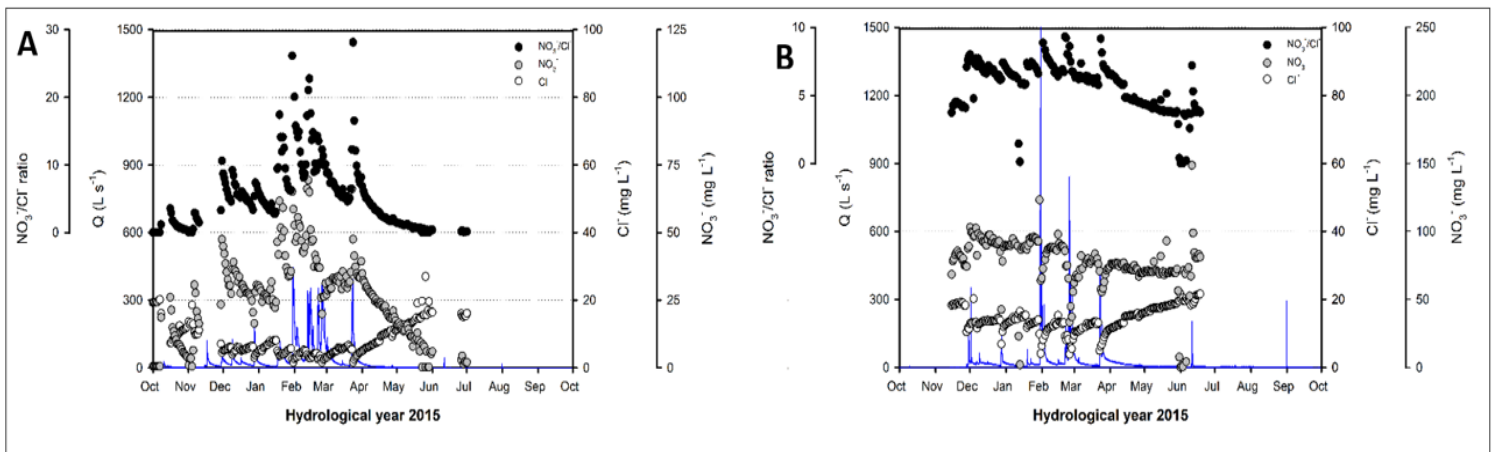


Figure 5.5: Nitrate concentration, chloride concentration, and nitrate/chloride ratio at the Latxaga (A) and La Tejería (B) watersheds.

Finally, at both watersheds the median phosphate concentration (PO_4^{3-}) was below the detection limit ($<0.05 \text{ mg PO}_4^{3-} \text{ L}^{-1}$) (Table 5.1). Only 15.4% and 27.2% of the samples were above that threshold at Latxaga and La Tejería, respectively. PO_4^{3-} differed across years, with yearly median values above the detection limit only for a few years (Fig. 5.6). No clear seasonal patterns were detected for PO_4^{3-} . However, an increment of concentration from spring until the end of summer was observed at La Tejería (Fig. 5.7).

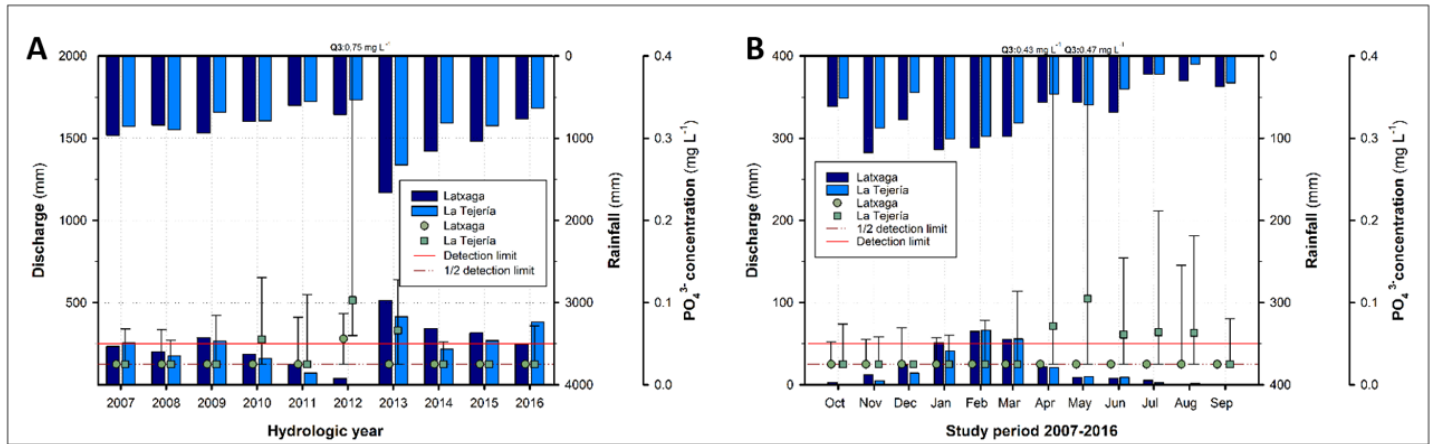


Figure 5.6: Annual (A) and monthly (B) distribution of rainfall, discharge, and median phosphate concentration with 25th and 75th percentiles at Latxaga and La Tejería.

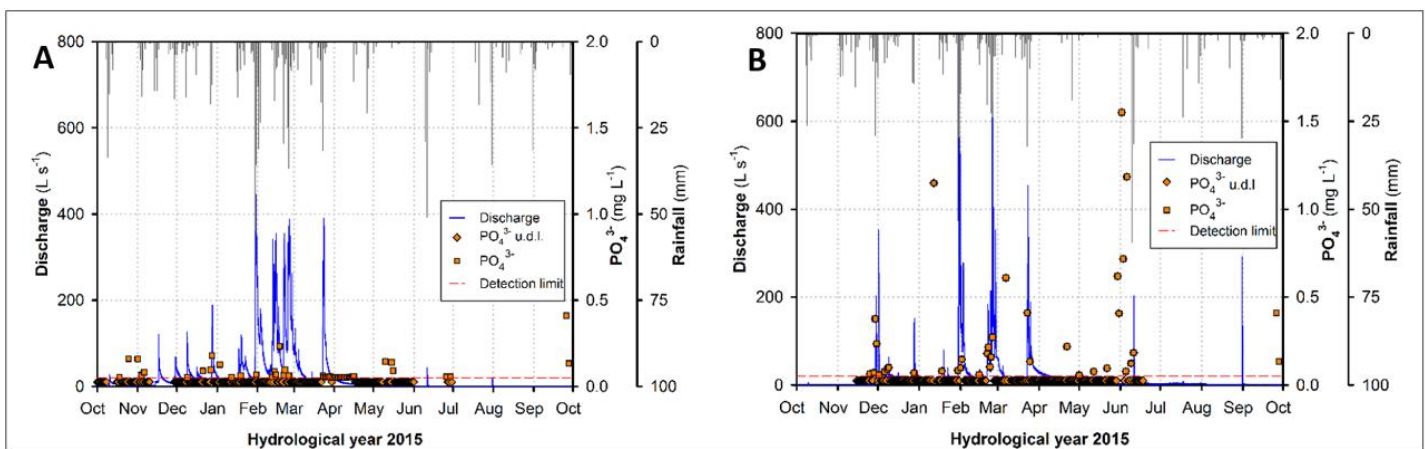


Figure 5.7: Rainfall, discharge, and phosphate concentration distribution in a typical hydrological year (2015) at Latxaga (A) and La Tejería (B)

5.3.3. Nutrient yields at both watersheds

The estimations obtained by different methods were consistent and showed approximately twice as much NO₃⁻-N yield at La Tejería (31.8 ± 16.0 kg NO₃⁻-N ha⁻¹ year⁻¹) than at Latxaga (17.0 ± 8.6 kg NO₃⁻-N ha⁻¹ year⁻¹) (Table 5.2). Regarding the NO₃⁻-N yield, a similar pattern was observed at both watersheds, where the NO₃⁻-N yield was generally controlled by the runoff of each watershed. The highest NO₃⁻-N yields were observed in the years with the highest runoffs, and vice versa. The year with the lowest NO₃⁻-N exportation at both watersheds was 2012 (1.1 and 0.6 kg ha⁻¹ year⁻¹ at Latxaga and La Tejería, respectively). The highest NO₃⁻-N yield at Latxaga occurred in 2015, and at La Tejería in 2016 (29.8 and 51.8 kg ha⁻¹ year⁻¹, Fig. 5.8A).

Seasonal distribution of the NO_3^- -N yield was similar at both watersheds, with the winter period (January, February, and March) presenting the higher exports, and summer and early autumn presenting the lower exports. February presented the higher exports at both watersheds, with 8.6 and 4.4 $\text{kg ha}^{-1} \text{ month}^{-1}$ at La Tejería and Latxaga, respectively. At both watersheds, around 51% was exported in winter (January-March) (Fig. 5.8B), whereas only 0.6% and 1.3% of the annual yield was exported in summer (July-September).

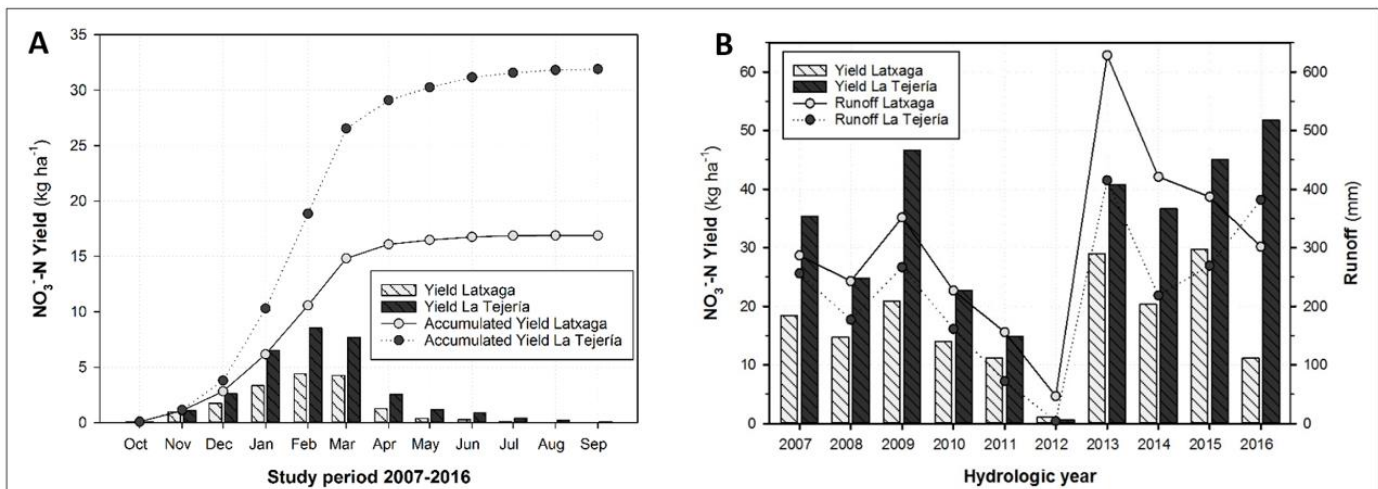


Figure 5.8: Monthly and monthly accumulated nitrate- N yield (A) and annual nitrate-N yield and runoff (B) at the Latxaga and La Tejería watersheds.

Regarding phosphate, La Tejería exported twice as much PO_4^{3-} -P ($71 \text{ g ha}^{-1} \text{ year}^{-1}$, Table 5.2) than Latxaga ($33 \text{ g ha}^{-1} \text{ year}^{-1}$). As shown for NO_3^- -N, differences in PO_4^{3-} -P yield across years followed a pattern similar to that of runoff. Throughout the study period, the year with the lowest PO_4^{3-} -P yield was 2012, with $8 \text{ g ha}^{-1} \text{ year}^{-1}$ at Latxaga and $10 \text{ g ha}^{-1} \text{ year}^{-1}$ at La Tejería. In contrast, the year with the highest PO_4^{3-} -P yield was 2013, with 63 and $267 \text{ g ha}^{-1} \text{ year}^{-1}$ at Latxaga and La Tejería, respectively (Fig. 5.9A). The seasonal distribution of the PO_4^{3-} -P yield was also similar for both watersheds: winter presented the highest exports (40%) and summer presented the lowest (2%). At La Tejería, January was the month with higher exports ($22 \text{ g ha}^{-1} \text{ month}^{-1}$) while the month with the highest exports at Latxaga was February ($7 \text{ g ha}^{-1} \text{ month}^{-1}$) (Fig. 5.9B).

Table 5.2: Yield estimations of nitrate-N and phosphate-P at Latxaga and La Tejería, with the methods described in Meals et al. (2013)

Yield estimations (kg ha ⁻¹ year ⁻¹)	Nitrate-N		Phosphate-P	
	Latxaga	La Tejería	Latxaga	La Tejería
Ratio estimator*	17.04	31.81	0.033	0.071
Regression**	20.11	37.84	0.033	0.068
Numeric integration	16.61	32.19	0.032	0.066

*The ratio estimator method employed was the Beale Ratio (Meals et al., 2013).

**The LOADEST software, developed by the US Geological Survey, was utilized for the Regression (Runkel et al., 2004).

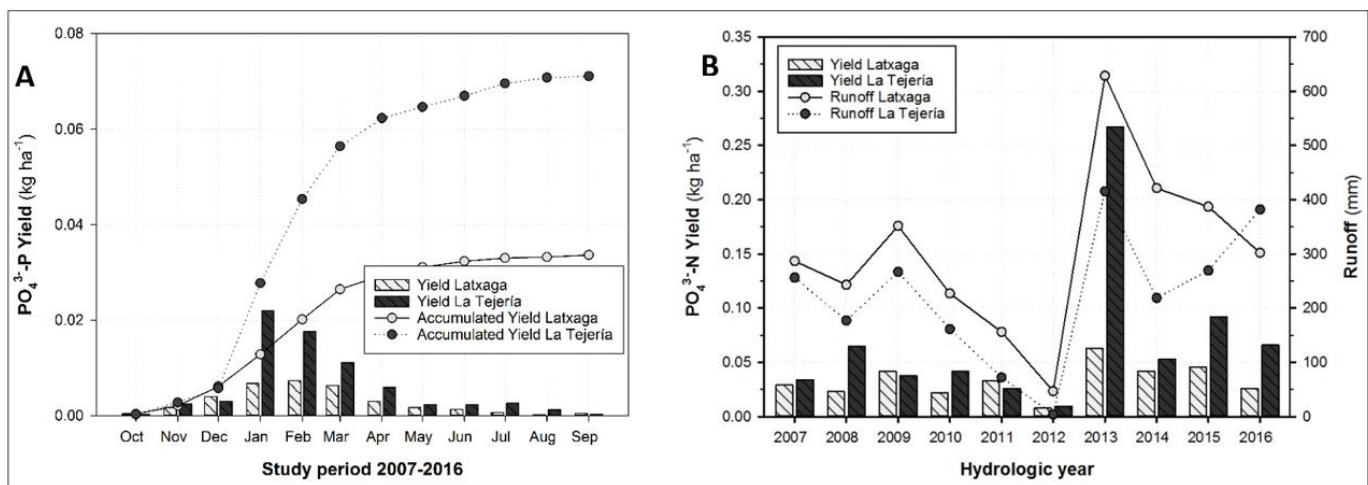


Figure 5.9: Monthly and monthly accumulated phosphate-P yield (A), and annual phosphate-P yield and runoff (B) at the Latxaga and La Tejería watersheds.

5.4. DISCUSSION

5.4.1. Hydrology patterns at both watersheds

At Latxaga and La Tejería, low rainfall in the summer as well as higher evapotranspiration requirements led to a lower soil moisture content in these months. Despite the existence of significant rainfall events, these did not generate considerable increases in runoff. At both watersheds, the increase of discharge started in autumn with the humid season. The role of antecedent soil moisture conditions in runoff generation is widely acknowledged. (e.g., Montaldo et al., 2007; Feki et al., 2018; Teegavarapu and Chinatalapudi, 2018; Wang et al., 2018). Higher soil moisture content implies, among other effects, a more significant response of a watershed to an event, generating increased runoff. This has been also reported by previous works carried out at these watersheds (Casalí et al., 2008; Giménez et al., 2012).

In contrast with the seasonal pattern of the runoff observed in Navarre and in other Mediterranean watersheds (Kalogeropoulos and Chalkias, 2013; Tuset et al., 2016), in northern Europe runoff was relatively homogeneous throughout the year (Lagzdins et al., 2012; Lloyd et al., 2016; Ockenden et al., 2016). In these regions, there was no significant difference between the dry period and the wet period as in the Mediterranean watersheds. This fact has enormous implications in the seasonal pattern of nutrient exports, as will be discussed in the following sections.

Hydrograph recessions were faster at La Tejería than at Latxaga, which could be related to the presence of tile drainage in the former (Gramlich et al., 2018). Tile drainage generates an increase in hydraulic conductivity while reducing the water storage capacity of the soil (Blann et al., 2009), leading to a faster recession to baseflow in the hydrographs.

5.4.2. NO_3^- dynamics in response to storm events

Events with high runoffs produced different responses at both watersheds. At Latxaga, high-flow events generally indicated higher NO_3^- during the event, whereas at La Tejería these events meant lower NO_3^- . These responses suggest a difference in the predominant pathways, with an apparent *piston effect* (mobilization of NO_3^- enriched water previously stored in soils) acting at Latxaga, and a dilution effect occurring at La Tejería, which is consistent with the probable effects of tile-

drainage (Keller et al., 2008). Despite the apparent dilution, the increasing $\text{NO}_3^-/\text{Cl}^-$ ratio indicates that new NO_3^- is being mobilized by high-flow events at both watersheds. In other words, net mobilization of new NO_3^- is occurring at La Tejería despite the significant decrease in concentration. The presence of tile drainage avoids a higher residence time of water and limits soil denitrification, not increasing the NO_3^- concentration of the subsurface water and generating this apparent dilution. However, these events enable the mobilization of NO_3^- from areas where it is not generally supplied, therefore producing this new supply of NO_3^- .

Despite these observations, the response to high-flow events did not influence the long-term behaviour of NO_3^- at the watersheds. There was a contradictory behaviour, in which the watershed experiencing a decrease in NO_3^- concentration (La Tejería) presented higher concentrations and yield throughout the study period. Again, tile drainage at La Tejería could have been a critical factor in explaining this behaviour. The increase in the concentration and export of nutrients due to the presence of tile drainage has been reported by several authors (McIsaac and Hu, 2004; David et al., 2010; Li et al., 2010; Gramlich et al., 2018). This dilution occurs as a consequence of lower residence times, bypass of riparian areas, etc. Besides, in particular cases, dilution could also enhance the hydrological response (higher peak flows, Gramlich et al., 2018), potentially diluting the NO_3^- . That is in fact what we observe at La Tejería, higher concentrations and yields. In contrast, at Latxaga, with the negligible presence of tile drainage, NO_3^- was lower throughout the entire study period, due to a longer residence time of nitrate, which produces higher denitrification. However, NO_3^- increased in high flow periods due to the absence of the dilution effect caused by lower connectivity between soil and stream.

5.4.3. Seasonal NO_3^- dynamics

Both watersheds followed a similar seasonal pattern, with winter maxima in concentration and loads. NO_3^- concentration started to increase in November following the basal application of fertilizers. Side-dressing application throughout winter and spring maintained NO_3^- relatively high, with a decline in March-May. Later on, after the harvest of winter cereal, minima concentrations and loads were observed. It is interesting to note the different behaviour across watersheds, with Latxaga reaching negligible NO_3^- values probably as a consequence of its wider, more diverse, and denser riparian vegetation (Chapter 2, Section 2.1). Riparian vegetation is considered one of the main factors limiting nutrient exports from watersheds (Tabacchi

et al., 2000; Dosskey et al., 2010). In contrast, La Tejería presented nearly no riparian vegetation (farm plots reach the edge of the stream) and, as a consequence, higher NO_3^- values remained until the stream dried. The $\text{NO}_3^-/\text{Cl}^-$ ratio provides an additional line of evidence to distinguish between dilution and evapoconcentration effects and NO_3^- sources or sinks. At the end of the crop cycle, the $\text{NO}_3^-/\text{Cl}^-$ ratio at La Tejería remained relatively stable, with only a minor decrease, which suggests that no significant NO_3^- sinks were at work. At Latxaga, in contrast, the $\text{NO}_3^-/\text{Cl}^-$ ratio decreased down to nearly zero values, clearly indicating a NO_3^- sink.

The seasonal distribution of NO_3^- -N yield was heavily conditioned by runoff, with the minor influence of concentration values. Approximately 51 % of the annual yield was generated between January and March, at both watersheds. This observation significantly differs from those obtained under different climatic conditions. For instance, at watersheds located in northern Europe, the yield was usually evenly distributed throughout the year, with no specific season accounting for most of the yield (e.g., Iital et al., 2014). Many authors have manifested the preponderance of discharge over concentration in NO_3^- -N export processes (e.g., Darwiche-Criado et al., 2015; Fučík et al., 2015; Sorando et al., 2018).

5.4.4. Interannual NO_3^- dynamics

According to the NO_3^- -N yields, a high runoff generally increases the nutrient yields (Fučík et al., 2017). In the case of Latxaga and La Tejería, years with higher runoffs produced higher NO_3^- -N yields. Runoff and NO_3^- -N yields followed similar patterns. Differences in NO_3^- -N yields could be explained by several factors such as antecedent soil moisture, tile drainage, and possible different fertilization practices in different watershed areas. The increase of the 2013 NO_3^- -N yield in comparison with 2012 was considerable. The leaching of NO_3^- -N produced in 2013 probably was generated not only by fertilization excess in 2013 but also by nitrogen surplus in 2012, when productivity was probably limited (very dry year), leading to a higher nitrogen surplus in this particular year. In addition, denitrification during 2012 was probably limited due to the low soil moisture and prevailing aerobic conditions in the soils (Martens, 2005; Skiba, 2008).

5.4.5. PO_4^{3-} concentration dynamics

Although dissolved P is considered the form with less contribution to P losses (Wu et al., 2012; Yaşar Korkanç and Dorum, 2019), it is the form measured at the watersheds assessed herein. The median PO_4^{3-} concentration at both watersheds was lower than the threshold detection limit. Such a low concentration occurred due to the low solubility of the phosphorous form present in soils with high pH (Merrington et al., 2002; Brady and Weil, 2008). Regarding seasonal distribution, an increase of concentration, above the detection limit, was appreciated in the spring and summer (April-August) at the La Tejería watershed. This high concentration appeared when the runoff was lower. The more energetic storm events are concentrated in these periods in Mediterranean catchments (Giménez et al., 2012). Storm events generate an energy-intensive runoff, mobilizing a substantial amount of sediments. Generally, an increase of flow during a storm event supposes an increment of sediments and, as a consequence, of particulate-P transport, as this is the main P-form in soils with high pH (Drewry et al., 2009). An increase of sediments and particulate-P would facilitate desorption or dissolution of phosphorous in the stream channel, producing an increase of PO_4^{3-} concentration (Sharpley, 1995). Conversely, at Latxaga these patterns were not observed, which could be associated with a more intense presence of riparian vegetation. It was verified that PO_4^{3-} and NO_3^- behave somewhat independently. While PO_4^{3-} concentration tends to increase in high flow events, as aforementioned, the behaviour of NO_3^- presented high variability across watersheds. NO_3^- is highly soluble while PO_4^{3-} was related to sediment concentration.

5.4.6. PO_4^{3-} -P yield

Both watersheds presented similar PO_4^{3-} -P yield patterns. Although the dynamics of PO_4^{3-} -P are influenced not only by the soluble form of P but also by particulate-P, the runoff is considered a crucial factor in the PO_4^{3-} -P yield (Sharpley, 1995) producing an increment of water discharge and increase of PO_4^{3-} -P yield (Fučík et al., 2017). Consequently, months with higher runoff also presented high PO_4^{3-} -P yield, differing from those with higher concentration, as aforementioned. Similarly, PO_4^{3-} -P yields are higher in years with higher runoff. However, it must be mentioned that the total P yield could be higher than the PO_4^{3-} -P yield reported herein. The phosphorous form considered herein only involved dissolved PO_4^{3-} , which can be 45-90% of total P (Merrington et al., 2002). In contrast with what has been described for concentrations, NO_3^- -N

and $\text{PO}_4^{3-}\text{-P}$ yield behaviours followed relatively similar patterns, as their exports were controlled by the available water flow.

5.4.7. Nutrient export controlling factors

This section enumerates the main factors that could be present at the studied watersheds (Fig. 5.10), focusing on understanding the differences in nutrient concentrations and yields, according to our observations and the available scientific literature on the topic. Although other factors could be important to other case studies, those included herein were considered to be relevant for La Tejería and Latxaga. It must be highlighted that it is not attempted to infer the controlling factors in agricultural watersheds from the two watersheds studied herein, but rather the other way around, using the available literature to underpin our knowledge of the processes at work.

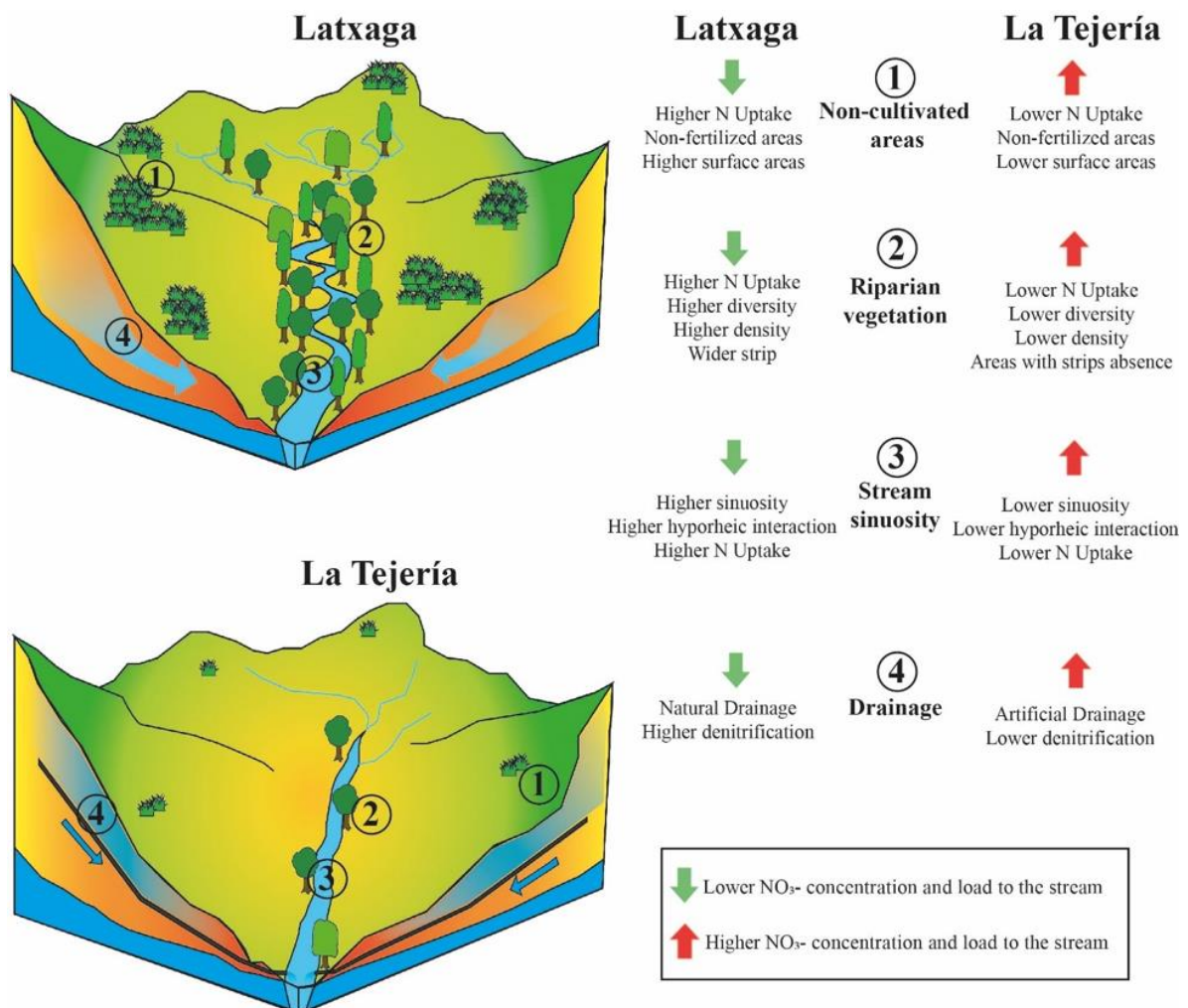


Figure 5.10: Schematics of the main controlling factors of nitrate dynamics

Soil characteristics and their effects on nutrient dynamics have been assessed previously (Lehmann and Schroth, 2003; Pärn et al., 2018). Empiric studies and simulation models have suggested that differences in organic matter quantity and quality led to differences in organic pools and carbon and nitrogen mineralization. The influence of texture is not sufficiently clear, although it is known that clay soils retain more organic matter than sandy ones when the same organic inputs are applied (Matus and Mairie, 2000). Denitrification regarding soil characteristics and texture has been also widely studied (Cambardella et al., 1999; Mastrocicco et al., 2011, 2019). Although some studies evidence a strong influence of texture on denitrification processes, with higher rates observed in soils with high content of clay and lower rates in soils with a high content of sand (D'Haene et al., 2003), other studies reported no significant differences regarding texture (Hofstra and Bouwman, 2005). Besides, a high preferential flow suggests higher nutrient transports to the subsoil (Brady and Weil, 2008) and lower residence time of nitrates in the soil, which could hinder denitrification processes. Despite the diversities between watersheds regarding soil organic matter content, depth, and texture, the differences were not sufficient to draw conclusions. Subtle differences in preferential flow (vertic conditions through the soil profile in ca. 40% of La Tejería's surface), however, could have contributed to nitrate leaching.

Every agrosystem encompasses a share of land that is not cultivated (i.e., unproductive areas). In general, these areas present limitations for cultivation – e.g., excessive slope or shallow soils. Casal et al. (2019) verified that non-cultivated areas retained an important fraction of nitrogen, leading to a decrease in the active fertilized area and consequently reducing nitrogen exports at a French catchment. Herein the share of unproductive areas at Latxaga (10.6 %) was almost five times higher than at La Tejería (2.3 %), and was, in general, closer to the stream. These unproductive areas did not receive any fertilization and could act as sinks of the nutrients originating from the upper parts of each watershed, affecting the total yield of nutrients.

Even if the riparian vegetation occupies a reduced area of the total watershed, its location near the water bodies enables it to act as a filter and/or sink of sediments and nutrients (Tabacchi et al., 2000; Dosskey et al., 2010; Chase et al., 2016; Neilen et al., 2017; Janssen et al., 2018). The width, density, and diversity of riparian vegetation have been reported to affect nutrient transports to streams (Broadmeadow and Nisbet, 2004; de Souza et al., 2013). For instance, herbaceous vegetation improves water infiltration and protects from runoff and erosion while woody vegetation protects streambanks from mass failure, and, in the case of senescent species, the

leaves increase the soil roughness, reducing the runoff (Dosskey et al., 2010). Moreover, the content of biomass is the primary indicator of nutrient uptake (Dosskey et al., 2010). As exposed in Section 2.1 of Chapter 2, there are essential differences in the riparian vegetation of the two watersheds: at Latxaga there is wider, denser, higher, and more diverse and developed riparian vegetation near the stream. At La Tejería, croplands reach the edge of the channel in many cases, with negligible riparian vegetation. According to scientific literature, when other conditions are similar, lower nutrient exports would be expected at Latxaga rather than at La Tejería.

The stream sinuosity index (ratio between the real length of a stream and the shortest straight line) is a parameter related to riparian vegetation, and its value at Latxaga was 1.13 m m^{-1} while La Tejería presented 1.04 m m^{-1} . Higher sinuosity causes a higher interaction of the water with the hyporheic zone of the bed (Peterson and Benning, 2013), increasing the potential of denitrification and nitrogen uptake in riparian areas. Although differences in sinuosity values could seem trivial, Lassaletta (2007) reported changes in average sinuosity, from 1.14 to 1.07 after land consolidation works, which could have induced changes in riparian vegetation and nutrient exports. Thus, the differences verified at Latxaga and La Tejería could be sufficient to produce higher interaction of water with the hyporheic zone and, as a consequence, decrease NO_3^- in stream water.

Although the natural characteristics of each watershed play essential roles regarding NO_3^- dynamics, management practices are also relevant. The impact of N fertilization on NO_3^- -N exports depends on different factors such as N fertilization rate, time and type of application, type of fertilizer, soil condition before the application, and crop phenology and characteristics. A linear relationship has been established between N application rates and the total nitrate leaching from soils - meaning that, under similar circumstances, an increase in N fertilizer rates produces an increase in mean leaching losses of NO_3^- -N (Liang et al., 2011; Muschietti-Piana et al., 2017). Consequently, it is imperative to control N fertilization rates, as N surplus (the N supplied in excess to the crop necessities) is considered the primary driver of N losses in croplands (Thorburn and Wilkinson, 2013). According to the recommended fertilization rates and average productivities, the N surplus at La Tejería ($46.7 \text{ kg N ha}^{-1} \text{ year}^{-1}$) was 11 % higher than at Latxaga ($41.9 \text{ kg N ha}^{-1} \text{ year}^{-1}$). Interestingly, a higher surplus was estimated for La Tejería (which received a lower amount of N) due to the higher productivities obtained at Latxaga. The nitrate yield from watersheds depends mainly on N surplus. Although this relationship is not linear, it

requires a threshold value below which N yield is negligible (Fenn et al., 2006; Ventura et al., 2008). At La Tejería, the N surplus 11 % higher supposed a NO_3^- -N yield 87 % higher. Besides, this threshold over which significant amounts of NO_3^- are leached depends on the available N retention capacity of the watershed. By comparing N yields and N surplus in the Navarrese watersheds, these thresholds can be estimated as approximately 15 and 25 $\text{kg N ha}^{-1} \text{ year}^{-1}$ for La Tejería and Latxaga, respectively, which are consistent with the differences previously discussed in riparian vegetation and other factors.

The presence of tile drainage at one of the watersheds is a relevant management practice that influences N exports (Arenas Amado et al., 2017). Tile drainage is typically employed in productive agricultural areas where natural drainage is poor (Randall and Goss, 2008; Gramlich et al., 2018). Several studies have remarked that tile drainage causes a considerable increase in the NO_3^- -N yield (Gentry et al., 1998; McIsaac and Hu, 2004; Woodley et al., 2018). Tile drainage acts as a bypass and decreases residence time and thus the interaction with soils and riparian vegetation, limiting in this way denitrification and nutrient uptake (McIsaac and Hu, 2004). For instance, in two wide regions in which the main differences were related to the intensity of drainage, McIsaac and Hu (2004) reported a N yield almost four times higher at an extensively drained area (21 m ha^{-1}) than at a relatively undrained area (0.7 m ha^{-1}). Tile drainage was present at La Tejería, and its density was estimated as approximately 25 m ha^{-1} . At Latxaga, no tile drains were observed nor reported by farmers. Given the importance of tile drainage in N exports, its presence/absence could be sufficient to explain the differences verified in the NO_3^- -N yield values of Latxaga and La Tejería.

Finally, explicitly focusing on PO_4^{3-} exports, several studies reported that sediments and phosphorous dynamics share an important connection (Kotti et al., 2000; Drewry et al., 2009; Shore et al., 2016; Odhiambo, 2018). A fraction of particulate-P can be desorbed from sediments when the latter is mobilized under high-flow conditions and transformed into a bioavailable form, generally PO_4^{3-} (Sharpley, 1995). Previous works carried out at the Navarrese watersheds reported that the median suspended sediment concentration was approximately five times higher and sediment yield was three times higher at La Tejería than at Latxaga (Merchán et al., 2019). This was mainly explained by the different characteristics in morphology and topography of each watershed (Casalí et al., 2008). Thus, the observed differences in PO_4^{3-} -P exports could be justified by these differences in sediment dynamics.

So far, the feasible influence of these controlling factors, according to our observations and available literature on the topic, has been examined separately, i.e., without considering possible interactions. The quantification of the effect of each factor and any possible synergies or counter effects deserve additional analyses such as statistical assessments and process modelling, which are outside the scope of the present chapter.

5.4.8. Comparison with other studies

The observations made at the Navarrese watersheds, regarding NO_3^- -N yields, were in agreement with those reported for arable watersheds all across Europe. In the United Kingdom, three catchments comparable to the Navarrese ones exported ca. 7-19 kg NO_3^- -N ha^{-1} year $^{-1}$, with an average nitrate concentration of ca. 6.5-35 mg NO_3^- L $^{-1}$ (Lloyd et al., 2016). In agricultural watersheds of the Baltic countries, Deelstra et al. (2014) reported nitrate yields of ca. 5-47 kg NO_3^- -N ha^{-1} year $^{-1}$. Other studies have confirmed the range of NO_3^- -N yield values: in Latvia (Lagzdins et al., 2012), Sweden (Kyllmar et al., 2014), Estonia (Iital et al., 2014) and Lithuania (Povilaitis et al., 2014). In Central Europe, a range of 10-50 kg NO_3^- -N ha^{-1} year $^{-1}$ was reported at different areas of a small catchment in the Czech Republic (Fučík et al., 2017). Regarding agricultural catchments in the Mediterranean region, the highest export of NO_3^- -N occurred in the December-March period (De Girolamo et al., 2017b). To the best of the authors' knowledge, there is scarce data regarding NO_3^- -N exports at small scale watersheds in Mediterranean regions. Larger watersheds in the Iberian Peninsula export 5-21.5 kg NO_3^- -N ha^{-1} year $^{-1}$, according to Romero et al. (2016). The results obtained for the Navarrese watersheds were of the same order of magnitude than those reported above.

Concerning water quality, the most critical P form is considered to be PO_4^{3-} due to its biological availability. However, phosphate usually does not represent an essential fraction of the total phosphorus load. Consequently, the PO_4^{3-} -P yield estimated at the Navarrese watersheds is only a fraction of the total P yield. Indeed, studies developed in northern Europe reported P loads that were two and three orders of magnitude higher than those observed at La Tejeria and Latxaga (Kyllmar et al., 2006; Pengerud et al., 2015).

5.5. CONCLUSIONS

Two experimental watersheds with similar climatic characteristics and management practices, and cultivated with rainfed cereals, have been assessed throughout ten years. Differences regarding water quality, mainly nitrate and phosphate concentrations and exports, have been observed.

Differences in nutrient concentration and yield obtained at these watersheds have demonstrated the relevance of the intrinsic characteristics of each watershed. Vegetation, tile drainage, and stream channel sinuosity were crucial factors affecting nutrient exports at the studied watersheds. Besides, riparian vegetation was considered to be a buffering factor in nutrient concentration, smoothing the nutrient concentration peak in specific periods.

An increase of vegetative elements in specific locations, better drainage management, and sufficient width of the riparian forest (which enables the stream to develop a specific sinuosity) would not only improve the water quality of streams in agricultural watersheds but would also produce more significant carbon sequestration, improvement in soil structure and soil fauna, decrease in erosion, and increase in the presence of aquatic organisms. These facts, combined with correct management choices, would contribute to the progress towards sustainable agriculture.

Although long-term water quality monitoring implemented in these watersheds and the suitable traceability of management practices within the watershed - which includes the influence of tile drainage, the evolution of riparian vegetation, development of non-cultivated areas, and land use - will help quantify the effect of each factor on the exports of nutrient pollution, a thorough analysis of the obtained data would be necessary. In this context, a non-linear time series analysis or watershed modeling would be suitable. These nature analyses would permit to obtain a causal interaction network among nutrient export controlling factors, thereby enabling the quantification of retention/export of nutrients by herein described controlling factors in the watershed. The knowledge of the interactions and quantification of factors would permit a better understanding of nutrient transport. In addition, the observations made in these watersheds, the in-depth analysis of controlling factors for nutrient export carried out in this study, and the proposed analysis such as modeling, will allow an adequate evaluation of agricultural watershed management tools to assess consequences in different scenarios regarding land use and management.

CHAPTER 6:
On the modeling of two agricultural
Mediterranean watersheds to quantify the
critical factors affecting dissolved nitrogen
exports

6.1. INTRODUCTION

The deterioration of aquatic ecosystems due to anthropogenic activities is a major global concern. Among the activities that affect water quality, agricultural practices are highlighted due to the high pressure exerted on natural aquatic ecosystems (Merrington et al., 2002; Durand et al., 2011). The use of fertilizers and management of agricultural land can contribute to the exports of nutrients to water bodies. Nitrogenous fertilizers are the most used worldwide (FAO, 2017), being essential to the adequate development of crops, but an excess can generate a surplus of nitrogen (N) in the soil. This surplus is not taken up by the crops and is lost through runoff and leaching, generally in the nitrate form (Durand et al., 2011).

An excess of nutrients in aquatic systems can produce significant environmental consequences, such as eutrophication. The main problems associated with eutrophication include dramatic algae blooms, deoxygenation of water bodies (causing fish mortality), alteration of the system's food chain, and growth of toxin-producing aquatic plants (Merrington et al., 2002). High concentrations of dissolved N (such as nitrate) in freshwater ecosystems not only affects the environment, but can also cause considerable health problems in humans. Excessive exposure to nitrate can cause methaemoglobinaemia and gastric cancer, among other diseases (World Health Organization, 2011). In addition, the ingestion of hazardous toxins produced in a eutrophic environment can cause significant health issues (World Health Organization, 2011).

Environmental concerns have led to the creation of legislative instruments by different governments and entities to mitigate the effects of nitrate. In Europe, the Nitrate Directive (91/676/CEE) limits the maximum concentration of nitrite in groundwater to 50 mg L⁻¹. The Water Framework Directive (2000/60/CE) identifies vulnerable areas to nitrate pollution for the implementation of conservation measures. Motivated by these environmental concerns, many European regions such as Baltic (e.g. Deelstra et al., 2014), Central Europe (e.g. Fučík et al., 2017) and Mediterranean (e.g. De Girolamo et al., 2017) countries, and British islands (e.g. Lloyd et al., 2016) have implemented watershed networks to monitor and quantify the status of water bodies.

In Navarre, northern Spain, the impact of agriculture on water bodies is also a concern. For this reason, the former Department of Agriculture, Livestock, and Food of the Government of Navarre implemented a network of small agricultural watersheds, encompassing the main agricultural land

uses and management practices in the region. Several studies related to water quality and nutrients have been conducted in these watersheds (Casalí et al., 2008, 2010; Merchán et al., 2018; Merchán et al., 2019; Hernández-García et al., 2020). A recent study evaluated two watersheds with similar land use, management and climate conditions, and reported that riparian vegetation and tile drainage significantly influenced N exports (Hernández-García et al., 2020, see Chapter 5).

Well-developed riparian vegetation on the streambank can act as a filter for pollutants and be an important nutrient and sediment sink (Dosskey et al., 2010; Chase et al., 2016). In addition, non-cultivated areas with spontaneous vegetation development can act as N sinks, retaining an important share of N and decreasing the fertilized surface of the watershed (Casal et al., 2019). However, tile drainage in a watershed implies in a decrease in the water residence time, and therefore, of the dissolved nutrients throughout the watershed – this causes less interaction between the nutrients and the soil, decreasing denitrification (Randall and Goss, 2008).

The quantification of the factors controlling nutrient dynamics is a complex task, but necessary to the establishment of measures directed to decrease the export of nutrients to freshwater ecosystems. Models are representations of real systems or processes, and watershed hydrological models are extremely useful to assess diverse scenarios regarding water, sediment or nutrients in a watershed, such as Soil water Assessment Tool (SWAT), Annualized Agricultural Non-Point Source model (AnnAGNPS), or the Better assessment Science Integrating Point and Non-point Sources model (BASINS), among others (Parajuli and Ouyang, 2013). The most adopted deterministic watershed hydrological models generally employ mainly three components (Novotny, 2008): i) hydrological component, related to the transit of water in the watersheds; ii) sediment component, based on erosion and transport processes, and iii) water quality component, focused on the dynamics of different nutrients and pollutants. The adjustment of models, which enables a fair representation of reality (considering its limitations), can aid in the decision-making process of managers.

This study builds upon Chapter 5 and quantifies the influence of the most significant factors on the dynamics of N in two Mediterranean rainfed watersheds. The contributions of this study are: (a) to evaluate a watershed hydrological model in the study area; (b) and to use the fitted model to quantify the influence of controlling factors on nitrogen dynamics, by applying different simulation scenarios in the watersheds.

6.2. METHODS

6.2.1. Experimental watersheds and data collection and analysis

The watersheds where the study of this chapter was conducted were the rainfed winter cereal watersheds of the agricultural watershed network of the Government of Navarre, namely Latxaga and La Tejería (Fig. 6.1). In the Section 2.1 of the Chapter 2 a thorough description of each watershed and its peculiarities is presented.

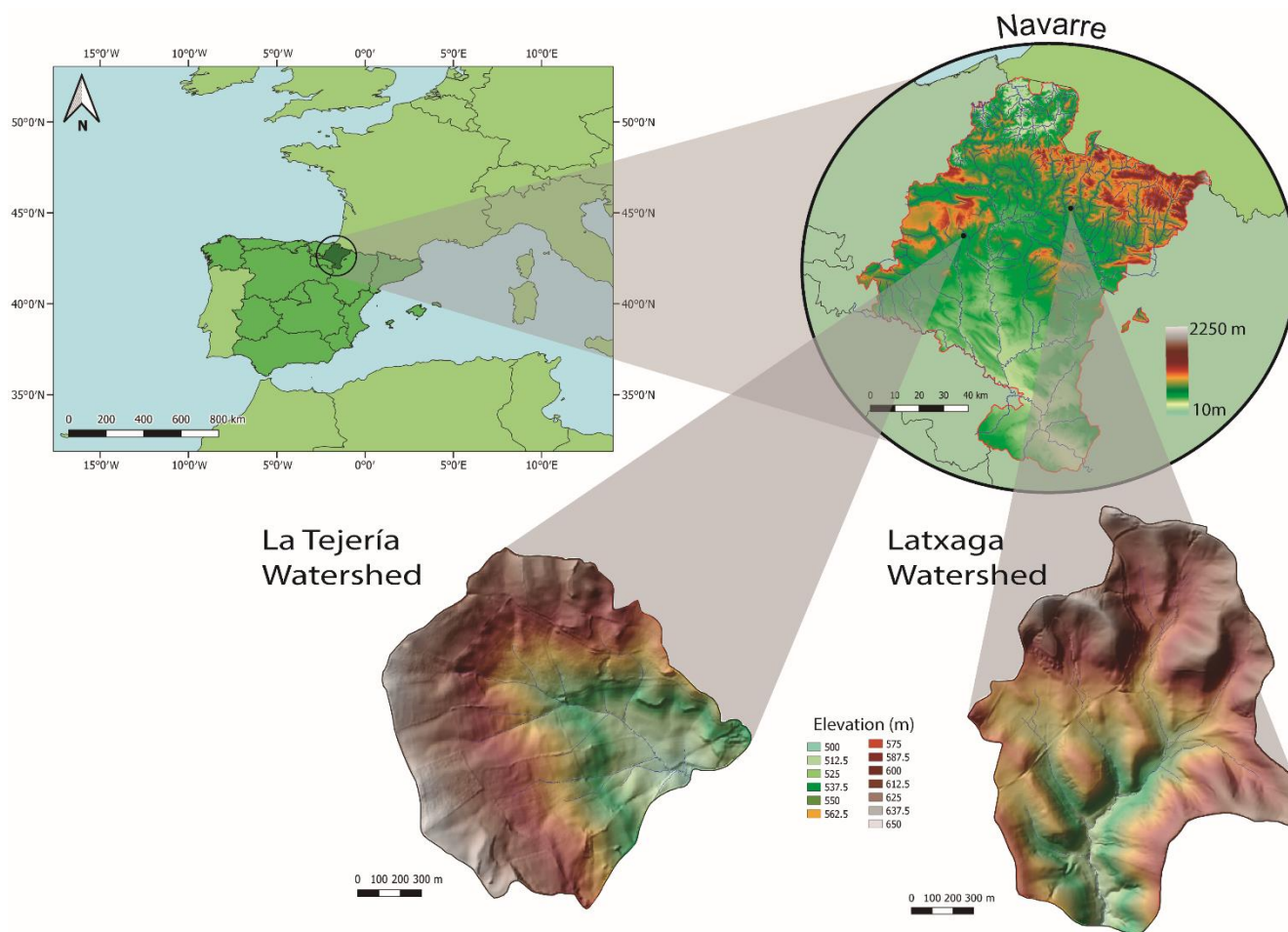


Figure 6.1: Location of the Latxaga and La Tejería watersheds, two experimental agricultural watersheds of the Government of Navarre.

The methodology employed for hydrological and meteorological data, and the collected water quality samples (with the correspond analysis) is described in the Chapter 2 Section 2.

6.2.2. AnnAGNPS model

The model used in this chapter was the Annualized Agricultural Non-Point Source Pollution (AnnAGNPS) model (version v5.51). The description of this model can be found in Section 2.3 of Chapter 2. This section describes the model operation, the main inputs required for its correct functioning, and the main processes simulated and evaluated in this chapter.

6.2.3. AnnAGNPS model inputs

The effective performance of AnnAGNPS requires a significant number of inputs. As can be observed in the Section 2.3.1. of Chapter 2.

Regarding topography, a digital elevation model (DEM) to generate the land units (cells) and stream reaches with TOPAGNPS software can be utilized to greatly simplify the development of the necessary AnnAGNPS input parameters. A 1 m DEM of the two watersheds was obtained by processing high-density LiDAR points information from the Government of Navarra (IDENA, 2019).

Climate information was collected from the automatic weather stations in each watershed. Precipitation, temperature, wind speed, wind direction, and solar radiation were obtained on a 10-minute basis. The information was grouped into daily values and incorporated into AnnAGNPS. The dew point was estimated from the relative humidity and average air temperature using the inverse of Tetens's equation (Chow et al., 1988).

The crop growth data required were obtained from different sources. Annual crop yield data of each crop were collected from the Government of Navarre datasets, obtaining the productions throughout the study period, ensuring an adequate crop yield range to calibrate the model (Government of Navarre, 2020). Other parameters related to cultivation, such as decomposition factor, residue/grain ratio, and cultivation uptake, were obtained from technical reports (Government of Aragon, 2000; Government of Navarre, 2020) and scientific literature (Vagstad et al., 1997; Liao et al., 2004; Rezig et al., 2014). Other parameters, such as phenological development at different stages of the crop, were obtained from different studies (Wang and Engel, 1998; Racca et al., 2015;).

Regarding crop management, the land use of each watershed was obtained from annual aerial imagery taken by the Government of Navarra. A thorough survey of the watershed was performed by checking all the drainage pipes to determine tile drainage, thus determining drainage density. The management operations of each crop were registered from information obtained from experts and compared with the technical sheets of each crop management (MARM, 2008). Average fertilization data were obtained from Casalí et al. (2008), from recommendations of local institutions (INTIA, 2018), and from the previously mentioned crop data sheets. Finally, data concerning grain stubble ratio were obtained from studies carried out in areas with similar characteristics (Government of Aragon, 2000; Government of Navarre, 2020)

Soil input data were collected from a detailed soil map of each watershed, developed by the (Government of Navarre, 2005a, 2005b) and reported by Casalí et al. (2008) (see Chapter 2, Section 2.1). From these maps, information was collected on a variety of physical (number of horizons, structure, texture and bulk density) and chemical parameters (pH and contents of N, phosphorus and carbon). Field capacity and wilting point of soils were estimated from the equations reported by Saxton et al. (1986), and the K factor was estimated from Wischmeier and Smith (1978) and Renard et al. (1997).

Runoff data were primarily based on the curve number (CN) obtained from the Technical Release 55 (USDA-NRCS, 1986), and adapted to the particular conditions of each watershed as previously reported by (Government of Navarre, 2005a, 2005b; Chahor et al., 2014; Hernández-García et al., 2020).

6.2.4. Processing of observed data

AnnAGNPS is used to perform daily simulations for the exports of water, sediments, and chemicals by runoff at the watershed outlet, but it cannot simulate baseflow.

Previous processing of the water flow and exported nitrogen was performed to compare AnnAGNPS simulation data with observed data. A recursive filter was applied to separate the baseflow from the direct runoff, to determine the baseflow at the watershed outlet. The filter employed was developed by Eckhardt (2005), and applied three times to flow data (Fig. 6.2). After the baseflow was determined, the runoff was obtained from the difference between total flow and baseflow. The suitability of the filter was confirmed previously in different watersheds of Navarre,

with satisfactory results (e.g., Chahor et al., 2014). The percentage of flow at the watershed outlet that corresponded to runoff was 38% at La Tejería, and 43% at Latxaga.

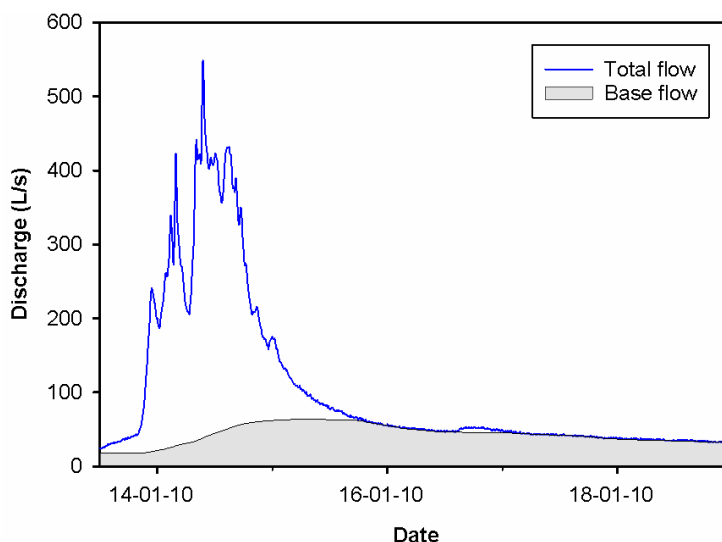


Figure 6.2: Discharge of total flow and baseflow at La Tejería throughout in six days.

In AnnAGNPS, the simulated N exports are those transported by direct runoff. Therefore, an estimation of the daily exports of nitrogen was carried out following the procedure developed by Vanni et al. (2001). Firstly, it was necessary to obtain the daily exports of dissolved N at the watershed outlet. This was accomplished by multiplying the daily concentration by the daily water discharge. Once the total N exports were obtained, the nitrogen concentrations before and after a storm event were obtained (in other words, the baseflow concentration before and after a runoff event). After the nitrogen and baseflow concentrations were obtained, a linear interpolation was applied between the two periods to obtain the baseflow concentration during the event. Similarly to the determination of total N exports at the watershed outlet, baseflow concentrations were multiplied by the baseflow, yielding the N exports from the baseflow at the watershed outlet. The difference between total N exports and N exports from the baseflow is the N exported by runoff.

6.2.5. Runoff calibration

For runoff calibration, an inverse calibration technique was applied to both watersheds, which required the procedures shown in Fig. 6.3. A unique calibration set including all available data was used to optimize the runoff component, for a better fit with the N export component. Model fitting was performed on a monthly scale. The processes within this calibration are: (1) global search of

the parameters selected; (2) local refinement to reduce the value range of the parameters selected, and (3) model performance evaluation, which employs various model-fit indices or metrics.

For the inverse calibration process, several iterations were necessary with the AnnAGNPS model in various parts of the processes (Fig. 6.3). Calibration was accomplished through a High Performance Computing (HPC), which enables simultaneous computation jobs and reduces computation time significantly, allowing multiple iteration processes. This study utilized the computer cluster of the research institutes at the Public University of Navarra. In this cluster each user can utilize 30 computing cores to execute parallel work with 128 GB RAM and 100 GB hard disk. The HPC works with Sun Grid Engine (SGE), which is a queue management system that optimally selects the solution node, for an effective and equal job execution (see Chapter 2, Section 2.4). The calibration scripts used herein were based on those developed by Muñoz-Carpena (2019) for Global Sensitivity and Uncertainty Analysis.

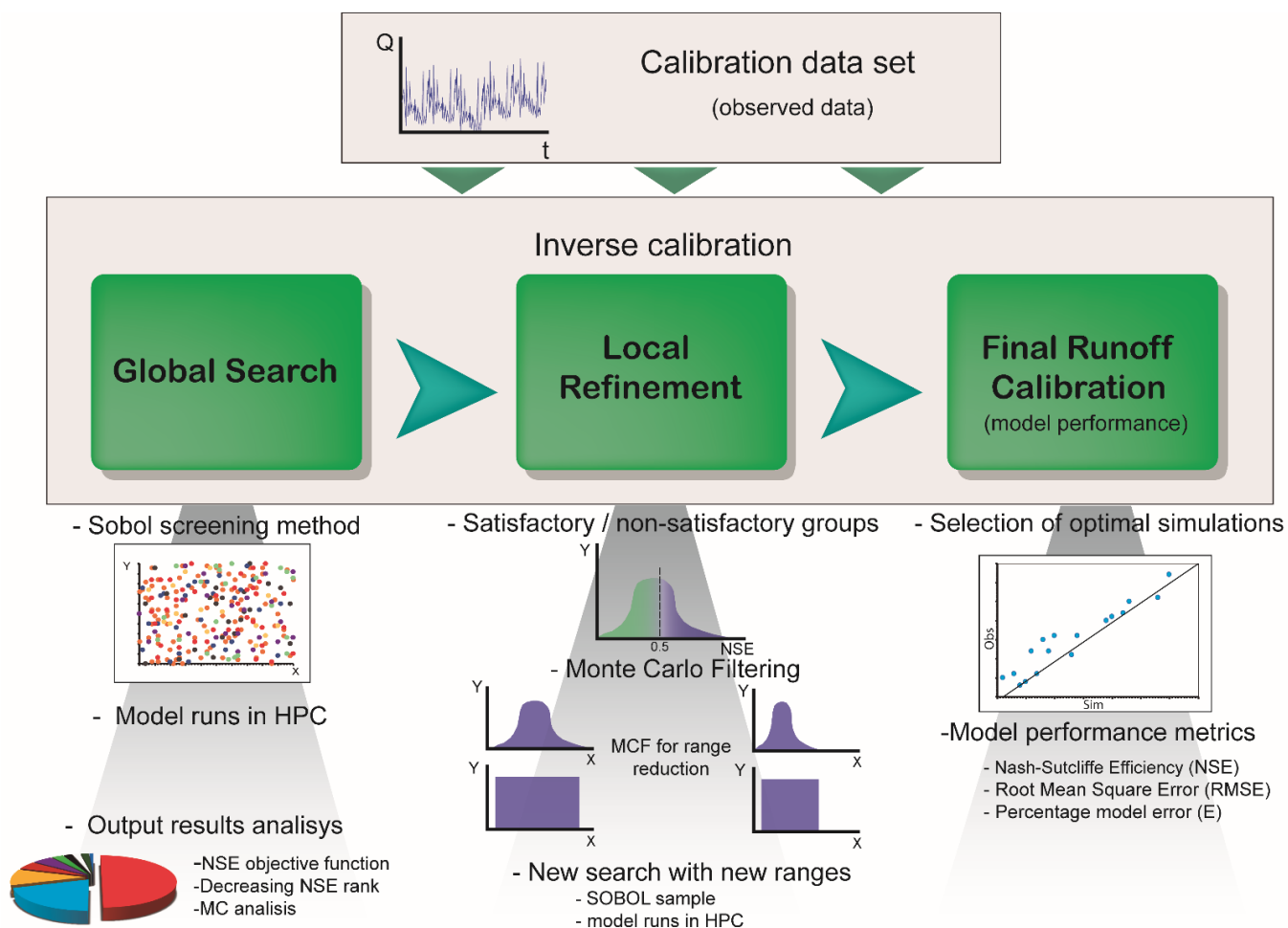


Figure 6.3: Schematics of runoff calibration.

6.2.5.1. Global search

The first step in runoff calibration is the definition of parameters. Runoff simulation in the AnnAGNPS model is based on the SCS Curve Number technique (see Chapter 2, Section 2.3.2.1) (Bingner et al., 2018). The variables considered in the calibration are the different CN values in the different soils and the different periods. The variables chosen were CN values for stubble soil, bare soil, bare soil after tillage, cultivation in winter, and cultivation in spring, and rangeland for the soils of hydrological groups B and C (Table 6.1).

After the selection of variables, a Monte Carlo global search analysis was performed with the Sobol screening method (Sobol, 1993, 2001). This method identifies the critical parameters for model optimization. The Sobol method is a global sensitivity analysis method in which a decomposition of the variance is performed. All variables vary simultaneously. This method determines the sensitivity independently of the linearity or monotonicity of the model (Baroni and Tarantola, 2014). In addition, this method is not only capable of assessing the sensitivity of each variable (Sobol first order index, S_i), but also enables the observation of the sensitivity of interactions (Sobol total order index), being one of the most capable models in detecting these interactions (Tang et al., 2007).

The global search process was structured in three steps: (1) generation of a Sobol sample, (2) execution of the model in the HPC, and (3) analysis of the execution results (Monte Carlo Analysis) (Fig. 6.3). The first and third steps were performed using the SimLab software (Saltelli et al., 2004; Tarantola and Becker, 2017), developed for global uncertainty and sensitivity analysis techniques.

For the first global search, the CN values chosen for the 12 variables, to be sampled at both watersheds, had a range of 30-100 with uniform distribution (Table. 6.1). This range was defined based on the values reported by USDA-NRCS (1986) and Ponce and Hawkins (1996), which confirmed that although CN values theoretically range from 0-100, values under 30-40 have not been observed in the environment. Combination of the 12 variables yielded a matrix with 13,312 combinations. These combinations were executed using HPC, and the results were exported to SimLab software, for the sensitivity analysis of the parameters based on the model's fit with observed data. This adjustment was made by applying the Nash-Sutcliffe coefficient (consolidated

in the prediction of hydrological models, Nash and Sutcliffe, 1970) as the objective function, and ranking each simulation based on the NSE value obtained, in decreasing order.

Table 6.1: Curve number and soil hydrological parameters (each soil hydrologic group corresponds to a different parameter).

Parameter	Hydrologic soil group	Description	Start Date
Stubble soil	B/C	Bare soil recently harvested with plant residue	1st Jul
Bare Soil	B/C	Bare soil after ploughing with moldboard	15th Sep
Bare Soil 2	B/C	Recently sown bare soil	15th Oct
Winter CN	B/C	Soil with crops in an early phenological state (e.g. germination, tilling in the cereal)	15th Dec
Spring CN	B/C	Soil with crops in an advanced phenological state (e.g. stem extension, maturation in the cereal)	15th Mar
Rangeland	B/C	Non-cultivated areas with shrubs	--

6.2.5.2. Local Refinement

After the first global analysis and determination of the parameters that explain the adjustment of the model, a Monte Carlo Filtering (MCF) was performed (Saltelli et al., 2004). The filter refined the range of the most sensitive variables in the model fit, comparing with a possible sub-range of important input factors and establishing a more accurate range of those that are not so important (Fig. 6.4). To this end, two groups of simulations were generated: for the satisfactory NSE coefficient values and for the non-satisfactory values. The threshold value for definition as satisfactory or non-satisfactory followed Moriasi et al. (2007, 2015), where $NSE = 0.5$ was considered the limit value for a satisfactory flow adjustment of a watershed scale model to a monthly time step.

The Kolmogorov-Smirnov test was then applied to identify candidates for the refinement (parameters with significant differences between satisfactory and non-satisfactory models, Fig. 6.4). It is important to know, that equifinality or nonuniqueness appear when alternative parameter sets produce similar results (Beven and Binley, 1992). The distributions of each candidate parameter were adjusted in range, for a new sampling (Fig. 6.4). For those parameters without significant differences between distributions, a more specific range was adjusted, based on scientific literature and good fit ranges obtained in this global analysis.

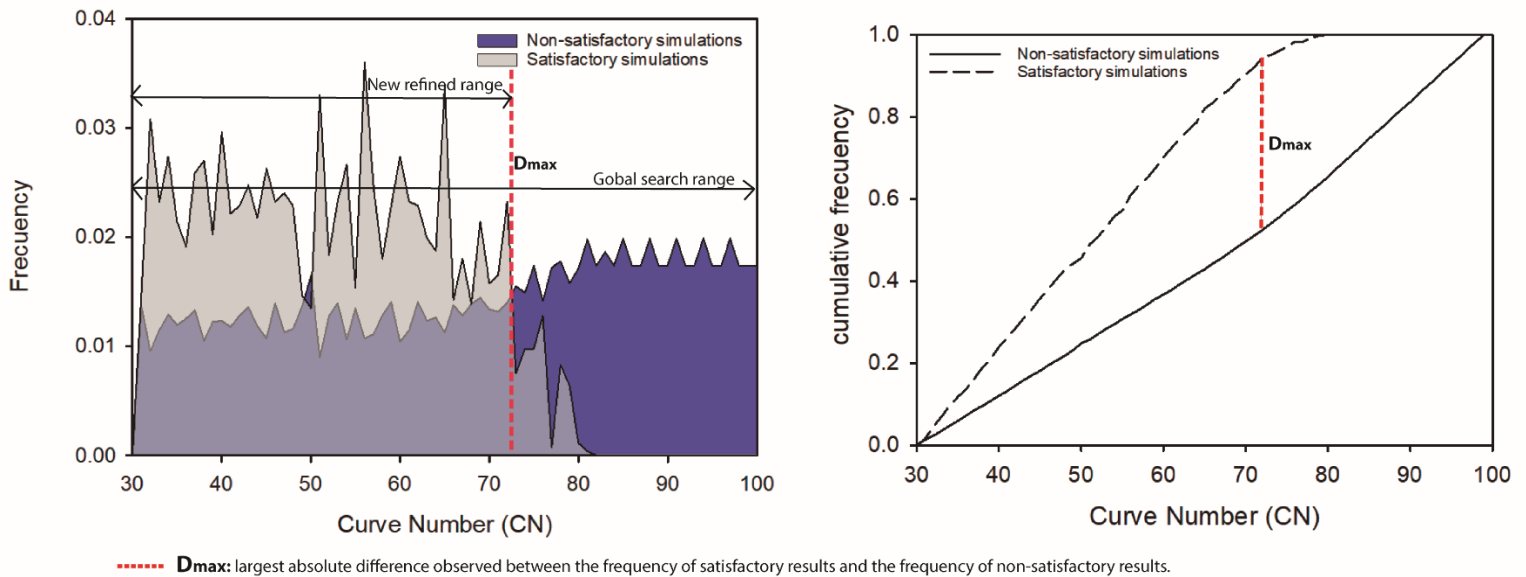


Figure 6.4: Monte Carlo Filtering of a critical parameter and new range definition.

6.2.5.3. Final runoff calibration

Finally, the process was repeated by re-sampling a Sobol screening matrix with the new refined ranges, followed by final model execution with HPC (13,312 runs). After model execution, the optimal simulation was selected as the one with the best adjustment and consistent parameters with scientific literature and intrinsic characteristics of the watersheds, ending the calibration process. Model performance followed the model-fit metrics described in the Section 6.2.8.

6.2.6. Dissolved nitrogen calibration and testing

For N calibration, the processes carried out were very similar to runoff calibration. Inverse calibration on a monthly scale was also used, but with subtle differences, as depicted in Fig. 6.5. As can be observed in Fig. 6.5, the dataset of N observations was divided into two independent subsets (tails and center) for model cross-validation with a “hold-out” method (Bennett et al., 2013).

This method consists of independent steps for calibration model and testing. The calibration period was March 2009-March 2014, and the testing periods were October 2006-February 2009 and April 2014-September 2016. Similarly to runoff calibration, the steps for N inverse calibration were: (1)

global search, (2) local refinement, and (3) model performance (with calibration and testing datasets). Due to the succession of processes and the number of model runs performed, HPC was essential for the viability of the calibration.

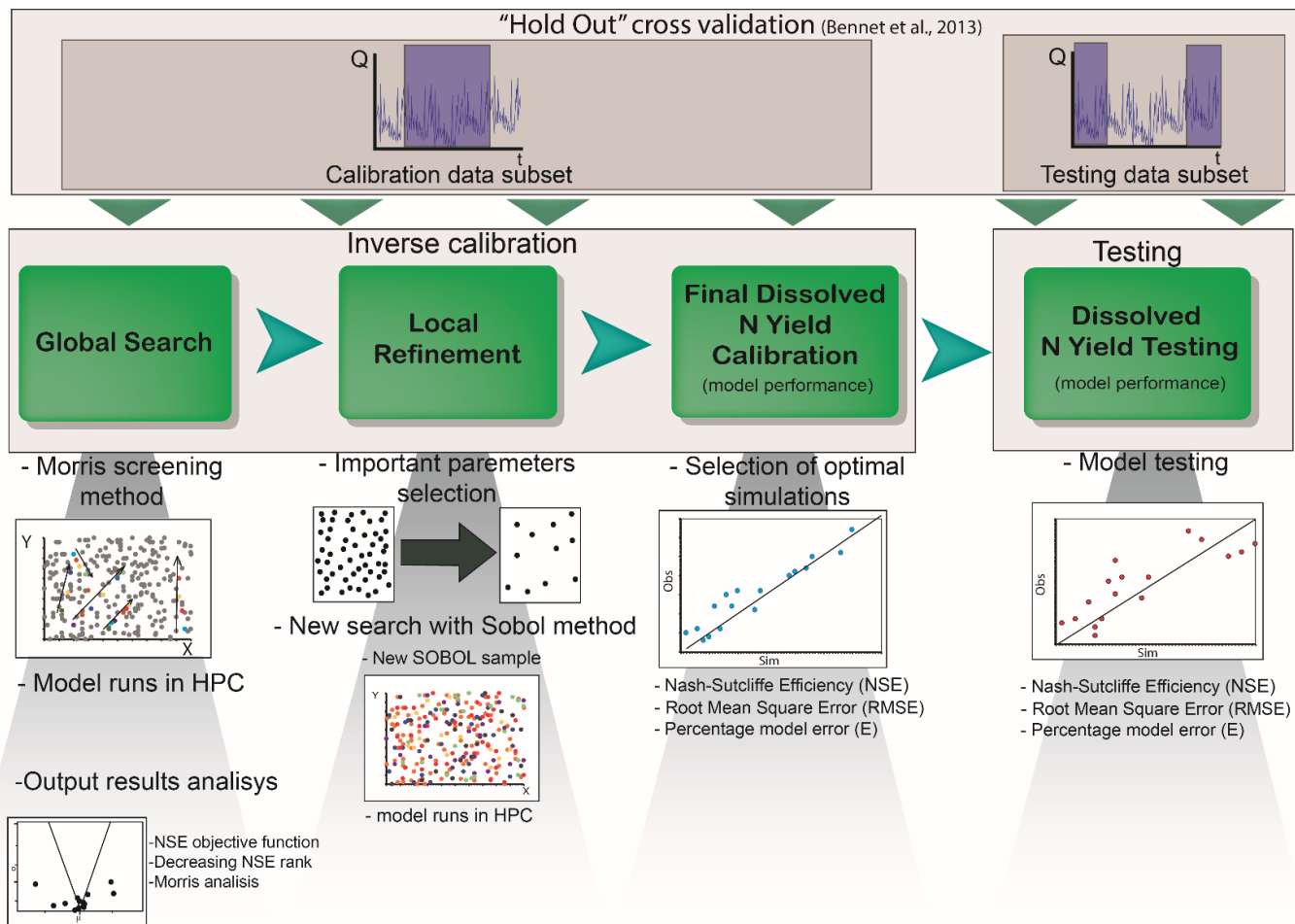


Figure 6.5: Procedure for dissolved N export calibration and testing.

6.2.6.1. Global search

The first step in N calibration was the detection of the parameters involved in the movement and export of N in the watersheds. To this end, each process related to N and simulated by AnnAGNPS was analyzed in detail (see Chapter 2 Section 2.3.2.2). Unlike what happened with runoff, the number of parameters involved in the N cycle was very high, assuming a total of 74 direct parameters (Table 6.2) that affected up to 141 parameters indirectly (i.e., if the clay content is a direct parameter, its alteration produces changes in the sand and silt content).

Sampling with the Sobol method was not viable due to the high number of model simulations for an adequate global search, which was unfeasible with the available resources. Therefore the Morris method was used to determine the most sensitive variables regarding N exports in the two watersheds.

Table 6.2: Parameters that influence the N cycle in AnnAGNPS, processes in which they are involved, and the distribution used in the defined ranges, based on scientific literature. In the case of clay, the variation range comprised the textural class of the horizon to be analyzed in each case, and reported in the soil map developed by the Government of Navarra (e.g. for a silty-clay horizon, the range analyzed was 40-60% clay content).

Parameter	Description	N cycle processes	Distribution
Yield	Yield per unit area at harvest.	Harvest	Normal
Fertilizer application	Fertilizer amount applied in each dose (two applications per year).	N input (Fertilizer)	Normal
CNR*	Carbon/N ratio for the crop	Humus mineralization	Triangular
Descomposition Coefficient	Coefficient of crop surface residue decomposition.	Humus mineralization	Triangular
Residue cover	Percentage of area covered by plant residue in each tillage activity (30%, 60%, 90%).	Harvest/humus mineralization	Uniform
Crop-Residue coefficient	Mass ratio of residue to yield.	Harvest	Normal
N uptake	N uptake per crop yield unit.	Plant Uptake	Normal
Fenological stage development	Accumulated fraction of time from planting to harvest for ending each of 4 growth stages (initial; development; mature; and senescence).	Plant Uptake	Uniform
N uptake in diferent fenological development	Fraction of Nitrogen uptake from planting to harvest for each of 4 growth stages (initial; development; mature; and senescence).	Plant Uptake	Uniform
Soil Organic content of 1st soil layer**	Organic carbon content in the first soil layer of each soil type.	Soil N content	Uniform
Soil Organic content of 2nd soil layer**	Organic carbon content in the second soil layer of each soil type.	Soil N content	Uniform
Soil Inorganic content of 1st soil layer**	Inorganic carbon content in the first soil layer of each soil type.	Soil N content	Uniform
Soil Inorganic content of 2nd soil layer**	Inorganic carbon content in the second soil layer of each soil type.	Soil N content	Uniform
Clay content of 1st soil layer**	Clay content in the first soil layer of each soil type.	Soil N content	Uniform
Clay content of 2nd soil layer**	Clay content in the seconf soil layer of each soil type.	Soil N content	Uniform

*Carbon Nitrogen Ratio

**the number of variables of these parameters depends on the number of soil types present in the watershed.

The Morris screening method (Morris, 1991) takes advantage of elementary effects computed at evenly spaced values of each parameter over its entire range, calculating the final effect from the average of the partial effects (Loizu et al., 2016). Therefore, this method obtains results with significantly fewer model runs and considerable reduction in computational costs, compared to other methods. Although this method presents lower computational cost, it does not detect individual interactions between parameters, as it only calculates the interaction of a parameter with the rest (Saltelli et al., 2000).

The global calibration steps are the same as those for runoff calibration: (1) generation of a Morris sample, (2) execution of the model with HPC, and (3) analysis of results. The first and third steps of this global search were carried out following Khare and Muñoz-Carpena (2014) and Khare et al. (2015).

Sample generation followed the scripts developed by Khare and Muñoz-Carpena (2014) for Morris Sampling Uniformity, from a Sample ASCII fac file, which contains parameter ranges and distributions, generated with SimLab Software (Tarantola and Becker, 2017). The sampling strategy used was Enhanced Sampling for Uniformity (Chitale et al., 2017), with eight minor input factors and 16 trajectories. The ranges of the direct variables and their distributions were obtained from data collected at the watersheds during the studied years by the Government of Navarre, and from widely adopted data identified in scientific literature. Simulations were ranked in decreasing NSE order.

After results were obtained, the elementary effects were evaluated with the objective of identifying the most sensitive variables, and reducing the number of these in a following iteration. Morris' sensitivity analysis was carried out employing the measurements and plots of the elementary effects developed by Khare and Muñoz-Carpena (2014). Variance and mean were evaluated for each parameter.

6.2.6.2. *Local Refinement*

Following the assessments of means and variances, parameters with linear (additive) and nonlinear (interactive) effects were selected as critical, excluding all parameters with negligible effects.

Once the number of variables was reduced to those that explain the N exports, new sampling of these variables was carried out with the Sobol method (sampling with this method is feasible due

to the reduction in variables, 12,288 runs). The ranges and distributions chosen for these variables were those observed in the field throughout the study period, and typical of the region.

6.2.6.3. *Final dissolved N calibration and testing.*

The best fitting model runs, consistent with the environment, were selected as optimal. Model performance followed the model-fit metrics described in Section 6.2.8. Finally, the set of calibration inputs was applied to the subset of testing data, to evaluate model performance.

6.2.7. Scenario simulations for controlling factors of dissolved N exports.

6.2.7.1. *Quantification scenarios of dissolved N export by tile drainage and vegetation at La Tejería and Latxaga, respectively.*

Two scenarios were proposed to quantify the factors that control the exports of nitrogen in the agricultural watersheds of Tejería and Latxaga.

All land units (cells) with spontaneous or riparian vegetation at Latxaga's watershed were replaced by cells with standard cereal management in the watershed. This was required to observe the effect of vegetation in non-cultivated areas and in riparian zones.

All cells with tile drainage were changed: drainage was removed, so that the effect of tile drainage could be appreciated.

After observing the effects of these changes on the exports of N, an analysis is carried out to verify the effects of variations in these factors on N exports.

6.2.7.2. *Scenarios for determining the effect of different tile drainage and spontaneous vegetation management in both watersheds.*

In addition to the proposed quantification scenarios, other scenarios have been simulated with different management in each watershed.

At Latxaga, two scenarios were simulated:

- A scenario in which the area of riparian vegetation and spontaneous vegetation increases from 12% of the watershed to 24% (ca. 52 ha), in order to simulate an increase in riparian vegetation. This increase occurred in cells close to the main channel (Fig. 6.6A)
- A scenario in which those cells in areas with poor cultivation conditions, and with riparian or spontaneous vegetation, were replaced by cultivation areas with tile drainage.

As at Latxaga, two other scenarios were simulated at La Tejería:

- A scenario in which the area of cultivated plots under tile drainage management increased considerably in cells close to the main channel. In this scenario the simulated area with artificial drainage covered 63 ha, ca. 38% of the watershed (Fig. 6.6B).
- A scenario in which those cells occupied by tile drainage were replaced by spontaneous or riparian vegetation without tile drainage, and considering the area not cultivable due to its limitations.

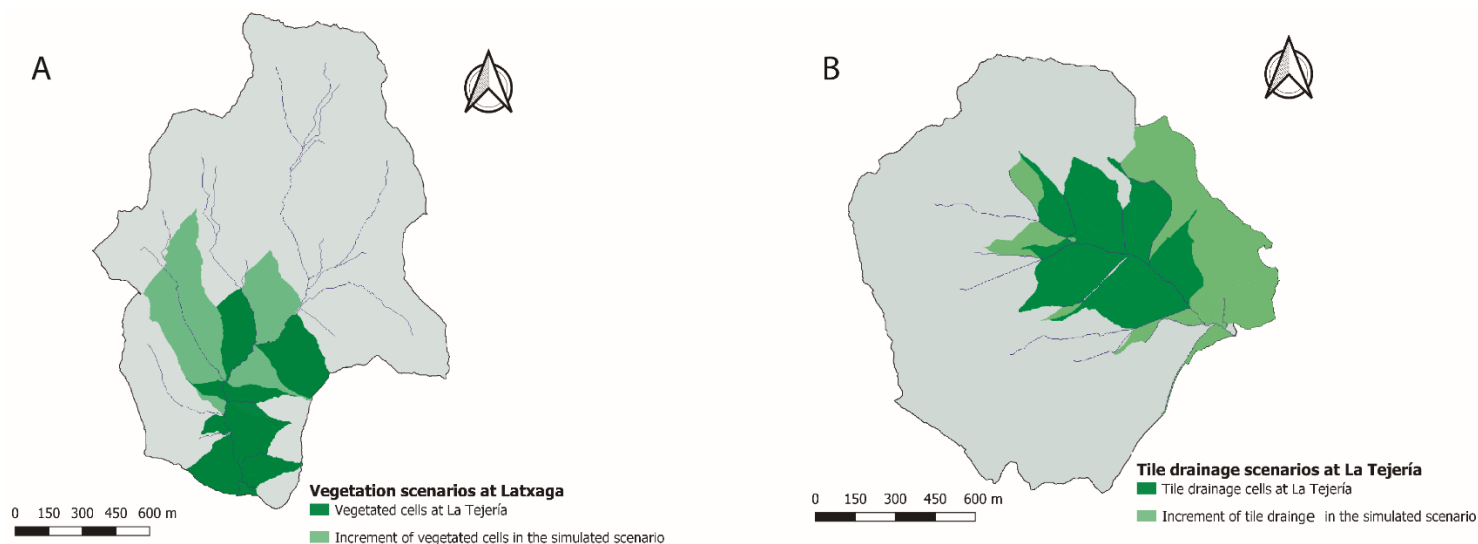


Figure 6.6: Increment of (A) tile drainage cells in simulated scenario at La Tejería, and (B) vegetated cells in simulated scenario at Latxaga.

6.2.8. Model Performance Metrics

The assessment of AnnAGNPS's performance was carried out by using Nash-Sutcliffe efficiency (NSE) (Equation 6.1), the root mean square error (RMSE) (Equation 6.2), and the percentage model error (E) (Equation 6.3):

$$NSE = 1 - \frac{\sum_{i=1}^n (P_i - O_i)^2}{\sum_{i=1}^n (P_i - \bar{O})^2}; \quad \text{Eq. 6.1}$$

$$RMSE = \sqrt{\frac{\sum_{i=1}^n (P_i - O_i)^2}{n}} \quad \text{Eq. 6.2}$$

$$E = \frac{P_i - O_i}{O_i} \quad \text{Eq. 6.3}$$

P_i is the predicted output, O_i is the observed output at time t , \bar{O} is the average observed output and n is the sample size.

NSE statistics ($-\infty < NSE < 1$, where $NSE=1$ indicates perfect model fit) provides a measure of the model's goodness-of-fit, calculated between measured and predicted values. NSE greater than 0.50 (Moriassi et al., 2007) or 0.65 (Ritter and Muñoz-Carpena, 2013) are often used as a threshold value, with satisfactory agreement between observed and simulated values. The less stringent criterium ($NSE \geq 0.5$), was used for the runoff refinement step and the more stringent criterium ($NSE \geq 0.65$) was utilized for the runoff calibration.

Statistical hypothesis testing was applied to verify model adequacy. This was accomplished with FITEVAL software (Ritter and Muñoz-Carpena, 2013), which is based on NSE fitting for the different simulations.

The hypothesis testing enables the identification of the significance (p-value) of the model performance exceeding a desirable minimum efficiency threshold in runoff ($NSE \geq 0.65$) (Ritter and Muñoz-Carpena, 2013).

For dissolved nitrogen calibration and testing, the threshold value selected for the definition of satisfactory simulations was $NSE \geq 0.35$, based on the performance measurements and evaluation criteria developed by Moriassi et al. (2015) for water quality models.

6.3. RESULTS AND DISCUSSION

This section presents the results of the calibrations and testing for runoff and N exports, and for the proposed scenarios.

6.3.1. Runoff calibration

The results obtained from the global analysis, local refinement, and model performance are presented below.

6.3.1.1. Global search

After carrying out the global search in the inverse calibration of runoff with the Sobol screening method, MonteCarlo analysis was performed considering the following parameters as critical for calibration, which explained more than 85% of runoff variability in the model (Fig. 6.7):

- Bare Soil, Winter CN and Spring CN in Soils with hydrologic group B in La Tejería;
- Bare Soil, Winter CN and Spring CN in Soils with hydrologic group C in Laxaga

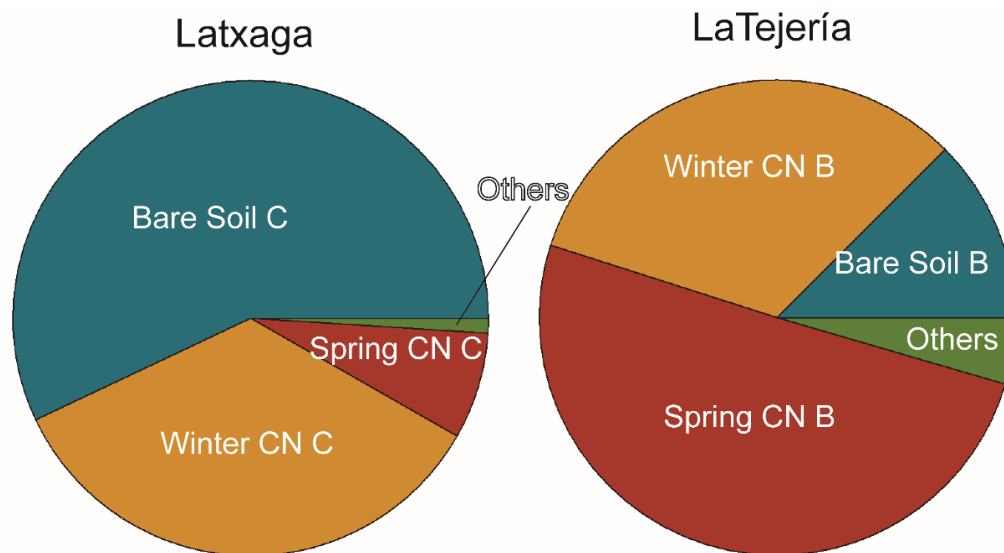


Figure 6.7: Sobol first order index distributions for runoff at Latxaga and La Tejería watersheds.

There are several causes for the importance of these parameters to runoff. The wet season occurs between the months of November-March for both watershed, producing a considerable increase in

runoff from the end of December/beginning of January to March/April, due to the increase of the humidity content of the soil (Hernández-García et al., 2020). The Winter CN parameter represents the curve number of the cereal in its first development stages, which happens in the January-March period, coinciding with the period of highest rainfall and runoff. The relevance of this parameter is related to this increase in runoff.

Spring CN refers to the curve number in the cereal crop in its advanced phenological development, from the end of March to the end of June. This period did not have as much precipitation (in comparison with the aforementioned period) but it includes considerable precipitation events that generated runoff. In addition, because this period occurs after the wet season, the soil moisture content at the watersheds is high, facilitating runoff generation. This is also the period before the dry season, when soil cracks appear, especially in watersheds with vertic soil features, such as La Tejería.

Another critical parameter for both watersheds was the Bare Soil curve number, which refers to the bare soil ploughed for management prior to sowing. This period occurs after summer, in mid-September, when the soil moisture content is very low after the dry period. At these watersheds, the vertic conditions of the soils have been previously reported (Government of Navarre, 2005a, 2005b; Hernández-García et al., 2020). The presence of cracks in low moisture soils due to the presence of expansive clays causes a modification of preferential flow, enhancing infiltration and thus decreasing runoff (Brady and Weil, 2008). The Bare soil period coincides with the end of summer, which is the period in which the soil is the driest, and therefore when the highest number of cracks appear. The occurrence of vertic conditions have been reported as more intense in La Tejería than in Latxaga (Government of Navarre, 2005b; Hernández-García et al., 2020). For this reason, cracks appear in La Tejería not only during the Bare Soil period, but also in late spring and summer.

The critical variables at La Tejería correspond to soils with hydrological group B and at Latxaga, correspond to soils with hydrological group C, due to the occupation of land in each watershed. At La Tejería, 77% of its area is occupied by soils classified as hydrological group B. And at Latxaga, 97% of its area is occupied by soils from hydrological group C (Government of Navarre, 2005a, 2005b).

Regarding the first order Sobol indices, it is observed that the sum of the first-order indices (S_i) is (S_i)=0.88 at La Tejería and (S_i)=0.95 at Latxaga. When $0.6 \leq \text{sum}(S_i) \leq 1$, the model is considered additive (most of the variance is explained by the sum of individual factor effects) (Saltelli et al., 2004). Such high values of (S_i) at both watersheds refers to negligible interactions between parameters (Table 6.3).

Table 6.3: Sobol first and total order indices, and interactions of runoff parameters for runoff at La Tejería and Latxaga watersheds.


Parameter	Hydrologic soil group	La Tejería			Latxaga		
		Sobol First order indices	Sobol Total order indices	Interactions	Sobol First order indices	Sobol Total order indices	Interactions
Stubble soil	B	0.013	0.034	0.020	0.001	0.001	0
Bare Soil	B	0.109	0.145	0	0	0	0
Bare Soil 2	B	0.001	0.028	0.027	0	0	0
Winter CN	B	0.283	0.348	0.064	0	0.001	0.001
Spring CN	B	0.439	0.512	0.073	0.001	0.001	0.000
Rangeland	B	0.020	0.029	0.008	0	0	0
Stubble soil	C	0	0.008	0.008	0.003	0.003	0
Bare Soil	C	0	0.017	0.017	0.550	0.570	0.019
Bare Soil 2	C	0.002	0.019	0.017	0	0.005	0.005
Winter CN	C	0.001	0.005	0.004	0.336	0.348	0.013
Spring CN	C	0.012	0.027	0.015	0.071	0.080	0.009
Rangeland	C	0	0.009	0.009	0.004	0.004	0

6.3.1.2. Local Refinement

Once the critical runoff generation parameters were obtained in the model, MCF was performed. Analysis included the critical parameters (defined as candidate for the refinement) and those with significant differences between the simulations with satisfactory results and non-satisfactory results. New and more accurate screening ranges for each parameter were obtained (Table 6.4). For parameters without significant differences and no critical influence on runoff, a more adjusted range was defined, supported by literature data (TR-55, USDA-NRCS, 1986).

Table 6.4: p-value between non-satisfactory and satisfactory results for each parameter, and first and refined ranges for runoff.

		La Tejería			Latxaga		
	Hydrologic soil group	First Range	p-value	Refined Range	First Range	p-value	Refined Range
Stubble soil	B	30-100	<0.01	40-62	30-100	<0.01	35-60
Bare Soil	B	30-100	<0.01	31-67	30-100	<0.01	31-54
Bare Soil 2	B	30-100	>0.1	49-76	30-100	>0.1	45-80
Winter CN	B	30-100	<0.01	35-78	30-100	<0.01	65-83
Spring CN	B	30-100	<0.01	31-67	30-100	<0.01	53-84
Rangeland	B	30-100	>0.1	56-72	30-100	>0.1	52-86
Stubble soil	C	30-100	<0.05	56-80	30-100	<0.01	55-68
Bare Soil	C	30-100	<0.01	50-65	30-100	<0.01	35-69
Bare Soil 2	C	30-100	>0.1	65-90	30-100	>0.1	45-90
Winter CN	C	30-100	<0.01	73-89	30-100	<0.01	66-84
Spring CN	C	30-100	<0.01	55-77	30-100	<0.01	53-84
Rangeland	C	30-100	>0.1	61-85	30-100	>0.1	61-90

 Runoff critical parameters at La Tejería

 Runoff critical parameters at Latxaga

The low curve numbers observed in the parameters that appear during and after the dry season occurred because of the presence of cracks, which significantly reduce the runoff potential in watersheds.

6.3.1.3. Model performance

After simulations were carried out with a Sobol matrix and the new refined ranges, the best combinations of parameters were selected, not only based on the best results, but also on the consistence with the environmental properties of the watershed of these factors (Table 6.5).

In the optimal result combination, low CN values are observed in both watersheds during the dry season. As discussed in the previous sections, the presence of cracks decreases the runoff potential

of the watershed, favoring infiltration (Brady and Weil, 2008; Cheng et al., 2021). The effects of cracks at La Tejería are more evident than at Latxaga as low CN values affect more parameters. Although cracks were observed at both watersheds, La Tejería presented larger and more numerous cracks (Government of Navarre, 2005a, 2005b; Hernández-García et al., 2020), with several cracks appearing in the months of April-May, before the dry season.

Regarding the rangeland variable in soils with hydrological group C, the CN value is slightly higher than expected. Even though the vegetated areas of rangeland can favor infiltration, their location, usually close to the channel, causes the saturation of soil in some periods and produces higher curve numbers than those expected.

Rangeland areas in other locations of the watershed are generally non-cultivable areas due to the shallow soil profile and high slope, with easier saturation and higher curve number values. The areas mainly occupied by low brush present an important amount of thick elements on the surface, decreasing in some cases infiltration and promoting runoff generation.

Table 6.5: Optimal model fit variables and model performance metrics for runoff at Latxaga and La Tejería.

<i>Parameter</i>	La Tejería		Latxaga	
	B	C	B	C
Stubble soil	46.6	71.8	50	55.5
Bare Soil	42.2	56.4	38	38.5
Bare Soil 2	64.5	74.5	89	89.5
Winter CN	71.1	78.3	73	73.5
Spring CN	48.5	75.2	71	71.5
Rangeland	61.3	61.5	77.5	89.5
<i>Model fit statistics</i>				
NSE	0.76		0.72	
RMSE	11364		15977	
E	<5%		-18.20%	

B and C refer to hydrological soil groups

Finally, model runoff was verified through model performance metrics (Table 6.5). It was observed that in both cases the model results were satisfactory, with a p-value > 0.1 , indicating less than 10 % probability of unsatisfactory results (Fig. 6.8).

The threshold for non-satisfactory models was set at $NSE=0.65$, as reported by Ritter and Muñoz-Carpena (2013). This threshold was stricter than that reported by Moriasi et al. (2007, 2015) as suitable runoff fit was required to achieve successful results in the dissolved N export calibration process.

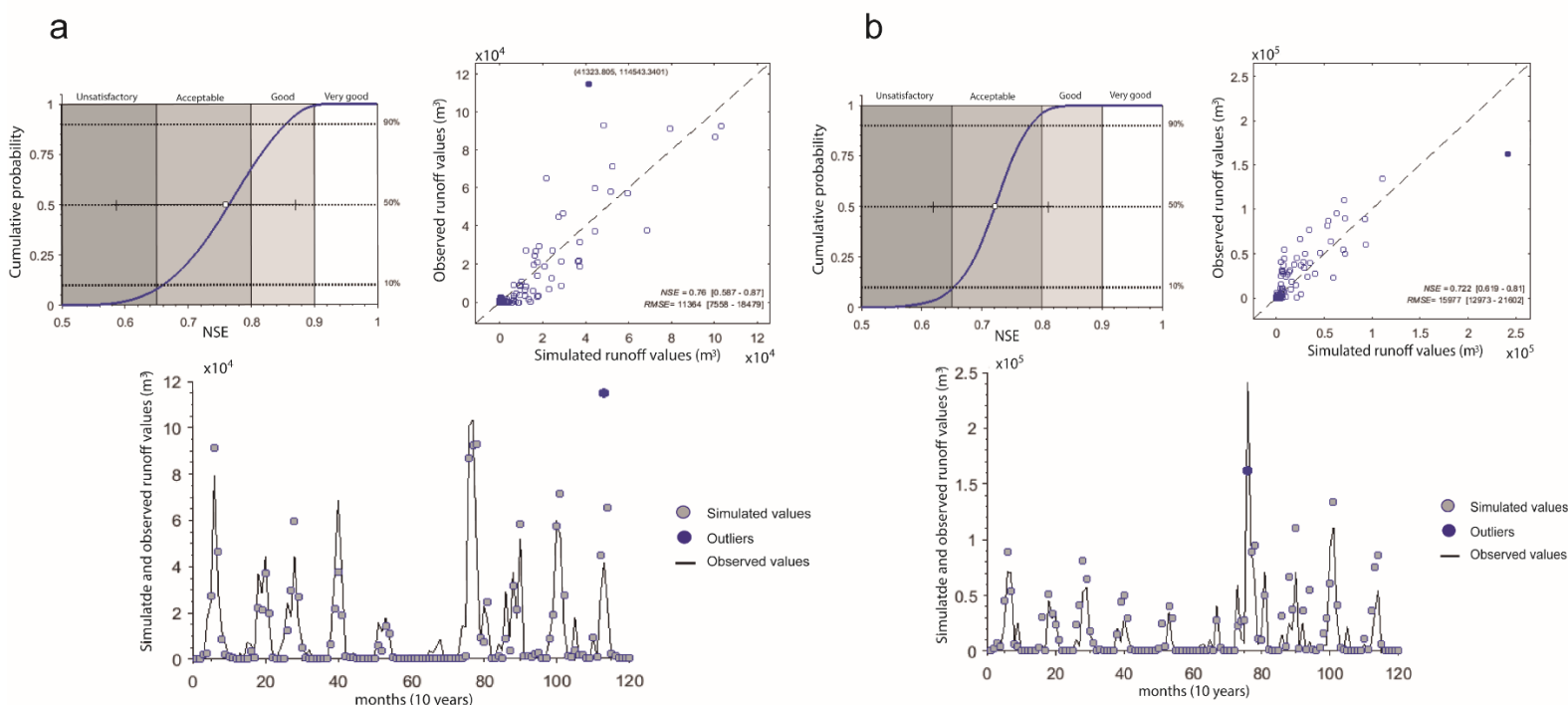


Figure 6.8: Observed and simulated values, and NSE probability for runoff at (a) La Tejería and (b) Latxaga watersheds.

6.3.2. Calibration and testing of dissolved N exports

The results obtained from the global analysis, local refinement, and model performance are presented below.

6.3.2.1. Global search

Due to the large number of variables required for the determination of N exports at both watersheds (74 parameters), global analysis was previously performed with the Morris method to detect the

most critical parameters for N exports.

Figure 6.9 shows the yield and residue decomposition coefficients (decompcoeff) as being the most sensitive, considering these two factors were crucial in model calibration. The parameters of soil texture and soil N content were not very influential – because these are more related to the exports of organic N (usually exported as particulates, not dissolved).

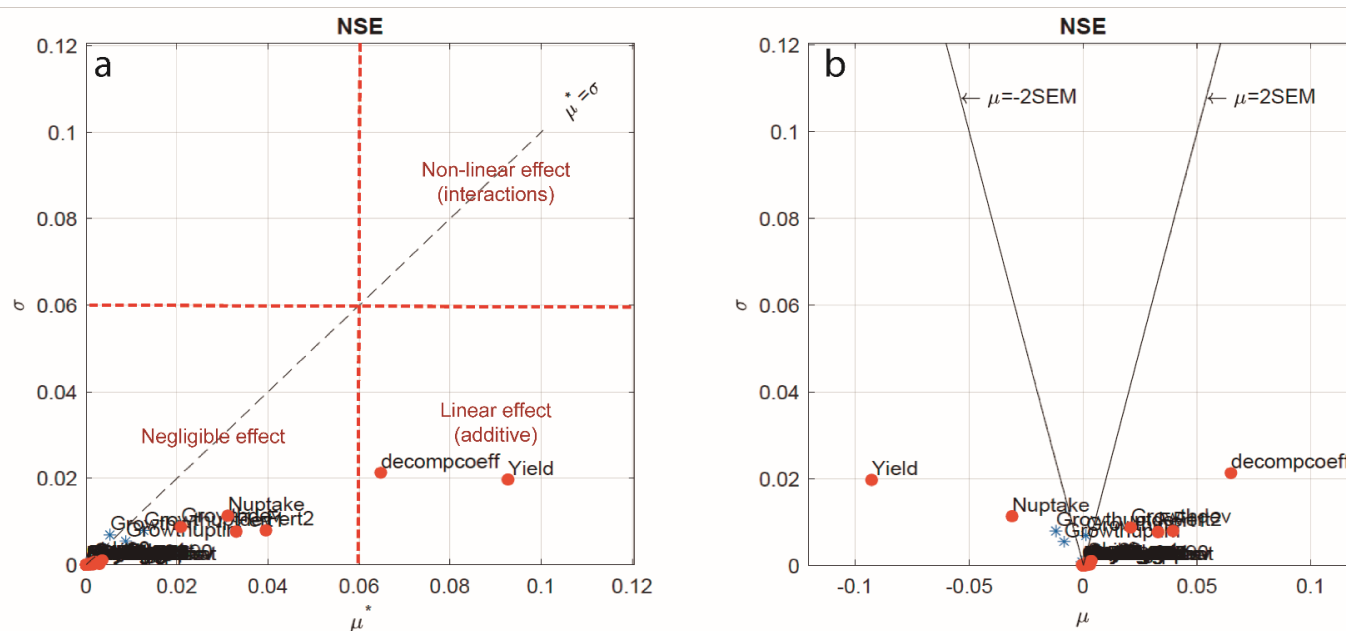


Figure 6.9: μ vs σ plot for selected parameters: (a) those parameters located above the black dotted line refer to interactions; (b) the $\mu = \pm 2$ SEM lines identify the factors with dominant non-additive/non-linear effects.

6.3.2.2. Local Refinement

As mentioned in the previous section, the parameters of cereal yield and residue decomposition coefficient were the most critical, displaying linear effects. This means that, similarly to runoff, the model is also additive for N exports, as no parameter in this analysis presented a non-linear effect (interactions) (Fig. 6.9a).

As shown in Fig. 6.9b, an increase in the decomposition coefficient led to an increment in N exports, due to the higher availability of dissolved forms. Conversely, an increment of the N yield implied in less N exports, due to a higher N content in the crop. In Fig. 6.9b, the N uptake parameter seems to affect the N exports.

In addition to the critical parameters, fertilization and N uptake were also included in the

calibration process. Although these parameters presented negligible effect, they were selected due to their important impact on dissolved N. Regarding fertilization, this parameter displayed wide variability throughout the study period, while N uptake was identified as a critical parameter in Fig. 6.9b. After the selection of new parameters, a Sobol sampling was carried out with the same ranges of the variables previously obtained from the yield and fertilization at the watersheds throughout the study period (Casalí et al., 2008; MARM, 2008; Government of Navarre, 2020). The decomposition coefficients and N uptake of the cereal were obtained from Government of Aragon (2000) and Government of Navarre (2020b) (Table 6.6).

Table 6.6: Range of selected critical parameters.

Input Factor	Unit	Factor ID	Range
Cereal yield	kg ha ⁻¹	Yield	2000-7000
Residue Decomposition Factor	unitless	Decompcoeff	0.0008-0.016
Fertilization in winter	kg N ha ⁻¹	Fert1	51.5-124
Fertilization in spring	kg N ha ⁻¹	Fert2	81-180
N Uptake	kg N kg yield ⁻¹	Nupt	0.017-0.033

6.3.2.3. Model performance and testing

The combinations of parameters with the best (or optimal) fit to the simulation were selected, based on consistent values with the environment and agricultural management of the watersheds (Table 6.7).

Table 6.7: Optimal combination factors for model performance, and model performance metrics at La Tejería and Latxaga watersheds.

Parameters		La Tejería		Latxaga	
		Calibration	Testing	Calibration	Testing
Cereal yield	kg ha ⁻¹	2,112		3,441	
Residue Decomposition Factor	unitless	0.014		0.015	
Fertilization in winter	kg N ha ⁻¹	109.4		81	
Fertilization in spring	kg N ha ⁻¹	136		106	
N Uptake	kg N kg yield ⁻¹	0.027		0.029	
<i>Model fit statistics</i>		<i>Calibration</i>	<i>Testing</i>	<i>Calibration</i>	<i>Testing</i>
NSE		0.72	0.51	0.52	0.45
RMSE		260.26	288.09	249	329.6
E		-13.2%	8.2%	-19.5	-14.4

Within these combinations of selected critical parameters, the low average yield reported for both watersheds was highlighted. The yield value at La Tejería and Latxaga was ca. 50% and ca. 30% lower than the average cereal yield reported in the area for the study period, respectively. This apparent low value could be partially caused by the uncertainties in the determination of the real cereal yield. The yield value considered suitable for Latxaga and La Tejería watersheds was that reported by the regional agricultural area to which each of these watersheds belong (Government of Navarre, 2020). These regional zones cover a larger area than that occupied by the watersheds, and even though the crop yield of Latxaga and La Tejería is considered representative of these agricultural areas, the generation of uncertainties in determining an exact cereal yield value is possible, and may occur an underestimation of this value. Due to this issue, the average crop yield of these watersheds may be slightly lower than the average annual cereal yield in the agricultural area. In addition, processes not incorporated in the N cycle by the AnnAGNPS model (e.g. nitrogen fixation), or the additive nature of the model, with no significant interactions between parameters and processes observed, are also important sources of possible uncertainties, which may influence the low cereal crop yield value. A yield value closer to the average yield generate unsatisfactory results in model simulations, producing a significant overestimation of results on low cereal yield years. The possibility of reducing these uncertainties in future versions of AnnAGNPS can help calibrate the model with annually updated data.

Regarding fertilization, even though the values in Latxaga and La Tejería are not exactly the same than the values described herein, are very similar to those reported by local governments. In addition, similar values have been reported in other works in these watersheds (Casalí et al., 2008). Moreover, these average values are based on the fertilization recommendations made by the local institutions (INTIA 2018), so uncertainties in the application may justify this slight difference.

Regarding model calibration performance metrics (Table 6.7), it is observed that the NSE values at La Tejería and Latxaga are over the threshold of $NSE \geq 0.35$ defined by Moriasi et al. (2015) for satisfactory nitrogen exports on a monthly basis in watersheds.

Moriasi et al. (2015) established $NSE \geq 0.35$ for acceptable simulations, $NSE \geq 0.5$ for good simulations, and $NSE \geq 0.65$ for very good simulations of N exports at a monthly scale. When verifying model error percentage (E), at both Latxaga and La Tejería an underestimation of the

mean N exports occurred, probably because of the uncertainties of parameters described, and the limitations of the model. Even so, the calibration results were satisfactory with *very good* and *good* model performances at La Tejería and Latxaga, respectively (Fig. 6.10).

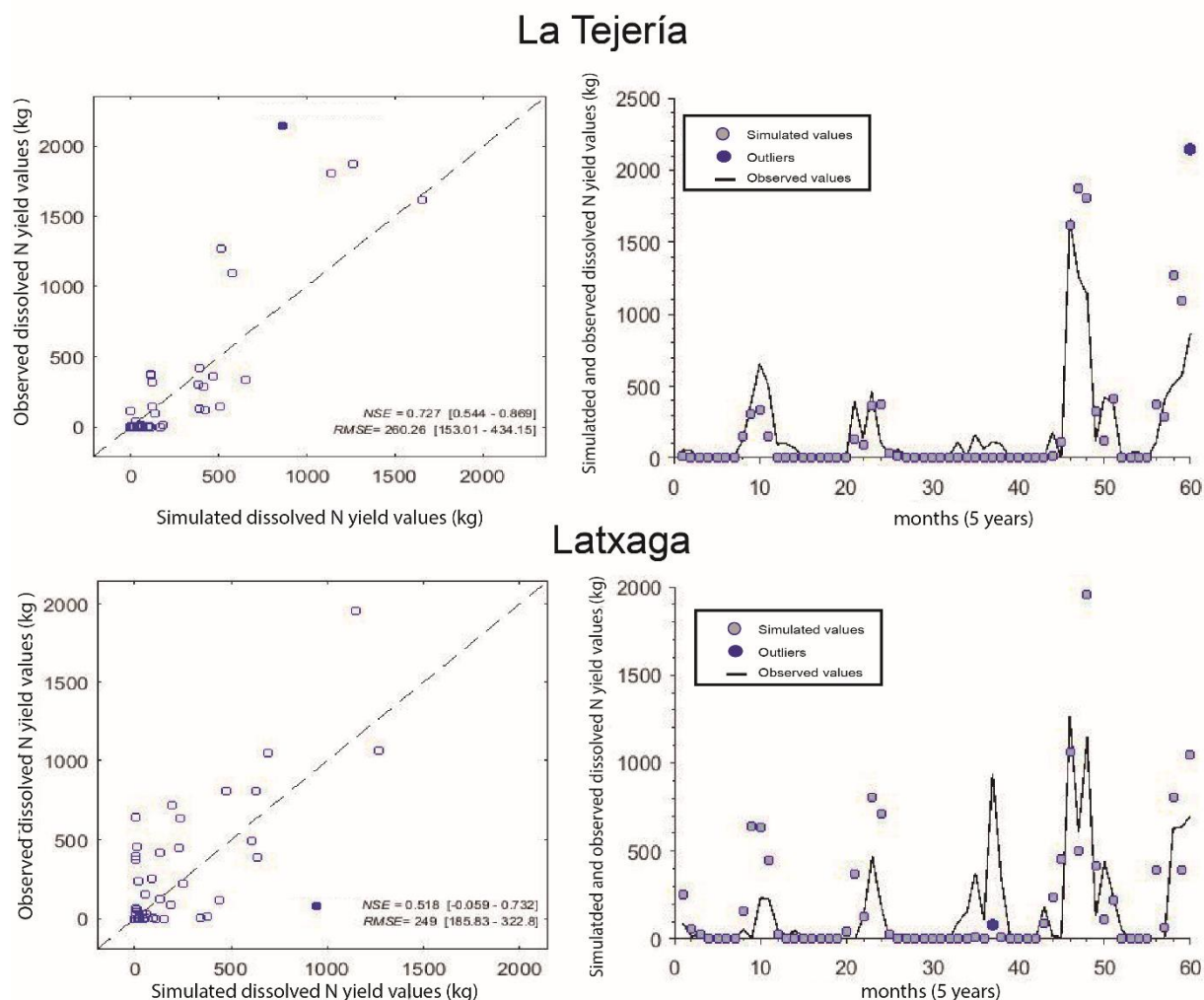


Figure 6.10: Observed and simulated values of dissolved N Yield calibration at La Tejería and Latxaga watersheds.

The results for performance metrics according to the testing also displayed NSE values above the threshold established by Moriasi et al. (2015) (Table 6.7). As occurred in calibration, during testing an underestimation was observed for the La Tejería model, possibly also to the uncertainties caused by input factors as cereal crop yield, by processed not considered by the model, or by the low interactions between parameters and processes of the model (Fig. 6.11).

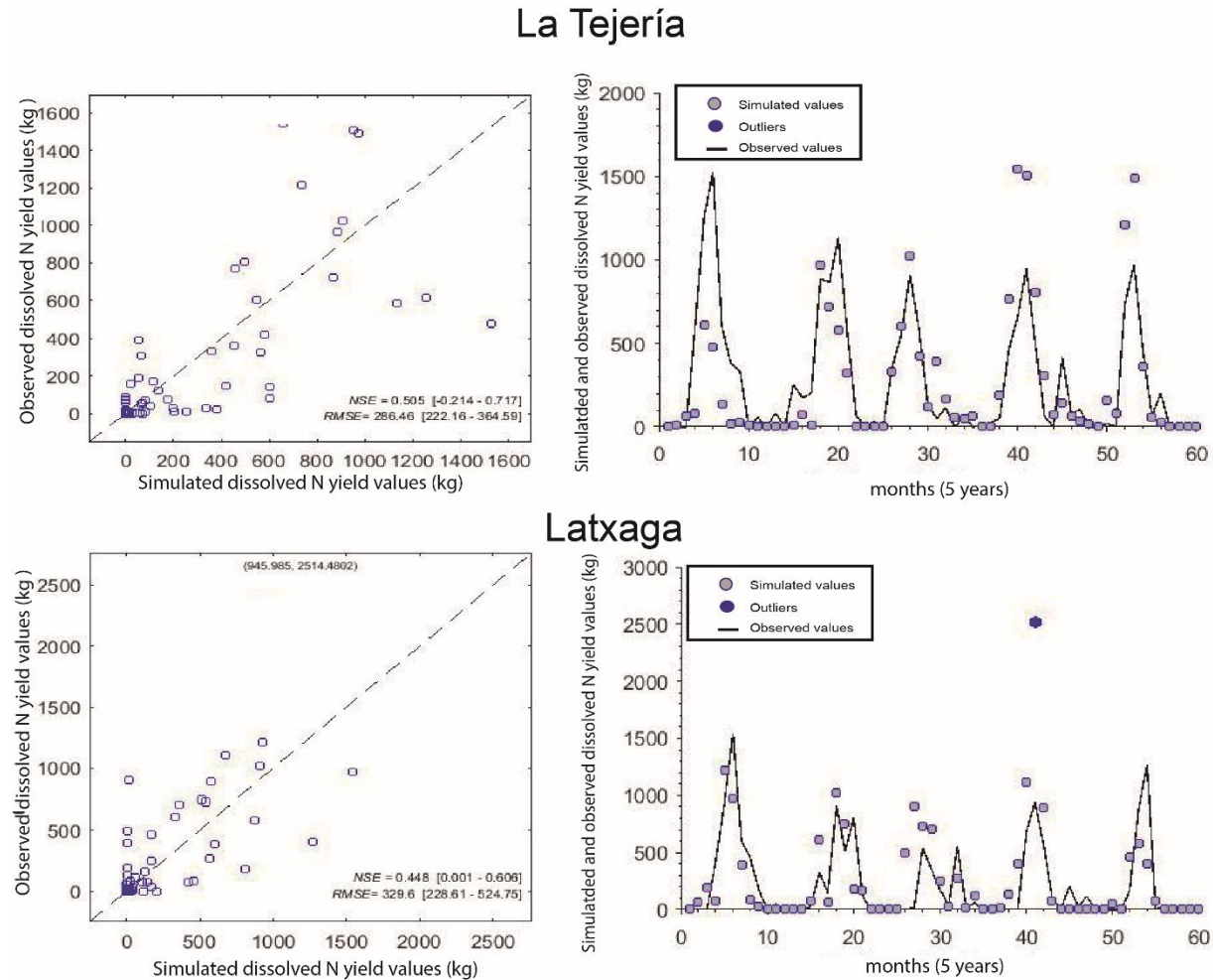


Figure 6.11: Observed and simulated values of dissolved N Yield testing at La Tejería and Latxaga watersheds.

After the analysis for calibration and testing results for N exports at La Tejería and Latxaga, the AnnAGNPS model was considered an adequate tool for the investigation of possible scenarios, and the assessment of N-related controlling factors.

6.3.3. Scenario simulations of the controlling factors of dissolved N exports

6.3.3.1. Quantification scenarios of dissolved N export by tile drainage and vegetation at La Tejería and Latxaga, respectively

Different scenarios were modeled to quantify the influences of tile drainage and non-cultivated areas (with spontaneous and riparian vegetation) on N exports.

When removing tile drainage at La Tejería, the average annual N reduction was approximately 12.4% (Table 6.8). Tile drainage is a widespread management practice in agricultural soils with poor drainage. Several studies have reported increases in NO_3^- concentration and yield in watersheds with tile drainage (Randall and Goss, 2008; Gramlich et al., 2018). The reduction of the residence time of NO_3^- due to the bypass effect produced by the tile drainage, and its reduced interaction with the environment (primarily riparian vegetation) significantly reduces denitrification (McIsaac and Hu, 2004).

However, at Latxaga, the removal of riparian areas and vegetated non-cultivable areas with spontaneous vegetation (which cover 11% of the watershed's surface) produced an increase of ca. 11.9% in N exports at the watershed outlet (Table 6.8). The presence of areas that are not arable (because of shallow soils or steep slopes) reduces the fertilizable area and can also be a sink of N from other areas of the watershed (Casal et al., 2019). In addition, the presence of well-developed riparian vegetation, with adequate width and plant density and diversity, favors infiltration and reduces surface runoff by acting as a nutrient sink, also becoming a sediment trap (Dosskey et al., 2010; Chase et al., 2016; Neilen et al., 2017). Well-developed riparian vegetation implies in a significant biomass content, which is the main indicator of N uptake (Dosskey et al., 2010).

Table 6.8: Annual averages of dissolved N for calibrated values and proposed quantification scenarios.

	Calibrated data (kg ha^{-1}) (Calibrated values)	Simulated scenario (kg ha^{-1}) (Absence of tile drainage and spontaneous vegetation at La Tejería and Latxaga respectively)	Variation
La Tejería	17.49	15.32	-12.4%
Latxaga	11.59	12.97	11.9%

Regarding monthly and annual data at Latxaga and La Tejería, it was observed that the largest differences between scenarios occurred in the periods with most rainfall (wet season and 2007, 2008 and 2013) (Fig. 6.12).

Dissolved N, like total dissolved solids (TDS), follows a very similar trend to that observed in the flow, with the highest water exports coinciding with the highest TDS exports and *vice versa* (Merchán et al., 2019). These pronounced TDS dynamics were not as evident for other agricultural

pollutants such as sediments, as these were also related to other characteristics such as the erosive potential of each event (Merchán et al., 2019).

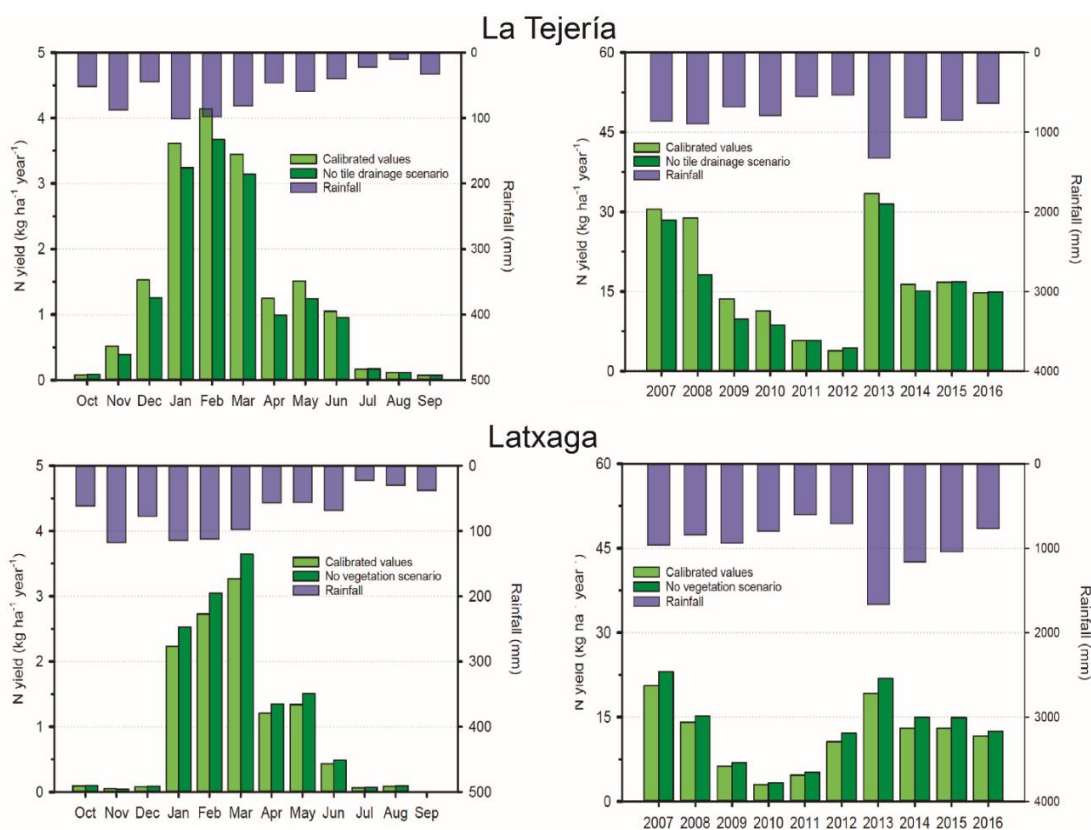


Figure 6.12: Average monthly and annual dissolved N yield for calibrated values and proposed scenarios at La Tejería and Latxaga.

The AnnAGNPS model, with its surface distribution in cells that act as sub-watersheds, limits possible interactions between cells. This lack of interaction prevents a cell with non-crop land use, with spontaneous vegetation or riparian vegetation, from interacting with cells presenting cereal land use. Due to this limitation, non-crop cells cannot act as N sinks for contiguous cells. This can bias the increase in exports at the watershed outlet, which could be higher than the values shown in Table 6.8. Even so, the increase in active fertilization area was well represented.

Another limitation of the model was the riparian buffer. AnnAGNPS enables the addition of a riparian vegetation buffer along the streambanks. As observed in previous studies in these watersheds (Hernández-García et al., 2020), the effect of riparian vegetation can lead to a change in nutrient dynamics. AnnAGNPS permits to consolidate vegetation continuously along the streams, but these buffers only act as sediment traps, and therefore do not reduce dissolved N transport. The addition of plant data to reduce N exports (e.g., N uptake) would improve the ability

of the model to predict N exports from watersheds. Nevertheless, the riparian vegetation at Latxaga was accurately represented by the cells contiguous to the watercourse through the correct selection of size, and hence this limitation of the model was reasonably solved.

Considering the discretization of the surface in cells and its limitations, at Latxaga and La Tejería the variation of dissolved N in watersheds was focused on those cells altered by simulating the proposed scenarios (at La Tejería all cells with the presence of tile drainage, and at Latxaga those non-cultivable cells with vegetation) (Fig. 6.13).

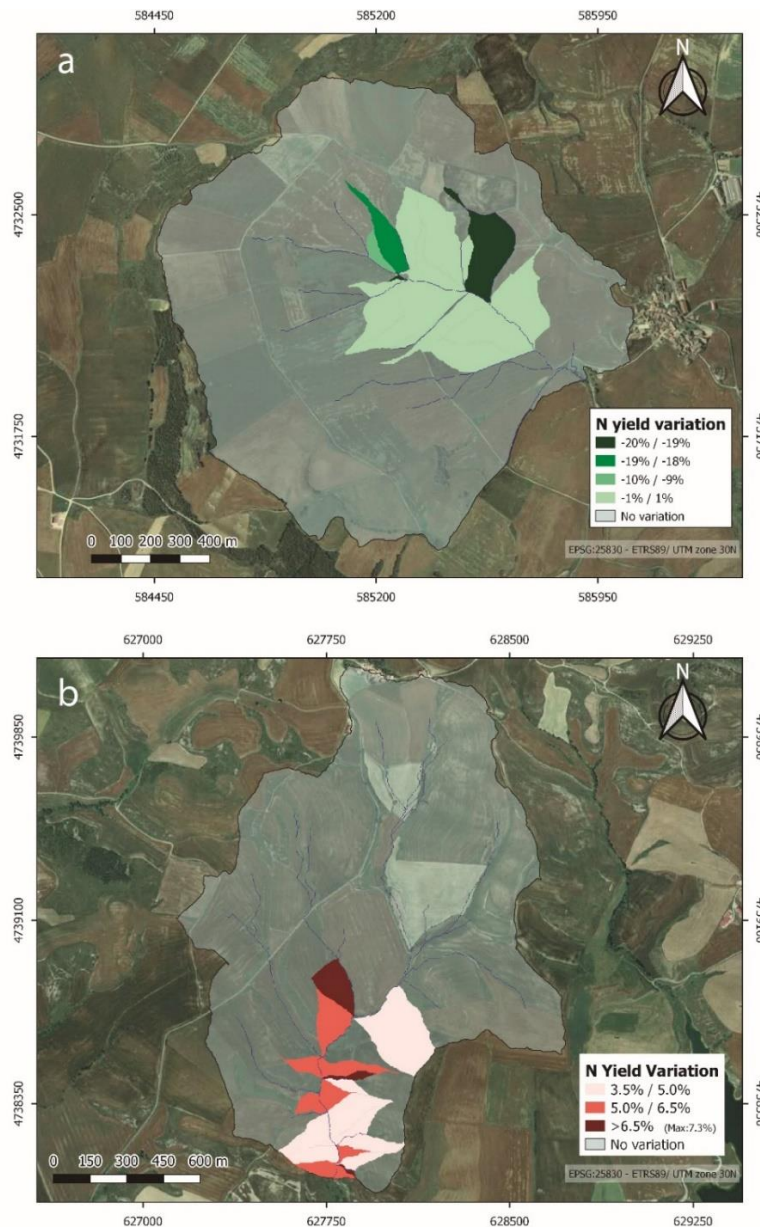


Figure 6.13: Dissolved N yield variations at the watershed outlet (a) La Tejería and (b) Latxaga, for calibrated simulation and proposed scenarios.

At La Tejería, the area affected by the modifications corresponds to 27 ha (ca. 16% of the total watershed) (Fig. 6.13a). These cells were located around the main channel. Further investigation of the cells that generate a higher variation in the dissolved N yield at the watershed outlet, 21% (5.7 ha) produce a reduction higher than 95% for dissolved N in this scenario. The intrinsic characteristics of these cells such as infiltration, average slope, and the decrease in the water table were considered key factors to explain the differences between cells in terms of N export reduction at this watershed.

At Latxaga, the area that suffered an increase in exports due to the change from spontaneous vegetation to cereal cultivated land was ca. 12% (25 ha) (Fig. 6.13b). In contrast with La Tejería, the cells involved in the variation of N yield did not present significant differences, with increases in the range of 3.7%-7.3% for dissolved N yield. Focusing on the most critical cells involved in dissolved N exports, approximately 10 ha (5%) were responsible for 70% of the increase in dissolved N yield exported at the watershed outlet. Unlike La Tejería, in this case the management of Latxaga was the main cause for this increase, due to the transformation of areas without fertilization and no cultivation into areas that receive annual inputs of fertilizers.

The results of the quantification scenarios of tile drainage and vegetation factors in La Tejería and Latxaga respectively, support the advances reported on the dynamics of N and its controlling factors in Chapter 5.

6.3.3.2. Scenarios for determining the effect of different tile drainage and spontaneous vegetation management in both watersheds.

Regarding the simulated scenarios with different management practices described in section 2.7.2, a similar trend to the quantification scenarios has been observed, but with subtle differences (Table 6.9).

At La Tejería, an increase in tile drainage area from 16% to 37% has resulted in only a 0.2% increase in dissolved N yield at the watershed outlet. Even though a more significant increase was expected, this small increment could be due to the characteristics of the soils in the cells where tile drainage was implemented. Generally, this type of drainage is implemented in soils with low infiltration characteristics. By installing these drains in good infiltration soils (without waterlogging problems), the effect of tile drainage can become negligible. In addition, the occurrence of cracks in these soils is recurrent and facilitates preferential flow (Brady and Weil,

2008). Moreover, AnnAGNPS calculates the CN daily, based on the antecedent moisture content of the soils. A soil without infiltration problems and with tile drainage would imply a soil with a longer dry period, so AnnAGNPS assigns a lower CN value than its actual value (see Chapter 2, Section 2.3.2.1). This leads to lower runoff produced and consequently lower contents of N dissolved in the water.

In the scenario where the cells with tile drainage at La Tejería are replaced by vegetated areas (mainly riparian vegetation due to their location close to the channel), there was a significant decrease in the dissolved N yield. If 16% of this area (mainly used to grow cereal crops but has infiltration problems) were dedicated to developing riparian vegetation, the dissolved N exported from the watershed would be 26% lower. It is important to emphasize that AnnAGNPS only considers the decrease in fertilized area, not considering the N sink effect of riparian vegetation (Dosskey et al., 2010). Therefore, the reported percentage decrease could be higher.

Table 6.9: Annual averages of dissolved N for calibrated values and proposed scenarios for determining the effect of different tile drainage and spontaneous vegetation management at both watersheds.

	La Tejería		Latxaga		
	Dissolved N yield (kg ha ⁻¹)	Variation (%)	Dissolved N yield (kg ha ⁻¹)	Variation (%)	
Calibrated values	17.49	--	Calibrated values	11.59	--
Scenario with increased tile drainage	17.52	0.2	Scenario with increased spontaneous and riparian vegetation	9.76	-15.8
Scenario with replacement of tile drainage cells with vegetation (Rangeland)	12.95	-26.0	Scenario with replacement of spontaneous vegetation cells (Rangeland) with tile drainage	13.82	19.2

Regarding the scenarios simulated at Latxaga, increases in vegetated areas from 12% to 25% (both spontaneous and riparian vegetation) lead to a decrease of 15.8% in the dissolved N yield at the watershed outlet. As in the previous case, only the effect of non-fertilized areas is considered.

On the other hand, vegetated cells were replaced by cells with cereal crops and tile drainage to simulate the transformation of vegetated areas (generally with poor infiltration) into arable areas with tile drainage. As a result, there was an increase of ca. 20% in dissolved N yield at the watershed outlet.

6.4. CONCLUSIONS

Quantification of the controlling factors of dissolved N exports with the AnnAGNPS model confirmed the effect of vegetation (riparian and spontaneous in non-cultivable areas) and of tile drainage in agrosystems with Mediterranean characteristics.

Regarding the model analysis, AnnAGNPS was found to be an additive model with very low interactions between parameters. The most sensitive parameters for runoff simulation were: i) the CN values set in the wettest periods, due to the higher runoff generation and; ii) the CN values set in the driest periods, due to the appearance of soil cracks affecting the preferential flow. Regarding dissolved N yield, our analysis showed crop yield and decomposition coefficient parameters as the most sensitive.

Despite the relative simplicity of the AnnAGNPS model, the results showed both for runoff (NSE=0.76 and NSE=0.72 in calibration at La Tejería and Latxaga respectively) and dissolved N yield (NSE=0.72 and NSE=0.52 in calibration, and NSE=0.51 and NSE=0.45 in testing at La Tejería and Latxaga respectively) can be considered as satisfactory according to the model performance metrics thresholds reported in the literature.

These simulations confirm the importance of tile drainage and spontaneous and riparian vegetation in non-cultivable areas at the studied watersheds. The absence of tile drainage at La Tejería watershed, and of riparian and spontaneous vegetation in non-cultivable areas at Latxaga, could lead to a decrease of ca. 12.4% and an increase of ca. 11.9% in N exports, respectively.

In both watersheds, a replacement between the poorly drained areas with tile drainage and vegetated areas would imply a variation in the N dissolved yield at the watershed outlet of ca. 20%.

Within the AnnAGNPS model, the crop yield parameter was the most critical for the simulation of N exports. However, a satisfactory model performance was not possible with a more suitable crop yield value. The reduction of the possible uncertainties of this parameter, combined with a complete representation of N cycle processes by the AnnAGNPS model and an increased interaction between parameters and processes within the model, would improve the accuracy of the model in terms of N exports. On the other hand, the addition of N retention characteristics (e.g., N uptake, plant phenologic cycle) to the vegetation buffer along the streambank would

improve the estimation of N content at the watershed outlet, when this vegetation is not correctly represented by the cells. This would allow the simulation of the interaction between cultivated areas and riparian vegetation.

Tile drainage and vegetation (riparian and non-cultivated areas) are considered very important factors for the retention/export of N in agrosystems. Although the analysis of the effect of tile drainage and vegetation provide a deeper understanding of the influence of different agricultural practices on N exports, the quantification of other variables (e.g., channel sinuosity, annual variability of preferential flow due to the presence of cracks, and the evaluation of different fertilization doses) would enable a more precise quantification of retention/export of N and expand the knowledge base of N dynamics in agricultural systems. In addition, the satisfactory performance of the model allows exploring many other effects in the watersheds, such as scenarios with different land uses, or different management practices that allow defining the best available management practices (BMPs) in the territory. Furthermore, this tool can also facilitate the study of larger areas of analysis, and the effect of climate change among other questions.

CONCLUSIONS

The dynamics of total dissolved solids, particularly nutrients such as N and P, are highly complex, with many processes involved. This thesis has contributed to deepening knowledge on these dynamics at a small agricultural watershed scale (detecting transport dynamics and identifying and quantifying the controlling factors). Nevertheless, the multitude of processes, elements, and interactions highlight these dynamics as a subject of great scientific interest with many unknowns to be investigated.

Analysis of the dynamics of total dissolved solids over a considerable period (10 years) at the outlet of agricultural watersheds has demonstrated an association with water flows. The temporal dynamics of TDS concentration and loads are controlled by the fact that TDS are conservative with water. The dynamics of concentration and total dissolved solids loads are mainly influenced by characteristics related to the geology of the study area, climate, and meteorological events. It was observed that fertilizer inputs and livestock manure from agricultural land uses increase the concentration of total dissolved solids in water drainages. Although natural factors predominantly control the export of total dissolved solids, contributions from agricultural land uses have an essential weight due to their anthropogenic origin, which allows a greater regulation of their loads. The yield of total dissolved solids in the watersheds with a significant extension of arable land was lower than the yield of suspended sediments. According to scientific literature, generally, the predominant yield in agricultural and non-agricultural watersheds is given by total dissolved solids. The high proportion of arable land in the studied watersheds and the environmental conditions increases the export of sediments. Suspended sediment yields are more predominant in these watersheds due to tillage (which breaks up soil aggregates), presence of fallow land, periods of bare soil, high moisture content of the soil, and the occurrence of erosive events.

Understanding the dynamics of total dissolved solids at the watershed outlet has contributed to expanding the knowledge base, even though some unknowns remain and must be clarified by future research. Smaller-scale analysis, such as at hillslope or plot scales, can help comprehend these dynamics and contribute to discretizing areas with specific land use. As observed, the influence of agricultural land use is highly relevant to understanding the dynamics of solutes (geological origin salts, nutrients, etc.) and their impact on total yield.

In this sense, mechanisms and techniques to observe and provide an interpretation of the processes occurring within a watershed are crucial. The accurate characterization can help define which areas

are responsible for a higher export of solutes and agricultural pollutants, such as nutrients. This avoids the black-box approach that sometimes hinders the analysis at the watershed outlet. This thesis has confirmed that the development of overlandflow connectivity indices can help understand, with a high level of details, the routes taken by particles within the watershed, thus defining which areas are more connected to each other and which are not. An OFC index that considers the major processes of runoff generation and particle transport is a useful tool in understanding both solute and sediment dynamics, shedding light on processes occurring in the watershed. Regarding the factors considered in the calculation of the OFC, the choice of the RUSLE C-factor as a weighting factor is a good parameter to incorporate the impediment of runoff generation or the transport of particles in agricultural watersheds. This factor is well established in the determination of runoff erosion, and is well suited to agricultural environments. However, the RUSLE C-factor, used for erosion prediction, causes the OFC index to be more easily related to the connectivity of sediment or particulate solutes or solutes attached to the soil, than to dissolved solutes. Therefore, a correct representation of surfaces with high runoff potential in the determination of the OFC is basic for accurate representation of runoff, and with this, all the solutes dissolved in it.

These indices have been successfully tested in alpine watersheds, with very satisfactory results. However, in agricultural watersheds, even though the results obtained herein were realistic and consistent with the definition of flow connectivity, it would be necessary to incorporate weighting factors to include information on different management practices. In this way, for example, the effect of tile drainage could be included.

The spatial distribution of OFC provided by these indices presents valuable information for understanding the behavior of different compounds in the watershed. However, their semi-quantitative nature does not enable comparisons between watersheds. The impossibility of comparing watersheds restricts the study of processes, as comparison with other study areas is hindered. The possibility of generating a quantifiable OFC index comparable with other watersheds would facilitate understanding nutrient and sediment dynamics in watersheds.

Determination of the controlling factors of nutrient dynamics helps determine the transport process of these solutes. Controlling factors have been identified at two rainfed winter cereal watersheds with similar management and climatic characteristics but with very different N and P nutrient

concentrations and yields. These differences have emphasized the relevance of the intrinsic characteristics of each watershed, some of them being crucial such as vegetation, tile drainage, and channel sinuosity. Riparian vegetation was considered a buffering factor in nutrient concentration, smoothing nutrient concentration peaks at specific periods. Identifying these controlling factors can help environmental managers of institutions and governments identify potentially vulnerable areas and act accordingly.

The ecological status of the watershed can be improved by increasing the vegetated areas in specific locations, improving drainage management and developing the width of riparian vegetation. In addition, an increase on species diversity and density would also improve water quality. Considering these factors in combination with best management practices can lead to significant carbon sequestration, improvement in soil structure and soil fauna, decrease in soil erosion, and increase in the presence of aquatic organisms in freshwater ecosystems, thus progressing towards sustainable agriculture.

Identifying the controlling factors of nutrient dynamics and determining their importance was possible due to the analysis of the data obtained from the long-term water quality monitoring in each watershed, adequate traceability of the management practices within the watershed, and their characterization. Future works can focus on thorough analyses for a deeper understanding of these dynamics. For instance, non-linear time series analysis can enable establishing a causal interaction network across the nutrient export controlling factors. This tool, as well as modeling, would permit the quantification of retention/export of nutrients by the herein described controlling factors in the watershed, with the advantage of quantifying the interactions between factors. This knowledge would allow a better understanding of nutrient transports. The quantification of effects at smaller scales (plot or slope), and the investigation on specific processes of these controlling factors (e.g., the vigor of riparian vegetation throughout the year, the activity of tile drains in wet periods) would help clarify how these processes act and how nutrients interact. Understanding these factors behavior would increase the knowledge of processes that occur in watersheds in terms of nutrient dynamics.

The capability of the AnnAGNPS model for the simulation of dissolved N yield at the watershed outlet was evaluated to quantify the effect of the leading nutrient controlling factors (tile drainage and vegetation) on N dynamics. The use of management models such as AnnAGNPS is relevant

and very useful for hydrologists and landscape managers. This type of tool enables an important prospection of scenarios, simulating different management options in the landscape. The results provided are very valuable, but require a prior evaluation. To this end, the runoff component was calibrated, and the dissolved N export component (dissolved N yield) was calibrated and tested. According to the Nash-Sutcliffe coefficient thresholds reported in scientific literature, the results were satisfactory for both runoff and dissolved N yields at the Latxaga and La Tejería watersheds. The inverse calibration evaluation method, employed jointly with screening methods, improved the model's performance. The capability to explore a comprehensive combination of sensitive parameters enables the optimization of the model, thus achieving highly satisfactory results.

The analysis of the AnnAGNPS model showed that it is an additive model, with few interactions between the parameters. For runoff simulation, the most sensitive parameters of the model were the CN values set in the wettest periods (due to higher runoff generation) and the CN values set in the driest periods (due to the appearance of soil cracks). For dissolved N yields, the analysis revealed crop yield and decomposition coefficient parameters as the most sensitive.

The satisfactory performance of the AnnAGNPS model at the Latxaga and La Tejería watersheds makes this model a suitable tool for quantifying the controlling factors of N dynamics. The quantification results showed a significant influence of vegetation and tile drainage factors at Latxaga and La Tejería. The effect of these two factors on the dissolved N yield was higher than 10%. Furthermore, different simulated scenarios showed variations of up to 25% in the dissolved N yield at the watershed outlet. However, these results must be considered with caution, as the AnnAGNPS model has some limitations. For example, this model does not assume any N retention process (e.g., N uptake) in the vegetation buffers along the streambank, so the interaction of dissolved N with these buffers is null. This problem, added to the absence of interaction between cells, means that the sink effect of vegetation is not adequately incorporated into the model, generating a bias in the export of dissolved N to be considered at the watershed outlet.

Despite these limitations, using a model such as AnnAGNPS for land assessment enables the simulation of scenarios that guide agriculture towards a more sustainable path through the implementation of best management practices. Furthermore, the satisfactory fit of the model to the Latxaga and La Tejería watersheds opens the possibility of using the model in other non-

gauged cereal watersheds of the region, or even in watersheds with the same use and management, on a larger scale. In addition, the high capacity of the model could be employed in the simulation of different intensive agriculture scenarios, such as irrigated agricultural systems with more than one crop per year, high fertilization rates, and high use of heavy machinery. These are frequent practices in vegetable production fields in the southern areas of Navarre.

REFERENCES

- Ali, G.A., Roy, A.G., 2009. Revisiting Hydrologic Sampling Strategies for an Accurate Assessment of Hydrologic Connectivity in Humid Temperate Systems 1, 350–374.
- Anning, D.W., Flynn, M.E., 2014. Dissolved-solids sources, loads, yields, and concentrations in streams of the conterminous United States, Scientific Investigations Report. Reston, VA. <https://doi.org/10.3133/sir20145012>
- Aranguren, M., Castell, A., Aizpurua, A., 2020. Wheat Yield Estimation with NDVI Values Using a Proximal Sensing Tool.
- Arenas Amado, A., Schilling, K.E., Jones, C.S., Thomas, N., Weber, L.J., 2017. Estimation of tile drainage contribution to streamflow and nutrient loads at the watershed scale based on continuously monitored data. *Environ. Monit. Assess.* 189. <https://doi.org/10.1007/s10661-017-6139-4>
- Arnold, J.G., Allen, P.M., Bernhardt, G., 1993. A comprehensive surface-groundwater flow model. *J. Hydrol.* 145, 47–69. [https://doi.org/10.1016/0022-1694\(93\)90004-S](https://doi.org/10.1016/0022-1694(93)90004-S)
- Arnold, J.G., Moriasi, D.N., Gassman, P.W., Abbaspour, K.C., White, M.J., Srinivasan, R., Santhi, C., Harmel, R.D., Van Griensven, A., Van Liew, M.W., Kannan, N., Jha, M.K., 2012. SWAT: Model use, calibration, and validation. *Trans. ASABE* 55, 1491–1508.
- Badr, E.A., El-sonbati, M.A.E., Nassef, H.M., 2013. Water Quality Assessment in the Nile River, Damietta Branch , Egypt. <https://doi.org/10.12816/0010762>
- Baroni, G., Tarantola, S., 2014. A General Probabilistic Framework for uncertainty and global sensitivity analysis of deterministic models: A hydrological case study. *Environ. Model. Softw.* 51, 26–34. <https://doi.org/10.1016/j.envsoft.2013.09.022>
- Bennett, N.D., Croke, B.F.W., Guariso, G., Guillaume, J.H.A., Hamilton, S.H., Jakeman, A.J., Marsili-Libelli, S., Newham, L.T.H., Norton, J.P., Perrin, C., Pierce, S.A., Robson, B., Seppelt, R., Voinov, A.A., Fath, B.D., Andreassian, V., 2013. Characterising performance of environmental models. *Environ. Model. Softw.* 40, 1–20. <https://doi.org/10.1016/j.envsoft.2012.09.011>
- Berka, C., Schreier, H., Hall, K., 2001. Linking water quality with agricultural intensification in a rural watershed. *Water. Air. Soil Pollut.* 127, 389–401. <https://doi.org/10.1023/A:1005233005364>
- Beven, K., Binley, A., 1992. The future of distributed models: Model calibration and uncertainty prediction. *Hydrol. Process.* 6, 279–298. <https://doi.org/10.1002/hyp.3360060305>
- Billen, G., Silvestre, M., Grizzetti, B., Leip, A., Garnier, J., Voss, M., Howarth, R., Bouraoui, F., Lepistö, A., Kortelainen, P., Johnes, P., Curtis, C., Humborg, C., Smedberg, E., Kaste, Ø., Ganeshram, R., Beusen, A., Lancelot, C., 2011. Nitrogen flows from European regional watersheds to coastal marine waters. *Eur. Nitrogen Assess.* 271–297. <https://doi.org/10.1017/cbo9780511976988.016>
- Bingner, R.L., Theurer, F.D., Yuan, Y., 2001. AnnAGNPS technical processes: Documentation version. Oxford,MS.
- Bingner, R.L., Theurer, F.D., Yuan, Y., Taguas, E. V, 2018. AnnAGNPS Technical Process,

version 5.5.

- Black, P.E., 1996. *Watershed Hydrology*, Second ed. ed. Lewis Publishers, New York.
- Blann, K.L., Anderson, J.L., Sands, G.R., Vondracek, B., 2009. Effects of agricultural drainage on aquatic ecosystems: A review. *Crit. Rev. Environ. Sci. Technol.* 39, 909–1001. <https://doi.org/10.1080/10643380801977966>
- Bœuf, G., Payan, P., 2001. How should salinity influence fish growth? *Comp. Biochem. Physiol. - C Toxicol. Pharmacol.* 130, 411–423. [https://doi.org/10.1016/S1532-0456\(01\)00268-X](https://doi.org/10.1016/S1532-0456(01)00268-X)
- Borselli, L., Cassi, P., Torri, D., 2008. Prolegomena to sediment and flow connectivity in the landscape: A GIS and field numerical assessment 75, 268–277. <https://doi.org/10.1016/j.catena.2008.07.006>
- Bracken, L.J., Croke, J., 2007. The concept of hydrological connectivity and its contribution to understanding runoff-dominated geomorphic systems 1763, 1749–1763. <https://doi.org/10.1002/hyp>
- Bracken, L.J., Wainwright, J., Ali, G.A., Tetzlaff, D., Smith, M.W., Reaney, S.M., Roy, A.G., 2013. Earth-Science Reviews Concepts of hydrological connectivity: Research approaches, pathways and future agendas. *Earth Sci. Rev.* 119, 17–34. <https://doi.org/10.1016/j.earscirev.2013.02.001>
- Brady, N.C., Weil, R.R., 2008. *The Nature and Properties of Soils*, 14th ed. PEARSON Prentice Hall, Upper Saddle River, New Jersey.
- Broadmeadow, S., Nisbet, T.R., 2004. The effects of riparian forest management on the freshwater environment: a literature review of best management practice. *Hydrol. Earth Syst. Sci.* 8, 286–305. <https://doi.org/10.5194/hess-8-286-2004>
- Bustamante, M.M.C., Martinelli, L.A., Pérez, T., Rasse, R., Ometto, J.P.H.B., Siqueira Pacheco, F., Machado Lins, S.R., Marquina, S., 2015. Nitrogen management challenges in major watersheds of South America. *Environ. Res. Lett.* 10. <https://doi.org/10.1088/1748-9326/10/6/065007>
- Butler, B.A., Ford, R.G., 2018. Evaluating Relationships Between Total Dissolved Solids (TDS) and Total Suspended Solids (TSS) in a Mining-Influenced Watershed. *Mine Water Environ.* 37, 18–30. <https://doi.org/10.1007/s10230-017-0484-y>
- Butterbach-Bahl, K., Nemitz, E., Zaehle, S., Billen, G., Boeckx, P., Erisman, J.W., Garnier, J., Upstill-Goddard, R., Kreuzer, M., Oenema, O., Reis, S., Schaap, M., Simpson, D., de Vries, W., Winiwarter, W., Sutton, M.A., 2011. Nitrogen as a threat to European water quality. *Eur. Nitrogen Assess.* 434–462. <https://doi.org/10.1126/science.333.6046.1083>
- Buttle, J.M., 1998. Fundamentals of Small Catchment Hydrology, in: Kendall, C., MacDonnel, J.J. (Eds.), *Isotope Tracers in Catchment Hydrology*. Elsevier B.V., Amsterdam, The Netherlands, pp. 1–49. <https://doi.org/10.1016/B978-0-444-81546-0.50008-2>
- Calsamiglia, A., García-comendador, J., Fortesa, J., López-tarazón, J.A., Crema, S., Cavalli, M., 2018. Effects of agricultural drainage systems on sediment connectivity in a small Mediterranean lowland catchment. *Geomorphology* 318, 162–171.

<https://doi.org/10.1016/j.geomorph.2018.06.011>

- Cambardella, C.A., Moorman, T.B., Jaynes, D.B., Hatfield, J.L., Parkin, T.B., Simkin, W.W., Karlen, D.L., 1999. Water Quality in Walnut Creek Watershed: Herbicides in Soils, Subsurface Drainage, and Groundwater. *J. Environ. Qual.* 28, 25–34. <https://doi.org/10.2134/jeq1999.00472425002800010004x>
- Carling, P.A., 1983. Particulate dynamics , dissolved and total load , in two small basins , northern Pennines , UK. *Hydrol. Sci.* 28, 355–375. <https://doi.org/10.1080/02626668309491976>
- Casal, L., Durand, P., Akkal-Corfini, N., Benhamou, C., Laurent, F., Salmon-Monviola, J., Vertès, F., 2019. Optimal location of set-aside areas to reduce nitrogen pollution: A modelling study. *J. Agric. Sci.* 1–13. <https://doi.org/10.1017/S0021859618001144>
- Casalí, J., Gastesi, R., Álvarez-Mozos, J., De Santisteban, L.M., Lersundi, J.D.V. de, Giménez, R., Larrañaga, A., Goñi, M., Agirre, U., Campo, M.A., López, J.J., Donézar, M., 2008. Runoff, erosion, and water quality of agricultural watersheds in central Navarre (Spain). *Agric. Water Manag.* 95, 1111–1128. <https://doi.org/10.1016/j.agwat.2008.06.013>
- Casalí, J., Giménez, R., Díez, J., Álvarez-Mozos, J., Del Valle de Lersundi, J., Goñi, M., Campo, M.A., Chahor, Y., Gastesi, R., López, J., 2010. Sediment production and water quality of watersheds with contrasting land use in Navarre (Spain). *Agric. Water Manag.* 97, 1683–1694. <https://doi.org/10.1016/j.agwat.2010.05.024>
- Cavalli, M., Trevisani, S., Comiti, F., Marchi, L., 2013. Geomorphology Geomorphometric assessment of spatial sediment connectivity in small Alpine catchments. *Geomorphology* 188, 31–41. <https://doi.org/10.1016/j.geomorph.2012.05.007>
- Cerdan, O., Govers, G., Bissonais, Y. Le, Oost, K. Van, Poesen, J., Saby, N., Gobin, A., Vacca, A., Quinton, J., Auerswald, K., Klik, A., Kwaad, F.J.P.M., Raclot, D., Ionita, I., Rejman, J., Rousseva, S., Muxart, T., Roxo, M.J., Dostal, T., 2010. Rates and spatial variations of soil erosion in Europe : A study based on erosion plot data. *Geomorphology* 122, 167–177. <https://doi.org/10.1016/j.geomorph.2010.06.011>
- Chahor, Y., Casalí, J., Giménez, R., Bingner, R.L., Campo, M.A., Goñi, M., 2014. Evaluation of the AnnAGNPS model for predicting runoff and sediment yield in a small Mediterranean agricultural watershed in Navarre (Spain). *Agric. Water Manag.* 134, 24–37. <https://doi.org/10.1016/j.agwat.2013.11.014>
- Chartin, C., Evrard, O., Lacey, J.P., Onda, Y., Cerdan, O., Cedex, G., 2017. The impact of typhoons on sediment connectivity : lessons learnt from contaminated coastal catchments of the Fukushima Prefecture (Japan). *Earth Surf. Process. Landforms* 42, 306–317. <https://doi.org/10.1002/esp.4056>
- Chase, J.W., Benoy, G.A., Hann, S.W.R., Culp, J.M., 2016. Small differences in riparian vegetation significantly reduce land use impacts on stream flow and water quality in small agricultural watersheds. *J. Soil Water Conserv.* 71, 194–205. <https://doi.org/10.2489/jswc.71.3.194>
- Chen, L., Fu, B., Zhang, S., Qiu, J., Guo, X., Yang, F., 2002. A comparative study on nitrogen-concentration dynamics in surface water in a heterogeneous landscape. *Environ. Geol.* 42,

424–432. <https://doi.org/10.1007/s00254-002-0547-6>

- Cheng, Q., Tang, C.S., Xu, D., Zeng, H., Shi, B., 2021. Water infiltration in a cracked soil considering effect of drying-wetting cycles. *J. Hydrol.* 593. <https://doi.org/10.1016/j.jhydrol.2020.125640>
- Childs, S.W., Hanks, R.J., 1975. Model of Soil Salinity Effects on Crop Growth. *Soil Sci. Soc. Am. J.* 39, 617–622.
- Chitale, J., Khare, Y., Muñoz-Carpena, R., Dulikravich, G.S., Martinez, C., 2017. An effective parameter screening strategy for high dimensional models. *Proc. ASME 2017 Int. Mech. Eng. Congr. Expo.* <https://doi.org/https://doi.org/10.1115/IMECE2017-71458>
- Chow, V. Te, Maidment, D.R., Mays, L.W., 1988. *Applied Hydrology*. McGraw-Hill, Singapore.
- Clunie, P., Ryan, T., James, K., Cant, B., 2002. Implications for rivers from salinity hazards: scoping study. Report to Murray–Darling Basin Commission, Strategic Investigations and Riverine Program—Project R2003. Arthur Rylah Institute, Department of Natural Resources and Environment, Melbourne., Heidelberg, Vic.
- Crawford, N., Burges, S., 2004. History of the stanford watershed model. *water Resour. IMPACT* 6.
- D’Haene, K., Moreels, E., De Neve, S., Daguilar, B.C., Boeckx, P., Hofman, G., Van Cleemput, O., 2003. Soil properties influencing the denitrification potential of Flemish agricultural soils. *Biol. Fertil. Soils* 38, 358–366. <https://doi.org/10.1007/s00374-003-0662-x>
- Daley, M.L., Potter, J.D., McDowell, W.H., 2009. Salinization of urbanizing New Hampshire streams and groundwater: Effects of road salt and hydrologic variability. *J. North Am. Benthol. Soc.* 28, 929–940. <https://doi.org/10.1899/09-052.1>
- Daniel, T.C., Sharpley, A.N., Lemunyon, J.L., 1998. (1998) Agricultural Phosphorus and Eutrophication: A Symposium Overview 257, 251–257.
- Danish Hydraulics Institute, 1993. MIKE SHE Water Movement Short Description.
- Darwiche-Criado, N., Comín, F.A., Sorando, R., Sánchez-Pérez, J.M., 2015. Seasonal variability of NO₃-mobilization during flood events in a Mediterranean catchment: The influence of intensive agricultural irrigation. *Agric. Ecosyst. Environ.* 200, 208–218. <https://doi.org/10.1016/j.agee.2014.11.002>
- David, M.B., Drinkwater, L.E., McIsaac, G.F., 2010. Sources of Nitrate Yields in the Mississippi River Basin. *J. Environ. Qual.* 39, 1657. <https://doi.org/10.2134/jeq2010.0115>
- De Girolamo, A.M., Balestrini, R., D’Ambrosio, E., Pappagallo, G., Soana, E., Lo Porto, A., 2017a. Anthropogenic input of nitrogen and riverine export from a Mediterranean catchment. The Celone, a temporary river case study. *Agric. Water Manag.* 187, 190–199. <https://doi.org/10.1016/j.agwat.2017.03.025>
- De Girolamo, A.M., D’Ambrosio, E., Pappagallo, G., Rulli, M.C., Lo Porto, A., 2017b. Nitrate concentrations and source identification in a Mediterranean river system. *Rend. Lincei* 28, 291–301. <https://doi.org/10.1007/s12210-016-0593-8>

- de Souza, A.L.T.D., Fonseca, D.G., Libório, R.A., Tanaka, M.O., 2013. Influence of riparian vegetation and forest structure on the water quality of rural low-order streams in SE Brazil. *For. Ecol. Manage.* 298, 12–18. <https://doi.org/10.1016/j.foreco.2013.02.022>
- De Vente, J., Poesen, J., Arabkhedri, M., Verstraeten, G., 2007. The sediment delivery problem revisited. *Prog. Phys. Geogr.* 31, 155–178. <https://doi.org/10.1177/0309133307076485>
- Deelstra, J., Iital, A., Povilaitis, A., Kyllmar, K., Greipsland, I., Blicher-Mathiesen, G., Jansons, V., Koskiaho, J., Lagzdins, A., 2014. Reprint of “Hydrological pathways and nitrogen runoff in agricultural dominated catchments in Nordic and Baltic countries.” *Agric. Ecosyst. Environ.* 198, 65–73. <https://doi.org/10.1016/j.agee.2014.06.032>
- Delgado, A., Quemada, M., Villalobos, F.J., 2016. Fertilizers, in: Villalobos, F.J., Fereres, E. (Eds.), *Principles of Agronomy for Sustainable Agriculture*. Springer International Publishing, pp. 321–340.
- Deyle, E.R., May, R.M., Munch, S.B., Sugihara, G., 2016. Tracking and forecasting ecosystem interactions in real time.
- Di Toro, D.M., Fitzpatrick, J.J., Thomann, R.V., 1983. *Water Quality Analysis Simulation Program (WASP) and Model Verification Program (MVP) - Documentation*. Westwood, NY.
- Djordjic, F., Börling, K., Bergström, L., 2004. Phosphorus leaching in relation to soil type and soil phosphorus content. *J. Environ. Qual.* 33, 678–684. <https://doi.org/10.2134/jeq2004.6780>
- Dosskey, M.G., Vidon, P., Gurwick, N.P., Allan, C.J., Duval, T.P., Lowrance, R., 2010. The role of riparian vegetation in protecting and improving water quality in streams. *J. Am. Water Resour. Assoc.* 46, 1–18. <https://doi.org/10.1111/j.1752-1688.2010.00419.x>
- Drewry, J.J., Newham, L.T.H., Croke, B.F.W., 2009. Suspended sediment, nitrogen and phosphorus concentrations and exports during storm-events to the Tuross estuary, Australia. *J. Environ. Manage.* 90, 879–887. <https://doi.org/10.1016/j.jenvman.2008.02.004>
- Durán Zuazo, V.H., Francia Martínez, J.R., García Tejero, I., Rodríguez Pleguezuelo, C.R., Martínez Raya, A., Cuadros Távira, S., 2012. Runoff and sediment yield from a small watershed in southeastern Spain (Lanjarón): implications for water quality. *Hydrol. Sci. J.* 57, 1610–1624. <https://doi.org/10.1080/02626667.2012.726994>
- Durand, P., Breuer, L., Johnes, P., 2011. Nitrogen processes in aquatic ecosystems, in: Mark A. Sutton; Clare M. Howard; Jan Willem Erisman; Gilles Billen; Albert Bleeker; Perine Grennfelt; Hans Van Grinsven; Bruna Grizzetti (Ed.), *The European Nitrogen Assessment*. Cambridge, pp. 127–146.
- Eckhardt, K., 2005. How to construct recursive digital filters for baseflow separation. *Hydrol. Process.* 19, 507–515. <https://doi.org/10.1002/hyp.5675>
- EEA, 2018. Gross nitrogen balance in Europe by country [WWW Document]. URL https://www.eea.europa.eu/data-and-maps/daviz/gross-nitrogen-balance-by-country-1#tab-chart_3
- Egamberdieva, D., Renella, G., Wirth, S., Islam, R., 2010. Secondary salinity effects on soil

- microbial biomass. *Biol. Fertil. Soils* 46, 445–449. <https://doi.org/10.1007/s00374-010-0452-1>
- Environmental and Hydraulics Laboratory, 1986. CE-QUAL-W2: A numerical two-dimensional, laterally averaged model of hydrodynamics and water quality; user's manual. Vicksburg, MS.
- EUROSTAT, 2016. Main annual crop statistics [WWW Document]. https://appsso.eurostat.ec.europa.eu/nui/show.do?dataset=apro_cpsh1&lang=en
- FAO, 2017. World fertilizer trends and outlook to 2020. Food Agric. Organ. United Nations 38.
- FAO, 2011. Climate change, water and food security. Rome Food Agric. Organ. United Nations. 204. <https://doi.org/ISSN 1020-1203>
- Feki, M., Ravazzani, G., Ceppi, A., Milleo, G., Mancini, M., 2018. Impact of Infiltration Process Modeling on Soil Water Content Simulations for Irrigation Management. *Water* 10, 850. <https://doi.org/10.3390/w10070850>
- Fenn, M.E., Poth, M.A., Lemly, A.D., Aber, J.D., McNulty, S.G., Ryan, D.F., Bormann, B.T., Johnson, D.W., Baron, J.S., Stottlemeyer, R., 2006. Nitrogen Excess in North American Ecosystems: Predisposing Factors, Ecosystem Responses, and Management Strategies. *Ecol. Appl.* 8, 706. <https://doi.org/10.2307/2641261>
- Ferrant, S., Oehler, F., Durand, P., Ruiz, L., Salmon-Monviola, J., Justes, E., Dugast, P., Probst, A., Probst, J.L., Sanchez-Perez, J.M., 2011. Understanding nitrogen transfer dynamics in a small agricultural catchment: Comparison of a distributed (TNT2) and a semi distributed (SWAT) modeling approaches. *J. Hydrol.* 406, 1–15. <https://doi.org/10.1016/j.jhydrol.2011.05.026>
- Fitzpatrick, R.W., Boucher, S.C., Naidu, R., Fritsch, E., 1994. Environmental consequences of soil sodicity. *Aust. J. Soil Res.* 32, 1069–1093. <https://doi.org/10.1071/SR9941069>
- Frisbee, M.D., Phillips, F.M., Weissmann, G.S., Brooks, P.D., Wilson, J.L., Campbell, A.R., Liu, F., 2012. Unraveling the mysteries of the large watershed black box : Implications for the streamflow response to climate and landscape perturbations 39, 1–6. <https://doi.org/10.1029/2011GL050416>
- Fučík, P., Hejduk, T., Peterková, J., 2015. Quantifying Water Pollution Sources in a Small Tile-drained Agricultural Watershed. *Clean - Soil, Air, Water* 43, 698–709. <https://doi.org/10.1002/clen.201300929>
- Fučík, P., Zajíček, A., Kaplická, M., Duffková, R., Peterková, J., Maxová, J., Takácová, Š., 2017. Incorporating rainfall-runoff events into nitrate-nitrogen and phosphorus load assessments for small tile-drained catchments. *Water (Switzerland)* 9, 18–21. <https://doi.org/10.3390/w9090712>
- Gaillardet, J., Dupré, B., Allègre, C.J., Négrel, P., 1997. Chemical and physical denudation in the Amazon River Basin. *Chem. Geol.* 142, 141–173.
- Gao, W., Gao, S., Li, Z., Lu, X.X., Zhang, M., Wang, S., 2014. Suspended sediment and total dissolved solid yield patterns at the headwaters of Urumqi River , northwestern China: a comparison between glacial and non-glacial catchments. *Hydrol. Process.* 28, 5034–5047.

<https://doi.org/10.1002/hyp.9991>

- Garbrecht, J., Martz, L.W., 1999. TOPAGNPS: An automated digital landscape analysis tool for topographic evaluation, drainage identification, watershed segmentation, and subcatchment parameterization.
- García-Ruiz, J.M., Beguería, S., Nadal-Romero, E., González-Hidalgo, J.C., Lana-Renault, N., Sanjuán, Y., 2015. A meta-analysis of soil erosion rates across the world. *Geomorphology* 239, 160–173. <https://doi.org/10.1016/j.geomorph.2015.03.008>
- García-Ruiz, J.M., López-Bermúdez, F., 2009. *La erosión del suelo en España*. Sociedad Española de Geomorfología, Zaragoza, Spain.
- Gastesi, R., 2014. Efectos de la actividad agraria sobre los recursos hídricos y la erosión del suelos: Análisis y modelado en cuencas experimentales en zona media de Navarra. Public University of Navarre. Doctoral Thesis
- Gay, A., Cerdan, O., Mardhel, V., Desmet, M., 2016. Application of an index of sediment connectivity in a lowland area. *J. Soils Sediments* 16, 280–293. <https://doi.org/10.1007/s11368-015-1235-y>
- Gentry, L., David, M., Smith, K., Kovacic, D., 1998. Nitrogen cycling and tile drainage nitrate loss in a corn/soybean watershed. *Agric. Ecosyst. Environ.* 68, 85–97.
- Giménez, R., Casalí, J., Grande, I., Díez, J., Campo, M.A., Álvarez-Mozos, J., Goñi, M., 2012. Factors controlling sediment export in a small agricultural watershed in Navarre (Spain). *Agric. Water Manag.* 110, 1–8. <https://doi.org/10.1016/j.agwat.2012.03.007>
- Godwin, K.S., Hafner, S.D., Buff, M.F., 2003. Long-term trends in sodium and chloride in the Mohawk River , New York : the effect of fifty years of road-salt application 124, 273–281. [https://doi.org/10.1016/S0269-7491\(02\)00481-5](https://doi.org/10.1016/S0269-7491(02)00481-5)
- Government of Aragon, 2000. *La relación paja-grano en los cereales (Una aproximación en condiciones de secano semiárido , en Aragón)*, Informaciones técnicas.
- Government of Navarre, 2020. *Producción de los principales productos agrícolas*. Departamento de Desarrollo Rural y Medio Ambiente [WWW Document]. URL https://www.navarra.es/home_es/Temas/Ambito+rural/Indicadores/agricultura.htm
- Government of Navarre, 2011a. *Mapa de suelos de la cuenca hidrológica experimental Oskotz-Muskitz*. 1:25.000. Soil Map and Report.
- Government of Navarre, 2011b. *Mapa de suelos de la cuenca agraria experimental de Landazuría*. 1:25.000. Soil Map and Report.
- Government of Navarre, 2005a. *Mapa de Suelos de la Cuenca experimental de Latxaga (Lizoáin-Arriasoiti y Urroz-Villa)* 1:25.000. Soil Map and Report.
- Government of Navarre, 2005b. *Mapa de Suelos de la Cuenca experimental de La Tejería (Villanueva de Yerri)* 1:25.000. Soil Map and Report.
- Government of Navarre, 2003a. *Cartografía Geológica de Navarra, Escala 1:25.000, 244-II(Rada)*. Geological map and report. 119 pp. [WWW Document]. URL

http://www.navarra.es/appsext/tiendacartografia/seleccion_hoja.aspx?idp=15

Government of Navarre, 2003b. Cartografía Geológica de Navarra, Escala 1:25.000, 244-IV(Arguedas). Geological map and reports. 120 pp [WWW Document]. URL http://www.navarra.es/appsext/tiendacartografia/seleccion_hoja.aspx?idp=15

Government of Navarre, 1996. Cartografía Geológica de Navarra, Escala 1: 25.000, 140-IV, Abárzuza. Geological Map and Report 115 pp. [WWW Document]. URL http://www.navarra.es/appsext/tiendacartografia/seleccion_hoja.aspx?idp=15 (accessed 1.3.21).

Government of Navarre, 1995. Cartografía Geológica de Navarra, Escala 1:25.000, 115-I(Irurtzun). Geological map and report. [WWW Document]. URL http://www.navarra.es/appsext/tiendacartografia/seleccion_hoja.aspx?idp=15

Government of Navarre, 1994. Cartografía Geológica de Navarra, Escala 1: 25.000, 142-I, Aoiz. Geological Map and Report 39 pp. [WWW Document]. URL http://www.navarra.es/appsext/tiendacartografia/seleccion_hoja.aspx?idp=15 (accessed 1.3.21).

Gramlich, A., Stoll, S., Stamm, C., Walter, T., Prasuhn, V., 2018. Effects of artificial land drainage on hydrology, nutrient and pesticide fluxes from agricultural fields – A review. *Agric. Ecosyst. Environ.* 266, 84–99. <https://doi.org/10.1016/j.agee.2018.04.005>

Grove, A.T., 1972. The Dissolver and Solid Load carried by some West African rivers: Senegal, Niger, Benue and Shari. *J. Hydrol.* 16, 277–300.

Guan, S., Fukami, K., Matsunaka, H., Okami, M., Tanaka, R., 2019. Assessing Correlation of High-Resolution NDVI with Fertilizer Application Level and Yield of Rice and Wheat Crops using Small UAVs. <https://doi.org/10.3390/rs11020112>

Haller, W., Sutton, D.L., Barlowe, W.C., 1974. Effects of Salinity on Growth of Several Aquatic Macrophytes 55, 891–894.

Hansen, L., Delgado, J.A., Ribaudó, M., 2012. Minimizing costs of reducing agricultural nitrogen loadings : choosing between on- and off-field conservation practices. *Environ. Econ.* 3, 98–113.

Hart, B.T., Bailey, P., Edwards, R., Hortle, K., James, K., McMahon, A., Meredith, C., Swadling, K., 1991. A review of the salt sensitivity of the Australian freshwater biota. *Hydrobiologia.*

Hart, B.T., Lake, P.S., Webb, J.A., Grace, M.R., 2003. Ecological risk to aquatic systems from salinity increases. *Aust. J. Bot.* 51, 689–702. <https://doi.org/10.1071/BT02111>

Haygarth, P.M., Chapman, P.J., Jarvis, S.C., Smith, R.V., 1998. Phosphorus budget for two contrasting grassland farming systems in the UK. *Soil Use Manag.* 14, 160–167.

Haynes, R.J., 1986. The decomposition process: Mineralization, immobilization, humus formation, and degradation, in: Haynes, R.J. (Ed.), *Mineral N in the Soil-Plant System*. Academic Press, Orlando, FL, pp. 52–126. <https://doi.org/10.1016/B978-0-12-334910-1.50006-6>

Hayter, E.J., Bergs, M.A., Gu, R., Mccutcheon, S.C., Smith, S.J., Whiteley, H.J., 1995. HSCTM-

- 2D , a finite element model for depth-averaged hydrodynamics, sediment and conatminant transport. Athens, GA.
- Heckmann, T., Cavalli, M., Cerdan, O., Foerster, S., Javaux, M., Lode, E., Smetanová, A., Vericat, D., Brardinoni, F., 2018. Indices of sediment connectivity : opportunities , challenges and limitations. *Earth-Science Rev.* 187, 77–108. <https://doi.org/10.1016/j.earscirev.2018.08.004>
- Helsel, D.K., Hirsch, R.M., 2002. *Statistical methods in water resources*. Reston, VA.
- Hengl, T., Reuter, H.I., 2008. *Geomorphometry: Concepts, Software, Applications. Developments in Soil Science*. Elsevier, Amsterdam.
- Hernández-García, I., Merchán, D., Aranguren, I., Casalí, J., Giménez, R., Campo-Bescós, M.A., Del Valle de Lersundi, J., 2020. Assessment of the main factors affecting the dynamics of nutrients in two rainfed cereal watersheds. *Sci. Total Environ.* 733. <https://doi.org/10.1016/j.scitotenv.2020.139177>
- Hofstra, N., Bouwman, A.F., 2005. Denitrification in agricultural soils: Summarizing published data and estimating global annual rates. *Nutr. Cycl. Agroecosystems* 72, 267–278. <https://doi.org/10.1007/s10705-005-3109-y>
- Hooda, P.S., Moynagh, M., Svoboda, I.F., Thurlow, M., Stewart, M., Thomson, M., Anderson, H.A., 1997. Streamwater nitrate concentrations in six agricultural catchments in Scotland. *Sci. Total Environ.* 201, 63–78. [https://doi.org/10.1016/S0048-9697\(97\)84053-3](https://doi.org/10.1016/S0048-9697(97)84053-3)
- Huang, J.C., Lee, T.Y., Lin, T.C., Hein, T., Lee, L.C., Shih, Y.T., Kao, S.J., Shiah, F.K., Lin, N.H., 2016. Effects of different N sources on riverine DIN export and retention in a subtropical high-standing island, Taiwan. *Biogeosciences* 13, 1787–1800. <https://doi.org/10.5194/bg-13-1787-2016>
- Hubbard, R.K., Sheridan, J.M., Marti, L.R., 1990. Dissolved and Suspended Solids Transport from Coastal Plain Watersheds. *J. Environ. Qual.* 19, 413–420.
- IDENA, 2019. Cartografía LiDAR en Navarra [WWW Document]. URL https://filescartografia.navarra.es/5_LIDAR/
- Iital, A., Klõga, M., Pihlak, M., Pachel, K., Zahharov, A., Loigu, E., 2014. Nitrogen content and trends in agricultural catchments in Estonia. *Agric. Ecosyst. Environ.* 198, 44–53. <https://doi.org/10.1016/j.agee.2014.03.010>
- INTIA, 2018. Fertilization requirements in Navarre. Pamplona, Spain. [Unpublished]
- INTIA, 2017. Agronomic management, farmers face-to-face inquiries, database. ProyectoLIFE Nitratos (LIFE + 10 ENV/ES/478). Pamplona, Spain.
- Janssen, M., Frings, J., Lennartz, B., 2018. Effect of grass buffer strips on nitrate export from a tile-drained field site. *Agric. Water Manag.* 208, 318–325. <https://doi.org/10.1016/j.agwat.2018.06.026>
- Jingsheng, C., Xuemin, G., Dawei, H., Xinghui, X., 2000. Nitrogen contamination in the Yangtze River system , China 107–113.
- Johanson, R.C., Imhoff, J.C., Kittle, J.L., Donigian, A.S., 1984. *Hydrologic Simulation Program-*

- Fortran (HSPF): User's Manual, Release 8. Washington, DC.
- Jones, C., Jacobsen, J., 2002. Nutrient management module No. 3: N cycling, testing and fertilizer recommendations.
- Jørgensen, S.E., Bendoricchio, G., 2001. Fundamentals of ecological modelling, Third edit. ed. Elsevier.
- Kalogeropoulos, K., Chalkias, C., 2013. Modelling the impacts of climate change on surface runoff in small Mediterranean catchments: Empirical evidence from Greece. *Water Environ. J.* 27, 505–513. <https://doi.org/10.1111/j.1747-6593.2012.00369.x>
- Keller, C.K., Butcher, C.N., Smith, J.L., Allen-King, R.M., 2008. Nitrate in Tile Drainage of the Semiarid Palouse Basin. *J. Environ. Qual.* 37, 353. <https://doi.org/10.2134/jeq2006.0515>
- Khare, Y., Muñoz-Carpena, R., 2014. Morris SU (Sampling Uniformity) code [WWW Document]. URL <https://abe.ufl.edu/faculty/carpena/software/SUMorris.shtml>
- Khare, Y.P., Muñoz-Carpena, R., Rooney, R.W., Martinez, C.J., 2015. A multi-criteria trajectory-based parameter sampling strategy for the screening method of elementary effects. *Environ. Model. Softw.* 64, 230–239. <https://doi.org/10.1016/j.envsoft.2014.11.013>
- Knisel, W.G., 1980. CREAMS A Field Scale Model for Chemicals / Runoff , and Erosion From Agricultural Management Systems. Tucson, Arizona.
- Kotti, M.E., Vlessidis, A.G., Evmiridis, N.P., 2000. Determination of phosphorous and nitrogen in the sediment of lake “Pamvotis” (Greece). *Int. J. Environ. Anal. Chem.* 78, 455–467. <https://doi.org/10.1080/03067310008041360>
- Kyllmar, Katarina, Bechmann, M., Deelstra, J., Iital, A., Blicher-Mathiesen, G., Jansons, V., Koskiahio, J., Povilaitis, A., 2014. Long-term monitoring of nutrient losses from agricultural catchments in the Nordic-Baltic region - A discussion of methods, uncertainties and future needs. *Agric. Ecosyst. Environ.* 198, 4–12. <https://doi.org/10.1016/j.agee.2014.07.005>
- Kyllmar, K., Carlsson, C., Gustafson, A., Ulén, B., Johnsson, H., 2006. Nutrient discharge from small agricultural catchments in Sweden. Characterisation and trends. *Agric. Ecosyst. Environ.* 115, 15–26. <https://doi.org/10.1016/j.agee.2005.12.004>
- Kyllmar, K., Stjernman Forsberg, L., Andersson, S., Mårtensson, K., 2014. Small agricultural monitoring catchments in Sweden representing environmental impact. *Agric. Ecosyst. Environ.* 198, 25–35. <https://doi.org/10.1016/j.agee.2014.05.016>
- Lagzdins, A., Jansons, V., Sudars, R., Abramenko, K., 2012. Scale issues for assessment of nutrient leaching from agricultural land in Latvia. *Hydrol. Res.* 43, 383. <https://doi.org/10.2166/nh.2012.122>
- Lasanta, T., Pérez Rontomé, M.C., Machín, J., Navas, A., Mosch, W., Maestro, M., 2001. La Exportación de solutos en un polígono de regadío de Bardenas (Zaragoza). *Rev. C&G* 15, 51–66.
- Lassaletta, L., 2007. Flujos superficiales de nutrientes en una cuenca agrícola de Navarra. Doctoral Thesis

- Lassaletta, L., Romero, E., Billen, G., Garnier, J., García-Gómez, H., Rovira, J. V., 2012. Spatialized N budgets in a large agricultural Mediterranean watershed: High loading and low transfer. *Biogeosciences* 9, 57–70. <https://doi.org/10.5194/bg-9-57-2012>
- Lehmann, J., Schroth, G., 2003. Nutrient Leaching, in: Schroth, G., Sinclair, F. (Eds.), *Trees, Crops, and Soil Fertility*. CABI, pp. 151–166. <https://doi.org/10.1079/9780851995939.0000>
- Lewis, W.M., Saunders, J.F., 1989. Concentration and transport of dissolved and suspended substances in the Orinoco River. *Biogeochemistry* 7, 203–240.
- Li, H., Sivapalan, M., Tian, F., Liu, D., 2010. Water and nutrient balances in a large tile-drained agricultural catchment: A distributed modeling study. *Hydrol. Earth Syst. Sci.* 14, 2259–2275. <https://doi.org/10.5194/hess-14-2259-2010>
- Li, Z., Luo, C., Xi, Q., Li, H., Pan, J., Zhou, Q., Xiong, Z., 2015. Assessment of the AnnAGNPS model in simulating runoff and nutrients in a typical small watershed in the Taihu Lake basin, China. *Catena* 133, 349–361. <https://doi.org/10.1016/j.catena.2015.06.007>
- Liang, X.Q., Xu, L., Li, H., He, M.M., Qian, Y.C., Liu, J., Nie, Z.Y., Ye, Y.S., Chen, Y., 2011. Influence of N fertilization rates, rainfall, and temperature on nitrate leaching from a rainfed winter wheat field in Taihu watershed. *Phys. Chem. Earth* 36, 395–400. <https://doi.org/10.1016/j.pce.2010.03.017>
- Liao, M., Fillery, I.R.P., Palta, J.A., 2004. Early vigorous growth is a major factor influencing nitrogen uptake in wheat. *Funct. Plant Biol.* 31, 121–129. <https://doi.org/10.1071/FP03060>
- Likens, G.E., 2001. Marine Freshwater Biogeochemistry, the watershed approach: some uses and limitations. *Mar. Freshw. Res.* 52, 5–12. <https://doi.org/10.1071/MF99188>
- Liu, X., Ju, X., Zhang, F., Pan, J., Christie, P., 2003. Nitrogen dynamics and budgets in a winter wheat-maize cropping system in the North China Plain. *F. Crop. Res.* 83, 111–124. [https://doi.org/10.1016/S0378-4290\(03\)00068-6](https://doi.org/10.1016/S0378-4290(03)00068-6)
- Llorens, P., Queralt, I., Plana, F., Gallart, F., 1997. Studying solute and particulate sediment transfer in a small mediterranean mountainous catchment subject to land abandonment. *Earth Surf. Process. Landforms* 22, 1027–1035.
- Lloyd, C.E.M., Freer, J.E., Collins, A.L., Johnes, P.J., Jones, J.I., 2014. Methods for detecting change in hydrochemical time series in response to targeted pollutant mitigation in river catchments. *J. Hydrol.* 514, 297–312. <https://doi.org/10.1016/j.jhydrol.2014.04.036>
- Lloyd, C.E.M., Freer, J.E., Johnes, P.J., Coxon, G., Collins, A.L., 2016. Discharge and nutrient uncertainty: Implications for nutrient flux estimation in small streams. *Hydrol. Process.* 30, 135–152. <https://doi.org/10.1002/hyp.10574>
- Loizu, J., Álvarez-Mozos, J., Casalí, J., Goñi, M., 2016. Evaluation of TOPLATS on three Mediterranean catchments. *J. Hydrol.* 539, 141–161. <https://doi.org/10.1016/j.jhydrol.2016.05.025>
- López-Vicente, M., Ben-Salem, N., 2019. Computing structural and functional flow and sediment connectivity with a new aggregated index: A case study in a large Mediterranean catchment. *Sci. Total Environ.* 651, 179–191. <https://doi.org/10.1016/j.scitotenv.2018.09.170>

- MAPAMA, 2018. Superficies y producciones anuales de cultivos [WWW Document].
- MARM, 2008. Cálculo de los costes de operación de cultivos en diferentes zonas agrícolas [WWW Document]. URL <https://www.mapa.gob.es/es/ministerio/servicios/informacion/plataforma-de-conocimiento-para-el-medio-rural-y-pesquero/observatorio-de-tecnologias-probadas/maquinaria-agricola/navarra.aspx>
- Martens, D.A., 2005. Denitrification, in: Hillel, D.B.T.-E. of S. in the E. (Ed.), *Encyclopedia of Soils in the Environment*. Elsevier, Oxford, pp. 378–382. <https://doi.org/10.1016/B0-12-348530-4/00138-7>
- Mastrocicco, M., Colombani, N., Castaldelli, G., 2019. Direct measurement of dissolved dinitrogen to refine reactive modelling of denitrification in agricultural soils. *Sci. Total Environ.* 647, 134–140. <https://doi.org/10.1016/j.scitotenv.2018.07.428>
- Mastrocicco, M., Colombani, N., Palpacelli, S., 2009. Fertilizers mobilization in alluvial aquifer: Laboratory experiments. *Environ. Geol.* 56, 1371–1381. <https://doi.org/10.1007/s00254-008-1232-1>
- Mastrocicco, M., Colombani, N., Palpacelli, S., Castaldelli, G., 2011. Large tank experiment on nitrate fate and transport: The role of permeability distribution. *Environ. Earth Sci.* 63, 903–914. <https://doi.org/10.1007/s12665-010-0759-0>
- Matus, F.J., Mairie, C.R., 2000. Carbon and Nitrogen. *Agric. Técnica* 60, 112–126. <https://doi.org/http://dx.doi.org/10.4067/S0365-28072000000200003>
- McIsaac, G.F., Hu, X., 2004. Net N input and riverine N export from Illinois agricultural watersheds with and without extensive tile drainage. *Biogeochemistry* 70, 251–271. <https://doi.org/10.1023/B: BIOG.0000049342.08183.90>
- Meals, D.W., Richards, R.P., Dressing, S.A., 2013. Pollutant Load Estimation for Water Quality Monitoring Projects, Tech Notes 8. Fairfax. <https://doi.org/10.13140/RG.2.1.2633.4243>
- Menció, A., Mas-pla, J., Otero, N., Regàs, O., Boy-roura, M., Puig, R., Bach, J., Domènech, C., Zamorano, M., Brusi, D., Folch, A., 2016. Nitrate pollution of groundwater; all right ..., but nothing else? *Sci. Total Environ.* 539, 241–251. <https://doi.org/10.1016/j.scitotenv.2015.08.151>
- Merchán, D., Auqué, L.F., Acero, P., Gimeno, M.J., Causapé, J., 2015. Geochemical processes controlling water salinization in an irrigated basin in Spain: Identification of natural and anthropogenic influence. *Sci. Total Environ.* 502, 330–343. <https://doi.org/10.1016/j.scitotenv.2014.09.041>
- Merchán, D., Casalí, J., Del Valle de Lersundi, J., Campo-Bescós, M.A., Giménez, R., Preciado, B., Lafarga, A., 2018. Runoff, nutrients, sediment and salt yields in an irrigated watershed in southern Navarre (Spain). *Agric. Water Manag.* 195, 120–132. <https://doi.org/10.1016/j.agwat.2017.10.004>
- Merchán, D, Casalí, J., Valle, J. Del, Lersundi, D., Campo-bescós, M.A., Giménez, R., Preciado, B., Lafarga, A., 2018. Runoff , nutrients , sediment and salt yields in an irrigated watershed in southern Navarre (Spain). *Agric. Water Manag.* 195, 120–132. <https://doi.org/10.1016/j.agwat.2017.10.004>

- Merchán, D., Causapé, J., Abrahão, R., 2013. Impact of irrigation implementation on hydrology and water quality in a small agricultural basin in Spain Impact of irrigation implementation on hydrology and water quality in a. *Hydrol. Sci. J.* 58, 1400–1413. <https://doi.org/10.1080/02626667.2013.829576>
- Merchán, D, Causapé, J., Abrahão, R., García-Garizábal, I., 2015. Assessment of a newly implemented irrigated area (Lerma Basin , Spain) over a 10-year period . II : Salts and nitrate exported. *Agric. Water Manag.* 158, 288–296. <https://doi.org/10.1016/j.agwat.2015.04.019>
- Merchán, D., Luquin, E., Hernández-García, I., Campo-Bescós, M.A., Giménez, R., Casalí, J., Del Valle de Lersundi, J., 2019. Dissolved solids and suspended sediment dynamics from five small agricultural watersheds in Navarre, Spain: A 10-year study. *Catena* 173, 114–130. <https://doi.org/10.1016/j.catena.2018.10.013>
- Merchán, D, Luquin, E., Hernández-García, I., Campo-Bescós, M.A., Giménez, R., Casalí, J., Valle, J. Del, Lersundi, D., 2019. Dissolved solids and suspended sediment dynamics from five small agricultural watersheds in Navarre , Spain : A 10-year study. *Catena* 173, 114–130. <https://doi.org/10.1016/j.catena.2018.10.013>
- Merrington, G., Winder, L., Prakinson, R., Redman, M., 2002. *Agricultural Pollution*. Spon Press, New York.
- Miller, R.E., Colbert, S.R., Morris, L.A., 2004. Effects of heavy equipment on physical properties of soils and on long-term productivity : a review of literature and current research.
- Millman, J.D., Farnsworth, K.L., 2001. *River Discharge to the Coastal Ocean: A Global Synthesis*. Cambridge University Press, Cambridge, UK.
- Moldanová, J., Grennfelt, P., Jonsson, Å., 2011. Nitrogen as a threat of air quality. *Eur. Nitrogen Assess.* 405–433. <https://doi.org/10.1017/CBO9780511976988.022>
- Montaldo, N., Ravazzani, G., Mancini, M., 2007. On the prediction of the Toce alpine basin floods with distributed hydrologic models. *Hydrol. Process.* 21, 608–621. <https://doi.org/10.1002/hyp>
- Montgomery, D.R., 2007. Soil erosion and agricultural sustainability. *PNAS* 104, 13268–13272. <https://doi.org/10.1073/pnas.0611508104>
- Moriasi, D.N., Arnold, J.G., Liew, M.W. Van, Bingner, R.L., Harmel, R.D., Veith, T.L., 2007. Model evaluation guidelines for systematic quantification of accuracy in watershed simulations. *Soil Water Div. ASABE* 50, 885–900.
- Moriasi, D.N., Gitau, M.W., Pai, N., Daggupati, P., 2015. Hydrologic and water quality models: Performance measures and evaluation criteria. *Nat. Resour. Environ. Syst. Community ASABE* 58, 1763–1785. <https://doi.org/10.13031/trans.58.10715>
- Morris, M.D., 1991. Factorial Sampling Plans for Preliminary Computational Experiments. *Technometrics* 33, 161–174. <https://doi.org/10.1080/00401706.1991.10484804>
- Muñoz-Carpena, R., 2019. HPC Scripts for Global Sensitivity and Uncertainty Analysis [WWW Document]. URL https://abe.ufl.edu/faculty/carpena/software/GSUA_HPC.shtml
- Muschietti-Piana, M. del P., Cipriotti, P.A., Urricariet, S., Peralta, N.R., Niborski, M., 2017. Using

- site-specific nitrogen management in rainfed corn to reduce the risk of nitrate leaching. *Agric. Water Manag.* 199, 61–70. <https://doi.org/10.1016/j.agwat.2017.12.002>
- Nadal-Romero, E., Lana-Renault, N., Serrano-Muela, P., Regüés, D., Alvera, B., García-Ruiz, J.M., 2012. Sediment balance in four catchments with different land cover. *Zeitschrift für Geomorphol.* 56, 147–168. <https://doi.org/10.1127/0372-8854/2012/S-00109>
- Nadal-Romero, E., Latron, J., Martí-Bono, C., Regüés, D., 2008. Temporal distribution of suspended sediment transport in a humid Mediterranean badland area: The Araguás catchment, Central Pyrenees. *Geomorphology* 97, 601–616. <https://doi.org/10.1016/j.geomorph.2007.09.009>
- Nash, J.E., Sutcliffe, J. V., 1970. River Flow Forecasting Through Conceptual Models Part 1-ADiscussion Of Principles. *J. Hydrol.* 10, 282–290. [https://doi.org/https://doi.org/10.1016/0022-1694\(70\)90255-6](https://doi.org/https://doi.org/10.1016/0022-1694(70)90255-6)
- Negrel, P., Roy, S., Petelet-giraud, E., Millot, R., Brenot, A., 2007. Long-term fluxes of dissolved and suspended matter in the Ebro River Basin (Spain). *J. Hydrol.* 342, 249–260. <https://doi.org/10.1016/j.jhydrol.2007.05.013>
- Neilen, A.D., Chen, C.R., Parker, B.M., Faggotter, S.J., Burford, M.A., 2017. Differences in nitrate and phosphorus export between wooded and grassed riparian zones from farmland to receiving waterways under varying rainfall conditions. *Sci. Total Environ.* 598, 188–197. <https://doi.org/10.1016/j.scitotenv.2017.04.075>
- Neill, C., Elsenbeer, H., Krusche, A. V, Lehmann, J., Markewitz, D., Figueiredo, R.D.O., 2006. Preface : Hydrological and biogeochemical processes in a changing Amazon : Results from small watershed studies and the large-scale Hydrological and biogeochemical processes in a changing Amazon : results from small watershed studies and the large-scale b. *Hydrol. Process.* 20, 2467–2476. <https://doi.org/10.1002/hyp.6210>
- Nielsen, D.L., Brock, M.A., Rees, G.N., Baldwin, D.S., 2003. Effects of increasing salinity on freshwater ecosystems in Australia. *Aust. J. Bot.* 51, 655–665. <https://doi.org/10.1071/BT02115>
- Nielsen, D.L., Hillman, T., 2000. The Status of Research into the Effects of Dryland Salinity on Aquatic Ecosystems A discussion paper arising from a salinity workshop Cooperative Research Centre for Freshwater Ecology.
- Novotny, V., 2008. Watershed Models, in: Jorgensen, S., Fath, B. (Eds.), *Encyclopedia of Ecology*. Elsevier B.V., Amsterdam, pp. 221–232. <https://doi.org/https://doi.org/10.1016/B978-008045405-4.00240-8>
- Novotny, V., 2003. *Water Quality: Diffuse Pollution and Watershed Management*, 2nd editio. ed. J. Wiley & Sons, New York.
- Novotny, V., 1994. *Water quality: Prevention, identification, and management of diffuse pollution*. Van Nostrand-Reinhold Publishers, New York, USA.
- O’Callaghan, J.N., Mark, D.M., 1984. The Extraction of Drainage Networks from Digital Elevation Data. *Comput. VisionmGraphics, Image Process.* 28, 323–344.

- Ocampo, C.J., Oldham, C., 2006. Hydrological connectivity of upland-riparian zones in agricultural catchments: Implications for runoff generation and nitrate transport. <https://doi.org/10.1016/j.jhydrol.2006.06.010>
- Ockenden, M.C., Deasy, C.E., Benskin, C.M.W.H., Beven, K.J., Burke, S., Collins, A.L., Evans, R., Falloon, P.D., Forber, K.J., Hiscock, K.M., Hollaway, M.J., Kahana, R., Macleod, C.J.A., Reaney, S.M., Snell, M.A., Villamizar, M.L., Wearing, C., Withers, P.J.A., Zhou, J.G., Haygarth, P.M., 2016. Changing climate and nutrient transfers: Evidence from high temporal resolution concentration-flow dynamics in headwater catchments. *Sci. Total Environ.* 548–549, 325–339. <https://doi.org/10.1016/j.scitotenv.2015.12.086>
- Ockenden, M.C., Hollaway, M.J., Beven, K.J., Collins, A.L., Evans, R., Falloon, P.D., Forber, K.J., Hiscock, K.M., Kahana, R., MacLeod, C.J.A., Tych, W., Villamizar, M.L., Wearing, C., Withers, P.J.A., Zhou, J.G., Barker, P.A., Burke, S., Freer, J.E., Johnes, P.J., Snell, M.A., Surridge, B.W.J., Haygarth, P.M., 2017. Major agricultural changes required to mitigate phosphorus losses under climate change. *Nat. Commun.* 8. <https://doi.org/10.1038/s41467-017-00232-0>
- Odhiambo, B.K., 2018. Sediment and Phosphorous Fluxes Analysis in Aquia Creek , a Sub-watershed of the Chesapeake Bay Basin , VA , USA.
- Oelmann, Y., Kreuziger, Y., Bol, R., Wilcke, W., 2007. Nitrate leaching in soil: Tracing the NO₃-sources with the help of stable N and O isotopes. *Soil Biol. Biochem.* 39, 3024–3033. <https://doi.org/10.1016/j.soilbio.2007.05.036>
- Ollivier, P., Hamelin, B., Radakovitch, O., 2010. Seasonal variations of physical and chemical erosion: A three-year survey of the Rhone River (France). *Geochim. Cosmochim. Acta* 74, 907–927. <https://doi.org/10.1016/j.gca.2009.10.037>
- Oster, J.D., Shainberg, I., 2001. Soil responses to sodicity and salinity: Challenges and opportunities. *Aust. J. Soil Res.* 39, 1219–1224. <https://doi.org/10.1071/SR00051>
- Outeiro, L., Úbeda, X., Farguell, J., 2010. The impact of agriculture on solute and suspended sediment load on a Mediterranean. *Earth Surf. Process. Landforms* 35, 549–560. <https://doi.org/10.1002/esp.1943>
- Pacheco-Betancur, 2013. Dinámica hidrológica y sedimentológica en una cuenca representativa mediterránea. In: Riera de Vernejà (1993-2012) (PhD dissertation, 213,pp). Universitat de Barcelona.
- Parajuli, P.B., Ouyang, Y., 2013. Watershed-scale hydrological modelling methods and applications, in: Bradley, P.M. (Ed.), *Current Perspectives in Contaminant Hydrology and Water Resources Sustainability*. InTech, Rijeka, Croatia, pp. 57–80. <https://doi.org/https://dx.doi.org/10.5772/47884>
- Pärn, J., Henine, H., Kasak, K., Kauer, K., Sohar, K., Tournebize, J., Uemaa, E., Välik, K., Mander, Ü., 2018. Nitrogen and phosphorus discharge from small agricultural catchments predicted from land use and hydroclimate. *Land use policy* 75, 260–268. <https://doi.org/10.1016/j.landusepol.2018.03.048>
- Pengerud, A., Stålnacke, P., Bechmann, M., Blicher-Mathiesen, G., Iital, A., Koskiaho, J.,

- Kyllmar, K., Lagzdins, A., Povilaitis, A., 2015. Temporal trends in phosphorus concentrations and losses from agricultural catchments in the Nordic and Baltic countries. *Acta Agric. Scand. Sect. B Soil Plant Sci.* 65, 173–185. <https://doi.org/10.1080/09064710.2014.993690>
- Peterson, E.W., Benning, C., 2013. Factors influencing nitrate within a low-gradient agricultural stream. *Environ. Earth Sci.* 68, 1233–1245. <https://doi.org/10.1007/s12665-012-1821-x>
- Pieri, L., Ventura, F., Vignudelli, M., Rossi, P., 2011. Nitrogen balance in a hilly semi-agricultural watershed in northern Italy. *Ital. J. Agron.* 6, 67–75. <https://doi.org/10.4081/ija.2011.e12>
- Planchon, O., Darboux, F., 2001. A fast , simple and versatile algorithm to fill the depressions of digital elevation models. *Catena* 46, 159–176.
- Ponce, V.M., Hawkins, R.H., 1996. Runoff Curve Number: Has it Reached Maturity? *J. Hydrol. Eng.* 1, 1–19.
- Povilaitis, A., Šileika, A., Deelstra, J., Gaigalis, K., Baigys, G., 2014. Nitrogen losses from small agricultural catchments in Lithuania. *Agric. Ecosyst. Environ.* 198, 54–64. <https://doi.org/10.1016/j.agee.2014.02.002>
- Que, Z., Seidou, O., Droste, R.L., Wilkes, G., Sunohara, M., Topp, E., Lapen, D.R., 2015. Using AnnAGNPS to Predict the Effects of Tile Drainage Control on Nutrient and Sediment Loads for a River Basin. *J. Environ. Qual.* <https://doi.org/10.2134/jeq2014.06.0246>
- Racca, P., Kakau, J., Kleinhenz, B., Kuhn, C., 2015. Impact of climate change on the phenological development of winter wheat, sugar beet and winter oilseed rape in lower Saxony, Germany. *J. Plant Dis. Prot.* 122, 16–27. <https://doi.org/10.1007/BF03356526>
- Randall, G.W., Goss, M.J., 2008. Nitrate Losses to Surface Water Through Subsurface, Tile Drainage, in: *Nitrogen in the Environment*. pp. 145–175. <https://doi.org/10.1016/B978-0-12-374347-3.00006-8>
- Renard, K.G., Foster, G.R., Weesies, G.A., McCool, D.K., Yoder, D.C., 1997. *Predicting Soil Erosion by water: A Guide to Conservation Planning with the Revised Universal Soil Loss Equation (RUSLE)*. U.S. Government, Washington, DC.
- Rezig, F.A.M., Elhadi, E.A., Abdalla, M.R., 2014. Decomposition and nutrient release pattern of wheat (*Triticum aestivum*) residues under different treatments in desert field conditions of Sudan. *Int. J. Recycl. Org. Waste Agric.* 3. <https://doi.org/10.1007/s40093-014-0069-8>
- Richards, R., 1998. Estimation of pollutant loads in rivers and streams: A guidance document for NPS programs. Prepared under Grant X998397-01-0;
- Ritter, A., Muñoz-Carpena, R., 2013. Performance evaluation of hydrological models : Statistical significance for reducing subjectivity in goodness-of-fit assessments. *J. Hydrol.* 480, 33–45. <https://doi.org/10.1016/j.jhydrol.2012.12.004>
- Romero, E., Garnier, J., Billen, G., Peters, F., Lassaletta, L., 2016. Water management practices exacerbate nitrogen retention in Mediterranean catchments. *Sci. Total Environ.* 573, 420–432. <https://doi.org/10.1016/j.scitotenv.2016.08.007>
- Runkel, R.L., Crawford, C.G., Cohn, T.A., 2004. Load Estimator (LOADEST): A FORTRAN

- Program for Estimating Constituent Loads in Streams and Rivers. U.S. Geol. Surv. Tech. Methods B. 4, Chapter A5 69.
- Saltelli, A., Tarantola, S., Campolongo, F., 2000. Sensitivity Analysis as an Ingredient of Modeling. *Stat. Sci.* 15, 377–395.
- Saltelli, A., Tarantola, S., Campolongo, F., Ratto, M., 2004. *Sensitivity Analysis in Practice: A Guide to Assessing Scientific Models*. John Wiley & Sons, Chichester, England.
- Saxton, K.E., Rawls, W.J., Romberger, J.S., Papendick, R.I., 1986. Estimating soil water characteristics-hydraulic conductivity. *Soil Sci. Soc. Am. J.* 50, 1031–1036.
- Scanlon, B.R., Jolly, I., Sophocleous, M., Zhang, L., 2007. Global impacts of conversions from natural to agricultural ecosystems on water resources : Quantity versus quality. *Water Resour. Res.* 43, 1–18. <https://doi.org/10.1029/2006WR005486>
- Sharpley, A.N., 1995. Dependence of Runoff Phosphorus on Extractable Soil Phosphorus. *J. Environ. Qual.* 24, 920. <https://doi.org/10.2134/jeq1995.00472425002400050020x>
- Sharpley, A.N., Halvorson, A.D., 1994. The Management of Soil Phosphorus Availability and its Impact on Surface Water Quality, in: Lal, R., Stewart, B.A. (Eds.), *Soil Processes and Water Quality*. Lewis Publishers, Boca Raton, USA.
- Shore, M., Jordan, P., Mellander, P.E., Kelly-Quinn, M., Daly, K., Sims, J.T., Wall, D.P., Melland, A.R., 2016. Characterisation of agricultural drainage ditch sediments along the phosphorus transfer continuum in two contrasting headwater catchments. *J. Soils Sediments* 16, 1643–1654. <https://doi.org/10.1007/s11368-015-1330-0>
- Skaggs, R.W., Fausey, N.R., Evans, R.O., 2012. Drainage water management. *J. Soil Water Conserv.* 67, 167–172. <https://doi.org/10.2489/jswc.67.6.167A>
- Skiba, U., 2008. Denitrification. *Encycl. Ecol.* 866–871. <https://doi.org/10.1016/B978-008045405-4.00264-0>
- Soana, E., Bartoli, M., Milardi, M., Fano, E.A., Castaldelli, G., 2019. An ounce of prevention is worth a pound of cure: Managing macrophytes for nitrate mitigation in irrigated agricultural watersheds. *Sci. Total Environ.* 647, 301–312. <https://doi.org/10.1016/j.scitotenv.2018.07.385>
- Sobol, I.M., 2001. Global sensitivity indices for nonlinear mathematical models and their Monte Carlo estimates. *Math. Comput. Simul.* 55, 271–280.
- Sobol, I.M., 1993. Sensitivity Analysis for Nonlinear Mathematical Models. *Math. Model. Comput. Exp.* 1, 407–414.
- Soil Survey Staff, 2014. *Keys to Soil Taxonomy*, 12th ed.
- Sorando, R., Comín, F.A., Sauvage, S., Sánchez-Pérez, J.M., Jiménez, J.J., 2018. Water resources and nitrate discharges in relation to agricultural land uses in an intensively irrigated watershed. *Sci. Total Environ.* 659, 1293–1306. <https://doi.org/10.1016/j.scitotenv.2018.12.023>
- Subramanian, V., 1979. Chemical and Suspended-Sediment Characteristics. *J. Hydrol.* 44, 37–55.

- Swiechowicz, J., 2002. Linkage of slope wash and sediment and solute export from a foothill catchment in the Carpathian foothills. *Earth Surf. Process. Landforms* 27, 1389–1413. <https://doi.org/10.1002/esp.437>
- Tabacchi, E., Lambs, L., Guilloy, H., Planty-Tabacchi, A.-M., Muller, E., Decamps, H., 2000. Open Archive Toulouse Archive Ouverte (OATAO) Impacts of riparian vegetation on hydrological processes. *Hydrol. Process.* 14, 2959–2976. [https://doi.org/10.1002/1099-1085\(200011/12\)14](https://doi.org/10.1002/1099-1085(200011/12)14)
- Tang, Y., Reed, P., Wagener, T., Van Werkhoven, K., 2007. Comparing sensitivity analysis methods to advance lumped watershed model identification and evaluation. *Hydrol. Earth Syst. Sci.* 11, 793–817. <https://doi.org/10.5194/hess-11-793-2007>
- Tarantola, S., Becker, W., 2017. SIMLAB Software for Uncertainty and Sensitivity Analysis, in: Ghanem, R., Higdon, D., Owhadi, H. (Eds.), *Handbook of Uncertainty Quantification*. Springer International Publishing, Cham, Switzerland, pp. 1979–200. <https://doi.org/10.1007/978-3-319-12385-1>
- Tarboton, D.G., 1997. A new method for the determination of flow directions and upslope areas in grid digital elevation models. *Water Resour. Res.* 33, 309–319.
- Tedeschi, A., Beltrán, A., Aragües, R., 2001. Irrigation management and hydrosalinity balance in a semi-arid area of the middle Ebro river basin (Spain). *Agric. Water Manag.* 49, 31–50.
- Teegavarapu, R.S. V, Chinatalapudi, S., 2018. Incorporating Influences of Shallow Groundwater Conditions in Curve Number-Based Runoff Estimation Methods. *Water Resour Manag.* 32, 4313–4327. <https://doi.org/https://doi.org/10.1007/s11269-018-2053-y> Incorporating
- Thorburn, P.J., Wilkinson, S.N., 2013. Conceptual frameworks for estimating the water quality benefits of improved agricultural management practices in large catchments. *Agric. Ecosyst. Environ.* 180, 192–209. <https://doi.org/10.1016/j.agee.2011.12.021>
- Tisdale, S., Nelson, W.L., Beaton, J.D., Halvin, J., 1993. *Soil Fertility and Fertilisers*. 5th edition. Prentice Hall, New Jersey, USA.
- Tiwari, T., Buffam, I., Sponseller, R.A., Laudon, H., 2017. Inferring scale-dependent processes influencing stream water biogeochemistry from headwater to sea. *Limnol. Oceanography* 62, 58–70. <https://doi.org/10.1002/lno.10738>
- Tuset, J., Vericat, D., Batalla, R.J., 2016. Rainfall, runoff and sediment transport in a Mediterranean mountainous catchment. *Sci. Total Environ.* 540, 114–132. <https://doi.org/10.1016/j.scitotenv.2015.07.075>
- USDA-NRCS, 1986. *Urban Hydrology for Small. (TR-55), Technical Release 55*. Washington, DC.
- USDA, 1972. *National Engineering Handbook. Hydrology Section. Chapters 1-4*. Washington, DC.
- USEPA, 2019. *Better Assessment Science Integrating point and Nonpoint Sources. BASINS 4.5-User's Manual*. Washington, DC.
- USEPA, 2015. *Nitrogen and Phosphorous Loads in Large Rivers [WWW Document]*. URL

<https://cfpub.epa.gov/roe/indicator.cfm?i=33#1>

- USEPA, 2000. BASINS Technical Note 6: Estimating hydrology and hydraulic parameters for HSPF. Washington, DC.
- Vagstad, N., Eggestad, H.O., Høyås, T.R., 1997. Mineral nitrogen in agricultural soils and nitrogen losses: Relation to soil properties, weather conditions, and farm practices. *Ambio* 26, 266–272. <https://doi.org/10.2307/4314603>
- Van Meter, K., Thompson, S.E., Basu, N.B., 2016. Human Impacts on Stream Hydrology and Water Quality, Stream Ecosystems in a Changing Environment. Elsevier Inc. <https://doi.org/10.1016/B978-0-12-405890-3.00011-7>
- Vanmaercke, M., Poesen, J., Verstraeten, G., Vente, J. De, Ocakoglu, F., 2011. Sediment yield in Europe: Spatial patterns and scale dependency. *Geomorphology* 130, 142–161. <https://doi.org/10.1016/j.geomorph.2011.03.010>
- Vanni, M.J., Renwick, W.H., Headworth, J.L., Auch, J.D., Schaus, M.H., 2001. Dissolved and particulate nutrient flux from three adjacent agricultural watersheds: A five-year study. *Biogeochemistry* 54, 85–114. <https://doi.org/10.1023/A:1010681229460>
- Ventura, M., Scandellari, F., Ventura, F., Guzzon, B., Rossi Pisa, P., Tagliavini, M., 2008. Nitrogen balance and losses through drainage waters in an agricultural watershed of the Po Valley (Italy). *Eur. J. Agron.* 29, 108–115. <https://doi.org/10.1016/j.eja.2008.05.002>
- Vidon, P.G.F., Hill, A.R., 2004. Landscape controls on nitrate removal in stream riparian zones 40, 1–14. <https://doi.org/10.1029/2003WR002473>
- Wang, E., Engel, T., 1998. Simulation of phenological development of wheat crops. *Agric. Syst.* 58, 1–24. [https://doi.org/10.1016/S0308-521X\(98\)00028-6](https://doi.org/10.1016/S0308-521X(98)00028-6)
- Wang, X., Yang, J., Liu, G., Yao, R., Yu, S., 2015. Impact of irrigation volume and water salinity on winter wheat productivity and soil salinity distribution. *Agric. Water Manag.* 149, 44–54. <https://doi.org/10.1016/j.agwat.2014.10.027>
- Wang, Y., You, W., Fan, J., Jin, M., Wei, X., Wang, Q., 2018. Effects of subsequent rainfall events with different intensities on runoff and erosion in a coarse soil. *Catena* 170, 100–107. <https://doi.org/10.1016/j.catena.2018.06.008>
- Wiegand, C., Anderson, G., Lingle, S., Escobar, D., 1996. Soil salinity effects on crop growth and yield - Illustration of an analysis and mapping methodology for sugarcane. *J. Plant Physiol.* 148, 418–424. [https://doi.org/10.1016/S0176-1617\(96\)80274-4](https://doi.org/10.1016/S0176-1617(96)80274-4)
- Wischmeier, W.H., Smith, D.D., 1978. Predicting rainfall erosion losses, Agriculture Handbook Number 537. Washington, DC.
- Withers, P.J.A., Jarvie, H.P., 2008. Delivery and cycling of phosphorus in rivers: A review. *Sci. Total Environ.* 400, 379–395. <https://doi.org/10.1016/j.scitotenv.2008.08.002>
- Withers, P.J.A., Sharpley, A.N., 1995. Phosphorus fertilizers, in: Reheigl, J.E. (Ed.), *Soil Amendments and Environmental Quality*. Lewis Publishers Inc., Boca Raton, USA, pp. 65–107.

- Woodley, A.L., Drury, C.F., Reynolds, W.D., Tan, C.S., Yang, X.M., Oloya, T.O., 2018. Long-term Cropping Effects on Partitioning of Water Flow and Nitrate Loss between Surface Runoff and Tile Drainage. *J. Environ. Qual.* 47, 820–829. <https://doi.org/10.2134/jeq2017.07.0292>.
- World Health Organization, 2011. Guidelines for drinking-water quality: guideline values for chemicals from industrial sources and human dwellings that are of health significance in drinking water, 4th ed. Geneva.
- Wu, X.Y., Zhang, L.P., Yu, X.X., 2012. Impacts of surface runoff and sediment on nitrogen and phosphorus loss in red soil region of southern China. *Environ. Earth Sci.* 67, 1939–1949. <https://doi.org/10.1007/s12665-012-1635-x>
- Yaşar Korkanç, S., Dorum, G., 2019. The nutrient and carbon losses of soils from different land cover systems under simulated rainfall conditions. *Catena* 172, 203–211. <https://doi.org/10.1016/j.catena.2018.08.033>
- Young, R.A., Onstad, C.A., Bosch, D.D., Anderson, W.P., 1989. AGNPS: A nonpoint-source pollution model for evaluating agricultural watersheds. *J. Soil Water Conserv.* March 44, 168–173.
- Yuan, Y., Bingner, R., Momm, H., 2018. Nitrogen Component in Nonpoint-Source Pollution Models, in: Delgado, J.A., Sassenrath, G.F., Mueller, T. (Eds.), *Precision Conservation: Geospatial Techniques for Agricultural and Natural Resources Conservation*. Madison, WI, pp. 27–64. <https://doi.org/10.2134/agronmonogr59.2013.0012>
- Yuan, Y., Bingner, R.L., Rebich, R.A., 2003. Evaluation of AnnAGNPS nitrogen loading in an agricultural watershed. *J. Am. Water Resour. Assoc.* 6649, 457–466.
- Yuan, Y., Mehaffey, M.H., Lopez, R.D., Bingner, R.L., Bruins, R., Erickson, C., Jackson, M.A., Division, S., Vegas, L., Quality, W., Exposure, E., 2011. AnnAGNPS Model Application for Nitrogen Loading Assessment for the Future Midwest Landscape Study. *Water* 3, 196–216. <https://doi.org/10.3390/w3010196>
- Zabaleta, A., Martínez, M., Uriarte, J.A., Antigüedad, I., 2007. Factors controlling suspended sediment yield during runoff events in small headwater catchments of the Basque Country. *Catena* 71, 179–190. <https://doi.org/10.1016/j.catena.2006.06.007>
- Zhou, Y., Xu, J.F., Yin, W., Ai, L., Fang, N.F., Tan, W.F., Yan, F.L., Shi, Z.H., 2017. Hydrological and environmental controls of the stream nitrate concentration and flux in a small agricultural watershed. *J. Hydrol.* 545, 355–366. <https://doi.org/10.1016/j.jhydrol.2016.12.015>

ANNEXES

ANNEX I: PRINCIPAL NUTRIENT CYCLES

Understanding the dynamics of total dissolved solids in a watershed is not a trivial task. The multitude of interactions and processes that each constituent experiences in a watershed is very difficult to quantify. For this reason, it is essential to achieve sufficient knowledge on the cycle of the primary and most complex constituents. In agricultural lands, nutrients play a fundamental role, and knowing which form of nutrients are present is vital in the adequate definition of dynamics. As previously mentioned, fertilizers composed of N and P are the most employed in agriculture. Therefore, knowledge of N and P cycles is crucial to understanding their dynamics.

Nitrogen cycle

The nitrogen nutrient cycle is considered the most complex cycle of all mineral nutrients because N can be found in solid, liquid, and gaseous forms (Jones and Jacobsen, 2002). The dynamics of N in agricultural soils are complex due to the biological and chemical processes involved (Yuan et al., 2018). In soils, N content is usually under 0.5 % and can be found as organic N associated with hummus or inorganic N, in soluble forms (mainly NO_3^- , NH_4^+). Fig.A.I.1 shows the main processes of the N cycle in agricultural lands, followed by a description.

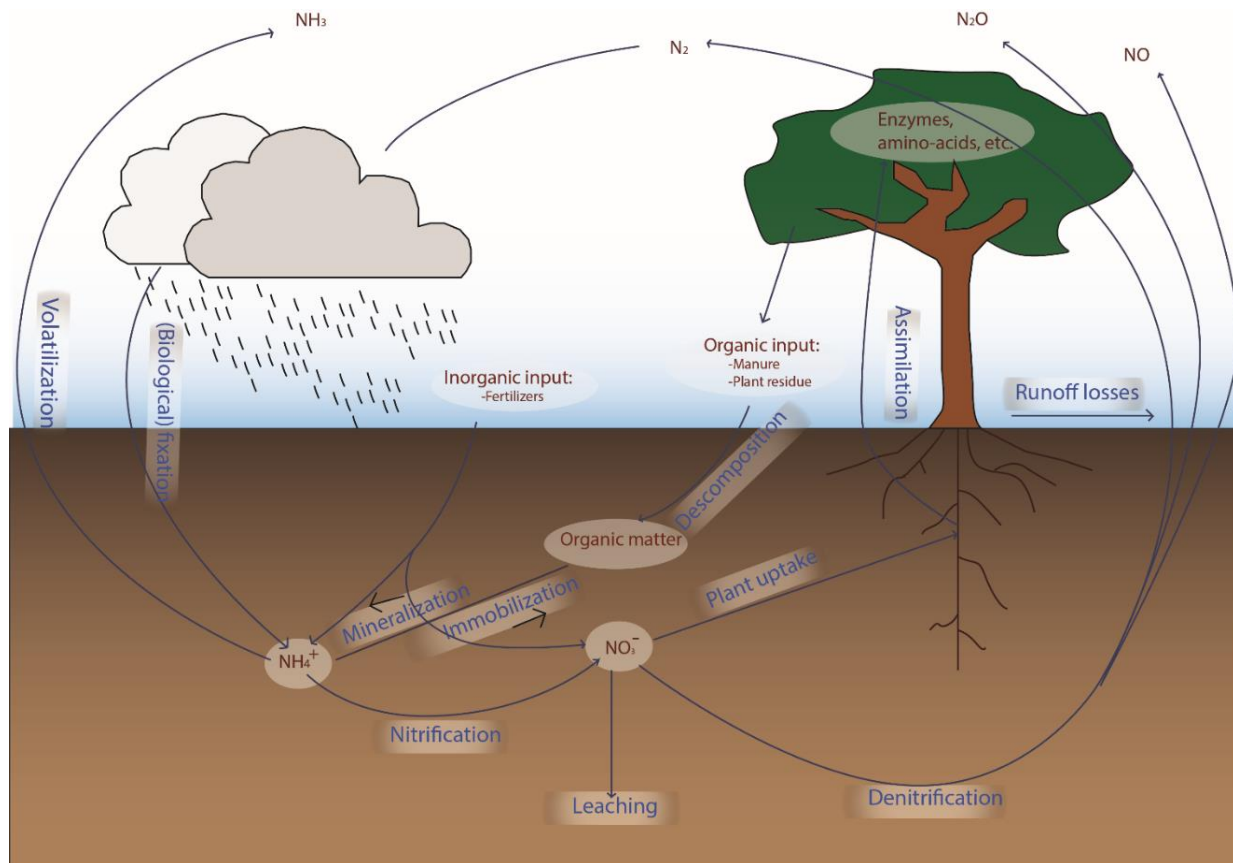


Figure A.I.1: Principal processes of the N cycle.

Nitrogen inputs: The main inputs of N in agricultural soils are a consequence of fertilizer or manure application. In addition, atmospheric deposition, plant residue, and fixation from soil bacteria also contribute to the increase of soil N (Novotny, 1994). Organic N and Ammonium N (NH_4^+) are frequently fixed to clays, preventing an immediate uptake by plants. Nitrate (NO_3^-) is the most soluble form of N in soils and is highly mobile. This high mobility makes it available for plants and also vulnerable to losses by runoff, leaching into deeper soil layers or groundwater.

Mineralization and immobilization: Mineralization occurs when the organic N breaks down and is transformed into less complex compounds of N. The liberation of carbon dioxide generally accompanies this process into the atmosphere. Contrary to this process, immobilization happens when microbial interactions transform simple forms of N (NO_3^- , NH_4^+) into more complex organic forms. Immobilization occurs more readily in zones with high C/N ratios (Yuan et al., 2018). There are several factors affecting immobilization, with soil moisture content being the most remarkable, followed by crop residues, soil temperature, and pH, to name a few (Haynes, 1986).

Nitrification and denitrification: Nitrification is the transformation of NH_4^+ into NO_3^- . This process occurs in aerated soils with high microorganism contents. Nitrification is carried out in two steps: firstly, NH_4^+ is transformed into NO_2^- by the interaction with Nitrosomonas; then, NO_2^- is finally transformed into NO_3^- by Nitrobacter, which are the microorganisms that control the transformation. The second reaction is much faster than the first one, with very low NO_2^- concentrations in soils (in many cases, insignificant). Nevertheless, NO_2^- is very soluble and easily moved by water. The requirements for nitrification include temperatures between 10-22 °C, pH values between 6-10, and adequate soil moisture. Regarding soil moisture, the nitrification rate decreases with decrease of soil moisture. However, saturated soils are not suitable for nitrification because of the decreasing oxygen content in the soil, which triggers this process. Denitrification reduces NO_3^- to gaseous forms, generally N_2O and N_2 , and is mainly carried out by microbial activity. An infrastructure that operates as a water bypass, reducing its residence time, can increase NO_3^- exports in freshwater ecosystems (Gramlich et al., 2018; Randall and Goss, 2008), so the presence of wetlands is essential and helpful in reducing nitrate upstream (Hansen et al., 2012; Skaggs et al., 2012).

Volatilization: This process occurs when ammonia (NH_3) is lost in gaseous form to the atmosphere. It generally occurs in soils with high pH, where NH_4^+ is more easily transformed into NH_3 . Increases in wind and temperature also contribute positively to this volatilization.

Biological nitrogen fixation: Incorporates atmospheric nitrogen into the biosphere, making it available to microorganisms. This fixation can occur in an abiotic manner (e.g., through precipitation, electrical discharges) or in a biotic way, through bacteria. Essential factors in the fixation process include the number of microorganisms available for fixation, light, temperature, humidity, oxygen concentration, and nitrogen compounds.

Nitrogen uptake and assimilation: These processes are highly interconnected. Nitrogen uptake occurs first, which is the absorption of nutrients by the plant. Then, the assimilation of nutrients occurs, forming organic N compounds such as amino-acids, pigments or enzymes. Assimilation requires a complex series of biochemical reactions at a high energy cost. These compounds are generated from environmental inorganic compounds such as NH_4^+ or NO_3^- .

Decomposition: This process breaks fresh organic residue into more simple organic components (humus), adding organic N to the soil. Essential factors to decomposition include soil moisture content, crop residues, soil temperature and pH, and the characteristics of the organic residue.

Leaching and runoff losses: Although there are numerous forms of nitrogen in the environment, NO_3^- is considered crucial. NO_3^- can be leached in considerable quantities as water flows through the soil profile due to its high mobility. An increase of water in the soil profile, or an increase of runoff, are crucial to nitrogen losses. These losses directly impact water quality due to the high mobility of NO_3^- , and the consequences can affect human health and environment. Although rainfall is a critical factor in the control of N losses, many other factors play important roles in quantifying these losses, such as fertilizer amounts, soil texture, and land use.

Phosphorous cycle

The cycle of P is primarily terrestrial, as it does not have critical gaseous components. All the P found in the terrestrial layer originates mainly from mineral weathering and anthropogenic contributions. Fig. A.I.2 shows the main processes of the P cycle in agricultural lands, followed by a description.

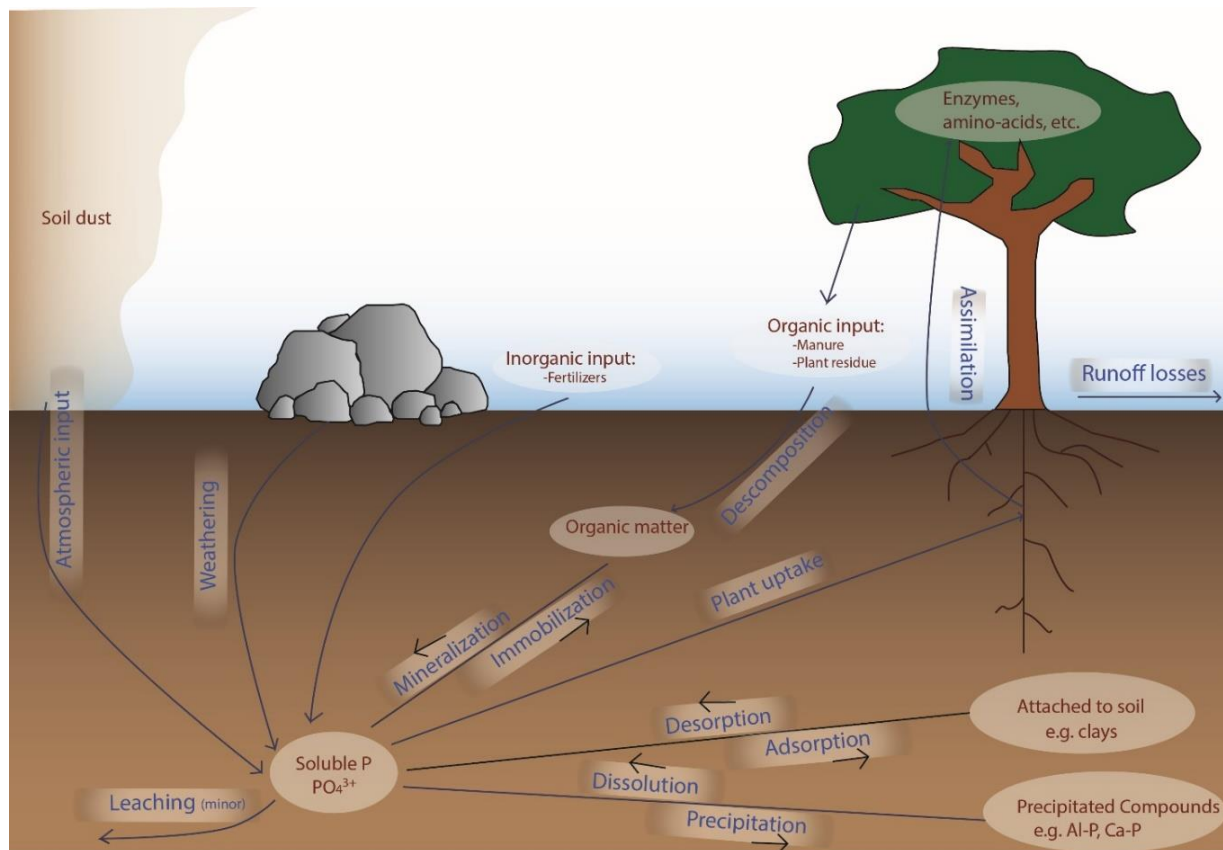


Figure A.I.2: Principal processes of the P cycle

Phosphorous inputs: In most ecosystems, the most outstanding contribution of phosphorus is due to the weathering of rocky material. However, in agrosystems, the application of fertilizers suppose an important input of P in the environment. In terms of phosphorus, management practices in agricultural soils have been reported to be very important. An apparent surplus of P has been shown, producing an essential change in the balance of P inputs and offtakes. Generally, fertilizers provide the soil with soluble and reactive phosphorus compounds (SRP), with ion phosphate (PO_4^{3-}) being the most usual for plant uptake.

Atmospheric inputs: Atmospheric inputs of P are limited (unlike N), as the gaseous phase is not predominant. The P content in the rain is generally very low, so the most common way in which P reaches the soil is by dry deposition, or by dust or soil carried by the wind.

Animal manure: Around 75% of the P consumed by livestock in its different forms is excreted (Haygarth et al., 1998). Phosphorus inputs to livestock feed are paramount because low P can lead to reduced milk yield, poor animal weight gain, reduced feed intake, and reduced fertility. However, an excess would produce a higher excretion of P, thus increasing the P content of the

soil and generating a surplus of the nutrient. Therefore, special care must be taken when feeding livestock to maintain the P balance (Withers and Sharpley, 1995).

Mineralization and immobilization: These transformations occur in aerated soils with high concentrations of microorganisms responsible for carrying out these processes. As in the N cycle, these transformations depend on various factors such as the range of soil, organic substrate, climatic and seasonal factors (Sharpley and Halvorson, 1994). Mineralization and immobilization take place simultaneously. Mineralization transforms the P into its inorganic form, and immobilization converts the inorganic P into biochemical compounds that are less available. Most organic phosphates from plants can be broken down by the phosphatase enzyme from microorganisms (Tisdale et al., 1993).

P distribution in soil: The distribution of P in soils is very diverse, and depending on its form, the effect on the environment can be very different. There are organic and inorganic forms of P in soils, classified in different pools (non-labile organic P, labile P, biomass P, organic P, dissolved P). Organic P is generally found in the first few centimeters of the soil because of its close relationship with organic matter. The P in soil solution represents less than 0002% of the total P (Merrington et al., 2002). The inorganic compounds of this soil solution are suitable for uptake by plants (plants mainly absorb phosphate ions). During the growing period, the P in soil solution is depleted and must be replaced to maintain adequate P levels for plant growth. The diffusion of P ions is very low, with very slow movement compared to other nutrients (e.g., N). This low mobility can produce areas where plant absorption is higher than the nutrients available due to the impossibility of replacing the P in the soil solution.

P sorption: When P is applied to the soil, there are several possible pathways. The P supplied can be taken up by the plant, kept as organic P, or even attached to the inorganic components of the soil. Precipitation leads to the retention and removal of P from the soil solution. This occurs when the concentration of P in the solution, combined with other relevant cations, exceeds the solubility product of the mineral (Merrington et al., 2002). Adsorption, however, occurs more commonly when the solution concentrations are low, although both mechanisms can work in parallel. P-sorption is initially fast, followed by slower processes in which less available P-forms are generated for the plants. Depending on the soil pH, there could be different insoluble forms. At low pH values, insoluble phosphates of Al and Fe are very common, and at high pH values,

insoluble phosphates of Ca appear (Brady and Weil, 2008). Due to the insoluble compounds in high and low pH values, the optimal value of this potential availability of P for plants is close to neutral (Merrington et al., 2002). Besides pH, other factors contribute to the P-sorption of soil, such as soil texture, temperature, organic matter content, and the different ions present in the soil, among others. The complexity of these factors and their relationship with P-sorption places emphasis on fertilization management.

Leaching and runoff losses: Although the best way to remove P from the soil in an agricultural system is through crop plant uptake, this is neither the only nor the most common way. P losses in agricultural systems are not generally high, but it has been proven that low P concentrations can generate significant environmental problems such as eutrophication (Merrington et al., 2002). Runoff P losses are the most common loss in agricultural systems, which vary in form, amount, and timing, depending on factors such as agricultural practices and hydrology. Most of the P lost through runoff is P-particulate, especially if there is significant sediment transport in runoff, which occurs primarily in storm events (Merrington et al., 2002). These particles can be desorbed and converted to soluble P in contact with the flow (Sharpley, 1995). P leaching in agricultural soils is very low, with very weak movement of P ions in the soil profile. Although sometimes the presence of drainage can decrease surface runoff and increase P leaching, this would mean a significant decrease in P losses by runoff. Therefore, runoff losses are higher than those from leaching, reducing the final balance of soil P loss.

**ANNEX II: HPC SCRIPTS FOR DISSOLVED
NITROGEN CALIBRATION IN THE AnnAGNPS
MODEL**

This Annex presents the bash scripts developed for AnnAGNPS calibration. These scripts are based on those reported by Muñoz-Carpena (2019). An example of the scripts for Linux, developed for runoff calibration at La Tejería watershed, is presented below.

All these scripts are original by Rafael Muñoz Carpena.

©2019. R. Munoz-Carpena, U. of Florida, carpena@ufl.edu

proc_matrix script.

```
# script used for the matrix generation. In this case, curve numbers for soil hydrologic group B and C.
```

```
tr -d '\r' <matrix.tmp> $1.tmp1
```

```
dm "if x1 < x7 then INPUT else "s1 s2 s3 s4 s5 s6 x1+0.5 s8 s9 s10 s11 s12"" <$1.tmp1 | dm "if x2 < x8 then INPUT else "s1 s2 s3 s4 s5 s6 s7 x2+0.5 s9 s10 s11 x6+0.5""|dm "if x3 < x9 then INPUT else "s1 s2 s3 s4 s5 s6 s7 s8 x3+0.5 s10 s11 s12"">$1.tmp2
```

```
dm "if x4 < x10 then INPUT else "s1 s2 s3 s4 s5 s6 s7 s8 s9 x4+0.5 s11 s12"" <$1.tmp2 |dm "if x5 < x11 then INPUT else "s1 s2 s3 s4 s5 s6 s7 s8 s9 s10 x5+0.5 s12""|dm "if x6 < x12 then INPUT else "s1 s2 s3 s4 s5 s6 s7 s8 s9 s10 s11 x6+0.5"">$1.tmp3
```

```
dm "'sens_class'" s1 s2 s3 s4 s5 s6 s7 s8 s9 s10 s11 s12 <$1.tmp3 >$1.txt
```

```
ln -sf $1.txt matrix.txt
```

```
rm $1.tmp1 $1.tmp2 $1.tmp3
```

make_jobs.sh script.

```
#!/bin/bash
```

```
## make jobs from matrix vectors
```

```
# Use: make_jobs.sh $1 $2
```

```
# where $1 is the total number of simulations (TOTALSIM) and $2 is the number of simulations in each job (SIMSJOB)
```

```
# prepare files
```

```

rm class_submit.sh Outputs/class_merge.sh

echo cat >tmp1.tmp

# bash while loop, divide TOTALSIM simulations into batches with SIMSJOB number of
simulations inside

COUNT=0

XSUB=1

TOTALSIM=$1

SIMSJOB=$2

while [ $COUNT -lt $TOTALSIM ]; do
    let COUNT0=COUNT+1
    let COUNT=COUNT+SIMSJOB
    sed -n "$COUNT0","$COUNT"p matrix.txt > matrix$XSUB.tmp
    cat class_GSA.job.top matrix$XSUB.tmp class_GSA.job.bottom > class_GSA$XSUB.tmp
    sed s/CCA/$XSUB/g < class_GSA$XSUB.tmp >class_GSA$XSUB.job
    echo Value of count is: $XSUB $COUNT0 $COUNT
    echo 'qsub' class_GSA$XSUB.job >>class_submit.sh
    echo TIEGEM$XSUB.out >>class_merge.tmp
    let XSUB=XSUB+1
done

echo 'cat ' > head.tmp

echo '>output.all' >>class_merge.tmp

cat head.tmp class_merge.tmp | tr '\n' ' ' > Outputs/class_merge.sh

echo -e "\nsed 's;/ /g' <output.all>output_all.txt" >> Outputs/class_merge.sh

# clean up!

rm *.tmp

```

class_GSA.job.top script

```
JOB_DIR=$HOME/TIEGEM/  
SRC_DIR=$HOME/TIEGEM/base  
DST_DIR=$HOME/TIEGEM/Outputs  
TMP_DIR=$HOME/scratch/SimulationsCCA  
#  
PATH=$HOME/bin.:$PATH  
#  
# Create and populate working directory to run in.  
#  
if [ ! -d $TMP_DIR ]; then  
  echo Making TMP_DIR = $TMP_DIR  
  mkdir -p $TMP_DIR  
fi  
cp -r $SRC_DIR $TMP_DIR  
rm Outputs/TIEGEMCCA.out  
cd $TMP_DIR/base  
echo pwd = `pwd`  
#  
# Start simulations  
# run java with SIMLAB GSUA table (matrix.txt)  
rm output.all
```

class_GSA.job.bottom script

```
#Done with simulations  
touch $DST_DIR/TIEGEMCACA.done  
  
#  
# Finish processing and copy results to user directory  
#  
# Copy all individual output files with the (numerical) order they belong  
cp output.all $DST_DIR/TIEGEMCCA.out  
cd $DST_DIR
```

class_submit.sh script

```
#execute jobs in HPC  
qsub class_GSA1.job  
qsub class_GSA2.job
```

qsub class_GSA3.job
qsub class_GSA4.job
qsub class_GSA5.job
qsub class_GSA6.job
qsub class_GSA7.job
qsub class_GSA8.job
qsub class_GSA9.job
qsub class_GSA10.job
qsub class_GSA11.job
qsub class_GSA12.job
qsub class_GSA13.job
qsub class_GSA14.job
qsub class_GSA15.job
qsub class_GSA16.job
qsub class_GSA17.job
qsub class_GSA18.job
qsub class_GSA19.job
qsub class_GSA20.job
qsub class_GSA21.job
qsub class_GSA22.job
qsub class_GSA23.job
qsub class_GSA24.job
qsub class_GSA25.job
qsub class_GSA26.job
qsub class_GSA27.job
qsub class_GSA28.job
qsub class_GSA29.job
qsub class_GSA30.job

class_merge.sh script

```
#Merge all jobs outputs in a single output file
```

```
cat TIEGEM1.out TIEGEM2.out TIEGEM3.out TIEGEM4.out TIEGEM5.out TIEGEM6.out  
TIEGEM7.out TIEGEM8.out TIEGEM9.out TIEGEM10.out TIEGEM11.out TIEGEM12.out  
TIEGEM13.out TIEGEM14.out TIEGEM15.out TIEGEM16.out TIEGEM17.out TIEGEM18.out  
TIEGEM19.out TIEGEM20.out TIEGEM21.out TIEGEM22.out TIEGEM23.out TIEGEM24.out  
TIEGEM25.out TIEGEM26.out TIEGEM27.out TIEGEM28.out TIEGEM29.out TIEGEM30.out  
>output.all
```

```
sed 's;/ /g' <output.all>output_all.txt
```

sens_class script.

```
#!/bin/bash
```

```
# create the table of substitutions for this run to be used by the AWK script "a_subs" based on  
the parameter specified in the command-line. par.txt substitute labels
```

```
for VAR in $*
```

```
do
```

```
    echo $VAR>>set1.par
```

```
done
```

```
abut par.txt set1.par | dm s1 x2 >substitute.tab
```

```
# Substitute command-line parameters into the XML input file for this simulation.
```

```
a_subs < general/rocurve.csv.ptr >general/rocurve.tmp
```

```
sed 's/ //g' <general/rocurve.tmp > general/rocurve.csv
```

```
#Run for this sample combination
```

```
echo '...running AnnAGNPS ...'
```



```
#rm output/outputInfo
```

```
agnps
```

```
# Process results
```

```
tail -3668 AnnAGNPS_TBL_Gaging_Station_Data_Hyd.txt |head -3653 |sed 's/\\/ /g' |dm s3 s1  
s16 >pred.tmp
```

```
perl -ane '$h{"@F[0 .. 1]}" += $F[2] }{ print "$_ $h{$_}\n" for keys %h' pred.tmp |dsort |dm s3  
>pred.txt
```

```
#Calculate Nash-Sutcliffe of Runoff
```

```
paste obs.txt pred.txt >nse1.in
```

```
nse nse1.in |dm s2 >>output.all
```

```
paste obs.txt pred.txt >Latxaga.in
```

```
# Clean-up
```

```
rm substitute.tab set1.par general/*.tmp
```

```
rm *.tmp* nse*.in pred.txt
```

**ANNEX III: PUBLICATIONS IN JOURNALS AND
CONFERENCE PROCEEDINGS DURING THE
DOCTORAL PROGRAM**

Manuscripts published in indexed journals.

Merchán, D., Luquin, E., Hernández-García, I., Campo-Bescós, M.A., Giménez, R., Casalí, J., Valle, J. Del, Lersundi, D., 2019. Dissolved solids and suspended sediment dynamics from five small agricultural watersheds in Navarre, Spain: A 10-year study. *Catena* 173, 114–130. <https://doi.org/10.1016/j.catena.2018.10.013>

Merchán, D., Sanz, L., Alfaro, A., Pérez, I., Goñi, M., Solsona, F., Hernández-García, I., Pérez, C., Casalí, J., 2020. Irrigation implementation promotes increases in salinity and nitrate concentration in the lower reaches of the Cidacos River (Navarre, Spain). *Sci. Total Environ.* 706, 135701. <https://doi.org/10.1016/J.SCITOTENV.2019.135701>

Hernández-García, I., Merchán, D., Aranguren, I., Casalí, J., Giménez, R., Campo-Bescós, M.A., Del Valle de Lersundi, J., 2020. Assessment of the main factors affecting the dynamics of nutrients in two rainfed cereal watersheds. *Sci. Total Environ.* 733. <https://doi.org/10.1016/j.scitotenv.2020.139177>.

Manuscripts in preparation for indexed journals.

Hernández-García, I., Muñoz-Carpena, R., Luquin, E., Campo-Bescós, M.A., Casalí, J., Merchán, D., Bingner, R. On the modeling of two agricultural Mediterranean watersheds to quantify the critical factors affecting dissolved nitrogen exports.

National Conference Presentations.

Hernández-García, I., Merchán, D., Luquin, E., Campo-Bescós, M.A., Giménez, R., Del Valle de Lersundi, J., Casalí, J., 2017. Nitrate-nitrogen concentration and yield in streams draining agricultural watersheds in Navarre (Spain). *Jornadas sobre Calidad Ecológica y Estado de Conservación de las Aguas*. Pamplona, Spain.

Luquin, E., Merchán, D., Hernández-García, I., Campo-Bescós, M.A., Giménez, R., Del Valle de Lersundi, J., Casalí, J., 2017. Sediment concentration and yield in streams draining agricultural

watersheds in Navarre (Spain). Jornadas sobre Calidad Ecológica y Estado de Conservación de las Aguas. Pamplona, Spain.

International Conference Presentations.

Merchán, D., Luquin, E., Hernández-García, I., Campo-Bescós, M.A., Giménez, R., Casalí, J., Valle, J. Del, Lersundi, D., 2018. Suspended sediment and dissolved solids concentrations and loads in small agricultural watersheds in Navarre. Terraenvision. Barcelona, Spain.

Hernández-García, I., Merchán, D., Aranguren, I., Luquin, E., Campo-Bescós, M.A., Giménez, R., Casalí, J., Del Valle de Lersundi, J., 2018. Understanding the differences in nitrate-nitrogen concentration and yield of two rainfed winter cereal watersheds in Navarre (Spain). European Geosciences Union Assembly (EGU). Vienna. Austria.

Hernández-García, I., Merchán, D., Luquin, E., Campo-Bescós, M.A., Giménez, R., Del Valle de Lersundi, J., Casalí, J., 2018. Agricultural land uses and their effects on water quality in Navarre (Spain). 21st World Soil Science Congress (WCSS21). Rio de Janeiro. Brazil.

Hernández-García, I., López-Vicente, M., Goñi, M., Merchán, D., Luquin, E., Campo-Bescós, M.A., Giménez, R., Del Valle de Lersundi, J., Casalí, J., Assessing current flow connectivity indexes to understand differences in sediment and nutrient dynamics in two Mediterranean watersheds in Navarre (Spain). 3rd Conference of Land Use and Water Quality (LUWQ). Aarhus Denmark

Hernández-García, I., Luquin, E., Gastesi, R., Gómez-Calero, J.A., López-Rodríguez, J.J., Casalí, J., Hayas, A., López-Uceda, A., Peña, A., 2020. Finding strategies to reduce soil erosion using modelling tools: A case study in olive orchards of Cordoba (Spain) including sheet and rill erosion, ephemeral and permanent gullies. European Geosciences Union Assembly (EGU). Vienna. Austria.